PHASE TRANSITIONS IN SPIN-PHONON SYSTEMS

A.P. Young

Department of Theoretical Physics
University of Oxford

A Thesis submitted for the degree of Doctor of Philosophy at Oxford University.

September 1973

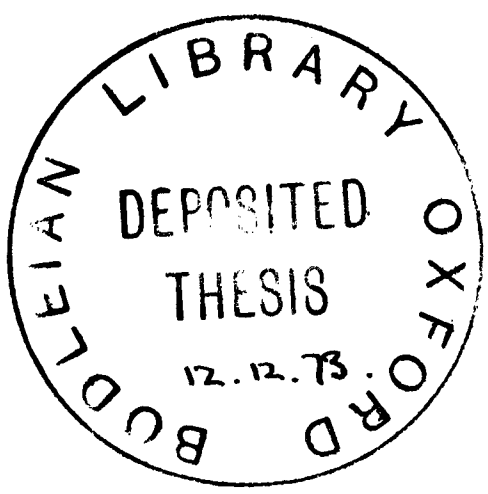

ACKNOWLEDGEMENTS

I should like to thank my supervisor, Dr. R.J. Elliott, for suggesting these problems and for much help and guidance while the work was being carried out. I am also very grateful to Dr. S.R.P. Smith for many interesting and helpful discussions. I thank Dr. D.K. Ray for his kind hospitality during my stay in Grenoble to complete a section of this work. My thanks go to Mrs. Pauline Grounds and Mrs. Margo Goodin for their care in typing the manuscript and their patience in deciphering my illegible handwriting. A grant from the S.R.C. is gratefully acknowledged.

Finally a special word of gratitude must go to my wife for her patience while my time was occupied writing this thesis, which accordingly is dedicated to her.

ABSTRACT

General symmetry arguments show that an elastic constant should vanish when a crystal undergoes a second order structural phase transition. A detailed theory of the elastic anomaly is developed for $DyVO_4$, $TbVO_4$, and $TmVO_4$, which have crystallographic phase changes caused by the Jahn-Teller effect at 14, 34 and 2.1°K respectively. The theory predicts that the elastic constant $\frac{1}{2}(c_{11}-c_{12})$ should fall to zero at the transition temperature T_D for $DyVO_4$ and that c_{66} should vanish for $TbVO_4$ and $TmVO_4$. These conclusions have been verified experimentally. For $DyVO_4$ the electron lattice interaction is predominantly of short range and a cluster theory has been used to interpret the results. For the other crystals a molecular field theory has been used to calculate the elastic constants under different thermodynamic regimes and the random phase approximation has been used in a treatment of the elementary excitations. In $TbVO_4$ and $TmVO_4$ the theory predicts that the elastic constant only falls to zero at T_D when measured at a sufficiently low frequency. This frequency dependence has been observed in $TbVO_4$ and is satisfactorily described by the theory.

At the first order 9.5°K phase change in DySb the elastic constant $\frac{1}{2}(c_{11}-c_{12})$ is observed to soften but not to vanish, consistent with general symmetry arguments. A theory of this anomaly has been developed within the molecular field approximation. Satisfactory agreement with experiment is obtained for $T>T_D$ but there are large unresolved

discrepancies in the low temperature phase.

A theory for the elastic constant and spontaneous polarization of the ferroelectric KH_2PO_4 has been developed. One of the lattice vibrational modes is written in a pseudo-spin formalism and four spin interactions have been included in the model. Although the theory gives a reasonable account of the data some discrepancies still remain.

Coupling between pairs of phonons and the soft mode in hydrogen bonded ferroelectrics has been investigated in the pseudospin model. An anomalous dielectric response is predicted similar to earlier work on the anharmonic phonon theory [71]. A frequency dependence of the elastic constants is expected but this has not yet been observed. An analysis of Raman scattering data shows that the low frequency anomaly is a small effect in KDP, KDA and CsDA contrary to an earlier analysis of the data [70].

When a magnetic field is applied in the hard direction of an anisotropic ferromagnet qualitative arguments show that an elastic constant should vanish when the moments line up parallel to the hard axis. These conclusions have been verified for a particular model of the ferromagnetic phase of Dy and Tb metal.

CONTENTS

CONTENTS

CONTENTS

INTRODUCTION

A transition between different phases of a pure substance is characterised by an 'order parameter' which is zero in one phase and non-zero in the other [1]. In part I of this thesis we shall be concerned with structural phase transitions where the crystal dimensions change as the temperature is reduced below the transition temperature T_D. Here the two phases are characterised by different crystal structures and the order parameter is the distortion in the low temperature phase. Transitions can conveniently be classified into those of the first order and those of the second order. In the former case the order parameter varies discontinuously at the transition temperature while for the latter it increases smoothly from zero as the temperature is reduced below T_D.

One can always express the order parameter in terms of the normal coordinates of the system in its high temperature phase. For second order transitions, the system offers no resistance to small changes in the order parameter when the transition temperature is reached otherwise the phase change would not occur spontaneously. It would be a coincidence if the restoring forces for several modes vanished at the same temperature so the order parameter can be expressed in terms of the normal coordinate of just one mode, which is called the 'soft mode'.

Consequently at T_D there is no resistance to small oscillations of the soft mode so fluctuations in it become

very large and its frequency tends to zero. If however the mode were already at zero frequency then it would remain so as the transition were approached while the fluctuations increased enormously. For $T<T_D$ the crystal distorts and higher order effects ignored in our treatment so far stabilise the mode again. The soft mode concept was introduced by Cochran [2] who showed that ferroelectric phase transitions are associated with an optic vibrational mode whose frequency tends to zero as the transition is approached.

For crystals whose dimensions change at a second order phase change an elastic constant must vanish at T_D for the distortion to occur with no external stress. The elastic constant determines the frequencies of long wavelength acoustic vibrations so in these transitions we expect the soft mode to belong to the acoustic and not the optic branch. In part I we shall investigate in detail a theory for the structural phase transition in several crystals and shall show that the soft mode is indeed a long wavelength acoustic vibration.

At 1st order transitions the resistance of the crystal to small changes in the order parameter does not vanish at the transition temperature. We do not therefore expect a mode to become soft although it is possible that the transition might be associated with a mode whose frequency becomes small, although not zero, as T approaches T_D.

The second part of this thesis concerns the elastic behaviour of anisotropic ferromagnets when there is strong

coupling between the magnetic moments and the lattice. In the absence of an applied magnetic field the moments lie along the easy direction, determined by anisotropy forces, which is a symmetry direction of the crystal. Suppose a magnetic field is applied in the hard direction, defined to be the least favourable orientation for the moments. Again this will be a symmetry axis of the crystal. As the field is increased the moments turn and, for fields greater than a critical value H_c, they will align parallel to the hard axis.

It is easy to see that the moments will point precisely along the hard axis for sufficiently large H, rather than at a small angle to it, by the following simple argument. The change in free energy caused by rotating the spins away from the hard direction through a small angle ϕ about a crystal axis is

$$\Delta F = -\mu(H\cos\phi - A\cos n\phi)$$

where μ is the magnetic moment, H is the applied field and A is a measure of the anisotropy energy which is assumed here to have n fold symmetry. Expanding ΔF to lowest order in ϕ one obtains

$$\Delta F = -\frac{\mu\phi^2}{2}\left(H - n^2A\right)$$

For sufficiently large H ΔF must be positive so the moments will lie precisely along the hard direction.

In other words for $H>H_c$ $\phi=0$ but for $H<H_c$ $\phi\neq0$. Since the lattice strains are coupled to the spins the variation of one of the strain components is qualitatively similar to ϕ. This situation corresponds precisely to a second

order structural phase transition except that the magnetic field H plays the role of temperature. Consequently all the previous arguments apply here and an elastic constant is expected to vanish at the transition (i.e. when $H=H_c$).

In part I we investigate structural phase changes in several crystals which have a small number of low lying energy levels, other than phonons, well separated from higher states. By writing operators acting on these levels in terms of spin operators it is possible to use the techniques developed for magnetic problems to describe the behaviour of many materials which are very different physically. This technique is extremely general and although we shall only consider a few systems in detail many of the conclusions reached have wider applicability.

Chapters 1 - 4 are devoted to a theoretical study of several rare earth vanadates, which undergo a structural phase transition caused by the cooperative Jahn-Teller effect. The transitions are driven by coupling between the low lying energy levels of the rare earth ions and lattice displacements. Many properties of these crystals have been measured - specific heat [5], [6], optical spectra [7], [8], [9], Raman spectra [10], [11] and X ray diffraction [12], [13], which show that the transition is of second order. In support of this work on the acoustic anomaly has already been presented [3]. Gehring et al. [14] have also developed a theory for the elastic constants in one of these materials $DyVO_4$ and from stress measurements on the optical spectrum have attempted to separate out the strain contributions to

the lattice coupling. In the present work we consider three crystals $DyVO_4$, $TbVO_4$ and $TmVO_4$ which, we believe, illustrate all the essential features of the elastic anomaly in this class of materials.

In Chapter 5 a theory is developed for the first order $9.5^{o}K$ phase transition in DySb where specific heat, susceptibility and neutron diffraction [42] measurements show that both a structural change and antiferromagnetic ordering appear. The elastic constants show a sizeable softening so electron-lattice as well as magnetic interactions are involved. An alternative treatment has been given by Levy et al. [43], [44]. This is considerably more complicated than our approach and, unlike our theory, has not been extended below the transition.

Chapters 6 and 7 are devoted to a rather lengthy study of the hydrogen bonded ferroelectric KDP and its isomorphs. Despite a wealth of theoretical and experimental investigations there is still no completely satisfactory description of these materials. Special attention is given in our treatment to the elastic anomaly which occurs at the ferroelectric transition but the same model is also used to discuss polarization and dielectric properties and Raman scattering data.

The second part of this thesis, concerned with elastic anomalies in anisotropic ferromagnets, develops a model for the ferromagnetic phase of the rare earth metals Dy and Tb. These materials have been extensively studied (see reference [1] of part II). Anisotropy forces and magneto-

elastic interactions are found to be large but nonetheless magnetic fields are available which are big enough to turn the moments from the easy to the hard direction. Dy and Tb are therefore suitable materials in which to investigate a possible elastic anomaly when the moments are turned into the hard direction by an applied field.

The first chapter of this thesis is concerned with the development of a model Hamiltonian capable of describing the acoustic properties of $DyVO_4$, $TbVO_4$ and $TmVO_4$. Above T_D they have the tetragonal zircon structure D_{4h}^{19} while below the transition the symmetry is reduced to orthorhombic with space groups D_{2h}^{28}, D_{2h}^{24} and D_{2h}^{24} respectively [10], [8]. For Dy^{3+} and Tb^{3+} the crystal field of the vanadates favours large moments in the basal plane as a result of which there are near degeneracies in the low lying electronic levels. This degeneracy is removed below T_D. The moments for Dy^{3+} lie at 45^o to those for Tb^{3+} and it is shown that this leads to a strong coupling to B_{1g} and B_{2g} lattice modes respectively. An instability in these modes reduces the symmetry to D_{2h}^{28} for $DyVO_4$ and D_{2h}^{24} for $TbVO_4$ in agreement with experiment and the corresponding elastic constants which we expect to vanish at T_D are $(c_{11}-c_{12})/2$ and c_{66} respectively. The quadrupole moments lie out of the basal plane in Tm^{3+} the lowest lying states forming a degenerate doublet which is split below T_D. This is different from the situation in Dy^{3+} and Tb^{3+} where the degeneracy is only approximate. We predict that $TmVO_4$ should distort in a B_{2g} mode, as observed, and the anomalous elastic constant is expected to be c_{66}.

The coupling of the lattice displacements to the electronic levels is investigated in §1.2 for a single complex around a rare earth site, operators acting on the electronic levels being written in terms of spin operators as in [10]. This discussion is extended to treat coupling to phonon modes and static strains in §1.3. Neglecting all but the most important interactions we show in §1.4 that the ion lattice coupling leads to an interaction between electronic levels on different sites which is responsible for the cooperative transition.

In Chapter 2 the static properties of our model are investigated using molecular field theory and the elastic constants under various thermodynamic regimes are calculated. For each crystal the isothermal elastic constant c_T vanishes at the transition as expected from the general considerations mentioned earlier.

In Chapter 3 the frequencies of the elementary excitations are calculated in the random phase approximation, with special emphasis on the acoustic phonon modes. The sound velocity calculated in this way corresponds to the elastic constant for the thermodynamic regime where the populations of the levels remain constant. We discuss this by considering the difference between 'collision dominated' or 'thermodynamic' modes and 'collision free' modes of the crystal. The frequency ω, at which a measurement would determine a particular thermodynamic elastic constant depends upon the relative magnitudes of ω and the spin-spin and spin-lattice relaxation rates, τ_{SS}^{-1} and τ_{SL}^{-1} respectively. We

propose an expression relating the observed value of c to the measuring frequency which we expect to be a satisfactory interpolation between the different thermodynamic results. At low frequencies the elastic constants of all our systems vanish as expected at T_D but for $TbVO_4$ and $TmVO_4$ the high frequency results do not fall to zero. This is interpreted in terms of a zero frequency spin mode of the same symmetry as the distortion. Such a mode exists for $TbVO_4$ and $TmVO_4$ but not for $DyVO_4$.

Chapter 4 compares the theory with the experimental results on $DyVO_4$ and $TbVO_4$ [3], there being no data on $TmVO_4$ at the time of writing. For $DyVO_4$ both the ultrasonic and Brillouin scattering data fall to zero at T_D, consistent with the theory. However there are large deviations from the molecular field results so a cluster theory has been developed to interpret the data. The details of the calculation are given in Appendix C. Modes in other symmetry directions are not expected to be strongly affected but in §4.1(b) we suggest a possible mechanism for the observation in [15] that $c_{44} \neq c_{55}$ below T_D. The elastic constant of $TbVO_4$, unlike $DyVO_4$ is found to be strongly frequency dependent and in particular does not vanish at the transition in the Brillouin scattering experiments although the ultrasonic data, measured at a much lower frequency, does fall to zero. Choosing a suitable value for τ_{SS} we find that the theory agrees satisfactorily with the measurements. Molecular field theory works well, so we have not extended the cluster theory to the four level Tb^{3+} system, and we

discuss why this is so when molecular field theory gives poor results for $DyVO_4$.

The symmetry of DySb is reduced from cubic to (almost) tetragonal below the transition. There are near degeneracies in the low lying electronic states similar to $DyVO_4$ and it is shown in §5.2 that this leads to strong coupling to lattice modes of E symmetry and a softening of the elastic constant $\frac{1}{2}(c_{11}-c_{12})$ in agreement with experiment. In §5.3 it is shown that the model predicts a first order transition as observed and expressions are calculated for the elastic constants in both phases. The two elastic constants corresponding to the components of the E symmetry strain are equal above the transition but this degeneracy is removed below T_D as required on symmetry grounds. Good agreement with the experimental data above the transition is found in §5.4 but the crystal is expected to harden considerably below the transition in contrast to the experiments which show an almost temperature independent behaviour in this region.

The treatment of KDP begins in §6.1 with a discussion of the crystal structure. Lattice displacements are written in terms of local normal coordinates in §6.2 and attention is focused on the four branches involving large proton displacements. By comparing this approach with an earlier theory of Slater [60] it appears plausible that one of these modes is unstable and causes the transition whereas the others are stable. It is found necessary to introduce four particle forces to represent the Slater theory exactly.

In §6.3 the local normal coordinate for the unstable mode, representing a combination of displacements of all the atoms in the cell, is described by a pseudospin formalism. Adding four particle interactions can lead to a first order transition as shown in §6.4. Polarization experiments show that the transition is indeed slightly first order so the four particle term is necessary to fit the polarization and elastic constant data with the same set of parameters as shown in §6.5. A fair description of the elastic constant data, but not the polarization measurements, can however be be obtained without this complication.

Chapter 7 investigates coupling of the soft mode in hydrogen bonded ferroelectrics to pairs of phonons in the light of Cowley's suggestion [70], [71], on the basis of an anharmonic phonon theory, that this leads to a large low frequency peak in the spectrum. After an introduction to Green functions and correlation functions in §7.1, it is shown in §7.2 that the same qualitative features are expected on the pseudospin model as on the anharmonic phonon theory. The necessary modifications to the theory for the elastic constants are discussed in §7.3 and a marked frequency dependence in c_{66} is expected. This effect has not yet been observed. The theory for Raman scattering intensity is developed for the pseudospin model and is found to be very similar to the anharmonic phonon description. From a careful analysis of the Raman data the low frequency peak in the spectrum of KDP, KDA and CsDA is found to be a small effect in contradiction to earlier results of [70], [84].

Section 8.1 gives a very brief introduction to the subject of rare earth metals. From qualitative arguments it is shown in §8.2 that an elastic anomaly should occur in the ferromagnetic phase of Dy and Tb when a field is applied in the hard direction. A particular model for these materials is discussed in §8.3. The elementary excitations are calculated in a spin wave theory leading to coupled magnon-phonon modes. In §8.4 the elastic constant is calculated and found to vanish at $H=H_c$ in agreement with the earlier qualitative arguments.

PART I

ELASTIC ANOMALIES IN CRYSTALS UNDERGOING STRUCTURAL PHASE TRANSITIONS

CHAPTER I

THE PSEUDO-SPIN HAMILTONIAN FOR $DyVO_4$, $TbVO_4$ AND $TmVO_4$

In this chapter we follow closely the arguements of [10] to obtain a model Hamiltonian capable of describing the observed acoustic properties of $DyVO_4$ and $TbVO_4$. Applying similar arguements to $TmVO_4$ we obtain the same Hamiltonian that is used in [8] and [11] to explain their optical absorption and Raman spectra respectively.

1.1 Structure of the electronic states

At room temperature the rare earth compounds discussed in this thesis have the tetragonal zircon structure with the general formula RVO_4, where R is the rare earth ion Dy, Tb or Tm, and their crystallographic space group is D_{4h}^{19} [16]. The structure is illustrated in figure 1; there are two formula units in the unit cell and they are related by an inversion operation so that all the rare earth sites are equivalent. It will be convenient to define two sets of axes (x,y,z) and (x',y',z) which are shown in figure 1; z is parallel to the fourfold rotation axis and (x,y) and (x',y') lie in the basal plane at 45^{o} to each other. Each rare earth ion is at a site of symmetry D_{2d} and the twofold rotation axes of D_{2d} in the basal plane are parallel to the x' and y' axes. The correspondence between the representations of D_{4h} and D_{2d} is shown in table1.1 below.

TABLE 1.1 CORRESPONDENCE BETWEEN REPRESENTATIONS OF D_{4h} and D_{2d}

Symmetry	Representation				
D_{4h}	A_{1g} B_{2u}	A_{2g} B_{1u}	B_{1g} A_{2u}	B_{2g} A_{1u}	E_g E_u
D_{2d}	A_1	A_2	B_2	B_1	E

In the undistorted phase of $DyVO_4$ ($T \geq T_D$) the low lying electronic levels of the Dy^{3+} ion are two nearly degenerate Kramers doublets with a separation ≈ 9 cm^{-1} [14]. The next electronic levels appear to be more than 100 cm^{-1} higher in energy [10] so we need only consider these four states in our discussion of the low temperature transition ($T_D = 14^0K$). In the distorted phase ($T < T_D$) the separation of the doublets increases reaching 27.5 cm^{-1} at $T = 4.5^0K$ [10]. The temperature dependence of these lowest electronic levels is shown in figure 2(a).

Below the transition temperature the ground electronic doublet has the spectroscopic splitting factors $g_x = 19$, $g_y < 1$, $g_z = 0.5$, [9]. The excited doublet has $g_y = 19$, and $g_x \approx g_z \approx 0$. The maximum g-value allowed for the $J = 15/2$ ground term of Dy^{3+} ($^6H_{15/2}$) is 20 and so we conclude that the two doublets correspond approximately to the states $|J_x = \pm J\rangle$ and $|J_y = \pm J\rangle$ (which we shall write as $|\pm J_x\rangle$ and $|\pm J_y\rangle$). By considering the operations of the double group D_{2d} we can show that in the undistorted phase the four states belong to the representations E' and E" (Γ^6 and Γ^7) and written explicitly are:

$$
\left.
\begin{aligned}
|E'\alpha'\rangle &= \tfrac{1}{2}[|J_x\rangle - |-J_x\rangle + i|J_y\rangle - i|-J_y\rangle] \\
|E'\beta'\rangle &= \tfrac{1}{2}[|J_x\rangle + |-J_x\rangle + |J_y\rangle + |-J_y\rangle] \\
|E''\alpha''\rangle &= \tfrac{1}{2}[|J_x\rangle - |-J_x\rangle - i|J_y\rangle + i|-J_y\rangle] \\
|E''\beta''\rangle &= \tfrac{1}{2}[-|J_x\rangle - |-J_x\rangle + |J_y\rangle + |-J_y\rangle]
\end{aligned}
\right\} \qquad (1.1)
$$

These states are orthogonal but not quite normalized because the basis states are not orthogonal.
($\langle J_x | \pm J_y\rangle = \langle -J_x | \pm J_y\rangle = 2^{-J}$).

In $TbVO_4$ for $T \geq T_D$ the low lying electronic levels of the Tb^{3+} ion consist of a doublet lying approximately halfway between two singlets [10]. Just above the transition the singlet-singlet separation is 22.9 cm^{-1} and the next electronic level is a doublet occuring at 91.5 cm^{-1} relative to the lower singlet. We shall include the effect of this level in a crude way in chapter 4 but here we consider only the four lowest lying states in our discussion of the transition ($T_D = 34^oK$). In the distorted phase the doublet splits as required by symmetry and the temperature variation of the energy levels is shown in figure 2(b). Below T_D, $g_{x'} = 16.3$, $g_{y'} = g_z = 0$, (for $g\beta h \gg 1.2\ cm^{-1}$) [7]. The maximum g-value for a pair of levels in the $^7F_6$ ground term of Tb^{3+} ($4f^8$) is 18 so it appears that our model for the states of maximum J is also applicable here. In the high temperature phase the basis states belong to representations A_1, B_1 and E of D_{2d} and written explicitly are:

$$
\left.
\begin{aligned}
|A_1\rangle &= \tfrac{1}{2}\left[|J_{x'}\rangle + |-J_{x'}\rangle - |J_{y'}\rangle - |-J_{y'}\rangle\right] \\
|B_1\rangle &= \tfrac{1}{2}\left[|J_{x'}\rangle + |-J_{x'}\rangle + |J_{y'}\rangle + |-J_{y'}\rangle\right] \\
|E_{x'}\rangle &= \tfrac{1}{\sqrt{2}}\left[|J_{x'}\rangle - |-J_{x'}\rangle\right] \\
|E_{y'}\rangle &= \tfrac{1}{\sqrt{2}}\left[|J_{y'}\rangle - |-J_{y'}\rangle\right]
\end{aligned}
\right\} \quad (1.2)
$$

In the undistorted phase of $TmVO_4$ the lowest electronic level is a doublet, belonging to the E representation of D_{2d}, separated by an energy of 50 cm^{-1} from the first excited level [8] which is ignored in our treatment of the transition ($T_D = 2^oK$). Below T_D the doublet splits, as it must in the reduced symmetry, and the separation at T = 0, determined by extrapolation of the experimental data is, ≈ 3 cm^{-1} [8]. The temperature variation of the levels is shown in figure 2(c). Above T_D, $g_z = 10.2$, $g_x \approx g_y \approx 0$, [8], [11]. The maximum g value in the $^3H_6$ ground term of $Tm^{3+}(4f^{12})$ is 14 so our model for the states of maximum J is not applicable here and indeed the states can be written as:

$$
\left.
\begin{aligned}
|E^+\rangle &= \alpha|M_J=5\rangle + \beta|M_J=1\rangle + \gamma|M_J=-3\rangle \\
|E^-\rangle &= \alpha|M_J=-5\rangle + \beta|M_J=-1\rangle + \gamma|M_J=3\rangle
\end{aligned}
\right\} \quad (1.3)
$$

where α, β and γ are coefficients. From the measured value of the g-factor it is evident that β and γ are relatively small compared with α, although it is not possible to determine the coefficients unambiguously without further information.

As discussed in [10] the crystal field produced by

the VO_4 complex is dominated by terms transforming like Y_2^0 and Y_4^4. The sign of the quadrupole moment relative to the J direction, given by the Elliott & Stevens [17] factor $\langle J||\alpha||J\rangle$ determines whether the moments lie in or out of the basal plane. Tb^{3+} and Dy^{3+} have the same sign of $\langle J||\alpha||J\rangle$ so the Y_2^0 component of the crystal field for the VO_4 complex must favour alignment of the moments in the basal plane. Tm^{3+} has the opposite sign of $\langle J||\alpha||J\rangle$ so we expect, in agreement with experiment, that the same crystal field should cause the moments to lie out of the basal plane. For Dy^{3+} and Tb^{3+} the Y_4^4 term determines the direction of the large moments in the basal plane. Since the fourth order coupling factor $\langle J||\beta||J\rangle$ has opposite signs for Dy^{3+} and Tb^{3+} we expect, again in agreement with observation, that the directions of the moments should be at 45^o to each other in these ions. If the Y_4^4 term acting on the Tm^{3+} ions in $TmVO_4$ were very small the lowest lying states would be the singlets consisting mainly of $|J_z = \pm J\rangle$. The Y_4^4 term must therefore be sufficiently large to raise the energy of these singlets above that of the E level, which is observed to be the ground level.

1.2 Coupling to lattice distortions

The interaction between the lattice distortions and the electronic states will be considered first for a single ion, confining our attention to the low lying states discussed in §1.1. If $Q_{T\alpha}$ represents a symmetrical combination of displacements on the ions surrounding the rare earth ion belonging to the α component of the representation Γ of D_{2d}, then by expanding the crystal field to first order in the displacements the interaction may be written

$$\mathcal{H}_s = \sum_{T\alpha} B_T Q_{T\alpha} O_{T\alpha} \qquad (1.4)$$

where $O_{\Gamma\alpha}$ is an appropriate operator acting on the electronic states and B_Γ is a coupling coefficient. Interaction terms quadratic in the lattice displacements will be discussed briefly in §4.1b.

We consider firstly the form of (1.4) for Dy^{3+}. The lowest four levels have symmetries E' and E" (figure 2a) and E' x E" = $B_1 + B_2 + E$. Operators invariant under time reversal thathave matrix elements within a Kramers doublet must transform according to a representation contained in the anti-symmetric product of the representation of that doublet [18]. In this case {E' x E'} = {E" x E"} = A_1 so (1.4) can be written

$$\mathcal{H}_s = \begin{array}{c} \begin{matrix} |E'\alpha'\rangle & |E'\beta'\rangle & |E''\alpha''\rangle & |E''\beta''\rangle \end{matrix} \\ \begin{bmatrix} -\Delta+\zeta_{A_1}Q_{A_1} & — & \zeta_{B_2}Q_{B_2}+i\zeta_{B_1}Q_{B_1} & -\zeta_E(Q_{E_x}+iQ_{E_y}) \\ — & -\Delta+\zeta_{A_1}Q_{A_1} & \zeta_E(Q_{E_x}-iQ_{E_y}) & \zeta_{B_2}Q_{B_2}-i\zeta_{B_1}Q_{B_1} \\ \zeta_{B_2}Q_{B_2}-i\zeta_{B_1}Q_{B_1} & \zeta_E(Q_{E_x}+iQ_{E_y}) & \Delta-\zeta_{A_1}Q_{A_1} & — \\ -\zeta_E(Q_{E_x}-iQ_{E_y}) & \zeta_{B_2}Q_{B_2}+i\zeta_{B_1}Q_{B_1} & — & \Delta-\zeta_{A_1}Q_{A_1} \end{bmatrix} \end{array} \quad (1.5)$$

where Δ is a static coupling of A_1 symmetry inserted to represent the initial crystal field splitting. For all our systems we consider only the traceless part of O_{A_1}.

Some idea of the relative sizes of the coupling coefficients can be obtained by assuming that the operators $O_{\Gamma\alpha}$ are of second rank.

$$\left.\begin{aligned} O_{A_1} &= J_z^2 - \tfrac{1}{3}J(J+1) \\ O_{B_1} &= J_{x'}^2 - J_{y'}^2 = J_x J_y + J_y J_x \\ O_{B_2} &= J_{x'}J_{y'} + J_{y'}J_{x'} = J_x^2 - J_y^2 \\ O_{E_x} &= J_x J_z + J_z J_x \\ O_{E_y} &= J_y J_z + J_z J_y \end{aligned}\right\} \quad (1.6)$$

Using the states (1.1) and operating with (1.6) it is found in [10] that coupling to the B_2 mode is strongest. If the soft mode is of this symmetry (corresponding to B_{1g} or A_{2u} lattice modes) the resulting site symmetry is C_{2v} (figure 2a) in agreement with experiment and the two doublets both belong to the representation E'.

It is convenient to transform (1.5) using approximate

eigenstates of the distorted phase

$$\mathcal{H}_S = \begin{array}{c} \begin{matrix} |A_1\rangle & |B_1\rangle & |E_{x'}\rangle & |E_{y'}\rangle \end{matrix} \\ \begin{bmatrix} \zeta_{B_2} Q_{B_2} & - & -\Delta + \zeta_{A_1} Q_{A_1} - i\zeta_{B_1} Q_{B_1} & \zeta_E (Q_{E_x} + i Q_{E_y}) \\ - & \zeta_{B_2} Q_{B_2} & -\zeta_E (Q_{E_x} - i Q_{E_y}) & -\Delta + \zeta_{A_1} Q_{A_1} + i\zeta_{B_1} Q_{B_1} \\ -\Delta + \zeta_{A_1} Q_{A_1} + i\zeta_{B_1} Q_{B_1} & -\zeta_E (Q_{E_x} + i Q_{E_y}) & -\zeta_{B_2} Q_{B_2} & - \\ \zeta_E (Q_{E_x} - i Q_{E_y}) & -\Delta + \zeta_{A_1} Q_{A_1} - i\zeta_{B_1} Q_{B_1} & - & -\zeta_{B_2} Q_{B_2} \end{bmatrix} \end{array} \quad (1.7)$$

where the wavefunctions are

$$\left.\begin{aligned} |\alpha_1\rangle &= \frac{1}{\sqrt{2}}\left[|E'\alpha'\rangle + |E''\alpha''\rangle\right] = \frac{1}{\sqrt{2}}\left[|J_x\rangle - |-J_x\rangle\right] \\ |\beta_1\rangle &= \frac{1}{\sqrt{2}}\left[|E'\beta'\rangle + |E''\beta''\rangle\right] = \frac{1}{\sqrt{2}}\left[|J_x\rangle + |-J_x\rangle\right] \\ |\alpha_2\rangle &= \frac{1}{\sqrt{2}}\left[|E'\alpha'\rangle - |E''\alpha''\rangle\right] = \frac{i}{\sqrt{2}}\left[|J_y\rangle - |-J_y\rangle\right] \\ |\beta_2\rangle &= \frac{1}{\sqrt{2}}\left[|E'\beta'\rangle + |E''\beta''\rangle\right] = \frac{1}{\sqrt{2}}\left[|J_y\rangle + |-J_y\rangle\right] \end{aligned}\right\} \quad (1.8)$$

For Tb^{3+}, which is a non Kramers ion, operators having matrix elements within a level must transform according to a representation contained within the symmetries product of the representation of that level [18]. In this case $[A_1 \times A_1] = [B_1 \times B_1] = A_1$ and $[E \times E] = A_1 + B_1 + B_2$ while $A_1 \times B_1 = B_1$ and $A_1 \times E = B_1 \times E = E$. Operating with (1.6) on the states (1.2) it is found that the B_1 coupling coefficient is largest [10] so we expect the distortion to be of this symmetry, corresponding to B_{2g} or A_{1u} lattice modes. Hence below T_D the site symmetry is D_2, in agreement with observation, and the levels belong to the A_1, B_3, B_2 and A_1 representations (figure 2b).

The Hamiltonian may be written in terms of the approximate eigenstates of the distorted phase as (see [10])

$$\mathcal{H}_s = \begin{array}{c} \begin{matrix} |a_1\rangle & |E_{x'}\rangle & |a_2\rangle & |E_{y'}\rangle \end{matrix} \\ \begin{bmatrix} \zeta_{B_1} Q_{B_1} & \zeta_E Q_{Ex'} & -\Delta + \zeta_{A_1} Q_{A_1} & - \\ \zeta_E Q_{Ex'} & \zeta_{B_1} Q_{B_1} & - & \zeta_{B_2} Q_{B_2} \\ -\Delta + \zeta_{A_1} Q_{A_1} & - & -\zeta_{B_1} Q_{B_1} & \zeta_E Q_{Ey'} \\ - & \zeta_{B_2} Q_{B_2} & \zeta_E Q_{Ey'} & -\zeta_{B_1} Q_{B_1} \end{bmatrix} \end{array} \qquad (1.9)$$

We have assumed the doublet lies exactly between the two singlets and denoted by the singlet-singlet energy separation by 2Δ. The basis states are:

$$\left.\begin{aligned} |a_1\rangle &= \frac{1}{\sqrt{2}}\left[|A_1\rangle + |B_1\rangle\right] = \frac{1}{\sqrt{2}}\left[|J_{x'}\rangle + |-J_{x'}\rangle\right] \\ |E_{x'}\rangle &= \frac{1}{\sqrt{2}}\left[|J_{x'}\rangle - |-J_{x'}\rangle\right] \\ |a_2\rangle &= \frac{1}{\sqrt{2}}\left[|A_1\rangle - |B_1\rangle\right] = \frac{1}{\sqrt{2}}\left[|J_{y'}\rangle + |-J_{y'}\rangle\right] \\ |E_{y'}\rangle &= \frac{1}{\sqrt{2}}\left[|J_{y'}\rangle - |-J_{y'}\rangle\right] \end{aligned}\right\} \qquad (1.10)$$

For Tm^{3+}, $[E \times E] = A_1 + B_1 + B_2$ and

$$\mathcal{H}_s = \begin{array}{c} \begin{matrix} |E^+\rangle & |E^-\rangle \end{matrix} \\ \begin{bmatrix} 0 & \zeta_{B_1} Q_{B_1} - i\zeta_{B_2} Q_{B_2} \\ \zeta_{B_1} Q_{B_1} + i\zeta_{B_2} Q_{B_2} & 0 \end{bmatrix} \end{array} \qquad (1.11)$$

In this system, where the degeneracy is due to symmetry we have an example of a true Jahn-Teller effect as originally proposed [19] and an A_1 distortion cannot split the levels. For a system such as $DyVO_4$, on the other hand, with accidental degeneracy an A_1 mode, which does not lower the symmetry, could cause a change in the separation of the E' and E" levels without admixing them. Although this type

of interaction does not cause a phase transition it can produce physically observable effects and is, for example, responsible for the anamalous heat capacity of cerium ethylsulphate [20].

Applying the operators (1.6) to the states (1.3) and noting that β and γ are small compared with α we find that the B_1 and B_2 coupling coefficients are roughly equal, as pointed out in [11]. For reasons that will be discussed in §4.2 the distortion below T_D is of B_1 symmetry so the resulting site symmetry is D_2 and the electronic levels transform like B_2 and B_3 (figure 2c). In a representation with the B_1 terms along the diagonal

$$\begin{array}{cc} |E_1\rangle & |E_2\rangle \\ \end{array}$$

$$\mathcal{H}_s = \begin{bmatrix} \zeta_{B_1} Q_{B_1} & -i\zeta_{B_2} Q_{B_2} \\ i\zeta_{B_2} Q_{B_2} & -\zeta_{B_1} Q_{B_1} \end{bmatrix} \tag{1.12}$$

where

$$|E_1\rangle = \frac{1}{\sqrt{2}}\left[|E^+\rangle + |E^-\rangle\right]$$

$$|E_2\rangle = \frac{1}{\sqrt{2}}\left[-|E^+\rangle + |E^-\rangle\right] \tag{1.13}$$

It is convenient to write the matrices (1.7) and (1.9) for Dy^{3+} and Tb^{3+} in terms of the following 4 x 4 matrices.

$$\sigma^x = \begin{bmatrix} . & . & 1 & . \\ . & . & . & 1 \\ 1 & . & . & . \\ . & 1 & . & . \end{bmatrix}, \quad \sigma^y = \begin{bmatrix} . & . & -i & . \\ . & . & . & -i \\ i & . & . & . \\ . & i & . & . \end{bmatrix}, \quad \sigma^z = \begin{bmatrix} 1 & . & . & . \\ . & 1 & . & . \\ . & . & -1 & . \\ . & . & . & -1 \end{bmatrix}$$

$$\tau^x=\begin{bmatrix} . & 1 & . & . \\ 1 & . & . & . \\ . & . & . & 1 \\ . & . & 1 & . \end{bmatrix}, \tau^y=\begin{bmatrix} . & -i & . & . \\ i & . & . & . \\ . & . & . & -i \\ . & . & i & . \end{bmatrix}, \tau^z=\begin{bmatrix} 1 & . & . & . \\ . & -1 & . & . \\ . & . & 1 & . \\ . & . & . & -1 \end{bmatrix} \qquad (1.14)$$

which obey the commutation relations

$$\underline{\sigma} \wedge \underline{\sigma} = 2i\,\underline{\sigma}, \quad \underline{\tau} \wedge \underline{\tau} = 2i\,\underline{\tau}, \quad [\underline{\sigma}, \tau] = 0$$

The matrix (1.7) for Dy^{3+} can be written

$$\mathcal{H}_s = (-\Delta + \zeta_{A_1} Q_{A_1})\sigma^x + \zeta_{B_2} Q_{B_2} \sigma^z + \left[\zeta_{B_1} Q_{B_1} \tau^x - \zeta_E (Q_{E_x} \tau^y + Q_{E_y} \tau^x)\right] \sigma^y \qquad (1.15)$$

while for Tb^{3+} we can write (1.9) as

$$\mathcal{H}_s = (-\Delta + \zeta_{A_1} Q_{A_1}) \tfrac{1}{2}(1+\tau^z)\sigma^x + \zeta_{B_1} Q_{B_1} \sigma^z + \zeta_{B_2} Q_{B_2} \tfrac{1}{2}(1-\tau^z)\sigma^x$$
$$+ \zeta_E \left[Q_{E_x}, \tfrac{1}{2}(1+\sigma^z) + Q_{E_y}, \tfrac{1}{2}(1-\sigma^z)\right] \tau^x \qquad (1.16)$$

We write (1.12) for Tm^{3+} as

$$\mathcal{H}_s = \zeta_{B_1} Q_{B_1} \sigma^z + \zeta_{B_2} Q_{B_2} \sigma^y \qquad (1.17)$$

where here σ^x, σ^y and σ^z are the 2 x 2 Pauli spin matrices.

1.3 Coupling to Phonons and Static Strains

In the preceeding section of this chapter we discussed the interaction between the electronic states and lattice displacements of a single complex surrounding a rare earth ion. Since the displacements of neighbouring complexes are, of course, coupled together it is best to describe these displacements in terms of normal modes of the whole system i.e. phonons. Denoting the branch index by j and the wavevector by $\underline{k}$ the displacements of the ions

in the crystal due to a single phonon may be written as $Q_j(\underline{k})$. If, for each site ρ in the lth unit cell centred at $\underline{R}(\ell)$ we define the electronic operators of different symmetries α by $O^{\alpha}(\rho, \ell)$ then the full interaction Hamiltonian can be written in the form

$$\mathcal{H}_{JT} = \sum_{\alpha\rho} \sum_{j\underline{k}} \zeta_j^{\alpha}(\rho, \underline{k}) Q_j(\underline{k}) O^{\alpha}(\rho, \underline{k}) \qquad (1.18)$$

where

$$O^{\alpha}(\rho, \underline{k}) = N^{-1/2} \sum_{\ell} O^{\alpha}(\rho, \ell) e^{-i\underline{k}.\underline{R}(\ell)} \qquad (1.19)$$

At $\underline{k} = 0$ symmetry requirements restrict the form of the $\zeta_j{}^{\alpha}(\rho, \underline{k})$ and in particular the branch index j must be compatible with the site symmetry of the electronic operator $O^{\alpha}(\rho, \ell)$ as given in table 1.

To make a solution of the problem more tractable we now approximate (1.18) by neglecting all but the most important interactions. In chapter 2 we shall calculate the static properties of our systems in a molecular field theory, in which we need only include terms in the Hamiltonian with non vanishing expectation values. All these systems are observed to order in an even $\underline{k} = 0$ mode, B_{1g} for $DyVO_4$ and B_{2g} for $TbVO_4$ and $TmVO_4$, consistent with our estimate of the magnitude of the coupling coefficients (see §§ 1.2 and 4.2). We therefore approximate our model Hamiltonian by neglecting all couplings to electronic operators other than the one which orders at $\underline{k} = 0$ (O^z in all cases) and the A_{1g} operator. Furthermore the A_{1g} coupling coefficients for $DyVO_4$ and $TbVO_4$ appear to be

relatively small (see §1.2 and [10]) so we put $C_{A_{1g}} = 0$.

In chapter three we investigate the elementary excitations for small $\underline{k}$ values in a simple theory equivalent to molecular field theory. Of particular interest are those excitations of the spin system with the same symmetry as the order parameter. In our theory they are not affected by couplings of different symmetries, which we therefore again ignore. However a more sophisticated theory would show that these other couplings affect the widths of the modes, as discussed qualitatively in chapter 3.

Because we are only concerned with the $\underline{k} = 0$ even modes for which all the rare earth ions are equivalent we can work with a simplified Hamiltonian, which assumes one site per unit cell, by defining operators such that

$$\sum_{j\rho} \zeta_j(\rho,\underline{k})\sigma^z(\rho,\underline{k}) = \sum_j \zeta_j(\underline{k})\sigma^z(\underline{k})$$

In what follows N refers to the number of rare earth ions. With the above approximations we can write the interaction Hamiltonian for all our systems in terms of phonon creation and annihilation operators, $a_j^+(\underline{k})$ and $a_j(\underline{k})$ respectively, by

$$\mathcal{H}_{JT} = \sum_{j\underline{k}} \xi_j(\underline{k})\sigma^z(\underline{k})[a_j^+(\underline{k}) + a_j(-\underline{k})] \qquad (1.20)$$

where the relationship between $\xi_j(\underline{k})$ and $\zeta_j(\underline{k})$ is given in Appendix B.

As $2\pi/k$ approaches wavelengths comparable with the crystal size the nature of the boundary conditions becomes important. To eliminate surface effects we follow Kanamori [21] and apply periodic boundary conditions with the result that there can be no $\underline{k} = 0$ acoustic mode and no change in the crystal dimensions. A static strain is therefore

added separately in this description and the phonon frequencies $\omega_j(\underline{k})$ and coordinates $Q_j(\underline{k})$ are those of a lattice with the observed strain but in the absence of any Jahn-Teller coupling. However, since the strain e which develops below T_D is small [12], [13], we neglect the resulting change in the phonon energies due to anharmonic effects.

The interaction of the electronic states with the static strain may be written as

$$\mathcal{H}_s = \eta e \sum_l \sigma^z(l) \qquad (1.21)$$

e must have the correct symmetry, B_{1g} in $DyVO_4$ and B_{2g} in $TbVO_4$ and $TmVO_4$, where (in the notation of appendix A) $e_{B1g} = e_{xx} - e_{yy}$ and $e_{B2g} = e_{xy} + e_{yx} = 2\, e_{xy}$. If the crystal has volume V the corresponding elastic energy is given by

$$\mathcal{H}_{el} = \frac{1}{2} V c_o e^2 \qquad (1.22)$$

where for $DyVO_4$, $c_o = (c_{11} - c_{12})/2$ and for $TbVO_4$ and $TmVO_4$ $c_o = c_{66}$ (see appendix A). The usual Hamiltonian for harmonic vibrations can be written in terms of phonon creation and annihilationoperators as

$$\mathcal{H}_p = \sum_{j\underline{k}} \hbar\omega_j(\underline{k}) \left[a_j^+(\underline{k}) a_j(\underline{k}) + \tfrac{1}{2}\right] \qquad (1.23)$$

The last term in our Hamiltonian represents the crystal field splitting and is

$$\mathcal{H}_c = -\Delta \sum_l \sigma^x(l) \qquad (1.24)$$

for $DyVO_4$ and

$$\mathcal{H}_c = -\Delta \sum_l \tfrac{1}{2}\left[(1+\tau^z)\sigma^x\right](l) \qquad (1.25)$$

for $TbVO_4$. There is no crystal field splitting for $TmVO_4$ but it is of interest to investigate the effect of a magnetic field h parallel to the z direction which interacts with the electronic states through a term

$$\mathcal{H}_c = -g\beta h \sum_l \sigma^x(l) \qquad (1.26)$$

Collecting expressions (1.20) - (1.26) together we may write the Hamiltonian in a form applicable to all our systems, as

$$\mathcal{H} = \sum_{j\underline{k}} \hbar\omega_j(\underline{k})\left[a_j^+(\underline{k})a_j(\underline{k}) + \tfrac{1}{2}\right] + \tfrac{1}{2}Vc_0e^2 + \eta e\sum_l \sigma^z(l)$$
$$+ \sum_{j\underline{k}} \xi_j(\underline{k})\,\sigma^z(\underline{k})\left[a_j^+(\underline{k}) + a_j(-\underline{k})\right] + \mathcal{H}_c \qquad (1.27)$$

1.4 Transformation to new coordinates

Spin-phonon Hamiltonians similar to (1.27) have been considered by many authors, [22] - [26]. As discussed by Elliott [27] the coupling term linear in phonon operators gives rise to an effective interaction between electronic states on different sites which causes the cooperative transition. Using second order perturbation theory and taking matrix elements between phonon states we find

$$\Delta E^{(2)} = \sum_{j\underline{k}} \left\{ \frac{|\langle n_j(\underline{k})-1|\mathcal{H}_{JT}|n_j(\underline{k})\rangle|^2}{\hbar\omega_j(\underline{k})} - \frac{|\langle n_j(\underline{k})+1|\mathcal{H}_{JT}|n_j(\underline{k})\rangle|^2}{\hbar\omega_j(\underline{k})} \right\}$$
$$= \frac{-1}{2N}\sum_{ll'}\sum_{j\underline{k}} \frac{2|\xi_j(\underline{k})|^2}{\hbar\omega_j(\underline{k})}\,\sigma^z(l)\sigma^z(l')\,e^{i\underline{k}\cdot[\underline{R}(l)-\underline{R}(l')]} \qquad (1.28)$$

Defining

$$J(\ell,\ell') = N^{-1}\sum_{j\underline{k}} \frac{2|\xi_j(\underline{k})|^2}{\hbar\omega_j(\underline{k})} e^{i\underline{k}\cdot[\underline{R}(\ell)-\underline{R}(\ell')]} \quad \text{For } \ell\neq\ell'$$

and

$$J(\ell,\ell) = 0 \qquad (1.29)$$

(1.28) becomes

$$\Delta E^{(2)} = -\tfrac{1}{2}\sum_{\ell\neq\ell'} J(\ell,\ell')\sigma^2(\ell)\sigma^2(\ell') - \sum_{j\underline{k}} |\xi_j(\underline{k})|^2/\hbar\omega_j(\underline{k}) \qquad (1.30)$$

We put $J(\ell,\ell) = 0$ because terms in (1.28) with $\ell = \ell'$ correspond to the constant Jahn-Teller self energy of a single complex, and are represented by the last term in (1.30), but do not contribute to the ordering. The Fourier transform of $J(\ell,\ell')$ is

$$J(\underline{k}) = \sum_j K_j(\underline{k}) - \frac{1}{N}\sum_{j\underline{k}'} K_j(\underline{k}') \qquad (1.31)$$

$$\text{Where} \quad K_j(\underline{k}) = 2|\xi_j(\underline{k}|^2/\hbar\omega_j(\underline{k}) \qquad (1.32)$$

the second term in (1.31) arising because $J(\ell,\ell) = 0$. $J(\underline{k})$ vanishes foroptic modes with no dispersion and $\xi_j(\underline{k})$ independent of $\underline{k}$ as it should because this situation corresponds to isolated complexes. It also vanishes for a model of the acoustic modes with a Debye frequency spectrum and $\xi \propto k^{\frac{1}{2}}$.

This problem bears a certain resemblance to that of the polaron [28] where a mobile electron interacts with the lattice through a term linear in the distortion analagous to $\mathcal{H}_{JT}$. It is well known that the distortion modifies the dielectric constant, (i.e. changes the interaction between two electrons a given distance apart) through exchange of virtual phonons in much the same way as $\mathcal{H}_{JT}$ leads to an interaction between electronic states on different sites.

Sears [22], for the magnetic equivalent of this problem, and Kobayashi [26] for the ferroelectric KDP used a decoupling scheme which effectively ignores the last term in (1.31). By taking the equations of motion to second order Elliott and Parkinson [23] were able to obtain $J(\underline{k})$ correctly when considering coupling to acoustic modes. Generalizing their treatment to include optic mode coupling we find certain inconsistencies. For example when $\mathcal{H}_c = 0$ the phonon frequencies should remain unchanged, as can readily be seen by taking the equations of motion of the phonon operators, but in their treatment one obtains a solution with the optic mode frequencies altered.

The problem is simplified if we use a transformation to displaced phonon operators [29]. This eliminates the term linear in the coupling coefficients and displays explicitly the interaction between electronic states on different sites so we need only take the equations of motion to first order.

Defining

$$\gamma_j(\underline{k}) = a_j(\underline{k}) + \frac{\xi_j(\underline{k})}{\hbar\omega_j(\underline{k})}\sigma^z(\underline{k}) \qquad (1.33)$$

then (1.27) becomes

$$\mathcal{H} = \sum_{j\underline{k}} \hbar\omega_j(\underline{k})\left[\gamma_j^+(\underline{k})\gamma_j(\underline{k}) + \tfrac{1}{2}\right] + \tfrac{1}{2}Vc_0e^2 - \eta e\sum_{\ell}\sigma^z(\ell) - \frac{1}{2}\sum_{\ell,\ell'} J(\ell,\ell')\sigma^z(\ell)\sigma^z(\ell') + \mathcal{H}_c \qquad (1.34)$$

with $J(\ell,\ell')$ given by (1.29).

Since we apply periodic boundary conditions, as

discussed in §1.3, the $\underline{k} = 0$ acoustic mode does not exist so we put $K_a(0) = 0$ in the expression for $J(0)$. For small $\underline{k}$, $\xi_a(\underline{k})$ is proportional to the strain and varies like $k^{\frac{1}{2}}$ (see appendix B) so $K_a(\underline{k})$ tends to a constant which depends upon the direction of the wavevector $\underline{k}$. Therefore there is a discontinuity in $J(\underline{k})$ at $k = 0$, the magnitude of which depends upon the direction from which $\underline{k}$ approaches zero.

If $\mathcal{K}_c = 0$ the spins and displaced phonons are decoupled, the phonon frequencies are unchanged as mentioned earlier and there is an interaction between the electronic states on different sites due to exchange of virtual phonons. For $\mathcal{K}_c \neq 0$, there is, in addition, a residual interaction between the displaced phonons and the spins due to the non-commutivity of $\mathcal{K}_c$ with the $\gamma_j(\underline{k})$ which mixes vibrational and electronic modes. We shall investigate this in detail in chapter 3 where the frequencies of the elementary excitations are calculated.

The final result of this chapter is expression (1.34) for the Hamiltonian with $\mathcal{K}_c$ given by (1.24), (1.25) or (1.26). In the next two chapters we investigate its static and dynamic properties, with particular emphasis on the elastic constants.

CHAPTER 2

STATIC PROPERTIES

In this chapter we investigate the static properties of Hamiltonian (1.34) using molecular field theory and in particular calculate the elastic constants for various thermodynamic regimes.

2.1 Equilibrium conditions

In the moleculor field approximation the Hamiltonian (1.34) for $TbVO_4$ can be written as

$$\mathcal{H}_{m.f.} = -\Delta\sum_{l}\tfrac{1}{2}\left[(1+\gamma^2)\sigma^x\right](l) - H_e\sum_{l}\sigma^z(l) + \tfrac{1}{2}NJ(0)\langle\sigma^z\rangle^2$$
$$+\tfrac{1}{2}Vc_0e^2 + \sum_{j\underline{k}} n_j(\underline{k})\hbar\omega_j(\underline{k}) \qquad (2.1)$$

where the effective field acting on σ^z is

$$H_e = J(0)\langle\sigma^z\rangle + \eta e \qquad (2.2)$$

and $n_j(\underline{k})$ is the phonon occupation number given by the usual Bose-Einstein distribution function

$$n_j(\underline{k}) = \left\{\exp\left[\hbar\omega_j(\underline{k})/kT\right] - 1\right\}^{-1} \qquad (2.3)$$

The term in $\langle\sigma^z\rangle^2$ in (2.1) represents the moleculor field self energy of $\frac{1}{2}J(0)\langle\sigma^z\rangle^2$ at each of the N unit cells. The energy levels of a single 'spin' are $\pm H_e$ and $\pm W$, where

$$W = \left(H_e^2 + \Delta^2\right)^{1/2} \qquad (2.4)$$

We calculate the elastic constants from the expressions for the free energy

$$F = E - TS \qquad (2.5)$$

where E is the expectation value of the Hamiltonian and S the entropy. It is given in the molecular field approximation by

$$F = -NkT\ln 2\left[\cosh\left(\frac{W}{kT}\right) + \cosh\left(\frac{H_e}{kT}\right)\right] + \tfrac{1}{2}NJ(0)\langle\sigma^z\rangle^2$$
$$+\tfrac{1}{2}Vc_0e^2 + F_p \qquad (2.6)$$

where

$$F_p = +kT \sum_{jk} \ln\left[1 - \exp\left(-\hbar\omega_j(k)/kT\right)\right]$$

is the phonon contribution to the free energy.

Because F is written in terms of Δ

$$\langle\sigma^x\rangle = \frac{-1}{N}\frac{\partial F}{\partial \Delta} = P_1 \frac{\Delta}{W}\tanh\left(\frac{W}{kT}\right) \qquad (2.7)$$

where P_1, the population of the singlet levels, is given by

$$P_1 = \cosh\left(\frac{W}{kT}\right)\Big/\left[\cosh\left(\frac{W}{kT}\right) + \cosh\left(\frac{H_e}{kT}\right)\right]^{-1} \qquad (2.8)$$

and $P_2 = 1 - P_1$ is the population of the levels which comprise the degenerate E doublet above T_D. Since $DyVO_4$ is effectively a two level system, the subsequent thermodynamic expressions, which will be derived for $TbVO_4$, can apply to $DyVO_4$ by putting $P_2 = 0$. In a magnetic field h the expressions for $TmVO_4$ are identical to those for $DyVO_4$ with Δ replaced by $g\beta h$ so we shall not discuss this case explicitly but only give the expressions for h = 0.

The equilibrium value of $\langle\sigma^z\rangle$ is given by the condition $\partial F/\partial\langle\sigma^z\rangle = 0$, i.e.

$$\langle\sigma^z\rangle = P_1(H_e/W)\tanh\left(\frac{W}{kT}\right) + P_2\tanh\left(\frac{H_e}{kT}\right) \qquad (2.9)$$

which is applicable to all our systems. The stress $\mathcal{S}$ corresponding to the strain e is given by

$$\mathcal{S} = \frac{1}{V}\left(\frac{\partial F}{\partial e}\right)_T = c_0 e - \frac{N}{V}\eta\langle\sigma^z\rangle \qquad (2.10)$$

and from the condition for mechanical equilibrium, $\mathcal{S} = 0$ we find that the equilibrium value of the strain is

$$\langle e\rangle = \frac{N}{V}\frac{\eta}{c_0}\langle\sigma^z\rangle \qquad (2.11)$$

Hence the interaction of the electronic states with the strain (1.21) may be written as

$$\mathcal{H}_s = -\mu \langle \sigma^z \rangle \sum_l \sigma^z(l) \tag{2.12}$$

where $\mu = (N/V)(\eta^2/Co)$, and the moleculor field H_e is given by $J'\langle\sigma^z\rangle$ with

$$J' = J(0) + \mu \tag{2.13}$$

It is shown in appendix B that μ is equal to $\lim_{K\to 0} K_a(\underline{k})$ where the limit is taken in the direction with maximum coupling. Remembering that $J(0)$ was defined with $K_a(0) = 0$ (see §1.3) we see that J' is just the maximum value of $J(\underline{k})$ for small $\underline{k}$. The discontinuity in $J(\underline{k})$ at $\underline{k} = 0$, due to there being no $\underline{k} = 0$ acoustic mode, is therefore exactly made up by the strain contribution which acts only at $k = 0$.

The transition occurs at $T = T_D$ when there is a solution $\langle\sigma^z\rangle \neq 0$ to (2.9), i.e.

$$1 = P_1 \frac{J'}{\Delta} \tanh\left(\frac{\Delta}{kT_0}\right) + P_2 \frac{J'}{kT_0} \tag{2.14a}$$

For $DyVO_4$ this simplifies to

$$1 = \frac{J'}{\Delta} \tanh\left(\frac{\Delta}{kT_0}\right) \tag{2.14b}$$

and for $TmVO_4$ to

$$kT_0 = J' \tag{2.14c}$$

2.2 Thermodynamic expressions for the elastic constants

The elastic constant relating the stress $\mathcal{S}$ to the strain e is defined by

$$c_\gamma = (\partial \mathcal{S}/\partial e)_\gamma$$

where γ specifies the thermodynamic conditions under which the elastic constant is measured. We shall discuss in

chapter 3 how these conditions are related to the frequency of measurement. Using (2.10) the elastic constants can be expressed as

$$\frac{c_\gamma}{c_0} = 1 - \frac{\mu}{\gamma}\left(\frac{\partial\langle\sigma^2\rangle}{\partial e}\right)_\gamma \qquad (2.15)$$

Defining g_γ, the susceptibility of the spin system with respect to the effect field H_e, by the relation

$$g_\gamma = \left(\frac{\partial\langle\sigma^2\rangle}{\partial H_e}\right)_\gamma$$

we see that the elastic constants can be expressed as

$$\frac{c_\gamma}{c_0} = \frac{1 - J' g_\gamma}{1 - J(0) g_\gamma} \qquad (2.16)$$

We may write this in two alternative forms

$$\frac{c_\gamma}{c_0} = 1 - \mu \tilde{G}_\gamma = \frac{1}{1 + \mu G_\gamma} \qquad (2.17)$$

where $\tilde{G}_\gamma = g_\gamma/[1-J(0)g_\gamma]$ is the full susceptibility of the spin system neglecting the strain coupling . μ and $G_\gamma = g_\gamma/[1-J'g_\gamma]$ is the susceptibility including all the spin interactions. G_γ and $\tilde{G}_\gamma$ are respectively the susceptibilities at zero stress and zero strain. Expressions similar to (2.17) were obtained by Dvorak [30] for the ferroelectric KDP, which we discuss in chapter 6. It is most convenient to give thethermodynamic results in terms of g_γ but in chapter 3 we shall discuss the frequency dependence of the elastic constants in terms of the full spin susceptibility G_γ.

The first thermodynamic regime which we consider, the 'isothermal' regime $\Upsilon = T$, is defined by keeping the temperature of the crystal constant. The other regimes of interest are adiabatic, but for a crystal with many

energy levels there are an infinite number of ways in which an adiabatic susceptibility can be defined. For our spin-phonon systems we find it convenient to consider three cases. At one extreme we can keep the populations of the levels constant, which is adiabatic the quantum mechanical sense. This result holds for an 'isolated' system, $\gamma = I$. At the other extreme, which is adiabatic in the thermodynamic sense and is called 'isentropic', $\gamma = S'$, thermal equilibrium is maintained while the entropy, expressed as a function of temperature and the other thermodynamic variables, remains constant. This distinction is made, for example, by Wilcox [31] and Tolman [32]. For our systems it is useful to define in addition the "essentially isolated" regime, $\gamma = S$, in which the spin system stays in thermal equilibrium with constant entropy while being unable to exchange energy with the phonons.

The expressions for the susceptibilities g_γ are as follows:

(a) In the 'perfectly isolated' regime, $\gamma = I$,

$$g_I = \frac{\Delta}{W^2} \langle \sigma^x \rangle \qquad (2.18a)$$

for both Dy and Tb while for Tm

$$g_I = 0 \qquad (2.18b)$$

(b) In the 'isothermal' regime, $\gamma = T$

$$g_T = g_I + \frac{1}{kT}\left[P_1\left(1 - \langle\sigma^z\rangle^2 - \Delta^2/W^2\right) + P_2\left(1 - \langle\sigma^z\rangle^2\right)\right] \qquad (2.19a)$$

for Dy and Tb with $P_2 = 0$ for Dy. For Tm

$$g_T = \frac{1}{kT}\left(1 - \langle\sigma^z\rangle^2\right) \qquad (2.19b)$$

(c) Results in the 'essentially isolated' regime, $\Upsilon = S$, are obtained by neglecting the phonon contribution, F_p, to the free energy (2.6). For Dy

$$g_S = g_T \tag{2.20a}$$

and for Tb

$$g_S = g_T - \frac{1}{KT}\frac{\left[P_1\left(H_e - W\langle\sigma^z\rangle\tanh\left(\frac{W}{KT}\right)\right) + P_2\left(H_e - H_e\langle\sigma^z\rangle\tanh\left(\frac{H_e}{HT}\right)\right)\right]^2}{P_1W_1^2 + P_2H_e^2 - \left[P_1W\tanh\left(\frac{W}{KT}\right) + P_2H_e\tanh\left(\frac{He}{HT}\right)\right]^2} \tag{2.20b}$$

which is an example of the general thermodynamic relationship.

$$g_T - g_S = T\left(\frac{\partial\langle\sigma^z\rangle}{\partial T}\right)^2_{H_e} / C_{H_e} \tag{2.21}$$

where C_{He} denotes the specific heat of the spin system at constant H_e. For Tm, $g_s = g_T$ above the transition while for $T < T_D$, $g_s = 0$ so $c_s = c_o$.

(d) In the 'isentropic' regime, $\Upsilon = S'$, the phonon contribution to the free energy is included. If we assume that the phonons are unaffected by the strain through anharmonic effects and denote the specific heat of the lattice by C_L, then $g_{s'}$ is obtained by replacing C_{H_e} in (2.21) by $C_{H_e} + C_L$ giving

$$g_{s'} = [g_S C_{H_e} + g_T C_L]/[C_{H_e} + C_L] \tag{2.22}$$

This leads to a relation between the susceptibilities G_Υ of the form

$$G_{s'} = [G_S C_\beta + G_T C_L]/[C_\beta + C_L] \tag{2.23}$$

where C_β is the specific heat of the spin system of constant stress. The corresponding expression for $c_{s'}$ is

$$c_{s'} = [c_S C_e + c_T C_L]/[C_e + C_L] \tag{2.24}$$

where C_e is the specific heat at constant strain.

If we neglect the phonons and confine our attention for a moment to the spin system the 'isentropic' susceptibility is g_s. As discussed in [31] $g_s = g_I$ if the populations of the spin levels, initially forming a canonical distribution, remain canonical when the stress is applied. This condition is satisfied, for example, with a system of equally spaced energy levels if the spectrum is uniformly expanded or contracted by the stress. For a non-degenerate two level system such as $DyVO_4$ this must always be the case so $g_s = g_I$ in agreement with our calculations. In more complicated systems, however, such as $TbVO_4$, $g_s \neq g_I$.

Above the transition $c_S = c_{S'} = c_T$ and at high temperatures all the elastic constants approach c_o whilst at T = 0 they are again all equal.

For $TmVO_4$

$$\frac{c_T}{c_o} = \frac{T - T_D(1-\langle\sigma^z\rangle^2)}{T - T_I(1-\langle\sigma^z\rangle^2)} \qquad (2.25)$$

where $kT_D = J'$ and $kT_I = J(0) = J' - \mu$. T_I is the 'clamped' transition temperature, at which the transition would take place if strain were forbidden (in practice, however, if the crystal were clamped, domains would form below T_D). Above T_D, $c_S = c_T$ and for $T < T_D$, $c_S = c_o$ while $c_I = c_o$ at all temperatures. (2.25) also holds for $DyVO_4$ if $\Delta \ll kT_D$. In the same limit the elastic constants of $TbVO_4$ above the transition are given by

$$\frac{c_I}{c_o} = \frac{2T - T_D}{2T - T_I}, \qquad \frac{c_S}{c_o} = \frac{c_T}{c_o} = \frac{T - T_D}{T - T_I} \qquad (2.26)$$

We see that

$$c_T \leq c_{S'} \leq c_S \leq c_I \leq c_o$$

for all our systems, consistent with the general results of [31].

General symmetry arguements show that an elastic constant should vanish at the transition andindeed we find from (2.14), (2.16), (2.19) and (2.21) that c_S and c_T fall to zero at T_D. However in $TbVO_4$ and $TmVO_4$, c_I remains finite and in chapter 3 we shall show that this is related to a zero frequency spin mode of these systems.

Equations (2.16) - (2.24) are the desired expressions for the elastic constants. We defer until the next chapter a discussion of how the different thermodynamic regimes are related to the time scale of measurement.

CHAPTER 3

DYNAMIC PROPERTIES

In §3.1 we calculate the frequencies of the elementary excitations by decoupling the equations of motion in the random phase approximation. A connection is made between the frequencies of acoustic modes, calculated by this method, and the thermodynamic elastic constants of chapter 2. §3.2 discusses the variation in elastic constant with measuring frequency.

3.1 Elementary excitations

3.1a $DyVO_4$ and $TmVO_4$

For Hamiltonian (1.34) we obtain the following equations of motion for the electronic operators σ^x, σ^y and σ^z and the mixed operators $\gamma_j(\underline{k})$:

$$
\begin{aligned}
\hbar \frac{d}{dt}\sigma^x(\underline{k}) &= N^{-1/2}\sum_{\underline{k}'} J(\underline{k}')\left[\sigma^y(\underline{k}+\underline{k}')\sigma^z(-\underline{k}') + \sigma^z(\underline{k}')\sigma^y(\underline{k}-\underline{k}')\right] \\
&\quad + 2\mu\langle\sigma^z\rangle\sigma^y(\underline{k}) - 2N^{-1/2}\sum_{\underline{k}'j}\xi_j(\underline{k}')\left[\sigma^y(\underline{k}+\underline{k}')\gamma_j(\underline{k}') + \gamma_j^\dagger(\underline{k}')\sigma^y(\underline{k}-\underline{k}')\right] \\
\hbar \frac{d}{dt}\sigma^y(\underline{k}) &= -N^{-1/2}\sum_{\underline{k}'} J(\underline{k}')\left[\sigma^x(\underline{k}+\underline{k}')\sigma^z(-\underline{k}') + \sigma^z(\underline{k}')\sigma^x(\underline{k}-\underline{k}')\right] + 2\Delta\,\sigma^x(\underline{k}) \\
&\quad - 2\mu\langle\sigma^z\rangle\sigma^x(\underline{k}) + 2N^{-1/2}\sum_{\underline{k}'j}\xi_j(\underline{k}')\left[\sigma^x(\underline{k}+\underline{k}')\gamma_j(\underline{k}') + \gamma_j^\dagger(\underline{k}')\sigma^x(\underline{k}-\underline{k}')\right] \\
\hbar \frac{d}{dt}\sigma^z(\underline{k}) &= -2\Delta\,\sigma^y(\underline{k}) \\
\hbar \frac{d}{dt}\gamma_j^\dagger(\underline{k}) &= i\hbar\omega_j(\underline{k}) - \frac{2\Delta\xi_j(\underline{k})\sigma^y(\underline{k})}{\hbar\omega_j(\underline{k})}
\end{aligned}
\qquad (3.1)
$$

These equations are valid for both $DyVO_4$ and $TmVO_4$ with $\Delta = 0$ for $TmVO_4$ (in zero magnetic field). We decouple in the random phase approximation by replacing products of operators AB by $\langle A\rangle B + \langle B\rangle A - \langle A\rangle\langle B\rangle$, which can be written as

$$(A - \langle A\rangle)(B - \langle B\rangle) = 0 \tag{3.2}$$

showing that correlations between A and B are neglected. This approximation, which is equivalent to the molecular field approximation, is suitable for calculating the dispersion relations of the elementary excitations but it does not enable one to study their lifetime, which is predicted to be infinite. We assume that ordering takes place in the $\underline{k} = 0$ modes so that the only non vanishing averages are

$$\langle \sigma^x(0)\rangle = N^{1/2}\langle \sigma^x\rangle, \qquad \langle \sigma^z(0)\rangle = N^{1/2}\langle \sigma^z\rangle$$

where $\langle \sigma^x\rangle$ and $\langle \sigma^z\rangle$ are given by the molecular field expressions (2.7) and (2.9). The normal mode frequencies ω are therefore given in this approximation by

$$\frac{1}{4}\hbar^2\omega\left[\omega^2 - \omega_E^2(\underline{k})\right] = \Delta\langle\sigma^x\rangle\omega^3\sum_j \frac{K_j(\underline{k})}{\omega^2 - \omega_j^2(\underline{k})} \tag{3.3}$$

where

$$\frac{1}{4}\hbar^2\omega_E^2(\underline{k}) = \left[J'\langle\sigma^z\rangle\right]^2 + \Delta\left[\Delta - J(\underline{k})\langle\sigma^x\rangle\right] \tag{3.4}$$

The solution $\omega = 0$ corresponds to oscillations of the spin parallel to the total molecular field $\underline{W}$ where

$$\underline{W} = J'\hat{\underline{z}} + \Delta\hat{\underline{x}} \tag{3.5}$$

For $TmVO_4$, $\Delta = 0$, the phonons have their unperturbed frequency $\omega_j(\underline{k})$ and the electronic excitation has energy $2J'\langle\sigma^z\rangle$ with no dispersion.

In the rest of this section we consider $DyVO_4$ concentrating on solutions of (3.3) for small $\underline{k}$ and ω. Since the optic phonon frequencies are much greater $\omega_E(\underline{k})$ or the acoustic phonon frequencies $\omega_a(\underline{k})$ we can neglect the optic mode terms on the right hand side of (3.3). Assuming further that only one acoustic branch couples to the electronic states (which is true in the symmetry directions for which the coupling is greatest) (3.3) becomes

$$\frac{1}{4}\hbar^2[\omega^2 - \omega_E^2(\underline{k})] = \Delta\langle\sigma^x\rangle \frac{\omega^2 K_a(\underline{k})}{\omega^2 - \omega_a^2(\underline{k})} \qquad (3.6)$$

Above T_D this agrees with the result of Elliott and Parkinson [23]. For small $\underline{k}$ (3.6) has the electron like solution

$$\frac{1}{4}\hbar^2\omega_e^2(\underline{k}) = [J'\langle\sigma^z\rangle]^2 + \Delta[\Delta - \{J(\underline{k}) - K_a(\underline{k})\}\langle\sigma^x\rangle] \qquad (3.7)$$

and the phonon like solution

$$\omega_p^2(\underline{k}) = \omega_a^2(\underline{k}) \frac{\omega_E^2(\underline{k})}{\omega_e^2(\underline{k})} \qquad (3.8)$$

At large $\underline{k}$ when $\omega_a(k) \gg \omega_E(\underline{k})$ the coupled mode frequencies tend to their unperturbed values $\omega_E(\underline{k})$ and $\omega_a(\underline{k})$. The coupling is greatest for acoustic modes which have the polarization and wavevector corresponding to the observed distortion. In $DyVO_4$ these are modes propagating parallel to the x' and y' axes transversly polarised in the basal plane, for which $K_a(\underline{k}) = \mu$ (appendix B), so that

$$\left.\begin{aligned} \lim_{k\to 0} \frac{\omega_p^2(k)}{\omega_a^2(k)} &= \frac{[J'\langle\sigma^z\rangle]^2 + \Delta[\Delta - J'\langle\sigma^x\rangle]}{[J'\langle\sigma^z\rangle]^2 + \Delta[\Delta - J(0)\langle\sigma^x\rangle]} \\ &= \frac{c_I}{c_0} = \frac{c_s}{c_0} \end{aligned}\right\} \qquad (3.9)$$

and the elastic constant determining the frequency of these modes is $c_I = c_S$ given by (2.16) and (2.18a). We shall discuss this point further in §3.1b.

The coupled mode frequencies for $T > T_D$ are plotted in figure 3. As T approaches T_D from above ω_E decreases because of the interaction between electronic states on different sites due to both acoustic and optic phonon coupling. In the region of the crossover of the dispersion curves the electronic and acoustic phonon branches repel so a decrease in ω_E in turn flattens the acoustic branch. When $T = T_D$ the acoustic phonon curve is horizontal and the transition takes place but the $\underline{k} = 0$ electronic mode given by

$$\frac{1}{4}\hbar^2\omega_e^2(0) = [J'\langle\sigma^z\rangle]^2 + \Delta[\Delta - J(0)\langle\sigma^x\rangle]$$

remains finite. The soft mode is therefore an acoustic phonon as expected from general arguements discussed in the introduction. Below T_D the distortion stabilises the modes, ω_e increases and the gradient of the acoustic phonon branch becomes finite again.

3.1b $TbVO_4$

The frequencies of the elementary excitations of $TbVO_4$ are calculated in the same manner as those of $DyVO_4$. The decoupled equations of motion of the operators $(1\pm\tau)\underline{\sigma}$ are

$$\left.\begin{aligned}
\hbar\frac{d}{dt}\left[(1\pm\tau^z)\sigma^x\right](\underline{k}) &= 2J'\langle\sigma^z\rangle\left[(1\pm\tau^z)\sigma^y\right](\underline{k}) \\
\hbar\frac{d}{dt}\left[(1+\tau^z)\sigma^y\right](\underline{k}) &= -2J'\langle\sigma^z\rangle\left[(1+\tau^z)\sigma^x\right](\underline{k}) - 4J(\underline{k})\langle\sigma^x\rangle\sigma^z(\underline{k}) \\
&\quad +2\Delta\left[(1+\tau^z)\sigma^z\right](\underline{k}) + 4\langle\sigma^x\rangle\sum_j \xi_j(\underline{k})\left[\gamma_j(-\underline{k}) + \gamma_j^+(\underline{k})\right] \\
\hbar\frac{d}{dt}\left[(1-\tau^z)\sigma^y\right](\underline{k}) &= -2J'\langle\sigma^z\rangle\left[(1-\tau^z)\sigma^x\right](\underline{k}) \\
\hbar\frac{d}{dt}\left[(1+\tau^z)\sigma^z\right](\underline{k}) &= -2\Delta\left[(1+\tau^z)\sigma^y\right](\underline{k}) \\
\hbar\frac{d}{dt}\left[(1-\tau^z)\sigma^z\right](\underline{k}) &= 0 \\
\hbar\frac{d}{dt}\gamma_j^+(\underline{k}) &= -i\hbar\omega_j(\underline{k}) - \frac{\Delta\xi_j(\underline{k})}{\hbar\omega_j(\underline{k})}\left[(1+\tau^z)\sigma^y\right](\underline{k})
\end{aligned}\right\} \quad (3.1$$

where $\langle\sigma^x\rangle$ and $\langle\sigma^z\rangle$ are given by their molecular field values (2.7) and (2.9). The operators involving $(1-\tau^z)$ give the dispersionless solutions

$$\hbar\omega_2(\underline{k}) = \pm 2J'\langle\sigma^z\rangle \quad (3.11$$

which is the same as the moleculor field energy $2H_e$ for the separation of the electronic levels forming the degenerate E doublet above T_D. There is also a zero frequency mode for all T due to the motion of $(1-\tau^z)\sigma^z$.

The remaining equations of motion are satisfied when

$$\frac{1}{4}\hbar^2\omega[\omega^2-\omega_E^2(\underline{k})] = \Delta\langle\sigma^x\rangle\omega^3\sum_j \frac{K_j(\underline{k})}{\omega^2-\omega_j^2(\underline{k})} \tag{3.12}$$

where

$$\frac{1}{4}\hbar^2\omega_E^2(\underline{k}) = [J'\langle\sigma^z\rangle]^2 + \Delta[\Delta - J(\underline{k})\langle\sigma^x\rangle] \tag{3.13}$$

As in $DyVO_4$ there is a zero frequency mode corresponding to oscillations along $\underline{W}$, which we ignore for the moment. Again we neglect the optic mode contribution to the right hand side of (3.12) and obtain for low ω and $\underline{k}$, the solution

$$\frac{1}{4}\hbar^2\omega_1^2(\underline{k}) = [J'\langle\sigma^z\rangle]^2 + \Delta[\Delta - \{J(\underline{k}) - K_a(\underline{k})\}\langle\sigma^x\rangle] \tag{3.14}$$

which is the electronic mode corresponding to the singlet-singlet excitation 2W in the molecular field theory (2.4) and the phonon like solution

$$\omega_p^2(\underline{k}) = \omega_a^2(\underline{k})\frac{\omega_E^2(\underline{k})}{\omega_1^2(\underline{k})} \tag{3.15}$$

The acoustic modes corresponding to the observed distortion propogate parallel to the x and y axes and are transversly polarized in the basal plane (appendix B). Again

$K_a(\underline{k}) = \mu$ for these modes so

$$\lim_{k\to 0} \frac{\omega_p^2(\underline{k})}{\omega_a^2(\underline{k})} = \frac{[J'\langle\sigma^z\rangle]^2 + \Delta[\Delta - J'\langle\sigma^x\rangle]}{[J'\langle\sigma^z\rangle]^2 + \Delta[\Delta - \mathcal{J}(0)\langle\sigma^x\rangle]} = \frac{c_I}{c_0} \qquad (3.16)$$

and the elastic constant determining their frequency is c_I. For $TbVO_4$ unlike $DyVO_4$ c_I does not equal c_S and in particular does not fall to zero at the transition temperature so the acoustic phonon branch does not have zero gradient. We shall see in §3.2 that this important difference between $TbVO_4$ and $DyVO_4$ is due to the zero frequency mode of $TbVO_4$ corresponding to the operator $(1-\tau^z)\sigma^z$ which has no equivalent in $DyVO_4$.

We now discuss why the equations of motion technique gives results corresponding to the 'isolated' thermodynamic regime. Because of collisions the single particle states have a lifetime $\Gamma_i(\underline{k})$ say, where the suffix i refers to a particular branch. If a disturbance of frequency ω propogates through the crystal, local thermal equilibrium is maintained if even the longest lived states have ample time to decay during one cycle of the disturbance

i.e. if $\omega \ll \Gamma_i(\underline{k})$ (3.17)

for all i and $\underline{k}$. A mode of frequency ω which satisfies this condition is said to be a 'thermodynamic' or 'collision dominated' mode. At the opposite extreme

$$\omega \gg \Gamma_i(\underline{k}) \qquad (3.18)$$

for all i and $\underline{k}$ the frequency is too high for collisions to have an effect and the populations of the states remain constant. If the frequency of a mode satisfies (3.18) it is said to be a 'collision free' mode.

For acoustic phonons the 'thermodynamic' regime corresponds to ordinary sound, sometimes called first sound,

zero sound. This distinction is made, for example by Kadanoff and Baym [33] for a weakly interacting fermi system and by Cowley [34] for an anharmonic crystal.

In our calculation of the elementary excitations we use a simple decoupling scheme which gives zero width to the single particle states. Hence we have effectively ignored collisions and the results will only be valid for modes in the zero sound region where the populations of the levels remain constant. The equation of motion method, therefore, gives results which correspond to the 'isolated' thermodynamic regime.

For $TbVO_4$ (3.15) does not predict the expected soft acoustic phonon branch. Instead the theory indicates that it is fluctuations in the zero frequency mode $(1-\tau^z)\sigma^z$ which diverge at T_D and cause the transition by splitting the degenerate E doublet. We know, however, that these results are only valid at frequencies large compared with the width of the modes. In the next section we shall show that for frequencies small compared with the width of $(1-\tau^z)\sigma^z$ the acoustic phonon branch does indeed flatten at T_D and become the soft mode.

The same considerations apply to $TmVO_4$ except that it is fluctuations in the zero frequency mode corresponding to σ^z which apparently cause the transition in our decoupling scheme.

3.2 Variation of the elastic constant with frequency

We can cast the expressions for the coupled mode frequencies for $DyVO_4$ and $TbVO_4$, (3.6) and (3.12) into a form similar to (2.17) by rearranging them as

$$\frac{\omega^2}{\omega_a^2(\underline{k})} = \frac{1}{1+\mu G(\underline{k},\omega)} = \frac{c(\underline{k},\omega)}{c_o} \tag{3.19}$$

where

$$G(\underline{k},\omega) = \frac{4\Delta\langle\sigma^x\rangle}{\omega_E^2(\underline{k}) - \omega^2} \tag{3.20}$$

It is easy to show, using a Green function technique, that $G(\underline{k},\omega)$ is just the spin susceptibility for Hamiltonian (1.34) neglecting the term involving displaced phonon coordinates $\gamma_j(\underline{k})$ (see (7.16)).

The contribution to the elastic anamaly from the coupling of the spin wave at $\omega_E(\underline{k})$ is seen to depend upon the frequency of measurement ω. If $\omega \gg \omega_E(\underline{k})$ one measures c_o and if $\omega \ll \omega_E(\underline{k})$ a measurement determines c_I. However at low ω there are further contributions to $G(\underline{k},\omega)$ because the equations of motion of the spin operators in the decoupling scheme of §3.1 give extra solutions at $\omega = 0$ which we now consider.

In general we expect some of these modes to correspond to energy fluctuations in the spin system. They will have a width determined by the rate at which such energy is dissipated into the lattice, i.e. by the spin-lattice relaxation time τ_{SL}. For example, in the analagous case of paramagnetic resonance such a mode arises from oscillations of the spin along

the field direction and has width τ_{SL}. The resonant mode in this case corresponds to oscillations of the spin component perpendicular to the field. This has a width determined by the spin-spin relaxation time τ_{SS}. In general for a 'spin'-phonon system there can be several modes. The energy oscillation mode must have the same symmetry as the hamiltonian, i.e. A_{1g}, but not all modes of this type will have width τ_{SL}^{-1}, since it may be possible to construct from operators of A_{1g} symmetry a zero frequency mode which does not cause fluctuations in the energy of the spin system. These, and modes of other symmetries, will have widths related to the time for the spins to come to local thermal equilibrium τ_{SS}.

If $\omega \gg \tau_{SS}^{-1}$ the populations of the spin levels must remain constant so G_I will be determined under these circumstances provided the measuring frequency is much less than that of the finite frequency modes.

If $\omega \gg \tau_{SL}^{-1}$ there is no energy transfer between the spins and the thermal phonons. Provided there is full response from all the other modes, a measurement of the susceptibility will be under conditions in which the entropy of the spin system remains constant so G_S is determined. If $\omega \ll \tau_{SL}^{-1}$ the spin system and the phonons have the same local temperature, the entropy of the total spin-phonon system remains constant and a different adiabatic susceptibility G_S, will be measured.

It is straightforward to show from thermodynamics that

$$G_T - G_{S'} = \frac{1}{kT}\left(\frac{\partial\langle\sigma^2\rangle}{\partial S}\right)^2 \langle \delta S^2 \rangle \qquad (3.21)$$

where $\langle \delta S^2 \rangle$ is the thermal average of the entropy fluctuations. Thus the difference between G_T and G_S, is due to fluctuations in σ^z caused by fluctuations in the entropy S, which is just a manifestation of the fluctuation dissipation theorem. The width of the mode involving these entropy fluctuations is determined from the heat diffusion equation to be $\Lambda k^2/\rho C_s$ where Λ is the thermal conductivity of the crystal and ρ is its density. If the measuring frequency is much less than this width a constant temperature is maintained over the whole crystal and G_T will be measured. Because of its k^2 dependence, the width for small k is always less than the measuring frequency which is linear in k so G_T can only be measured in a static compressibility experiment with the sample in thermal contact with a heat bath.

The conclusions reached above are consistent with those of Kwok & Schultz [35] who showed quite generally that the difference between the 'isothermal' and 'isolated' susceptibilitie is due to zero frequency modes. We now apply these general considerations to $DyVO_4$, $TbVO_4$ and $TmVO_4$.

Pytte [100] has also pointed out that the elastic constants are frequency dependent but his discussion is much less complete than ours

(i) For $T > T_D$

The phonon branch under consideration (of B_{1g} symmetry for D and B_{2g} symmetry for Tb and Tm) does not couple to the A_{1g} zero frequency modes so $G_T = G_{S'} = G_S$ and hence $c_T = c_{S'} = c_S$. In Dy there is only one zero frequency spin mode, which corresponds to the oscillations of the moment along the direction

of the total molecular field, and it is of A_{1g} symmetry so all the elastic constants for $\omega \ll \omega_E$ are equal. However for Tb and Tm there is a B_{2g} zero frequency spin mode (corresponding to the motion of the operator $(1-\tau^z)\sigma^z$ for Tb and σ^z for Tm), which gives a difference between c_I and c_S.

(ii) For $T < T_D$

The phonon branches of interest become A_{1g} in the reduced symmetry so there can be coupling to the spin-lattice zero frequency modes. For Dy and Tm there is just one A_{1g} mode whose width correspond to a spin lattice relaxation time so $c_I = c_S \neq c_{S'}$. The characterization of the various A_{1g} modes is not well defined below T_D for Tb, but we suppose it is still possible to define distinct spin-lattice and spin-spin relaxation times. i.e. $c_I \neq c_S \neq c_{S'}$. In all cases there can be coupling to the heat diffusion mode so c_T has a separate value.

The results for the c_γ given in chapter 2 are consistent with the above conclusions as of course they must be.

Assuming a Lorentzian form for the response of the zero frequency modes we expect that, for small $\underline{k}$, $G(\underline{k},\omega)$ is given by

$$G(\underline{k},\omega) = G_I \frac{\omega_E^2(\underline{k})}{\omega_E^2(\underline{k}) - \omega^2} + \frac{G_S - G_I}{1 - i\omega\tau_{ss}} + (G_T - G_S)F(\omega) \qquad (3.23)$$

where

$$F(\omega) = \left(\frac{C_L}{C_S + C_L}\right)\frac{1}{1 - i\omega\tau_{SL}} + \frac{C_S}{C_S + C_L}\delta(\omega) \qquad (3.24)$$

The last term in (3.23) vanishes for $T > T_D$ where $G_S = G_T$. Below T_D the first term in $F(\omega)$ distinguishes between G_S and G_S, and the second term permits a measurement of G_T at $\omega = 0$. We speculate that the frequency dependence of $\mathbf{c}(\underline{k},\omega)$ can be satisfactorily described by (3.19) with $G(\underline{k},\omega)$ given by (3.23).

For $T > T_D$, the expression for the elastic constant becomes

$$c(\underline{k},\omega) = c_I + \frac{c_S - c_I}{1 - i\omega\tau_{ss}(c_S/c_I)} \qquad (3.25)$$

Hence for sufficiently low frequencies the gradient of the acoustic phonon branch becomes zero at T_D and the soft mode is a long wavelength acoustic phonon as expected. For Dy, $c_I = c_S$ so we do not expect measurements above the transition to be frequency dependent. Since c_S tends to zero as $T \to T_D$ it is clear that we must investigate the behaviour of τ_{SS} in the region just above T_D for $TbVO_4$ and $TmVO_4$.

The difference $G_S - G_I$ and hence $c_S - c_I$ arises from fluctuations in an operator $(1-\tau^z)\sigma^z$ for Tb and σ^z for Tm) which is related to the order parameter. The lifetime of these fluctuations is expected to show critical showing down as $T \to T_D$. According to the theory of irreversible thermodynamics [36], [1]

$$\tau_{ss}^{-1} = \gamma\beta \qquad (3.26)$$

where γ is a kinetic coefficient and β is the second derivative of the entropy with respect to $(1-\tau^z)\sigma^z$ for Tb

or σ^z for Tm. This is related to the mean square fluctuations in this variable by

$$\langle [(1-\tau^z)\sigma^z]^2 \rangle = k/\beta \tag{3.27}$$

for Tb with a similar expression for Tm. In the classical region where $kT \gg \hbar\omega$, where ω gives a typical frequency of the fluctuations (3.27) is equal to kTG where G is the appropriate susceptibility. In this case it is $(G_S - G_I)$ which gives the strength of this mode's contribution to the general susceptibility (3.23).

Accordingly we expect that τ_{SS} has a behaviour which may be described above T_D by the expression

$$\tau_{ss} = 2kT(G_s - G_I)/\alpha \tag{3.28}$$

where α has the dimensions sec^{-1} and should be independent of T, so that τ_{SS} approaches the constant value α^{-1} at high T. For the ferroelectric KDP Garland and Novotny [37] and Litov and Garland [38] have measured the relaxation time of the polarization fluctuations (which correspond to τ_{SS} in the spin model) and find that it varies like $(T-T_D)^{-1}$ near T_D, consistent with (3.28).

The main result of this chapter is expression (3.19) for $c(\underline{k},\omega)$ with $G(\underline{k},\omega)$ given by (3.23). For $T > T_D$ we can simplify these equations to (3.25) and use (3.28) for τ_{SS}.

CHAPTER 4

COMPARISON OF THEORY WITH EXPERIMENT

Up to the time of writing there have been no measurements on the elastic anomaly of $TmVO_4$* although such measurements would undoubtedly be interesting, especially to envestigate the effect of a magnetic field parallel to the z axis. We expect that in zero field there should be a strong frequency dependence in the measurements but for a large field the results above T_D should be independent of frequency. Ultrasonic and Brillouin data have been obtained for $DyVO_4$ and $TbVO_4$ [3] which we compare with the theory in §§4.1a and 4.2. In 4.1b we give a brief discussion of the behaviour of elastic constants c_{44} and c_{55} for $DyVO_4$, which have also been measured [15].

4.1 $DyVO_4$

4.1a The anomaly in $(c_{11}-c_{12})/2$. [3]

The Brillouin scattering results of J. R. Sandercock are shown in figure 4. They have the same qualitative features as the ultrasonic data of Melcher and Scott [39] and in both cases the elastic constant $(c_{11}-c_{12})/2$ falls to zero at the transition. This is expected from the discussion of §3.2 because the measuring frequencies for the ultrasonic data (~10MHz) and for the Brillouin data (~10GHz) are both much less than that of the finite frequency electronic mode ω_E. There is some disagreement

*But see additional note on page 50.

in the measured values of the transition temperature; Sandercock finds $T_D = 13^oK$ while Melcher and Scott give 14.8^oK and Cooke et al [5] give 14^oK. These discrepancies appear to be outside the experimental error and are perhaps due to imperfections in the crystals which vary from sample to sample.

Using the values $J' = 13.75\ cm^{-1}$ obtained from Raman scattering [10] and $\Delta = 4.5\ cm^{-1}$ from optical absorption [14] the molecular field expression (2.14b) predicts a transition temperature of 20^oK so evidently short range correlations, which cause deviations from molecular field theory, are important in $DyVO_4$. Indeed Melcher and Scott find it is not possible to fit their ultrasonic data with molecular field theory over the whole temperature range $T > T_D$. Gehring et al. [14] also found that their stress measurements showed large deviations from molecular field theory and estimated that only a small number of nearest neighbours, $z \sim 4$, contributed to J'.

The interaction between electronic states on different sites is made up of contributions from the optic modes $J_o(\ell, \ell')$ and acoustic modes $J_a(\ell, \ell')$. One expects $J_o(\ell, \ell')$ to be of short range because $J_o(\underline{k})$, the Fourier transform of $J_o(\ell, \ell')$ varies smoothly over the whole Brillouin zone. There is, however, an infinite range interaction arising from the discontinuous behaviour of $J_a(\underline{k})$ at $k = 0$, discussed in §1.4. The strain contribution acting at $k = 0$ is μ so the size of this discontinuity is

$$\mu - \lim_{k \to 0} K_a(\underline{k}) \qquad (4.1)$$

which is zero for $\underline{k}$ in the direction of maximum coupling (see appendix B). The infinite range coupling parameter J_∞ is equal to the average of (4.1) over all directions of $\underline{k}$, i.e. $J_\infty = \mu - \nu$ where

$$\nu = \langle \lim_{k \to 0} K_a(\underline{k}) \rangle \qquad (4.2)$$

Molecular field theory breaks down when short range interactions are important, which is presumably the case for $DyVO_4$.

To take account of short range interactions in $DyVO_4$ a cluster theory has been developed which extends the constant coupling approximation of Kasteleijn and Van Kranendonk [40] the interaction being split into short and long range components. The short range part is assumed to be an interaction $j\,\sigma^z(\ell)\sigma^z(\ell')$ between a Dy ion and its four nearest neighbours while the long range part, which is treated as a molecular field, is taken to be the infinite range interaction $J_\infty = \mu - \nu$ (4.2). We require

$$J' = 4j + \mu - \nu \qquad (4.3)$$

so μ and ν can be regarded as parameters to be varied to get the best agreement with the data. Details of the calculation are given in appendix C. Using $J' = 13.75\ cm^{-1}$ and $\Delta = 4.5 cm^{-1}$ the solid curve in figure 4 is obtained with $\mu = 9.7 cm^{-1}$, $\nu = 9.95 cm^{-1}$ and $c_o = 10.78 \times 10^{11}$ dyn cm^{-2} and agrees satisfactorily with the experimental data above T_D. It follows from (4.3) that $4j = 14 cm^{-1}$ showing that the interaction is dominated by the short range coupling and the term in ν roughly cancels the strain coupling μ.

Small charges in the measured value of T_D cause large variations in the value taken for ν but do not greatly change the shape of the curve.

Gehring et al [14] obtain $\mu \sim 10cm^{-1}$ from stress measurements on the optical spectrum of $DyVO_4$ which agrees with our result within to the experimental errors. In the temperature range $60 < T < 150^oK$, where there is no significant difference between the molecular field theory and the cluster theory, Melcher and Scott obtain $\mu = 12.97cm^{-1}$ (and $J' = 12.85cm^{-1}$) from molecular field theory. However it is apparent from figure 1 of Melcher and Scott's paper that c_o decreases with increasing temperature due to lattice anharmonicity. It is better, therefore, to estimate μ from the data near T_D using a cluster theory, as is done here, because c_S changes much more rapidly in this region than c_o.

Below T_D the cluster theory is unsatisfactory (see appendix C). However at $T = 0$ the deviations from the fully ordered state should be small (appendix C) so the simple molecular field result (2.16), (2.20) should be a good approximation; it gives $c = 9.95 \times 10^{11}$ $dyncm^{-2}$ which is substantially less than the measured value of $11.4 \times 10^{11} dyn.cm^{-2}$. Melcher and Scott noted a similar discrepancy in their ultrasonic data. Presumably there is an additional mechanism which causes c_o to vary with temperature at low temperatures but without a model of this effect we have not attempted to fit the data below T_D.

4.1b Changes in other elastic constants

We do not expect the other elastic constants to vary strongly with temperature because the coupling coefficients to modes of other symmetries are considerably less (see §1.2). However Goredetsky et al [15] have investigated, by ultrasonic techniques, the frequencies of acoustic modes propogating parallel to the z axis. Above T_D they find that the frequencies of vibrations polarized parallel to the x axis and to the y axis are equal but that this degeneracy is removed below the transition. The corresponding elastic constants are c_{44} and c_{55} respectively so these results are consistent with the general symmetry requirements (A.12) and (A.13).

To explain this data it is necessary to go beyond coupling terms linear in the strains (1.21). Among the many possible quadratic terms it can be shown that symmetry requirements allow

$$\frac{1}{2} c_0 \left(\frac{V}{N}\right) \epsilon \left(e_{xz}^2 - e_{yz}^2\right) \sum_l \sigma^z(l)$$

where ϵ is a dimensionless coupling coefficient. In molecular field theory this leads to expressions for c_{44} and c_{55} of the form

$$\frac{c_{44}}{c_0} = 1 + \epsilon \langle \sigma^z \rangle, \qquad \frac{c_{55}}{c_0} = 1 - \epsilon \langle \sigma^z \rangle$$

where c_0 is the value of c_{44} $(= c_{55})$ above the transition. Experimentally $c_{44} - c_{55}$ varies like $\langle \sigma^z \rangle$ as expected but the increase in elastic constant for one mode does not equal the decrease for the other. This is interpreted in

[15] as an effect of domain formation. Equating $c_{44} - c_{55}$ to $2\epsilon \langle\sigma^z\rangle$ we find that $\epsilon = 0.85$.

An alternative explanation for this splitting lies in the point mentioned in §1.3 that the phonon frequencies $\omega_j(\underline{k})$ (and the unperturbed elastic constants c_o) refer to the distorted lattice and vary with the strain through anharmonic phonon effects. This mechanism would also cause $c_{44} - c_{55}$ to vary like $\langle\sigma^z\rangle$. D'Ambrogio et al. [41] have proposed that the splitting of the optic E modes below T_D, which they observe by Raman scattering, is caused by this effect.

4.2 $TbVO_4$ [3]

The ultrasonic results of S. B. Palmer and the Brillouin scattering data of J. R. Sandercock are plotted in figure 5. As with $DyVO_4$ there is disagreement over the value of the transition temperature; the measurements are 34.7 ± 0.5^oK (ultrasonics) and 33^oK (Brillouin) compared with previous values of 34^oK (Raman scattering [10]) and 35^oK (optical absorption [7]).

Since T_D is much closer to its molecular field value in $TbVO_4$ than in $DyVO_4$ it does not seem necessary to apply the cluster theory to the four level Tb^{3+} system. However since the results are taken up to room temperature we have modified the molecular field theory of chapter 2 to allow for population of the higher energy levels of Tb^{3+}. In [10] a doublet was reported at $90cm^{-1}$ and the

presence of this level has been allowed for crudely by multiplying the susceptibilities g_I, g_S and g_T by a factor

$$2[2+\exp(-129.5/T)]^{-1}$$

The ultrasonic measurements, which were made at a frequency of 14MHz, fall to zero at $T = T_D$ so c_S $(=c_T)$ is presumably being measured above the transition temperature. The solid curves of figure 5 show the values of c_I, c_S and c_T obtained from (2.16), (2.18a), (2.19a) and (2.20b) using $J' = 25.0\text{cm}^{-1}$, $\mu = 35.7\text{cm}^{-1}$, $\Delta = 9\text{cm}^{-1}$ [>] and $c_o = 1.49 \times 10^{11}$ dyn.cm^{-2}. The agreement between c_S and the ultrasonic data is excellent between T_D and room temperature. μ is seen to be large (of the same order of magnitude as T_D) so using (3.25) and (3.28) we find it possible to distinguish three frequency regimes in our measurements of the elastic anomaly of $TbVO_4$ for $T \geq T_D$:

(i) $\omega \gg \alpha$, c_I is measured at all temperatures.

(ii) $\omega \sim \alpha$, The measured elastic constant is intermediate between c_I and c_S and close to T_D the imaginary part becomes comparable with the real part.

(iii) $\omega \ll \alpha$, c_S is measured until the temperature is very close to T_D where the damping becomes large.

α is related to the spin-spin relaxation time by (3.28). The measuring frequency in the Brillouin scattering experiments is shown on the right hand side of figure 5. We see that the data lies between c_I and c_S in the high

temperature phase and does not fall to zero at T_D. This together with the observation that the linewidth increases near T_D [3], suggests that the phonon frequencies are comparable with α (i.e. regime (ii)) so the elastic constant is expected to be frequency dependent as described by (3.25). The real part of $c(\underline{k},\omega)$ is plotted as the dashed curve in figure 5 using the value $\alpha/2\Pi$ = 27.5 GHz in (3.28) and shows satisfactory agreement with the experimental data. The following expression for the frequency dependence of c_{66} at $T = T_D$ is obtained from (2.17), (3.25) and (3.28):

$$\mathrm{Re}\ c(\underline{k},\omega) = \frac{c_I}{1+(c_I \mu\alpha/c_0 k T_D \omega)^2} = \frac{c_I}{1+(8.38/\nu)^2} \qquad (4.4)$$

where ν is the frequency in GHz. This gives a rough fit to the experimental results as shown in figure 6.

Below T_D there is little difference between c_I and c_S and, allowing for the discrepancies in the transition temperature, the Brillouin data lies reasonably close to these curves. As with $DyVO_4$ the measurements at very low temperatures are higher than the theory predicts but the effect is smaller here. Because of the large damping it was not possible to obtain ultrasonic measurements between 18°K and T_D but the values in the range from 10°K to 18°K lie between c_S and c_T indicating that c_S, is being measured (see (2.24)). The electronic specific heats are likely to be comparable in this temperature range and the spin lattice relaxation rate τ_{SL}^{-1} is probably greater than the measuring frequency of 14MHz.

Molecular field theory works well for $TbVO_4$ (except at very low temperatures) but it was found necessary to use a cluster theory to explain satisfactorily the measurements on $DyVO_4$ so we wish to comment further on the differences between these systems.

At least part of the difference stems from the very large anisotropy in the elastic constants. For $DyVO_4$, $c_o = (c_{11} - c_{12})/2 = 10.78 \times 10^{11}$ dyn cm^{-2} whereas for $TbVO_4$ $c_o = c_{66} = 1.49 \times 10^{11}$ dyn cm^{-2}. Hence we expect from (2.12) that μ should be larger for $TbVO_4$ than for $DyVO_4$ (assuming that the coupling coefficients are roughly equal) in agreement with observation. Furthermore, in the region of small $\underline{k}$, $K_a(\underline{k})$ is much more strongly peaked about the direction of maximum coupling for $TbVO_4$ than for $DyVO_4$. This is possibly the explanation of why, for $DyVO_4$, the term in ν almost cancels the strain coupling μ in expression (4.2) for the infinite range coupling parameter J_∞, so the system is dominated by the relatively strong short range interaction. For $TbVO_4$, on the other hand, μ is much bigger than ν and $J_\infty = (\mu - \nu)$ is substantially larger than the short range coupling. In particular if the short range contribution is zero then $\mu = 35.7$ cm^{-1} and $\nu = \mu - J' = 10.7$ cm^{-1}.

As pointed out in [11] the large anisotropy in the elastic constants for rare earth vanadates with the tetrogonal zircon structure is responsible for $TmVO_4$ ordering in a B_{2g} rather than a B_{1g} mode even though the coupling coefficients appear to be roughly equal (see §1.2).

From the specific heat data of [6] it is evident that the interaction is of long range so presumably acoustic phonon coupling is dominant. $TmVO_4$ will therefore distort in the mode with smaller restoring forces, i.e. the B_{2g} mode. $DyVO_4$, on the other hand, orders in a B_{1g} mode because the anisotropy in the elastic constants is more than outweighed by the large B_{1g} coupling coefficient (§1.2).

Additional Note:

Melcher, Pytte and Scott [95] have recently measured the elastic constants of $TmVO_4$. They find that c_{66} vanishes at the transition as expected but there is, in addition, an appreciable softening of $\frac{1}{2}(c_{11}-c_{12})$ showing that coupling of B_{1g} symmetry, while smaller than B_{2g} coupling, is not completely negligable. This fits in with the above discussion where it was pointed out that $TmVO_4$ orders in the B_{2g} rather than the B_{1g} mode because the restoring forces are lower, the coupling coefficients being roughly equal.

As a further point Pytte and Feder [96] have recently proved that the equation

$$\frac{c_\gamma}{c_0} = \frac{1}{1+\mu G_\gamma}$$

(see (2.17)), shown in Chapter 2 to be valid in molecular field theory, is in fact exact for $TmVO_4$ where $\Delta=0$.

CHAPTER 5

THE ELASTIC PROPERTIES OF DySb. [46]

5.1 Introduction.

There has recently been a good deal of interest in the properties of DySb, [42], [43] and [44], which undergoes a single first order phase change at 9.5°K where the crystal symmetry is lowered from cubic to tetragonal and the moments of the Dy^{3+} ions order antiferromagnetically. Bucher et al. [42] have estimated the crystal field splittings of the electronic levels of the Dy ions and find that the ground level is an $E'(\Gamma_6)$ doublet with a $U(\Gamma_8)$ quadruplet only 14.5°K above it, the remaining levels being at a much higher energy. This near degeneracy between the lowest levels suggests that the transition might be driven by Jahn-Teller coupling as in $DyVO_4$. (see Chapter 1).

The shear elastic constant $\frac{1}{2}(c_{11}-c_{12})$ has been measured by ultrasonics, [43] and B.Lüthi (private communication). It is found to soften considerably below 100°K and, at the transition temperature T_D, has reduced to about 0.42 of its high temperature value. Despite the transition being of first order there is no marked discontinuity in $\frac{1}{2}(c_{11}-c_{12})$ at T_D and, in the ordered phase, the elastic constant is almost independent of temperature. This behaviour is in contrast to that in Jahn-Teller driven transitions in the rare earth vanadates where the crystals harden considerably below the transition (see Chapter 4).

Levy and coworkers, [43] and [44], have developed a

theory which provides a good description of the ultrasonic measurements above T_D. However their model is very complicated, since it includes all 16 electronic levels of the Dy ions in the lowest (J=15/2) multiplet, and has not been extended to the low temperature phase. They conjecture that the almost temperature independent behaviour of $\frac{1}{2}(c_{11}-c_{12})$ below T_D is an effect of domain formation.

The theory for the rare earth vanadates discussed in chapters 1-4 of this thesis is relatively simple because we consider only the lowest electronic energy levels, which are well separated from the states of next highest energy. Since Bucher et al. [42] predict that in DySb there are similarly a small number of low lying states well apart from the rest of the levels it seemed interesting to apply the same methods here and in particular to calculate the elastic constants below the transition. The theory which is developed in this chapter yields a simple analytic expression for the elastic constants above T_D which, like Levy's more complicated model, agrees satisfactorily with the experimental results. However the calculations in the low temperature phase do not give a good description of the data even by taking a domain average of the results. We conclude that there must be an additional mechanism, not considered in our treatment or that of [43] and [44], which affects the elastic constants below the transition.

5.2 The model Hamiltonian.

Following the approach of Chapter 1 we use the known

properties of the low lying states of the Dy^{3+} $^6H_{15/2}$ multiplet to estimate the relative sizes of the coupling between these states and lattice distortions of different symmetries. DySb crystallizes in the rocksalt structure so the Dy ions lie at points with O^h symmetry. The fourth and sixth rank terms of the corresponding crystal field Hamiltonian have been estimated in [42] by interpolation between the spectroscopically measured values in PrSb and TmSb. They find $A^o_4\langle r^4\rangle = 86\pm6\,^oK$ and $A^o_6\langle r^6\rangle = 4.2\pm1.2\,^oK$ for which the ground state is an $E'(\Gamma_6)$ doublet with a $U(\Gamma_8)$ quadruplet at $14.5\,^oK$, the next highest level being an $E''(\Gamma_7)$ doublet at $80\,^oK$. We shall consider only the E' and U levels in our treatment of the transition at $9.5\,^oK$. The crystal field corresponds closely to the value $x = -1$, where x is defined by Lea Leask and Wolf [45], who have tabulated explicitly the states in this limit. From their data we estimate that 99% of $|J_z = \pm J\rangle$ and by symmetry equal amount of $|J_x = \pm J\rangle$ and $|J_y = \pm J\rangle$ are contained in the E' and U levels. Hence it seems that $|J_z = \pm J\rangle$, $|J_y = \pm J\rangle$ and $|J_x = \pm J\rangle$ (which we shall abbreviate to $|\pm J_z\rangle$, $|\pm J_y\rangle$ and $|\pm J_x\rangle$ respectively) form a good set of basis states, and this conjecture is strengthened by the measurements of [42] who find that the Dy ions order with almost the maximum moment.

By considering the operations of the double group O^h we can show that in the undistorted phase these six states do belong to the representations E' and U as required and written explicitly are

$$
\begin{aligned}
|E'\alpha'\rangle &= \frac{1}{\sqrt{12}}\left[2\sqrt{2}\,|-J_z\rangle + |J_x\rangle - |-J_x\rangle + i\,|J_y\rangle - i\,|-J_y\rangle\right] \\
|E'\beta'\rangle &= \frac{-1}{\sqrt{12}}\left[2\sqrt{2}\,|J_z\rangle + |J_x\rangle + |-J_x\rangle + |J_y\rangle + |-J_y\rangle\right] \\
|U'\kappa\rangle &= \frac{1}{2}\left[|J_x\rangle + |-J_x\rangle - |J_y\rangle - |-J_y\rangle\right] \\
|U'\lambda\rangle &= \frac{1}{\sqrt{6}}\left[\sqrt{2}\,|-J_z\rangle - |J_x\rangle + |-J_x\rangle - i\,|J_y\rangle + i\,|-J_y\rangle\right] \\
|U'\mu\rangle &= -\frac{1}{\sqrt{6}}\left[\sqrt{2}\,|J_z\rangle - |J_x\rangle - |-J_x\rangle - |J_y\rangle - |-J_y\rangle\right] \\
|U'\nu\rangle &= -\frac{1}{2}\left[|J_x\rangle - |-J_x\rangle - i\,|J_y\rangle + i\,|-J_y\rangle\right]
\end{aligned}
\qquad (5.1)
$$

These states are orthogonal but not quite normalised because the basis states are not orthogonal.

$$|\langle \pm J_x | \pm J_y\rangle| = |\langle \pm J_y | \pm J_z\rangle| = |\langle \pm J_z | \pm J_x\rangle| = 2^{-J}$$

The interaction between the lattice distortions around a single ion and the electronic levels (5.1) can be written in a form indentical to (1.4) i.e.

$$\mathcal{H}_s = \sum_{\Gamma\alpha} B_\Gamma Q_{\Gamma\alpha} O_{\Gamma\alpha} \qquad (5.2)$$

where the symbols are defined in §1.2.

By replacing the O_{Γ_α} by second rank tensors Elliott et al. [3] were able to show for $DyVO_4$ that coupling to B_2 modes was dominant. This is essentially because J is large so matrix elements of the form $\langle J^i | O_{\Gamma_\alpha} | J^j\rangle$, where i, j = x, y, or z, can only be large if i=j and $O_{\Gamma_\alpha} \sim J_i^2$. For example $\langle J^x | O_{\Gamma_\alpha} | J^y\rangle$ will be small for any O_{Γ_α} which is a second rank tensor because no second rank tensor will turn J^y into J^x for J= 15/2. However $\langle J^x | J_x^2 | J^x\rangle$ $(=J^2)$ is large.

Applying these results to DySb it follows that the largest coupling will be to operators which have only diagonal

matrix elements in the representation $|\pm J_x\rangle$, $|\pm J_z\rangle$, $|\pm J_z\rangle$. Even if we represent the O_{Γ_a} by fourth or sixth rank tensors it still seems probable that this result will hold because of the large value of J. In addition operators which couple to lattice displacements must be even under time reversal so it follows that there are only two independent traceless operators with the desired properties, namely

$$O_{\varepsilon_1} = J_z^2 - \tfrac{1}{3} J(J+1)$$

and

$$O_{\varepsilon_2} = \tfrac{1}{\sqrt{3}} (J_x^2 - J_y^2) \qquad (5.3)$$

Hence we expect coupling to lattice distortions of E symmetry to be strongest, in agreement with the observation that the low temperature phase is tetragonal. From now on we put equal to zero the coupling coefficients for all operators except (5.3).

Acting on states (5.1) with operators (5.3), $\mathcal{H}_S$ becomes

$$\mathcal{H}_S = \begin{array}{c} \begin{array}{cccccc} |E'\alpha'\rangle & |E'\beta'\rangle & |U'\kappa\rangle & |U'\lambda\rangle & |U'\mu\rangle & |U'\nu\rangle \end{array} \\ \begin{bmatrix} -2\Delta & 0 & 0 & \sqrt{2}\xi_E Q_{\varepsilon_1} & 0 & \sqrt{2}\xi_E Q_{\varepsilon_2} \\ 0 & -2\Delta & -\sqrt{2}\xi_E Q_{\varepsilon_2} & 0 & -\sqrt{2}\xi_E Q_{\varepsilon_1} & 0 \\ 0 & -\sqrt{2}\xi_E Q_{\varepsilon_2} & -\xi_E Q_{\varepsilon_1}+\Delta & 0 & -\xi_E Q_{\varepsilon_2} & 0 \\ \sqrt{2}\xi_E Q_{\varepsilon_1} & 0 & 0 & \xi_E Q_{\varepsilon_1}+\Delta & 0 & -\xi_E Q_{\varepsilon_2} \\ 0 & -\sqrt{2}\xi_E Q_{\varepsilon_2} & -\xi_E Q_{\varepsilon_2} & 0 & \xi_E Q_{\varepsilon_1}+\Delta & 0 \\ \sqrt{2}\xi_E Q_{\varepsilon_2} & 0 & 0 & -\xi_E Q_{\varepsilon_2} & 0 & -\xi_E Q_{\varepsilon_1}-\Delta \end{bmatrix} \end{array} \qquad (5.4)$$

where $\xi_E = \frac{1}{3} J(J-\frac{1}{2}) B_E$ and a term of A_1 symmetry has been added to represent the initial crystal field splitting 3Δ.

Since the antiferromagnetic order occurs at the same temperature as the structural phase transition we must take account of magnetic interactions between the Dy^{3+} ions and we assume that it is a simple Heisenberg exchange. A crystalline distortion will modify the value of the exchange interaction and we believe that this type of coupling is responsible for the distortion along a [111] axis observed by neutron diffraction in addition to the tetragonal strain [42]. The magnetic structure is such that all the moments in a plane perpendicular to this [111] axis are parallel to each other but antiparallel to those on neighbouring planes. Since this distortion is small (0.1%) compared with the tetragonal distortion (0.7%) we neglect the effects of the modulation of the exchange interaction by lattice strains in this treatment.

It is useful to define the following operators acting on the Dy^{3+} ion at the ℓth site:

$$\underline{m}(\ell) = \epsilon_\ell \, \underline{J}(\ell)/J$$

$$q_1(\ell) = O_{E_1}(\ell)/[(2J/3)(J-\tfrac{1}{2})] = 3[J_z^2 - \tfrac{1}{3}J(J+1)]/[2J(J-\tfrac{1}{2})]$$

$$q_2(\ell) = O_{E_2}(\ell)/[(2J/3)(J-\tfrac{1}{2})] = \sqrt{3}[J_x^2 - J_y^2]/[2J(J-\tfrac{1}{2})] \qquad (5.5)$$

where ϵ_ℓ is equal to +1 or -1 depending upon which sublattice the Dy ion on the ℓth site lies. These operators are normalised so that

$$-1 \leq \langle \underline{m}(\ell) \rangle \leq 1 \quad \text{and} \quad -1 \leq \langle q_1(\ell) \rangle \leq 1.$$

An electronic level scheme consisting of a doublet and a quadruplet can be represented by two pseudospins $\underline{\ell}=1$ and

$\underline{s}=\frac{1}{2}$. If the separation between the levels is 3Δ then the crystal field Hamiltonian $\mathcal{H}_c$ can be written

$$\mathcal{H}_c = \Delta \sum_{l} \underline{\ell}(l) . \underline{\sigma}(l) \tag{5.6}$$

where $\sigma=2\underline{s}$.

The new basis states $|\ell_z s_z\rangle$ can be written in terms of (5.1) as

$$\begin{aligned}
|1\,\tfrac{1}{2}\rangle &= |u'\kappa\rangle = \tfrac{1}{2}\left[|J_x\rangle + |-J_x\rangle - |J_y\rangle - |-J_y\rangle\right] \\
|1-\tfrac{1}{2}\rangle &= -\sqrt{\tfrac{2}{3}}\,|E'\alpha'\rangle + \sqrt{\tfrac{1}{3}}\,|u'\lambda\rangle = -\tfrac{1}{2}\left[|J_x\rangle - |-J_x\rangle + i\,|J_y\rangle - i\,|-J_y\rangle\right] \\
|0\,\tfrac{1}{2}\rangle &= \sqrt{\tfrac{1}{3}}\,|E'\alpha'\rangle + \sqrt{\tfrac{2}{3}}\,|u'\lambda\rangle = |-J_z\rangle \\
|0-\tfrac{1}{2}\rangle &= \sqrt{\tfrac{1}{3}}\,|E'\beta'\rangle + \sqrt{\tfrac{2}{3}}\,|u'\mu\rangle = -|J_z\rangle \\
|-1\,\tfrac{1}{2}\rangle &= \sqrt{\tfrac{2}{3}}\,|E'\beta'\rangle - \sqrt{\tfrac{1}{3}}\,|u'\mu\rangle = -\tfrac{1}{2}\left[|J_x\rangle + |-J_x\rangle + |J_y\rangle + |-J_y\rangle\right] \\
|-1-\tfrac{1}{2}\rangle &= -|u'\nu\rangle = \tfrac{1}{2}\left[|J_x\rangle - |-J_x\rangle - i\,|J_y\rangle + i\,|-J_y\rangle\right]
\end{aligned} \tag{5.7}$$

and the operators (5.5) become

$$\begin{aligned}
q_1 &= -(3/2)\left[\ell_z^2 - \tfrac{1}{3}\ell(\ell+1)\right], \\
q_2 &= -(\sqrt{3}/2)\left[\ell_x^2 - \ell_y^2\right] \\
\text{and} \quad m_\alpha &= (\ell_\alpha^2 - 1)\sigma_\alpha \\
\text{where } \alpha &= x, y \text{ or } z.
\end{aligned} \tag{5.8}$$

Since the lattice displacements around different ions are of course coupled it is useful to relate the displacements around a single site to the normal modes of the crystal i.e. phonons. Following the discussion in Chapter 1 we can write the electron lattice coupling as

$$\mathcal{H}_{JT} = \frac{-1}{\sqrt{N}} \sum_{l} \left[\xi_j^{(1)} q_1(l) + \xi_j^{(2)} q_2(l)\right]\left[a_j^{+}(\underline{k}) + a_j(-\underline{k})\right] e^{i\underline{k}\cdot\underline{R}(l)} \tag{5.9}$$

(c.f. (1.20)) where $a^{+}_{j}(\underline{k})$ and $a_j(\underline{k})$ are creation and

annihilation operators for a phonon of wavevector $\underline{k}$ and branch index j, and $\xi_j^{(1)}(\underline{k})$ and $\xi_j^{(2)}(\underline{k})$ are coupling coefficients. Including the usual phonon Hamiltonian, the elastic energy and coupling to static strains (c.f. (1.23), (1.22) and (1.21) respectively) we can write our model Hamiltonian for DySb as

$$\begin{aligned}\mathcal{H} = &\tfrac{1}{2} V c_0 (e_1^2 + e_2^2) + \sum_{j\underline{k}} \hbar\omega_j(\underline{k}) \left[a_j^+(\underline{k}) a_j(\underline{k}) + \tfrac{1}{2}\right] \\ &- \eta \sum_l \left(e_1 q_1(l) + e_2 q_2(l)\right) - \sum_{j\underline{k}} \left[\xi_j^{(1)} q_1(\underline{k}) + \xi_j^{(2)} q_2(\underline{k})\right]\left[a_j^+(\underline{k}) + a_j(-\underline{k})\right] \\ &- \tfrac{1}{2} \sum_{l\neq l'} I(l,l')\, \underline{m}(l).\underline{m}(l') + \mathcal{H}_c\end{aligned} \tag{5.10}$$

where $\mathcal{H}_c$ represents the crystal field splitting, η is the static strain coupling parameter, V is the volume of the crystal and $I(l, l')$ represents the magnetic interaction between Dy ions on sites l and l'. Also

$$e_1 = \tfrac{1}{\sqrt{3}}(2e_{zz} - e_{xx} - e_{yy}),$$

$$e_2 = e_{xx} - e_{yy}$$

and

$$c_0 = \tfrac{1}{2}(c_{11} - c_{12})$$

(see Appendix A).

As discussed in Chapter 1 it is useful to transform to displaced phonon operators $\gamma_j^+(\underline{k})$. The transformation appropriate to this problem is

$$\gamma_j^+(\underline{k}) = a_j^+(\underline{k}) + \frac{\xi_j^{(1)}(\underline{k})\, q_1(\underline{k})}{\hbar\omega_j(\underline{k})} + \frac{\xi^{(2)}(\underline{k})\, q_2(\underline{k})}{\hbar\omega_j(\underline{k})} \tag{5.11}$$

Since q_1 and q_2 commute the γ's obey correct phonon commutation relations. Levy [44] uses the same transformation but has a very general Hamiltonian involving non-commuting electronic operators. As he points out, this is unsatisfactory

unless only the coupling to a set of commuting operators is large. By using the known properties of the low lying states of the dysprosium ions we have been able to show that this is indeed the case for DySb. In the treatment of [43] and [44] the elastic constants are calculated using molecular field theory and we believe that within this approximation the criticism made above does not affect the final results.

In terms of the new operators (5.11) our model Hamiltonian can be written

$$\begin{aligned}\mathcal{H} = {} & \tfrac{1}{2}NC_0(e_1^2+e_2^2) + \sum_{j\underline{k}}\left[\gamma_j^+(\underline{k})\gamma_j(\underline{k})+\tfrac{1}{2}\right]\hbar\omega_j(\underline{k}) \\ & - 3\sum_{l}\left[e_1 q_1(l)+e_2 q_2(l)\right] - \tfrac{1}{2}\sum_{l\neq l'}\{K(ll')\left[q_1(l)q_1(l')+q_2(l)q_2(l')\right] \\ & + 2L(l,l')q_1(l)q_2(l')\} - \tfrac{1}{2}\sum_{l\neq l'} I(l,l')\underline{m}(l).\underline{m}(l') + \mathcal{H}_c .\end{aligned} \tag{5.12}$$

There are also terms in (5.12) involving $q_1^{\,2}(l)+q_2^{\,2}(l)$, which just give a constant, while the coefficient of $q_1(l)q_2(l)$ vanishes by symmetry. $K(l,l')$ are related to the $\xi_j(\underline{k})$ by

$$\left.\begin{aligned}K(l,l') &= 2\sum_{j\underline{k}}\frac{|\xi_j^{(1)}(\underline{k})|^2}{\hbar\omega_j(\underline{k})}\exp\left[i\underline{k}.(\underline{R}(l)-\underline{R}(l'))\right] \\ &= 2\sum_{j\underline{k}}\frac{|\xi_j^{(2)}(\underline{k})|^2}{\hbar\omega_j(\underline{k})}\exp\left[i\underline{k}.(\underline{R}(l)-\underline{R}(l'))\right]\end{aligned}\right\} l'\neq l$$

$$K(l,l) = 0 \tag{5.13}$$

$$L(l,l') = 2\sum_{j\underline{k}}\frac{|\xi_j^{(1)*}(\underline{k})\xi_j^{(2)}(\underline{k})|}{\hbar\omega_j(\underline{k})}\exp\left[i\underline{k}.\left[\underline{R}(l)-\underline{R}(l')\right]\right] \tag{5.14}$$

The Fourier transforms of $K(l,l')$ and $L(l,l')$ are

$$K(\underline{k}) = 2\sum_{j}\frac{|\xi_j^{(1)}(\underline{k})|^2}{\hbar\omega_j(\underline{k})} - \frac{2}{N}\sum_{j\underline{k}'}\frac{|\xi_j^{(1)}(\underline{k}')|^2}{\hbar\omega_j(\underline{k}')} \tag{5.15}$$

$$L(\underline{k}) = 2\sum_{j}\frac{|\xi_j^{(1)*}(\underline{k})\xi_j^{(2)}(\underline{k})|}{\hbar\omega_j(\underline{k})} \tag{5.16}$$

where the second term in (5.15) comes from putting K(1,1)=0. Notice that L($\underline{k}$=0) vanishes by symmetry. Quadrupole-quadrupole coupling by other mechanisms than coupling through the phonons, such as direct electric forces or polarization of the conduction electrons, can be included in (5.12) and simply modifies the value of K(ℓ, ℓ').

5.3 Calculation of the elastic constants.

To investigate the types of ordering which can occur with this Hamiltonian we firstly neglect the magnetic interaction and use Landau theory [1], expanding the free energy as a power series in the q_1 and q_2. Writing $q_1=q\cos\theta$ and $q_2=q\sin\theta$ then

$$F = F_0 + a(T)q^2 + bq^3\cos 3\theta + cq^4 + \cdots \qquad (5.17)$$

The existence of a cubic term shows that the transition is of first order as observed. Minimising F with respect to θ it follows that $\theta=n\Pi/3$ where n is an integer so the quadrupoles order along one of the crystalline axes. The magnetic interaction cannot affect this result since we have taken it to be isotropic. We choose the quadrupolar ordering direction to be parallel to the z axis i.e. below T_D $\langle q_1\rangle\neq 0$, $\langle q_2\rangle=0$ and since this is the preferred direction in the crystal the magnetic ordering will also occur parallel to the z axis.

In the molecular field approximation (5.12) becomes

$$\mathcal{H}_{m.f.} = -H_1\sum_{\ell} q_1(\ell) - H_2\sum_{\ell} q_2(\ell) - \underline{H}_m\sum_{\ell}\underline{m}(\ell)$$
$$+\tfrac{1}{2}Vc_0(e_1^2+e_2^2) + \sum_{j\underline{k}}\hbar\omega_j(\underline{k})n_j(\underline{k}) \qquad (5.18a)$$

where $$H_1 = K(0)\langle q_1\rangle + \eta e_1,$$
$$H_2 = K(0)\langle q_2\rangle + \eta e_2$$
and $$H_\alpha = I\langle m_\alpha\rangle,$$

(5.18b)

are the molecular fields acting on the quadrupoles q_1 and q_2 and the magnetic moment $\underline{m}$ respectively,

$$K(0) = \sum_{l'} K(l,l') \quad , \quad I = \sum_{l'} I(l,l')$$

and $n_j(\underline{k})$ is the phonon occupation number (2.3). We have implicitly assumed that the ordering takes place in a $\underline{k}=0$ mode as observed. The Hamiltonian appropriate to a single electronic site can now be expressed in terms of the basis states (5.7) as

$$\mathcal{H}(l) = \begin{array}{c} \begin{matrix} |1\,\tfrac{1}{2}\rangle & |1\,{-\tfrac{1}{2}}\rangle & |0\,\tfrac{1}{2}\rangle & |0\,{-\tfrac{1}{2}}\rangle & |{-1}\,\tfrac{1}{2}\rangle & |{-1}\,{-\tfrac{1}{2}}\rangle \end{matrix} \\ \begin{bmatrix} \Delta+\frac{H_1}{2} & \frac{1}{2}(H_x-iH_y) & 0 & 0 & \frac{\sqrt{3}}{2}H_2 & -\frac{1}{2}(H_x+iH_y) \\ \frac{1}{2}(H_x+iH_y) & -\Delta+\frac{H_1}{2} & \sqrt{2}\Delta & 0 & -\frac{1}{2}(H_x-iH_y) & \frac{\sqrt{3}}{2}H_2 \\ 0 & \sqrt{2}\Delta & -H_1+H_2 & 0 & 0 & 0 \\ 0 & 0 & 0 & -H_1-H_2 & \sqrt{2}\Delta & 0 \\ \frac{\sqrt{3}}{2}H_2 & -\frac{1}{2}(H_x+iH_y) & 0 & \sqrt{2}\Delta & -\Delta+\frac{H_1}{2} & \frac{1}{2}(H_x-iH_y) \\ -\frac{1}{2}(H_x-iH_y) & \frac{\sqrt{3}}{2}H_2 & 0 & 0 & \frac{1}{2}(H_x+iH_y) & \Delta+\frac{H_1}{2} \end{bmatrix} \end{array} \qquad (5.19)$$

(5.19) is complicated to diagonalise as it stands but if we use the previous result that $\langle q_2\rangle=\langle m_x\rangle=\langle m_y\rangle=0$ the energy levels can easily be calculated. We find

$$\lambda'_1 = \tfrac{1}{2}\left[-\Delta + H_z - \tfrac{H_1}{2} + \left\{8\Delta^2 + \left(\Delta + H_z - 3\tfrac{H_1}{2}\right)^2\right\}^{1/2}\right]$$

$$\lambda'_2 = \tfrac{1}{2}\left[-\Delta + H_z - \tfrac{H_1}{2} - \left\{8\Delta^2 + \left(\Delta + H_z - 3\tfrac{H_1}{2}\right)^2\right\}^{1/2}\right]$$

$$\lambda'_3 = \tfrac{1}{2}\left[-\Delta - H_z - \tfrac{H_1}{2} + \left\{8\Delta^2 + \left(\Delta - H_z - 3\tfrac{H_1}{2}\right)^2\right\}^{1/2}\right]$$

$$\lambda'_4 = \tfrac{1}{2}\left[-\Delta - H_z - \tfrac{H_1}{2} - \left\{8\Delta^2 + \left(\Delta - H_z - 3\tfrac{H_1}{2}\right)^2\right\}^{1/2}\right]$$

$$\lambda'_5 = \lambda'_6 = \Delta + \frac{H_1}{2} \qquad (5.20)$$

Since the elastic constants are second derivatives of the free energy with respect to the strains it follows that to determine $c^{(2)}(=\partial^2 F/\partial \varepsilon_2^2)$ we must calculate the change in the energies of the levels due to an applied stress up to second order in $\langle H_2 \rangle$. Below the transition the point group symmetry is lowered from O^h to C^{4h} for which m_z and q_1 transform like A, as indeed they must since they have non zero averages in this phase. The other quadrupolar operator, q_2, transforms like B whereas m_x and m_y belong to the E representation. Since (m_x, m_y) have a different symmetry from q_2 the averages $\langle m_x \rangle$ and $\langle m_y \rangle$ are still zero even in an applied stress which causes $\langle q_2 \rangle$ to be non zero. Hence it follows from (5.19) that the energy levels $\lambda_i (i=1\ldots6)$ may be written to order $\langle H_2 \rangle^2$ as

$$\lambda_i = \lambda'_i + \tfrac{1}{2} a_i \langle H_2 \rangle^2 \qquad (5.21)$$

where

$$a_1 = \frac{\frac{3}{2}\left(\lambda'_1 + H_1 - H_z\right)}{\left(2\lambda'_1 + \Delta + \frac{H_1}{2} - H_z\right)\left(\lambda'_1 - \Delta - \frac{H_1}{2}\right)}$$

$$a_2 = \frac{3}{2}\frac{(\lambda_2' + H_1 - H_z)}{(2\lambda_2' + \Delta + \frac{H_1}{2} - H_z)(\lambda_2' - \Delta - \frac{H_1}{2})}$$

$$a_3 = \frac{3}{2}\frac{(\lambda_3' + H_1 + H_z)}{(2\lambda_3' + \Delta + \frac{H_1}{2} + H_z)(\lambda_3' - \Delta - \frac{H_1}{2})}$$

$$a_4 = \frac{3}{2}\frac{(\lambda_4' + H_1 + H_z)}{(2\lambda_4' + \Delta + \frac{H_1}{2} + H_z)(\lambda_4' - \Delta - \frac{H_1}{2})}$$

$$a_5 = \frac{3}{2}\frac{(\Delta + \frac{3H_1}{2} - H_z)}{2\Delta(\frac{3H_1}{2} - H_z)}$$

$$a_6 = \frac{3}{2}\frac{(\Delta + 3H_1/2 + H_z)}{2\Delta(\frac{3H_1}{2} + H_z)} \qquad (5.22)$$

Since q_2 does not couple to q_1 or the magnetization by symmetry (5.22) should be evaluated for $T \geq T_D$ with $\langle q_1 \rangle = \langle m_z \rangle = 0$. However (5.22) becomes indeterminate in this limit but by going back to the original Hamiltonian (5.19) it is easy to show that the energy levels to order $\langle H_2 \rangle^2$ are then given by

$$\lambda_1 = \lambda_3 = \quad \Delta - \frac{H_2}{2} + \frac{H_2^2}{12\Delta}$$

$$\lambda_2 = \lambda_4 = \quad -2\Delta - \frac{H_2^2}{6\Delta}$$

$$\lambda_5 = \lambda_6 = \quad \Delta + \frac{H_2}{2} + \frac{H_2^2}{12\Delta} \qquad (5.23)$$

The free energy $F(=\langle \mathcal{H}_{m.f.} \rangle - TS)$ is given in this approximation by

$$F = -Ng + \tfrac{1}{2}Vc_0(e_1^2 + e_2^2) + \tfrac{1}{2}N K(0)[\langle q_1 \rangle^2 + \langle q_2 \rangle^2] + \tfrac{1}{2} I \langle m_z \rangle^2 + F_p \qquad (5.24a)$$

where

$$g = -kT \ln\left[\sum_{i=1}^{6} e^{-\lambda_i / kT}\right] \qquad (5.24b)$$

is the Gibbs free energy per electronic site written in terms of the molecular fields (5.18b), and F_p is the phonon

contribution (§2.1). Equating $(\partial g/\partial H_1)$ and $(\partial g/\partial H_z)$ to $-\langle q_1\rangle$ and $-\langle m_z\rangle$ respectively we obtain the following self-consistency conditions:

$$\langle q_1\rangle = \frac{1}{4}\left[P_1(1+3f_1)+P_2(1-3f_1)+P_3(1+3f_2)+P_4(1-3f_2)-2P_5-2P_6\right]$$

$$\langle q_2\rangle = -\sum_{i=1}^{6} P_i \alpha_i H_2 \qquad (T<T_D).$$

$$\langle q_2\rangle = 2P_1\left(\frac{1}{2}-\frac{H_2}{6\Delta}\right)+2P_2\,\frac{H_2}{3\Delta}+2P_5\left(-\frac{1}{2}-\frac{H_2}{6\Delta}\right) \qquad (T\geq T_D).$$

$$\langle m_z\rangle = \frac{1}{2}\left[-P_1(1+f_1)+P_2(-1+f_1)+P_3(1+f_2)+P_4(1-f_2)\right] \qquad (5.25)$$

where

$$P_i = e^{-\lambda_i/kT}/Z$$

$$Z = \sum_{i=1}^{6} e^{-\lambda_i/kT} \qquad (5.26)$$

$$f_1 = \frac{\Delta+H_z-3H_1/2}{\left[8\Delta^2+(\Delta+H_z-3H_1/2)^2\right]^{1/2}}$$

$$f_2 = \frac{\Delta-H_z-3H_1/2}{\left[8\Delta^2+(\Delta-H_z-3H_1/2)^2\right]^{1/2}}. \qquad (5.27)$$

The stresses $\mathcal{S}_1$ and $\mathcal{S}_2$ corresponding to the strains e_1 and e_2 are given by

$$\mathcal{S}_1 = \frac{1}{V}\left(\frac{\partial F}{\partial e_1}\right)_T = c_0 e_1 - \frac{N}{V}\left(\frac{\partial g}{\partial H_1}\right)\left(\frac{\partial H_1}{\partial e}\right) \qquad (5.28a)$$

and similarly $$= c_0 e_1 - \frac{N}{V}\eta\langle q_1\rangle$$

$$\mathcal{S}_2 = \frac{1}{V}\left(\frac{\partial F}{\partial e_2}\right)_T = c_0 e_2 - \frac{N}{V}\eta\langle q_2\rangle \qquad (5.28b)$$

Hence the equilibrium value of the strain e_1 is given by

$$\langle e_1\rangle = \frac{N}{V}\,\frac{\eta}{c_0}\langle q_1\rangle \qquad (5.29)$$

so that we can replace H_1 in (5.25) and (5.27) by $K'\langle q_1\rangle$, where

$$K' = K(0) + \mu$$

with

$$\mu = \left(\frac{N}{V}\right)\frac{\eta^2}{c_0} \tag{5.30}$$

when calculating the thermal averages $\langle q_1\rangle$ and $\langle m_z\rangle$. The elastic constants $c^{(1)}$ and $c^{(2)}$ corresponding to the strains e_1 and e_2 are given by (c.f. (2.16))

$$\frac{c_\gamma^{(1)}}{c_0} = \frac{1 - K' g_\gamma^{(1)}}{1 - K(0) g_\gamma^{(2)}}, \quad \frac{c_\gamma^{(2)}}{c_0} = \frac{1 - K' g_\gamma^{(2)}}{1 - K(0) g_\gamma^{(2)}} \tag{5.31}$$

where

$$g_\gamma^{(1)} = \left(\frac{\partial\langle q_1\rangle}{\partial H_1}\right)_\gamma, \quad g_\gamma^{(2)} = \left(\frac{\partial\langle q_2\rangle}{\partial H_2}\right)_\gamma \tag{5.32}$$

The subscript 'γ' specifies the thermodynamic constraints under which the elastic constants are to be calculated. Above T_D we may evaluate (5.32) easily using (5.25) and remembering that there is no coupling to the magnetization. We find

$$g_I^{(1)} = g_I^{(2)} = \frac{2}{3\Delta}\frac{\left(1 - e^{-3\Delta/kT}\right)}{\left(2 + 4e^{-3\Delta/kT}\right)} \tag{5.33}$$

$$g_T^{(1)} = g_T^{(2)} = g_I^{(1)} + \frac{1}{kT}\frac{e^{-3\Delta/kT}}{(2 + 4e^{-3\Delta/kT})} \tag{5.34}$$

where γ=I refers to the 'isolated' regime and γ=T to the 'isothermal' regime discussed in Chapter 2. The 'essentially

isolated' value, $\gamma=s$, is obtained from the general thermodynamic relationship (c.f. (2.21)).

$$g_T^{(\alpha)} - g_S^{(\alpha)} = T\left(\frac{\partial \langle q_\alpha \rangle}{\partial T}\right)^2 / C_{H_\alpha} \tag{5.35}$$

where $\alpha=1$ or 2 and C_{H_α} is the specific heat of the electronic system at constant H_α. It follows that

$$g_S^{(1)} = g_T^{(1)} \quad , \quad g_S^{(2)} = g_T^{(2)} \tag{5.36}$$

above T_D. Note that (5.33), (5.34) and (5.36) show that $c_\gamma^{(1)}=c_\gamma^{(2)}$ in the cubic phase, as expected in this symmetry.

Below the transition the results are much more complicated because the degeneracy of the electronic levels is removed and because the magnetization m_z as well as the quadrupole moment q_1 couples to the strain e_1. The calculations are given in Appendix D and we shall simply mention here that we find $c_\gamma^{(1)} \neq c_\gamma^{(2)}$ as expected in the reduced symmetry and $c_s^{(2)}=c_T^{(2)}$ but $c_s^{(1)} \neq c_T^{(1)}$ as follows from (5.35).

5.4 Comparison of Theory with experiment.

The ultrasonic data of [43] is shown in figure 7; note that the temperature scale has been expanded below T_D to show the data more clearly. Since the results are taken up to 80°K we have modified the theory of §5.3 in a crude way to allow for thermal population of the E'' doublet at 80°K, multiplying $g_\gamma^{(1)}$ and $g_\gamma^{(2)}$ by a factor

$$3\left[3+\exp(-80/T)\right]^{-1} \tag{5.37}$$

The solid line in figure 7 for $T>T_D$ is the theoretical value for c_T calculated from (5.31), (5.32), (5.33), (5.34) and (5.37) using $\mu=16.0^oK$, $k(0)= -6.4^oK$, $c_o=1.05c(325^oK)= 7.8 \times 10^{11}$ dyn cm^{-2} and with $3\Delta=14.5^oK$, the value given by [42]. The agreement is seen to be satisfactory. Moran et al. [43] used the same value of Δ and c_o to fit their data but took $\mu=15.5^oK$ and $K= -4.4^oK$.

For crystals with the rocksalt structure the k=0 optic phonons have odd symmetry under inversion whereas the electronic operators we consider must be even because they connect states belonging to the same multiplet. Hence there is no contribution to $K(\underline{k}=0)$ from optic modes as pointed out in [43] and [44].

On the other hand the lattice structure does not put any restriction on the wavevector dependence of the acoustic phonon coupling. The electronic states can interact with the strains set up by the long wavelength acoustic modes, since these are even under inversion. It follows that $f_a(\underline{k}) \alpha k^{\frac{1}{2}}$ (Appendix B) so $K_a(\underline{k})$ is independent of k for small k. Hence there is, in our view, an important contribution to $K(\underline{k})$ from the acoustic modes in contradiction to the assertion of Levy, [43],[44]. K(0) neglects the contribution from the static strain (which just corresponds to the k=0 acoustic mode) and is therefore entirely due to the self energy term in (5.15) plus quadrupole-quadrupole coupling via other mechanisms. We find $K(0)\sim -0.4\mu$ which we believe is a reasonable value for the self energy and suggests that coupling via other mechanisms is relatively unimportant.

The magnetic coupling parameter I is determined from the requirement that the transition occurs at $9.5^{o}K$ and we find $I=24.5^{o}K$. If there were no magnetic interactions the total quadrupole coupling $K'=K(0)+_{\mu}$ would be insufficient to overcome the crystal field splitting and no transition would occur, although there would be a considerable softening of the elastic constant. Hence it is the magnetic interaction which provides the driving force for the transition in DySb.

The full lines in figure 7 below T_D are the theoretical values for $c_s^{(1)}$, $c_T^{(1)}$ and $c_T^{(2)}(=c_s^{(2)})$ obtained with the same values of parameters that were used in the high temperature fit. Since the measuring frequencies in ultrasonic experiments ($\sim 10MH_z$) are likely to be less τ_{SL}^{-1} (see §3.2) we expect the data to correspond to the 'isentropic' regime, $\gamma=s'$, discussed in §2.2. c_s' is given by (2.24) and lies between c_s and c_T. We have plotted the form of $c_{s'}^{(1)}$ schematically as the dashed curve in figure 7. The experimentally measured elastic constant, which represents a domain average, should lie between $c_{s'}^{(1)}$, and $c_{s'}^{(2)}$. In particular it should have a discontinuity at T_D and be almost equal to c_0 at T=0.

The ultrasonic data of [43] which is shown in figure 7 for comparison is clearly very different from these predictions. We have tried without success to remedy this discrepancy by including in our model the effects of modulation of the quadrupole-quadrupole interaction $K(\ell,\ell')$ by lattice strains. We do not believe that this discrepancy

is due to the simple model we have taken for the Dy^{3+} states since below the transition population of the higher levels, ignored in our treatment, is negligible. It would appear that there is an additional mechanism acting in the ordered phase which is not included in our treatment or that of Levy, [43] and [44]. In particular the experimental results in this region cannot be explained in terms of domain formation as was postulated in [43].

CHAPTER 6

THE ELASTIC PROPERTIES OF HYDROGEN BONDED FERROELECTRICS

In chapters 1-5 we showed that crystals which have effectively only a small number of electronic states per unit cell can be described by a pseudospin Hamiltonian. This technique is however more general [27] and can be applied to any system with a small number of low lying states well separated from those of higher energy. In this chapter we show that, with certain assumptions, highly anharmonic lattice vibrations can be described in terms of pseudospin operators. A detailed model for hydrogen bonded ferroelectrics will be developed and compared with the experimental data for KH_2PO_4 (KDP for short), paying particular attention to the anomaly in the elastic constant c_{66}.

6.1 Crystal structure.

The structure of the hydrogen bonded ferroelectric KDP has been determined by X-ray [47] and neutron [48] diffraction in both the ferroelectric and paraelectric phases. Above the transition the space group is D_{2d}^{12} and the structure is body centred tetragonal with two formula units in the primitive unit cell. We denote the direction containing the fourfold improper rotation of D_{2d} as the z axis and the two twofold axes at right angles to z as the x and y axes. The basis vectors of the tetragonal unit cell (which is not the primitive unit cell) are parallel to the x, y and z axes and are of length a=7.45Å, b=a and c=6.96Å respectively.

Each phosphorous ion is surrounded by four oxygens at the corners of an almost regular tetrahedron. Hydrogen bonds, which lie almost in the x-y plane, link an oxygen on one phosphate group to an oxygen on a neighbouring group. The K and P ions alternate each other at a distance c/2 in the direction of the z axis. A projection of the structure perpendicular to the z axis, showing for clarity only the oxygen ions and the protons, is given in figure 8a.

It will be necessary to consider the form of the primitive unit cell when discussing the lattice dynamics of KDP and this is shown schematically in figure 8b. Only the phosphate groups and the hydrogen bonds are indicated, again for reasons of clarity. The centres of the phosphate groups lie on two interpenetrating body centred tetragonal lattices, indicated by the open circles (sublattice A) and the filled circles (sublattice B) in the figure. We have chosen the corners of the cell to lie at the centre of phosphate sites on sublattice A and there is just one phosphate group of sublattice B contained within the cell. The hydrogen bonds are indicated schematically by the dashed lines. All the bonds meeting at a PO_4 group on sublattice B are entirely contained within a single cell whereas each of the bonds attached to a PO_4 group on sublattice A lie in a different cell. Each bond links a phosphate group on sublattice A to a phosphate group on sublattice B. These facts will be useful when we come to discuss the lattice dynamics of KDP in §6.2.

At 122°K a transition, which is slightly first order [49], occurs from the piezoeelectric phase described above to a ferroelectric phase. The low temperature structure is orthorhombic with space group C_{2V}^{19} so the ordering takes place in a $\underline{k}=0$ B_2 mode. The basis vectors of the orthorhombic unit cell in the x-y plane are rotated about the z axis by 45° with respect to the axes of the tetragonal unit cell of D_{2d} and are of unequal length.

Above the transition the distribution of the protons is symmetrical about the centre of the bonds but below T_D all the protons in a single domain are near the 'upper' or the 'lower' oxygens of the phosphate groups depending upon the polarity. This ordering is accompanied by a smaller displacement of the K and P ions parallel to the z axis, the positions of the oxygens being little affected. Since the hydrogens move almost in the x-y plane the spontaneous polarization, which is parllel to the z axis, is caused mainly by this relatively small shift of the K and P ions.

6.2 Local Normal Coordinates.

Large isotope effects are observed in this class of materials; for example the transition temperature of 122°K [49] in KDP is raised to 223°K [50] on deuteration. This suggests that the motion of the protons along the bonds plays an important role. A complete group theoretical analysis of all the normal modes at the symmetry points in the Brillouin zone has been given by Shur [51]. He finds that there are four modes which involve large motions of the

hydrogens along their bonds. At $\underline{k}=0$ these belong to the A_2, B_2 and E representations of D_{2d} and the corresponding proton eigenvectors are shown in figure 9. Since the displacements in the B_2 mode correspond to the static ordering which appears in the ferroelectric phase it must be an instability in this mode which causes the transition.

The eigenvectors of the soft mode in KDP have not been directly measured because of difficulties in doing coherent neutron scattering in a material containing hydrogen, which has a large inelastic cross section. However the eigenvectors of the soft mode in deuterated KDP have been determined [50], [52] and found to involve large displacements of the hydrogens along their bonds corresponding to the B_2 mode of figure 9 as expected. The mode is found to be of a relaxational type i.e. the real part of the frequency is zero. From these results it appears that a description of the soft mode as a phonon is not likely to be successful. This is because phonons are resonant modes (i.e. the real part of the frequency is finite and the imaginary part, caused by weak anharmonic forces, is relatively small) whereas, in KD_2PO_4 at least, the soft mode is of the relaxational type. It is worth mentioning here that the spectrum of the soft mode in KDP has been measured by light scattering [53] and also found to be overdamped. However its width is an order of magnitude greater than in deuterated KDP, which is another example of the large isotope effect in this class of materials.

We shall overcome the above mentioned difficulties in a phonon description of the soft mode by considering a model

similar to that proposed by Elliott [27]. This description, which will be called the 'local mode tunnelling theory', treats the unstable mode as a tunnelling motion of the ions. It is rather like the proton tunnelling model proposed much earlier by Blinc [55] but is based more on lattice dynamical principles.

The normal coordinate of wavevector $\underline{k}$ belonging to the jth branch can be written as (see B.4)

$$Q_j(\underline{k}) = \frac{1}{N^{1/2}M^c} \sum_{\alpha,l} e^{i\underline{k}.\underline{R}(l)} \epsilon^*_{\alpha j}(\underline{k})\, m_\alpha\, u_\alpha(l) \qquad (6.1)$$

where the suffix α is summed over all three component directions for each of the atoms in the unit cell and the suffix l refers to the unit cell centred at $\underline{R}(l)$. As discussed by Thomas [56] it is useful to define local normal coordinates $v_j(l)$. If we write

$$v_j(l) = \frac{1}{M^c} \sum_\alpha m_\alpha\, u_\alpha(l)\, \epsilon^*_{\alpha j}(0) \qquad (6.2)$$

then the normal coordinates for $\underline{k}\sim 0$ are given by

$$Q_j(\underline{k}) \simeq \frac{1}{N^{1/2}} \sum_l v_j(l)\, e^{i\underline{k}.\underline{R}(l)} \qquad (6.3)$$

Moore and Williams [54] suggest that (6.3) will be valid up to a wavevector $\underline{K}_m$ where

$$k_m \sim 1/R \qquad (6.4)$$

and R is an 'effective range' of the intercell forces.

It is also possible to define local normal coordinates in a different way, which can represent normal modes of any

wavevector, by analogy, with the usual theory of Wannier functions for electronic states. We wish to construct functions $w_j(\ell)$ localised around the cell centred at $\underline{R}(\ell)$ such that

$$Q_j(\underline{k}) = \frac{1}{N^{1/2}} \sum_{\ell} w_j(\ell)\, e^{i\underline{k}.\underline{R}(\ell)} \tag{6.5}$$

Inverting (6.5) yields

$$w_j(\ell) = \frac{1}{N^{1/2}} \sum_{\underline{k}} Q_j(\underline{k})\, e^{-i\underline{k}.\underline{R}(\ell)} \tag{6.6}$$

so from (6.6) and (6.1) it follows that

$$w_j(\ell) = \frac{1}{NM^c} \sum_{\underline{k}} \sum_{\ell'\alpha} e^{-i\underline{k}.[\underline{R}(\ell)-\underline{R}(\ell')]}\, \epsilon^*_{\alpha j}(\underline{k})\, m_\alpha\, u_\alpha(\ell). \tag{6.7}$$

Note that, unlike $v_j(\ell)$, the $w_j(\ell)$ involve displacements in cells ℓ', where ℓ' is close to ℓ, as well as in cell ℓ itself. Kohn [57] has discussed the nature of the $w_j(\ell)$ for the particularly simple case of a linear chain with two atoms per unit cell. However for three dimensional lattices there are problems connected with localisation of the $w_j(\ell)$ as there are with Wannier functions [58], [59]. Since we are only interested in the region around $\underline{k}=0$ we shall avoid these difficulties and go back to (6.2).

The Hamiltonian for lattice vibrations in the harmonic approximation is

$$\mathcal{H} = \sum_{j\underline{k}} \frac{P_j(\underline{k})P_j(-\underline{k})}{2M^c} + \frac{1}{2}M^c \sum_{j\underline{k}} \omega_j^2(\underline{k})\, Q_j(\underline{k})\, Q_j(-\underline{k}) \tag{6.8}$$

(see Appendix B) which can be expressed in terms of the local coordinates $v_j(\ell)$ as

$$\mathcal{H} = \sum_{j\ell} \frac{p_j^2(\ell)}{2M^c} + \frac{1}{2}\sum_{j\ell} A_j v_j^2(\ell) + \frac{1}{2}\sum_{j}\sum_{\ell'\neq\ell} U_j(\ell,\ell')[v_j(\ell)-v_j(\ell')]^2 \qquad (6.9)$$

where $p_j(\ell)$ is the momentum conjugate to $v_j(\ell)$ and $U_j(\ell,\ell')$ is the coupling between local normal coordinates in cells ℓ and ℓ', which gives rise to dispersion in the jth branch. The frequency of the mode at $\underline{k}=0$ is given by

$$\omega_j^2(0) = \frac{A_j}{M^c} \qquad (6.10)$$

We expect that (6.9) gives a good description of the normal modes $Q_j(\underline{k})$ for $k<k_m$ (see (6.4)) but to represent modes of large $\underline{k}$ accurately we should strictly include non-diagonal terms of the form $v_j(\ell)v_{j'}(\ell')$ where j' and j refer to different branches. Since we are concerned here specifically with the region around $\underline{k}=0$ we shall ignore this complication and assume that (6.9) is a satisfactory harmonic Hamiltonian.

We consider the form of (6.9) for the four local normal coordinates involving a large motion of the protons along their bonds (figure 9). Neglecting for a moment the displacements of the other ions we can write

$$\begin{aligned}
v_{A_2}(\ell) &= \tfrac{1}{2}[q_1(\ell) - q_2(\ell) + q_3(\ell) - q^4(\ell)] \\
v_{B_2}(\ell) &= \tfrac{1}{2}[q_1(\ell) + q_2(\ell) + q_3(\ell) + q^4(\ell)] \\
v_{E_1}(\ell) &= \tfrac{1}{2}[q_1(\ell) - q_2(\ell) - q_3(\ell) + q^4(\ell)] \\
v_{E_2}(\ell) &= \tfrac{1}{2}[q_1(\ell) + q_2(\ell) - q_3(\ell) - q^4(\ell)]
\end{aligned} \qquad (6.11)$$

where $q_i(\ell)$ is the displacement of the ith proton in the cell relative to the centre of the bond. (6.11) does not satisfy

the normalization condition (B.3) but this is unimportant in what follows. The relative signs of the $q_i(\ell)$ have been chosen so they are all positive for v_{B_2}, the soft mode. It is useful to write the potential energy appropriate to a single cell in terms of the q_i. Considering only quadratic terms we obtain

$$A(\ell) = a \sum_{i=1}^{4} q_i^2(\ell) + U\left[(q_1(\ell) - q_3(\ell))^2 + (q_2(\ell) - q_4(\ell))^2\right] + V\left[(q_1(\ell) - q_2(\ell))^2 + (q_3(\ell) - q_4(\ell))^2 + (q_1(\ell) - q_4(\ell))^2 + (q_2(\ell) - q_3(\ell))^2\right] \tag{6.12}$$

By symmetry the interaction U between the two 'upper' hydrogens (1 and 3) is equal to the interaction between two lower hydrogens (2 and 4) but does not equal the interaction V between an upper and a lower.

Suppose the protons are displaced by an amount ±d from the centre of the bonds. There are $2^4=16$ possible combinations shown in the first column of table 6.1 below and the corresponding energies are indicated in the second column.

The energies have been written in terms of the proton coordinates $q_i(\ell)$ rather than the $v_j(\ell)$ so that a comparison can be made between our model and an earlier theory of KDP proposed originally by Slater [60] and later modified by Takagi [61] and Silsbee, Uehling and Schmidt [62]. This theory assumes that there are two stable positions for each proton symmetrically situated about the centre of the bond. Slater assumed that the configurations with lowest energy where those with two 'upper' or two 'lower' hydrogens adjacent

TABLE 6.1

Relative energies of the different proton configurations according to the local mode theory and the Slater-Takagi model.

Configuration		Energy (Local Mode Theory)	Energy (Slater-Takagi Theory)
A)	1 	ad^2	0
	2 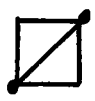	"	"
B)	3 	$(a+2(U+V))d^2$	ϵ
	4 	"	"
	5 	"	"
	6 	"	"
C)	7 	$(U+2V+a)d^2$	w
	8 	"	"
	9 	"	"
	10 	"	"
	11 	"	"
	12 	"	"
	13 	"	"
	14 	"	"
D)	15 	$(4V+a)d^2$	w_1
	16 		"

to a phosphate group, i.e. nos. 1 and 2 in table 6.1. From figure 9 it is clear that these configurations correspond to the unstable B_2 mode. Those configurations with an 'upper' and a 'lower' hydrogen (nos. 3 to 6 in table 6.1) have, according to Slater, a somewhat higher energy ϵ while those with one or three hydrogens adjacent to a given phosphate (nos. 7 to 14) have a much higher energy w. The states with no (15) or four (16) hydrogens should have a still higher energy w_1. Usually in the Slater-Takagi model one lets $w_1 \to \infty$. These energies are indicated in the third column of table 6.1.

Although there are three parameters in the Slater-Takagi theory, ϵ, w and w_1 there are effectively only two in the local mode theory, U and V. If we wish to represent the Slater picture exactly, we must add to (6.12) an additional term involving displacements of all four hydrogens, i.e.

$$b'(l) = -W' q_1(l) q_2(l) q_3(l) q_4(l') \tag{6.13}$$

Four particle forces of this type have been discussed by Tokunaga and Matsubara [63] and more recently by Blinc [64]. Three particle interactions are forbidden by symmetry since it follows from the inverse transformation to (6 11) that $q_i q_j q_k$ cannot contain the identity representation.

Quartic terms can also arise from the motion of a single proton along its bond so combining this contribution with (6.13) the quartic terms involving displacements in cell l

can be written as

$$B(l) = b \sum_{i=1}^{4} q_i^4(l) - W' q_1(l)\, q_2(l)\, q_3(l)\, q_4(l). \tag{6.14}$$

It seems reasonable that the coefficient b is positive since for sufficiently large displacements the protons must be repelled by the oxygen ions. Comparing the second and third columns in table 6.1 we expect that V is large and positive whereas U is large and negative. It is difficult to estimate the size of W' since it depends upon the precise values taken for ϵ, w and w_1.

Since each of the four protons in (6.12) and (6.13) are in the same unit cell it follows from the discussion in §6.1 that they all lie on bonds connected to the same phosphate group on sublattice B. There must, in addition, be equivalent interactions between those protons whose bonds join the same phosphate on sublattice A. Each of these protons is labelled by a different unit cell index. The potential energy term in our Hamiltonian is therefore written as

$$\mathcal{V} = \sum_{l} \left(A(l) + B(l) \right) + \sum_{l<l'<l''<l'''} \left[A(l,l',l'',l''') + B(l,l',l'',l''') \right] \tag{6.15}$$

where $A(l)$ and $B(l)$ are given by (6.12) and (6.14) respectively,

$$\begin{aligned} A(l,l',l'',l''') = {} & + U\left[(q_1(l) - q_3(l''))^2 + (q_2(l') - q_4(l'''))^2 \right] \\ & + V\left[(q_1(l) - q_2(l'))^2 + (q_3(l'') - q_4(l'''))^2 \right. \\ & \left. + (q_1(l) - q_4(l'''))^2 + (q_2(l') - q_3(l''))^2 \right] \end{aligned} \tag{6.16}$$

and

$$B(l,l',l'',l''') = -W' q_1(l)\, q_2(l')\, q_3(l'')\, q_4(l''') \tag{6.17}$$

The summation in the second term of (6.15) runs over each distinct set of values l, l', l'' and l''' such that each of these cells contains a hydrogen bond which meet at the same phosphate group.

Equation (6.15) has been expressed in terms of proton displacements to make a connection with the Slater-Takagi model. However it is not in a form useful for discussing lattice dynamics, which are best treated in terms of local normal coordinates (6.2). Employing the reverse transformation to (6.11) the potential energy (6.15) becomes rather complicated so each term will be considered separately.

$A(l)$ can be expressed in terms of the $v_j(l)$ as

$$A(l) = \tfrac{1}{2}\left[A_{B_2} v^2_{B_2}(l) + A_{A_2} v^2_{A_2}(l) + A_E\left(v^2_{E_1}(l) + v^2_{E_2}(l)\right)\right] \tag{6.18}$$

where

$$\tfrac{1}{2} A_{B_2} = a \qquad \tfrac{1}{2} A_E = a + 2(U+V) \tag{6.19}$$

and

$$\tfrac{1}{2} A_{A_2} = a + 4V$$

The coefficients A_{B_2}, A_E and A_{A_2} are just proportional to the energies of configuration A,B and D given in the second column of table 6.1. In §6.3 we shall make the crucial assumption that A_{B_2} is negative which means that the B_2 mode is unstable. It is apparent from table 6.1 that the coefficients

A_E and A_{A_2} are larger than A_{B_2} so for simplicity we shall assume that they are positive. These modes are therefore stable, in agreement with the lattice dynamical calculation of Fujiwara [65], and will not play an important role in the transition.

The term $B(\ell)$ in (6.15) can be written in terms of local normal coordinates as

$$\frac{1}{4}(b-W')\sum_j v_j^4(l) + \frac{W'}{2} v_{B_2}^2(l)\left(v_{A_2}^2(l)+v_{E_1}^2(l)+v_{E_2}^2(l)\right)$$
$$+ \frac{W'}{2} v_{A_2}^2\left(v_{E_1}^2+v_{E_2}^2\right) + \frac{W'}{2} v_{E_1}^2 v_{E_2}^2$$
$$+ \frac{W'}{2} v_{A_2} v_{B_2} v_{E_1} v_{E_2} \qquad (6.20)$$

The coefficient b-W' is expected to be positive since for sufficiently large displacements the potential must be repulsive. Hence the potential in which v_{B_2} moves is in the shape of the double well drawn in figure 10a(i). To a first approximation the non-diagonal terms in (6.20) can be decoupled by writing

$$v_{\Gamma_\alpha}^2 v_{\Gamma_\beta}^2 = \langle v_{\Gamma_\alpha}^2\rangle v_{\Gamma_\beta}^2 + \langle v_{\Gamma_\beta}^2\rangle v_{\Gamma_\alpha}^2 \qquad (6.21)$$

where Γ_α and Γ_β refer to different symmetries. This simply gives a relatively small correction to the coefficients of the quadratic terms (6.19).

$A(\ell,\ell',\ell'',\ell''')$ can be written as

$$A(l,l',l'',l''') = u\left[\left(v_{B_2}(l)-v_{B_2}(l'')\right)^2+\left(v_{B_2}(l')+v_{B_2}(l''')\right)^2\right]$$
$$+ v\left[\left(v_{B_2}(l)-v_{B_2}(l')\right)^2+\left(v_{B_2}(l'')-v_{B_2}(l''')\right)^2\right.$$
$$\left.+\left(v_{B_2}(l)-v_{B_2}(l''')\right)^2+\left(v_{B_2}(l')-v_{B_2}(l'')\right)^2\right] \qquad (6.22)$$

+ corresponding terms for v_{A_2}, v_{E_1} and v_{E_2}

+ terms involving v's of different symmetry.

The terms involving v's of different symmetry must vanish when we take space Fourier transforms and consider modes near $\underline{k}=0$.

The term $B(\ell, \ell', \ell'', \ell''')$ of (6.15) becomes

$$\frac{1}{4} W' v_{B_2}(\ell) v_{B_2}(\ell') v_{B_2}(\ell'') v_{B_2}(\ell''') \tag{6.23}$$

plus many other unimportant terms involving displacements of the A_2 and E modes which do not play an important role in the transition.

So far only short range forces have been considered but since there is a polarization associated with the soft B_2 mode dipolar interactions, which are of long range, must also be present. Adding these terms to the two particle forces described by (6.22) and neglecting the E and A_2 modes the model Hamiltonian may be written as

$$\mathcal{H} = \sum_{\ell} \mathcal{H}^{\circ}(\ell) - \frac{1}{2} \sum_{\ell,\ell'} U(\ell,\ell') [v_f(\ell) - v_f(\ell')]^2 - \frac{1}{4} \sum_{\ell,\ell',\ell'',\ell'''} W(\ell,\ell',\ell'',\ell''') v_f(\ell) v_f(\ell') v_f(\ell'') v_f(\ell''') \tag{6.24}$$

where the soft mode has been labelled by the suffix 'f' to distinguish it from other stable B_2 modes. $\mathcal{H}^{\circ}(\ell)$ is given by

$$\mathcal{H}^{\circ}(\ell) = \frac{p_f^2(\ell)}{2M^c} + \frac{1}{2} A v_f^2(\ell) + \frac{1}{4} B v_f^4(\ell) \tag{6.25}$$

where $A<0$ and $B>0$. $U(\ell, \ell')$ includes dipolar and short range contributions to the two particle interactions while the short range four particle interactions are described by $W(\ell, \ell', \ell'', \ell''')$. The potential corresponding to $\mathcal{H}^{\circ}(\ell)$ is in the form of a double well (figure 10.a(i)).

In the paraelectric phase the system is as likely to be in one well as in the other but intercell forces drive the system cooperatively into one of the wells by raising the energy of this well relative to the other (figure 10.a(ii)). Such transitions are said to be of the 'order disorder' type. At the other extreme, in so-called 'displacive' transitions of which barium titanate [66] is a typical example the coefficient A is positive above the transition leading to a single well potential (figure 10.b(i)). However A is temperature dependent and varies like

$$A = a(T - T_0)$$

An instability occurs at $T=T_D$ when A vanishes (figure 10.b(ii)) and in the low temperature phase the potential is in the form of a double well with the energy of one well raised relative to the other by intercell forces (figure 10.b(iii)) as for order disorder transitions. It will be noted from figure 10 that the main difference between the potentials for displacive and order disorder transitions occurs above T_D. In the local mode theory displacive and order disorder transitions are treated on an equal footing, there is no fundamental difference between them. Indeed the basic formalism introduced so far is applicable to either type.

It is natural to ask of there is any direct evidence for a double well above the transition in hydrogen bonded ferroelectrics. The answer appears to be in the affirmative, certainly for the deuterated compounds. Since the deuteron has a quadrupole moment it can be used to probe electric field gradients in the neighbourhood of dueteron bonds.

Deuteron magnetic resonance on KD_2PO_4 [67] and KD_2AsO_4 and $C_sD_2AsO_4$ [68] show that the largest component of the electric field gradient tensor remains essentially unchanged during the phase transition, which is to be expected if the average distance from the oxygen ions remains unchanged. This is consistent with the potential being in the form of a double well above and below the transition. An anomalous increase in the spin-lattice relaxation rate as T_D is approached from above has been explained by Bline et al. [68] as being due to some form of collective deuteron motion, which is again consistent with the picture presented here. It was not however possible to determine from the experiments whether the deuterons move from one equilibrium position to another by jumping over the barrier or by a true quantum mechanical tunnelling process.

To summarize this section the local mode picture has been compared with the Slater model in some detail. From this comparison it appears plausible that the A_2 and E modes involving a motion of the protons along the bonds are stable, whereas the B_2 mode is not. Furthermore it has been found necessary to introduce four particle interactions to represent the Slater model in detail. We are left with the difficulty of obtaining a realistic model for the unstable mode incorporating the large anharmonicity in a manageable way. This problem is worthy of a section in its own right, so we close this rather lengthy discussion here and encourage the interested reader to press on to §6.3.

6.3 The Pseudospin Hamiltonian.

In the previous section we suggested that the potential for the unstable mode is in the form of the double well shown in figure (10.a(i). If the barrier is sufficiently high the ground state is doubly degenerate corresponding to the system being localised in one or other of the wells. There can in practise be tunnelling from one well to the other so the ground state degeneracy is lifted. It will be assumed here that the tunnelling frequency is small compared with the energies of the excited vibrational states. Furthermore we assume that these excited states are not populated to any significant extent at temperatures in the region of the transition so we shall ignore them.

The Hamiltonian $\mathcal{H}^{o}(\ell)$, defined in (6.25) acts, therefore, on the states $|\ell L\rangle$ and $|\ell R\rangle$ corresponding to the system being approximately localised in the left and right hand wells of the ℓth cell respectively. Neglecting the possibility of intercell tunnelling the eigenstates of the full Hamiltonian (6.24) are linear combinations of product wavefunctions of the form

$$\psi = |1\alpha_1\rangle |2\alpha_2\rangle \cdots\cdots |N\alpha_N\rangle \tag{6.26}$$

where α takes the values L or R. Since any 2x2 Hermitian matrix can be written as a linear combination of the Pauli spin matrices and the unit matrix we can write $\mathcal{H}$ in terms of spin operators. Taking matrix elements of $\mathcal{H}$ between states (6.26) and ignoring constant terms one obtains

$$\mathcal{H} = -\Delta \sum_{l} \sigma^{x}(l) - \frac{1}{2} \sum_{l,l'} \mathcal{J}(l,l')\sigma^{z}(l)\sigma^{z}(l') - \frac{1}{4} \sum_{l,l',l'',l'''} J^{(4)}(l,l',l'',l''')\sigma^{z}(l)\sigma^{z}(l')\sigma^{z}(l'')\sigma^{z}(l''') \tag{6.27}$$

where

$$\Delta = \langle lR | \mathcal{H}_0(l) | lL \rangle,$$

$$\mathcal{J}(l,l') = U(l,l') \langle lR | v_f(l) | lR \rangle \langle l'R | v_f(l') | l'R \rangle$$

and

$$J^4(l,l',l'',l''') = W(l,l',l'',l''') \langle lR | v_f(l) | lR \rangle \langle l'R | v_f(l') | l'R \rangle \times \langle l''R | v_f(l'') | l''R \rangle \langle l'''R | v_f(l''') | l'''R \rangle$$

The matrix elements, written in the form $\langle l'\alpha | \mathcal{O} | l'\beta \rangle$ are understood to mean [54]

$$\langle l'\alpha | \mathcal{O} | l'\beta \rangle = \int_{-\infty}^{\infty} dv_f \, \psi_{l'}^{\alpha^*}(v_f) \, \mathcal{O} \, \psi_{l}^{\beta}(v_f) \tag{6.28}$$

It has been implicitly assumed in (6.27) that we take as origin for v the midpoint of the double well. In this case

$$\langle lR | v_f | lL \rangle = \langle lL | v_f | lR \rangle$$

$$\langle lR | v_f | lR \rangle = -\langle lL | v_f | lL \rangle \tag{6.29}$$

and

$$\langle lR | v_f^2 | lR \rangle = \langle lL | v_f^2 | lL \rangle$$

The operator $\sigma^z(l)$ is directly related to $v_f(l)$ by

$$v_f(l) = g(f)\sigma^z(l) \tag{6.30}$$

where

$$g(f) = \langle lR | v_f | lR \rangle \tag{6.31}$$

The eigenfunctions of the operator $\sigma^z(l)$ are $|lL\rangle$ and $|lR\rangle$. Below T_D one of these states is occupied in preference

to the other leading to a non zero expectation value of σ^z. Since the polarization from the unstable mode is proportional to $\langle v_f \rangle$, which is in turn proportional to $\langle \sigma^z \rangle$ by (6.30), the preferential occupation of one of the wells leads to a spontaneous polarization as expected.

The soft mode corresponds to the motion of the operator σ^z, which involves tunnelling of the system from one well to another. It must be stressed that this tunnelling involves all the atoms in the cell as distinct from the proton tunnelling model of Blinc [55] where only motion of the protons is considered. Recently Montgomery and Paul [69] have determined the symmetries of the four modes involving large proton displacements (figure 9) assuming they are tunnelling modes. They find that the symmetries are identical to those of the corresponding normal co-ordinates give by Shur [51], i.e., they belong to the A_2, B_2 and E representations of D_{2d}, so the symmetry arguments that have been used so far remain unchanged.

Interactions between σ^x and σ^z of the form

$$-\frac{1}{2}\sum_{l,l'} J^{xz}(l,l')\,\sigma^x(l)\,\sigma^z(l')$$

do not give a contribution to the ordering in molecular field theory because symmetry arguments show that $\sum_{l' \neq l} J^{xz}(l,l')=0$. The operator σ^y is imaginary whereas σ^x and σ^z are real so σ^y changes sign under time reversal although σ^x and σ^z remain unaltered. This behaviour, which is different from that of real spins, shows that there cannot be terms involving the products $\sigma^x\,\sigma^y$ or $\sigma^z\sigma^y$.

Symmetry does, however, allow coupling of the form

$$-\frac{1}{2}\sum_{l,l'} J^{xx}\sigma^{x}(l)\sigma^{x}(l')$$

which represents the effect of the tunnelling in one cell on the tunnelling in a neighbouring cell. Since this involves the overlap of wavefunctions in different cells we expect that $J^{xx}(l,l')$ is very small compared with the tunnelling frequency 2Δ (6.27) and can be neglected.

In §6.2 the interactions between the soft mode and the other modes involving large proton displacements were found to be unimportant, essentially because these other modes are of different symmetry (A_2 and E) to the soft mode (B_2). It is important, however, to consider the effect of coupling the unstable mode to other modes of the same symmetry. This can arise for instance from the interaction of the polarization of one mode with the electric field of the other. Terms such as $v_f(l)v_j(l')$ (where $j(\neq f)$ refers to a branch which has B_2 symmetry at $\underline{k}=0$) are forbidden because the v's were chosen explicitly to eliminate these cross terms (see (6.9)). However a term such as

$$\mathcal{H}_{SL} = -\frac{1}{N}\sum_{l,l'j}{}' F(l,l')\,v_f^3(l)\,v_j(l') \qquad (6.32)$$

is allowed by symmetry. On taking Fourier transforms (6.32) can be expressed as

$$\mathcal{H}_{SL} = -\frac{1}{N^{1/2}}\sum_{\underline{k},j}\zeta_j(\underline{k})\,e^{i\underline{k}\cdot\underline{R}(l)}\sigma^{z}(l)\,Q_j(\underline{k}) \qquad (6.33)$$

where $\zeta_j(\underline{k})$ is related to $F(l,l')$ by

$$\zeta_j(\underline{k}) = \sum_{l'} F(l,l')\langle lR|v_f^3(l)|lR\rangle e^{-i\underline{k}\cdot\underline{R}(l')} \qquad (6.34)$$

There are also terms involving $\sigma^x Q$ which represent a modulation of the tunnelling frequency by lattice vibrations. It is difficult to estimate the size of this effect but since it does not play an important role in the transition we shall ignore it for simplicity.

It has been suggested by Cowley et al., [70] and [71], that coupling of the soft mode to pairs of phonons is large in hydrogen bonded ferroelectrics. In terms of local normal coordinates these interactions can be represented by

$$-\frac{1}{N^{3/2}} \sum_{l,l',l''} \sum_{j,j'} M_{jj'}(l,l',l'')\, v_j(l)\, v_{j'}(l')\, v_{j'}(l') \tag{6.35a}$$

which are written as

$$-\frac{1}{N} \sum_{l} \sum_{\substack{j,j' \\ \underline{k},\underline{k}'}} N_{jj'}(\underline{k},\underline{k}')\, \sigma^z(l)\, e^{+i\underline{k}\cdot\underline{R}(l)}\, Q_j(\underline{k}')\, Q_{j'}(-\underline{k}-\underline{k}') \tag{6.35b}$$

in the tunnelling theory. Terms involving three spin operators such as

$$-\frac{1}{N} \sum_{l} \sum_{\underline{k},\underline{k}'} \tau(\underline{k},\underline{k}')\, \sigma^z(l)\, e^{i\underline{k}\cdot\underline{R}(l)}\, \sigma^z(\underline{k}')\, \sigma^z(-\underline{k}-\underline{k}') \tag{6.36}$$

are also allowed as well as interactions involving two phonons and one spin. Chapter 7 will be devoted to a study of the effects of (6.35) and (6.36) but for the time being we shall neglect them.

Static strain coupling (c.f. (1.21)) is of the form

$$\mathcal{H}_s = \gamma e \sum_l \sigma^z(l) \tag{6.37}$$

where $e = e_{B_2} = 2\epsilon_{xy}$ (Appendix A). As discussed earlier the polarization is proportional to σ^z so (6.37) represents the

piezoelectric coupling.

The branch j=f in the phonon Hamiltonian (6.8) has been treated in terms of pseudospin operators (6.27) but the other branches j≠f will still be described as harmonic phonons, i.e:

$$\mathcal{H}_{ph} = \sum_{\substack{j\neq f \\ \underline{k}}} \left[a_j^+(\underline{k}) a_j(\underline{k}) + \tfrac{1}{2} \right] \hbar\omega_j(\underline{k}) \tag{6.38}$$

Adding the elastic energy

$$\mathcal{H}_{el} = \tfrac{1}{2} V c_0 e^2 \tag{6.39}$$

(c.f. (1.22)) where $c_0 = c_{66}$ (Appendix A) and combining (6.27), (6.33), (6.37), (6.38) and (6.39) the model Hamiltonian is written as

$$\begin{aligned}\mathcal{H} = &- \Delta \sum_l \sigma^x(l) - \tfrac{1}{2} \sum_{l,l'} J(l,l') \sigma^z(l)\sigma^z(l') - \gamma e \sum_l \sigma^z(l) \\ &- \tfrac{1}{4} \sum_{l,l',l'',l'''} J^{(4)}(l,l',l'',l''') \sigma^z(l)\sigma^z(l')\sigma^z(l'')\sigma^z(l''') + \tfrac{1}{2} V c_0 e^2 \\ &+ \sum_{j\neq f} \sum_{\underline{k}} \left[a_j^+(\underline{k}) a_j(\underline{k}) + \tfrac{1}{2} \right] \hbar\omega_j(\underline{k}) - \sum_{j\,\underline{k}} \xi_j(\underline{k}) \left[a_j^+(\underline{k}) + a_j(-\underline{k}) \right] \sigma^z(\underline{k})\end{aligned} \tag{6.40}$$

where the relationship between $\zeta_j(\underline{k})$ and $\xi_j(\underline{k})$ is given by (B.10). Applying the transformation (1.33) to displaced phonon operators $\gamma_j(\underline{k})$ (6.40) becomes *

$$\begin{aligned}\mathcal{H} = &- \Delta \sum_l \sigma^x(l) - \tfrac{1}{2} \sum_{l,l'} J(l,l') \sigma^z(l)\sigma^z(l') - \gamma e \sum_l \sigma^z(l) \\ &- \tfrac{1}{4} \sum_{l,l',l'',l'''} J^{(4)}(l,l',l'',l''') \sigma^z(l)\sigma^z(l')\sigma^z(l'')\sigma^z(l''') + \tfrac{1}{2} V c_0 e^2 \\ &- \sum_{j\neq f} \sum_{\underline{k}} \left[\gamma_j^+(\underline{k}) \gamma_j(\underline{k}) + \tfrac{1}{2} \right] \hbar\omega_j(\underline{k})\end{aligned} \tag{6.41}$$

Although it is hard to determine from first principles the parameters that appear in (6.41) it is nonetheless a relatively simple description of a complicated lattice

---

*In (6.41) $J(l,l')$ is given by

$$J(l,l') = q(l,l') + \sum_{j\,\underline{k}} \frac{2|\xi_j(\underline{k})|^2}{\hbar\omega_j(\underline{k})} \exp\left[i\underline{k}\cdot(\underline{R}(l) - \underline{R}(l')) \right]$$

dynamical system. Indeed apart from the four spin term (6.41) is formally identical with the model Hamiltonian for $DyVO_4$ (1.34), whose properties have been fully discussed in chapters 2 and 3.

The pseudospin formalism for KDP was first suggested by DeGennes [72] to describe Blinc's proton tunnelling model [55], and later extended to include proton-phonon coupling by Kobayashi [73]. It is important to stress that in their treatment the pseudospins refer to the tunnelling of a single proton only We believe it is more satisfactory to focus attention on the displacements of all the atoms in the unit cell, observed below T_D by neutron diffraction [48], as is done in the local mode theory. A particular advantage of this approach is that only one pseudospin per unit cell is required instead of four in the proton tunnelling picture. It will be shown in §6.5 that this leads to substantially better agreement with polarization and dielectric measurements.

6.4 Calculation of the elastic constants.

The model Hamiltonian (6.41) for KDP is slightly different from that for $DyVO_4$ (1.34) because of the addition of the term involving four spin operators. In this section it will be shown that only small modifications are necessary to the theory of the elastic constants discussed in Chapter 2 but that the temperature dependence of the order parameter is greatly altered by the extra term and in fact a first order transition is possible.

In the molecular field approximation the energy E, is given by

$$E = -N\Delta\langle\sigma^x\rangle - \tfrac{1}{2}NJ(0)\langle\sigma^z\rangle^2 - \eta e\langle\sigma^z\rangle$$

$$- \tfrac{1}{4}J^{(4)}(0)\langle\sigma^z\rangle^4 + \tfrac{1}{2}Vc_0e^2 + \sum_{j\neq f}\sum_{\underline{k}} n_j(\underline{k})\hbar\omega_j(\underline{k}) \qquad (6.42)$$

where $J^{(4)}(0) = \sum_{l'l''l'''} J^{(4)}(l,l',l'',l''')$

and $H_e = J(0)\langle\sigma^z\rangle + \eta e + J^4(0)\langle\sigma^x\rangle^4$

(6.43)

is the z component of the molecular field $\underline{W}$, given by

$$\underline{W} = H_e\,\hat{\underline{z}} + \Delta\,\hat{\underline{x}}$$

and $n_j(\underline{k})$ is the phonon occupation number (2.3). In this approximation the entropy S can be written as

$$S = -\frac{N}{2}\left\{(1+\langle\sigma\rangle)\ln\left(\frac{1+\langle\sigma\rangle}{2}\right) + (1-\langle\sigma\rangle)\ln\left(\frac{1-\langle\sigma\rangle}{2}\right)\right\} \qquad (6.44)$$

where

$$\langle\sigma\rangle = \left[\langle\sigma^x\rangle^2 + \langle\sigma^z\rangle^2\right]^{1/2}$$

is the expectation value of the spin component parallel to the molecular field $\underline{W}$.

Minimising the free energy F=E - TS with respect to $\langle\sigma^x\rangle$ and $\langle\sigma^z\rangle$ the following self consistency conditions are obtained:

$$\langle\sigma^x\rangle = \frac{\Delta}{W}\tanh\left(\frac{W}{kT}\right)$$

$$\langle\sigma^z\rangle = \frac{He}{W}\tanh\left(\frac{W}{kT}\right) \qquad (6.45)$$

The stress of B_2 symmetry is given by

$$\beta = \frac{1}{V}\left(\frac{\partial F}{\partial e}\right)_T = c_0e - \eta\frac{N}{V}\langle\sigma^z\rangle \qquad (6.46)$$

and the elastic constant, evaluated under thermodynamic constraints specified by the suffix γ (see Chapter 2 for a discussion of the possible thermodynamic regimes) is given

by

$$\frac{c_\gamma}{c_0} = 1 - \frac{\mu}{3}\left(\frac{\partial\langle\sigma^z\rangle}{\partial\epsilon}\right)_\gamma \qquad (6.47)$$

or

$$\frac{c_\gamma}{c_0} = \frac{1 - [J' + 3J^{(4)}(0)\langle\sigma^z\rangle^2]\,g_\gamma}{1 - [J(0) + 3J^{(4)}(0)\langle\sigma^z\rangle^2]\,g_\gamma}$$

where

$$\mu = \left(\frac{N}{V}\right)\frac{\gamma^2}{c_0}, \quad g_\gamma = \left(\frac{\partial\langle\sigma^z\rangle}{\partial H_e}\right)_\gamma$$

and

$$J' = J(0) + \mu$$

(c.f. (2.13)). Since the expression (6.45) for $\langle\sigma^z\rangle$ is identical with that for $DyVO_4$ when written in terms of H_e the g_γ are formally given by the same expressions as for $DyVO_4$, i.e., (2.18), (2.19), (2.20) and (2.22), with C_{H_e}, the specific heat of the spin system at constant H_e given by

$$C_{He} = \frac{1}{k}\left(\frac{W}{T}\right)^2\left[1 - \tanh^2\left(\frac{W}{kT}\right)\right]$$

However the temperature variation of $\langle\sigma^z\rangle$ and hence the elastic constants can be very different in the two cases. This can easily be seen by putting $\Delta=0$ for simplicity and using Landau's [1] theory of second order phase transitions, expanding the free energy as a power series in $\langle\sigma^z\rangle$. One obtains

$$\frac{F}{Nk} = \frac{1}{2}\left(kT - J'\right)\langle\sigma^z\rangle^2 + \frac{1}{12}\left(kT - 3J^{(4)}(0)\right)\langle\sigma^z\rangle^4 + \frac{kT}{30}\langle\sigma^z\rangle^6 + \cdots \qquad (6.48)$$

If the coefficient of $\langle\sigma^z\rangle^4$ is positive at the transition, i.e. if $kT_D > 3J^{(4)}(0)$ it is well known that the transition is

of second order and occurs when the coefficient of $\langle\sigma^z\rangle^2$ vanishes, i.e. $kT_D=J'$. Just below T_D one can readily show that

$$\langle\sigma^z\rangle \propto (T_D-T)^{1/2} \tag{6.49}$$

On the other hand if $kT_D\leq 3J^{(4)}(0)$ the transition is of first order. Recent measurements of the specific heat [81] and polarization [49] indicate that the phase change in KDP is, indeed just first order, the difference between T_D and the temperature θ at which the polarization would extrapolate to zero being only $0.026^{\circ}K$. This implies that $3J^{(4)}(0)-kT_D$ is small but positive for which the theory predicts

$$\langle\sigma^z\rangle \propto (\theta-T)^{1/4} \tag{6.50}$$

We do not expect that making Δ non zero will qualitatively affect these conclusions.

The frequencies of the elementary excitations can easily be calculated using the techniques of Chapter 3. The approximation used there was to ignore correlations between pairs of operators AB by putting

$$(A-\langle A\rangle)(B-\langle B\rangle)\approx 0 \tag{6.51}$$

Because of the extra term involving four spin operators in (6.41) it is now necessary to decouple products of four operators ABCD. The approximation corresponding to (6.51) is

$$(A-\langle A\rangle)(B-\langle B\rangle)(C-\langle C\rangle)(D-\langle D\rangle)=0$$

where products such as ABC are calculated by setting

$$(A-\langle A\rangle)(B-\langle B\rangle)(C-\langle C\rangle) = 0$$

and so on. One finally obtains the result that ABCD is replaced in this approximation by

$$A\langle B\rangle\langle C\rangle\langle D\rangle + B\langle C\rangle\langle D\rangle\langle A\rangle + C\langle D\rangle\langle A\rangle\langle B\rangle + D\langle A\rangle\langle B\rangle\langle C\rangle - 3\langle A\rangle\langle B\rangle\langle C\rangle\langle D\rangle. \tag{6.52}$$

The decoupled equations of motion corresponding to (3.1) are *

$$\begin{aligned}
\hbar \frac{d}{dt}\sigma^x(\underline{k}) &= 2\left[J'\langle\sigma^z\rangle + J^{(4)}(0)\langle\sigma^z\rangle^3\right]\sigma^y(\underline{k}) \\
\hbar \frac{d}{dt}\sigma^y(\underline{k}) &= -2\left[J'\langle\sigma^z\rangle + J^{(4)}(0)\langle\sigma^z\rangle^3\right]\sigma^x(\underline{k}) + 2\Delta\sigma^z(\underline{k}) \\
&\quad - 2\langle\sigma^x\rangle\left[J(\underline{k}) + 3J^{(4)}(\underline{k})\langle\sigma^z\rangle^2\right]\sigma^z(\underline{k}) \\
&\quad + 2\langle\sigma^x\rangle\sum_j \xi_j(\underline{k})\left[\gamma_j^+(\underline{k}) + \gamma_j(-\underline{k})\right] \\
\hbar \frac{d}{dt}\sigma^z(\underline{k}) &= -2\Delta\sigma^y(\underline{k}) \\
\hbar \frac{d}{dt}\gamma_j(\underline{k}) &= -i\hbar\omega_j(\underline{k}) - 2\Delta\frac{\xi_j(\underline{k})}{\hbar\omega_j(\underline{k})}\sigma^y(\underline{k})
\end{aligned} \tag{6.53}$$

and it is straightforward to show that the frequency of the acoustic branch $\omega_p(\underline{k})$ is given by

$$\lim_{k\to 0}\frac{\omega_p^2(\underline{k})}{\omega_a^2(\underline{k})} = \frac{1-\left(J'+3J^{(4)}(0)\langle\sigma^z\rangle^2\right)q_I}{1-\left(J(0)+3J^{(4)}(0)\langle\sigma^z\rangle^2\right)q_I} \tag{6.54}$$

In other words the equation of motion technique gives results for the elastic constants which correspond to the 'isolated' thermodynamic regime, as expected from the discussion of §3.1b.

---

* n.b. In (6.53) $J^{(4)}(\underline{k})$ is defined by

$$3J^{(4)}(\underline{k}) = \sum_{l,l',l'',l'''} J^{(4)}(l,l',l'',l'''\,)\left[e^{i\underline{k}\cdot[\underline{R}(l)-\underline{R}(l')]} + e^{i\underline{k}\cdot[\underline{R}(l)-\underline{R}(l'')]} + e^{i\underline{k}\cdot[\underline{R}(l)-\underline{R}(l''')]}\right]$$

6.5 Comparison of Theory with Experiment.

6.5(a) Neglecting four particle interactions.

If we neglect the term in (6.41) involving four spin operators, which, it will be recalled, was introduced to account of the Slater theory, the model for KDP is identical to that for $DyVO_4$ so the elastic constants are given by expressions (2.16), (2.18), (2.19), (2.20) and (2.22) with the averages $\langle\sigma^x\rangle$ and $\langle\sigma^z\rangle$ determined from (2.7) and (2.9). It was shown in Chapter 3 that a measurement of the sound velocity above the transition should determine $c_S(=c_T)$ and should vanish at $T=T_D$. In the low temperature phase one should measure c_S if $\omega\gg\tau_{SL}^{-1}$ and c_S, if $\omega\ll\tau_{SL}^{-1}$, where τ_{SL} is the spin-lattice relaxation time. The physical significance of the different thermodynamic regimes is discussed in §2.2.

For ferroelectric crystals it is necessary to specify the electrical boundary conditions in which the theory is valid. Since no account has been taken of a macroscopic electric field $\underline{E}$, the theory will only hold if $\underline{E}=0$ so the crystal must be short circuited during the measurement. The elastic constant determined under these conditions is denoted by c^E and is clearly strongly affected by coupling between the strains and the spin mode. In the opposite limit, where the polarization $\underline{P}$ is kept constant there is no response from the spin modes because $\underline{P}$ is proportional to $\langle\sigma^z\rangle$ so $c^P=c_o$. An experiment on an isolated crystal keeps the electric displacement $\underline{D}$ constant and, provided the dielectric constant is high, this is virtually equivalent to keeping $\underline{P}$ constant, i.e. $c^D\simeq c^P=c_o$.

The Brillouin scattering [74] and ultrasonic [37] measurements of c_{66}^{E} for KDP are plotted in figure 11. Above T_D the results lie on the same curve and fall to zero at the transition as expected, but no ultrasonic data could be obtained below T_D because of excessive damping. The solid curve of figure 11 is a plot of c_S, calculated from (2.16) and (2.20a), using values of $J'=134^{o}K$, $\Delta=67^{o}K$, $\mu=3.6^{o}K$ and $c_o=7.0 \times 10^{10}$ dyn.cm.$^{-2}$. An excellent fit to the data is obtained both above and below the transition. It was not, however, possible to obtain good agreement in the low temperature phase between the measurements and the theory for c_{S},, (see 2.22)) using reasonable values for the lattice specific heat C_L.

J' was chosen to give the correct transition temperature ($T_D=122^{o}K$), c_o is the value given by [37] for c^D near the transition. Kaminov and Damen [75] give a value of $71^{o}K$ for Δ. The frequency of the spin like mode $\omega_e(0)$ given by (3.6) would vanish at a temperature T_I called the 'clamped' transition temperature and from our data $T_D-T_I=4^{o}K$. This agrees with the value obtained from measurements of the high and low frequency susceptibilities [76].

The magnitude of the spontaneous polarization per unit volume, P, is given by

$$P = P_o \langle \sigma^z \rangle \qquad (6.55)$$

where P_0 is the dipole moment when fully ordered. P_0 can be estimated from the Curie constant in the paraelectric

phase, Neglecting Δ, which should be a good approximation for deuterated KDP, it can easily be shown (see §7.2) that the susceptibility above the transition is given in molecular field theory by

$$\chi^{zz} = \frac{V P_0^2}{N n} \frac{1}{k(T-T_0)} \qquad (6.56)$$

where n is the number of 'spins' per unit cell. In the local mode theory n=1 whereas in the proton tunnelling model n=4. Hence P_0 is related to the Curie constant C by

$$P_0 = \left(n \frac{N}{V} k C\right)^{1/2} \qquad (6.57)$$

Hill and Ichiki [77] find $C=322^{\circ}K$ for deuterated KDP so using (6.57) the local mode theory predicts $P_0=5.05_{\mu} C/cm.^3$. For small Δ the theory of Chapter 2 shows that $\langle \sigma^z \rangle \to 1$ as $T \to 0$ so we expect the saturation polarization to be given by P_0. This is in reasonable agreement with the experimental value [78] of 6.15 $_{\mu}C/cm.^3$. The discrepancy is perhaps due to an expansion of the bond in the ferroelectric phase. It is worth pointing out that the proton tunnelling model assumes four spins per unit cell so (6.57) is not well obeyed, as pointed out by Cochran [79].

For KDP, $C=256^{\circ}K$ [76] so (6.57) predicts $P_0=4.54$ $_{\mu}C/cm.^3$ which compares satisfactorily with the saturation polarization [78] of 5.12 $_{\mu}C/cm.^3$. However one should probably include the tunnelling frequency Δ in a treatment of KDP in which case the saturation value of P is less than P_0 and the agreement is not so good. In addition (6.57) is slightly modified (see §7.2) also in a way to make the agreement worse.

Considering the crude nature of the approximations that have been made and the possibility of an expansion of the bond length in the ferroelectric phase we feel that the disagreement between (6.57) and the experimental results is not large enough to discredit the local mode theory.

The temperature dependence of polarization just below the transition is, however, less well described. The most recent measurements are those of Benepe and Reese [80] who used a polaroelectrocaloric technique based on measurement of the temperature changes produced by adiabatic changes in the polarization. They find that the polarization jumps discontinuously to $P=1.87\ \mu C/cm.^2$ and that near the transition $P \alpha (\theta-T)^{1/6}$ where $\theta=T_D+0.026^{\circ}K$.

As mentioned in §6.4 the theory predicts a second order phase change with $P \alpha (T_D-T)^{\frac{1}{2}}$ when the four spin interaction parameter $J^{(4)}(0)$ is set equal to zero which cannot possibly explain the data of [49]. Cummins (preprint) has also pointed out that a simple Landau type theory gives a very poor fit to the polarization data. It would appear, then, that the agreement between the theory for c_S and the Brillouin scattering data in the ferroelectric phase is fortuitous. Furthermore it is probable in a highly anharmonic crystal such as KDP that τ_{SL}^{-1} is greater than the frequency of the phonons generated in the Brillouin scattering experiment ($\sim 10^{10} H_z$) so one would expect from the discussion of §3.2 to measure c_S,(2.22) rather than c_S(2.20a).

Benepe and Reese have proposed a phenomenological form for the free energy of KDP which fits their polarization data

and the specific heat data of [81] very well. They took

$$F = \tfrac{1}{2}\alpha P^2 + \tfrac{1}{4}\beta P^4 + \tfrac{1}{8}\delta P^8 \qquad (6.58)$$

with $\alpha=(4\Pi/C)(T-\theta)=3.867 \times 10^{-3}(T-\theta)$, $\beta=-4.4 \times 10^{-12}$cm.^{4}/esu^2 and $\delta=2.96 \times 10^{-27}$cm.^{12}/esu, where C is the Curie constant and $\theta=T_D-0.012^{\circ}$K. The coefficient of P^4 is small but negative so the transition is slightly first order. The expression (6.58) neglects a possible sixth order term but includes the coefficient of P^8 so

$$P \propto (\theta - T)^{1/6} \qquad (6.59)$$

close to the transition as observed. Cummins (preprint) has shown that the same free energy gives a satisfactory description of the elastic constant data. He calculates the 'true' adiabatic modulus assuming the crystal comes to local thermal equilibrium, which is equivalent to c_S, in the spin model. As discussed in the previous section adding a four spin term to the Hamiltonian, to represent the restrictions on the proton configurations proposed by Slater, can lead to a fourth order term which is small but negative as required. There does not, however, seem to be any justification for neglecting the sixth order term in our model. Nonetheless we might expect to obtain a better description of the data by including four spin interactions, as discussed in the next section.

6.5(b) Including four particle interactions.

The polarization data of Benepe and Reese [49] is shown in figure 12 together with the older data of Von Arx

and Bantle [82]. We shall assume that the recent measurements of [49] are the more reliable. The full curve in figure 12 is calculated from the free energy (6.58) and gives an excellent fit to the data. The best fit in the pseudo-spin model is obtained with $J^{(4)}(0)=49.8^{o}K$ and $P_0=7.86\ \mu C/cm.^3$, as shown by the dashed curve in figure 12. We took $\Delta=67^{o}K$ (and hence $J'=134^{o}K$ to give T_D correctly) as in the previous section but a comparable fit was obtained for a range of values of Δ. The agreement is not so good as for Benepe and Reese's theory because the observed temperature dependence of $P \propto (\theta-T)^{\frac{1}{2}}$ is built into their theory whereas we predict $P \propto (\theta-T)^{\frac{1}{4}}$. Well below T_D $\langle\sigma^z\rangle \to 0.925$ so the saturation polarization is calculated to be $7.26\ \mu C/cm.^3$ which is significantly larger than the measured value of $5.12\ \mu C/cm.^3$ [78]. This discrepancy is again due to the theory predicting the wrong power law behaviour below T_D.

The theory for the elastic constants is unchanged above the transition by the inclusion of the four spin term except that c_S no longer tends to zero at T_D but at a slightly lower temperature θ. However taking the parameters from the fit to the polarization data one obtains $T_D-\theta=0.045^{o}K$, which is too small to be detected.

Figure 13 shows the experimental results of Brody and Cummins [74] together with the theory for c_S, $c_{S'}$, and c_T using the parameters taken from the fit to the polarization data and with $\mu=3.6^{o}K$, which gives the best fit to the data for c_{66} above T_D. Good agreement between the theory for $c_{S'}$ and the data is obtained with $C_L=4.2Nk$. C_L can be determined

from the specific heat measurements of [80], [81] by subtracting off the anomolous part, which is the contribution from the pseudospins. The value given in [80] is 63.8 J/mol, $=2\times 63.8/8.32$ Nk$= 15.6$ Nk, the factor of 2 arising because there are two formula units in the unit cell. This is considerably larger than the value taken above to fit the data.

It appears that including a term in the Hamiltonian to represent the Slater-Takagi model in detail can give a better fit to the data than the simple theory of §6.5(i). There are, however, a number of unsatisfactory features, namely the polarization does not extrapolate to the measured value at low temperatures and one must take too small a value for the lattice specific heat in the theory for c_S.

It is worth mentioning that there are many hydrogen bonded ferroelectrics isomorphic to KDP [82] and in all cases the transition is observed to be slightly first order, although the transition temperatures vary considerably. The four spin interaction parameter $J^{(4)}(0)$ must be within a narrow range of values to obtain this behaviour, in particular for zero tunnelling $J^{(4)}(0)$ must be slightly greater than $\frac{1}{3}J'$. It seems remarkable that J', which determines the transition temperature, should vary considerably from substance to substance yet the ratio of $J^{(4)}(0)$ to J' be almost identical in each case.

Blinc and Svetina [83] have investigated the behaviour of a pseudospin Hamiltonian similar to (6.41) in a four particle cluster theory. In the limit of $\Delta=0$ their results are identical with those of Silsbee, Uehling and Schmidt [62],

whose treatment is basically an extension of Slater's [60]. For $\Delta \neq 0$ however the results of [83] are very complicated and are not satisfactory at very low temperatures since an anti-Curie temperature, where the ordering disappears, is predicted. Nonetheless we feel it would be interesting to extend the theory of [83] to calculate the elastic constants and to compare the estimate for the spontaneous polarization with the data of Benepe and Reese to see if the difficulties in our molecular field treatment can be overcome.

On the other hand the phenomenological free energy (6.58) proposed by Benepe and Reese does fit the data very well and differs from our model principally in neglecting the coefficient of P^6. There is, unfortunately, no existing microscopic model which leads to a free energy of this form. It would appear then that a completely satisfactory theory of hydrogen bonded ferroelectrics has yet to appear.

CHAPTER 7

EFFECT OF TWO PHONON COUPLING ON THE LOW FREQUENCY PROPERTIES OF HYDROGEN BONDED FERROELECTRICS

It has recently been shows by Cowley and Coombs [71] on the basis of weakly anharmonic phonon theory that coupling between the soft mode and pairs of phonons, in ferroelectrics which are piezoelectric above the transition, leads to an anomalous dielectric response at low frequency. From an analysis of Raman scattering data [70], [84] they suggest that this effect is large in the hydrogen bonded ferroelectrics KDA and CsDA.

In §7.2 it will be shown that a similar anomaly in the dielectric response is expected for the pseudospin model discussed in Chapter 6. The effect of two phonon coupling on the elastic constants will be considered in §7.3. The theory for the Raman scattering intensity in the pseudospin model is shown to be very similar to that in the anharmonic phonon description. From a careful analysis of the data [85] we conclude that the size of this anomalous low frequency behaviur is much smaller than was first suggested [70], [71], [84].

7.1 Green functions and correlation functions.

Many properties of crystals can be described in terms of retarded Green functions $G^{AB}(t)$ and their corresponding

Fourier transforms $G^{AB}(\omega)$ defined by

$$G^{AB}(t) = \ll A(t), B(0) \gg$$

$$= \frac{2\pi i}{\hbar} \theta(t) \langle [A(t), B(0)] \rangle \qquad (7.1)$$

and

$$G^{AB}(\omega) = \frac{1}{2\pi} \int_{-\infty}^{\infty} G^{AB}(t) e^{i\omega t} dt \qquad (7.2)$$

where A(t) and B(t) are operators in the Heisenberg representation, $\theta(t)$ is the unit unit step function defined by

$$\theta(t) = \begin{cases} 1 & t > 0 \\ 0 & t < 0 \end{cases}$$

and [A,B] indicates the commutator of A with B. Apart from a numerical factor (7.1) is just the definition adopted by Zubarev [86] who shows that $G^{AB}(\omega)$ is a response function of the system. The system is assumed to be initially in thermal equilibrium so the probability P_i of the system being in the ith state is determined by a canonical distribution. An external force $Fe^{i\omega t}$ is applied slowly while the system remains isolated, that is the probabilities P_i remain unchanged. To account for this perturbation a term such as $-BFe^{i\omega t}$ must be added to the Hamiltonian. On taking the limit $F \to 0$ Zubarev shows that

$$\langle A(t) \rangle = G^{AB}(\omega) F e^{i\omega t}. \qquad (7.3)$$

$G^{AB}(\omega=0)$ is therefore the static susceptibility evaluated for the 'isolated' thermodynamic regime discussed in §2.2. The Green functions must have poles at frequences of the

elementary excitations since fluctuations occur at these frequencies with no external force.

To investigate the dynamics of crystals it is interesting to study certain correlation functions $J^{AB}(t)$ and their Fourier transforms $J^{AB}(\omega)$ defined by

$$J^{AB}(t) = \langle B(0) A(t) \rangle \tag{7.4a}$$

$$\text{and} \quad J^{AB}(\omega) = \frac{1}{2\pi} \int_{-\infty}^{\infty} J^{AB}(t) e^{i\omega t} dt. \tag{7.4b}$$

The Fourier transform of $\langle A(t)\ B(0) \rangle$ is related to $J^{AB}(\omega)$ by [86]

$$\frac{1}{2\pi} \int_{-\infty}^{\infty} \langle A(t)\ B(0) \rangle e^{i\omega t} dt = e^{\hbar\omega/kT} J^{AB}(\omega). \tag{7.5}$$

From the fluctuation dissipation theorem [87] which relates thermal fluctuations to the dissipative part of the appropriate complex susceptibility, it can be shown that

$$J^{AB}(\omega) = \frac{\hbar}{\pi} \frac{Im\ G^{AB}(\omega)}{e^{\hbar\omega/kT} - 1} \tag{7.6}$$

There are Kramers-Kronig relations between the real and imaginary parts of G [86] so a knowledge of J is sufficient to determine G completely. However the boundary conditions are difficult to define for the correlation functions so it is easier to determine the Green functions first of all and then use (7.6) to calculate the correlation functions.

To evaluate $G^{AB}(\omega)$ one starts by writing the equation of motion of $G^{AB}(t)$

$$i\hbar \frac{d}{dt} \ll A(t), B(0) \gg = -2\pi \delta(t) \langle [A, B] \rangle + \ll [A(t), \mathcal{H}(t)], B(0) \gg \tag{7.7}$$

Taking the Fourier transform of (7.7) and assuming $G^{AB}(t\to\infty)=0$ one obtains the equation of motion of $G^{AB}(\omega)= \ll A,B \gg_\omega$

$$\hbar\omega \ll A,B \gg_\omega = -\langle [A,B] \rangle + \ll [A,\mathcal{H}], B \gg \tag{7.8}$$

This equation involves Green functions of a higher order for which one can again write equations of the form (7.8). The resulting chain of equations must be decoupled at some stage. Assuming this can be done $G^{AB}(\omega)$ and hence $J^{AB}(\omega)$ are determined.

7.2 An anomalous dielectric response at low frequencies.

Interactions between the soft mode and pairs of phonons are of the form (6.35) which can be written as

$$\mathcal{H}_{2p} = \frac{1}{2N^{1/2}} \sum_{\underline{k},1,2} V(\underline{k},1,2)\, \sigma^z(\underline{k})\, A_1 A_2 \tag{7.9}$$

where, for ease of notation, the two suffices j and $\underline{k}$ have been replaced by a single suffix 1,2 etc., and

$$A_1 = a_1 + a_{-1}^+ \tag{7.10}$$

To keep the treatment as simple as possible the four spin terms in (6.41) will be neglected. This has no effect in molecular field theory above the transition, which is the main region of interest here. In this section the difference between the displaced phonon operators γ, defined by (1.33) and the unperturbed phonon operators a will be neglected. A correct treatment of the phonons, necessary to calculate the elastic constants, will be discussed in §7.3.

Since the polarization is proportional to $\langle \sigma^z \rangle$ the contribution of the soft mode to the dielectric response is determined by the Green function $\ll\sigma^z(\underline{k}),\sigma^z(-\underline{k})\gg$. From (7.8) the equation of motion of $\ll\sigma^z(\underline{k}),\sigma^z(-\underline{k})\gg$ is

$$\hbar\omega \ll\sigma^z(\underline{k}),\sigma^z(-\underline{k})\gg = -2i\Delta \ll\sigma^y(\underline{k}),\sigma^z(-\underline{k})\gg \tag{7.11a}$$

and similarly the equation of motion of $\ll\sigma^y(\underline{k})\sigma^z(-\underline{k})\gg$ is

$$\begin{aligned}\hbar\omega \ll\sigma^y(\underline{k}),\sigma^z(-\underline{k})\gg = {} & -2i\Delta\langle\sigma^x\rangle + 2i\Delta \ll\sigma^z(\underline{k}),\sigma^z(-\underline{k})\gg \\ & - \frac{2i}{N^{1/2}} \sum_{\underline{k}'} J(\underline{k}') \ll\sigma^x(\underline{k}+\underline{k}')\sigma^z(-\underline{k}'),\sigma^z(-\underline{k})\gg \\ & - \frac{2i}{2N} \sum_{\underline{k}',1,2} V(\underline{k}',1,2) \ll\sigma^x(\underline{k}+\underline{k}')A_1A_2,\sigma^z(-\underline{k})\gg\end{aligned} \tag{7.11b}$$

The three spin Green function in (7.11b) is decoupled in the same approximation that was used in Chapter 3 for the equations of motion of the operators, i.e. we set

$$\ll\sigma^\alpha\sigma^\beta,\sigma^\gamma\gg = \langle\sigma^\alpha\rangle\ll\sigma^\beta,\sigma^\gamma\gg + \langle\sigma^\beta\rangle\ll\sigma^\alpha,\sigma^\gamma\gg \tag{7.12}$$

To decouple the Green functions involving phonon operators satisfactorily it is necessary to consider products of two phonon operators as a single entity and write

$$\ll\sigma^\alpha A_1A_2,\sigma^\beta\gg = \langle\sigma^\alpha\rangle\ll A_1A_2,\sigma^\beta\gg + \langle A_1A_2\rangle\ll\sigma^\alpha,\sigma^\beta\gg. \tag{7.13}$$

Considering only the high temperature phase, for which $\langle\sigma^z\rangle = \langle A_1A_2\rangle = 0$, one obtains from (7.11), (7.12) and (7.13)

$$\begin{aligned}\hbar^2(\omega_E^2(\underline{k})-\omega^2)\ll\sigma^z(\underline{k}),\sigma^z(-\underline{k})\gg = {} & 4\Delta\langle\sigma^x\rangle \\ & + \frac{4\Delta\langle\sigma^x\rangle}{2N^{1/2}} \sum_{1,2} V(\underline{k},1,2) \ll A_1A_2,\sigma^z(-\underline{k})\gg,\end{aligned} \tag{7.14}$$

where

$$\frac{1}{4}\hbar^2\omega_E^2(\underline{k}) = \Delta\left[\Delta - J(\underline{k})\langle\sigma^x\rangle\right] \tag{7.15}$$

as in (3.4). We denote by $G_o^{zz}(\underline{k},\omega)$ the value of $\langle\langle\sigma^z(\underline{k}),\sigma^z(-\underline{k})\rangle\rangle$ when the coefficients V are set equal to zero, i.e.

$$G_o^{zz}(\underline{k},\omega) = \frac{4\Delta\langle\sigma^x\rangle}{\hbar^2(\omega_E^2(\underline{k})-\omega^2)} \tag{7.16}$$

The static electric susceptibility χ (see §6.5(i)) is given by

$$\chi = \frac{P_o^2}{Nn}\, G_o^{zz}(0,0) \tag{7.17}$$

if two phonon coupling is unimportant. For $\Delta\to 0$ (7.17) becomes

$$\chi = \frac{P_o^2}{Nn}\,\frac{1}{k(T-T_0)} \tag{7.18}$$

the result quoted in (6.56).

Omitting most of the symbols for clarity (7.14) can be written symbolically as

$$G^{zz} = G_o^{zz} + G_o^{zz}\, V\, G^{pp,z} \tag{7.19}$$

where

$$G^{pp,z} = \langle\langle\, A\,A,\,\sigma^z\rangle\rangle$$

Following the same arguments it is straightforward to show that

$$G^{z,pp} = G_o^{zz}\, V\, G^{pp,pp} \tag{7.20}$$

where $G^{pp,pp} = \langle\langle A\,A\,,\,A\,A\rangle\rangle$

is the two phonon Green function. From time reversal symmetry one can prove that $G^{z,pp}=G^{pp,z}$ so combining this result with (7.19) and (7.20) one finds

$$G^{zz} = G_o^{zz} + G_o^{zz} V\ G^{pp,pp} V\ G_o^{zz} \tag{7.21}$$

In the absence of coupling to the spins it is easy to calculate the two phonon Green function, which is denoted by $G_o^{pp,pp}$ in this limit. The phonons propagate independently so decoupling can be performed immediately to give

$$\begin{aligned} G_o^{pp,pp}(1,2,t) &= \ll A_1(t)\ A_2(t),\ A_{-1}(0)\ A_{-2}(0) \gg \\ &= \langle A_1(t) A_{-1}(0)\rangle \ll A_2(t),\ A_{-2}(0)\gg \\ &\quad + \langle A_{-2}(0) A_2(t)\rangle \ll A_1(t), A_{-1}(0)\gg \end{aligned} \tag{7.22}$$

In the absence of interactions the single phonon Green function $\ll A_1, A_{-1}\gg$ is equal to

$$\frac{2\omega_1}{\hbar(\omega_1^2-\omega^2)} = \frac{1}{\hbar(\omega_1+\omega)} + \frac{1}{\hbar(\omega_1-\omega)} \tag{7.23}$$

and the equivalent correlation function can be calculated from (7.6). Performing a convolution integral on (7.22) yields

$$\begin{aligned} G_o^{pp,pp} &= \frac{n_1+n_2+1}{\hbar(\omega+\omega_1+\omega_2)} + \frac{n_1+n_2+1}{\hbar(-\omega+\omega_1+\omega_2)} + \frac{n_1-n_2}{\hbar(\omega+\omega_2-\omega_1)} \\ &\quad + \frac{n_2-n_1}{\hbar(\omega+\omega_1-\omega_2)} \end{aligned} \tag{7.24}$$

where n_α is the usual phonon occupation number (2.3). The

equation of motion of $G^{pp,pp}$ the full 2 phonon Green function, can be expressed in terms of $G_o^{pp,pp}$ as

$$G^{pp,pp} = G_o^{pp,pp}\left[1 + V G^{z,pp}\right]. \tag{7.25}$$

Rearranging (7.19), (7.21) and (7.25) yields the desired expression for G^{zz}

$$G^{zz} = \frac{G_o^{zz}}{1 - V G_o^{pp,pp} V G_o^{zz}}. \tag{7.26}$$

Comparing (7.26) with the Dyson equation

$$G = G_o/[1 - \Sigma G_o]$$

one sees that the self energy Σ is given by

$$\Sigma = V G_o^{pp,pp} V. \tag{7.27}$$

In other words the propagation of a spin wave is altered by the spin wave decaying into a pair of virtual phonons which propagate independently (in this approximation) as described by $G_o^{pp,pp}$ before recombining to form the spin wave again. Including the suffices equation (7.26) becomes

$$G^{zz}(\underline{k},\omega) = \frac{4\Delta\langle\sigma^x\rangle}{4\Delta\left[\Delta - \{J(\underline{k}) + V(\underline{k},\omega)\}\langle\sigma^x\rangle\right] - \hbar^2\omega^2} \tag{7.28}$$

where

$$V(\underline{k},\omega) = \frac{1}{2N}\sum_{1,2}|V(\underline{k},1,2)|^2\left\{\frac{n_1+n_2+1}{\hbar(\omega+\omega_1+\omega_2)} + \frac{n_1+n_2+1}{\hbar(-\omega+\omega_1+\omega_2)} + \frac{2(n_2-n_1)}{\hbar(\omega+\omega_1-\omega_2)}\right\}. \tag{7.29}$$

Cowley and Coombs [71] have derived a very similar result for a weakly anharmonic phonon model by diagrammatic techniques. It will be noticed that in the spin model, two phonon coupling leads to an extra contribution to the spin-spin interaction $J(\underline{k})$, which is both frequency and temperature dependent.

As pointed out in [71], the first term in (7.29) is not well behaved in the limit $\underline{k}\to 0$, $\omega\to 0$ if modes 1 and 2 belong to the same branch and so have the same energy. This difficulty arises because of the rather unphysical assumption that the two phonons propagate freely so the frequencies $\pm\omega_1$ for example that appear in (7.29) are the poles of the single particle Green function for a perfect crystal (7.23). In practice interactions with other modes lead to damping and provided this small the Green function may be written as

$$\frac{2\omega_1}{\hbar(\omega_1^2 - i\omega\gamma_1 - \omega^2)} \tag{7.30}$$

which has poles at

$$\omega_\pm = -\frac{i\gamma}{2} \pm \omega_1 \tag{7.31}$$

if $\gamma_1 \ll \omega_1$. Hence the first term inside the curly brackets of (7.29) becomes

$$2\cdot\frac{i\gamma(\partial n/\partial\omega)}{\hbar(\omega + i\gamma_1)} = \frac{2n_1(n_1+1)}{kT}\cdot\frac{1}{1-i\omega\tau_1} \tag{7.32}$$

where

$$\tau_1 = 1/\gamma_1$$

The spin wave will also have a width γ_s which would appear in a more sophisticated theory. Assuming all the phonons have the same lifetime, which we denote by τ_{LL}, then for small $\underline{k}$ and ω

$$G^{zz}(\underline{k},\omega) = \frac{4\Delta\langle\sigma^x\rangle}{k^2\left[\bar{\omega}_E^2(\underline{k}) - i\omega\gamma_s - \omega^2\right] - 4\Delta\langle\sigma^x\rangle \frac{L}{1-i\omega\tau_{LL}}} \qquad (7.33)$$

where

$$L = \frac{1}{N}\frac{1}{kT}\sum_{1,2} |V(\underline{k},1,2)|^2 n_1(n_1+1) \qquad (7.34)$$

and where the terms in $V(\underline{k},\omega)$ that are well behaved at $\omega=0$ have been incorporated into $\bar{\omega}_E^2(\underline{k})$. At high temperatures L is proportional to T so we can write

$$L = \alpha kT \qquad (7.35)$$

where α is a dimensionless parameter.

At high frequencies, where $\omega\tau_{LL} \gg 1$, this is similar to the simple result (7.16) for G_o^{zz} where the susceptibility arises from a mode at finite frequency. However at low frequencies there is an additional contribution to (7.33) which increases the real part of the dielectric constant and also increases the damping.

For $\Delta \ll kT$

$$\bar{\omega}^2\omega_E^2 = 4\Delta^2\left[1 - \frac{T_o}{T}\right] \qquad (7.36)$$

where T_o is related to the transition temperature T_D, at which (7.33) diverges, by

$$T_D = T_o(1+\alpha) \qquad (7.37)$$

Consequently as T approaches T_D from above $\bar{\omega}_E$ decreases but it is the response at low frequencies which diverges and induces the transition before $\bar{\omega}_E$ becomes zero.

These results can readily be extended to the ferroelectric phase. The equation of motion of the one phonon Green function $\ll A_1, A_{-1} \gg$ is

$$\hbar^2[\omega_1^2 - \omega^2] \ll A_1, A_{-1} \gg = 2\hbar\omega_1 + \frac{2\hbar\omega_1}{N^{1/2}} \sum_{2,\underline{k}} V(\underline{k},1,2) \ll \sigma^2(\underline{k})\, A_2, A_1 \gg \tag{7.38}$$

The simplest approximation is to decouple at this stage so

$$\hbar^2[\omega_1^2 - \omega^2] \ll A_1, A_{-1} \gg = 2\hbar\omega_1 [1 + \langle\sigma^2\rangle \sum_2 V(0,1,2) \ll A_2, A_{-1} \gg \tag{7.39}$$

Calculating the equations of motion for $\ll A_2, A_{-1} \gg$ and decoupling in the same way one obtains a set of linear equations for all Green functions of the form $\ll A_\alpha A_{-1} \gg$ where the modes α and 1 are coupled because of the non zero average of σ^z. These equations can in principle be solved to obtain the new eigenvalues ω_α' and eigenvectors A_α'.

As a particularly simple example consider the symmetry allowed coupling to a doubly degenerate branch of E symmetry at $\underline{k}$=0. One finds

$$\begin{aligned} \hbar^2[\omega^2 - \omega_1^2]\, A_1 &= 2\hbar\omega_1 \langle\sigma^z\rangle V(0,1,2)\, A_2 \\ \hbar^2[\omega^2 - \omega_1^2]\, A_2 &= 2\hbar\omega_1 \langle\sigma^z\rangle V(0,1,2)\, A_1 \end{aligned} \tag{7.40}$$

so

$$\hbar\omega_1' \simeq \hbar\omega_1 \pm |V(0,1,2)| \langle\sigma^z\rangle \tag{7.41}$$

Hence the E modes are split below the transition as expected in the reduced symmetry.

The decoupled equations of motion for the spin Green functions in the ordered phase are

$$\hbar\omega \ll \sigma^z(\underline{k}), \sigma^z(-\underline{k}) \gg = -2i\Delta \ll \sigma^y(\underline{k}), \sigma^z(-\underline{k}) \gg$$

$$\hbar\omega \ll \sigma^y(\underline{k}), \sigma^z(-\underline{k}) \gg = -2i\Delta + 2i\Delta \ll \sigma^z(\underline{k}), \sigma^z(-\underline{k}) \gg$$

$$- 2iJ(\underline{k}) \langle \sigma^x \rangle \ll \sigma^z(\underline{k}), \sigma^z(-\underline{k}) \gg - 2iJ' \ll \sigma^y(\underline{k}), \sigma^z(-\underline{k}) \gg$$

$$- \frac{2i}{2N^{1/2}} \sum_{1,2} V(\underline{k}, 1, 2) \langle \sigma^x \rangle \ll A_1 A_2, \sigma^z(-k) \gg$$

$$- \frac{2i}{2N^{1/2}} \sum_{1,2} V(0,1,2) \langle A_1 A_2 \rangle \ll \sigma^x(\underline{k}), \sigma^z(-\underline{k}) \gg$$

$$\hbar\omega \ll \sigma^x(\underline{k}), \sigma^z(-\underline{k}) \gg = 2i \left[J' \langle \sigma^z \rangle + \sum_{1,2} V(0,1,2) \langle A_1 A_2 \rangle \right] \ll \sigma^y(\underline{k}), \sigma^z(-\underline{k}) \gg \tag{7.42}$$

Thermal averages such as $\langle A_1 A_2 \rangle$ are determined from the equations of motion $A_1 A_2$. For example

$$i\hbar \frac{d}{dt} [a_1^+ a_2] = \hbar [\omega_2 - \omega_1] a_1^+ a_2 - \frac{1}{N^{1/2}} \sum_{\underline{k},3} V(\underline{k}, 3, 2) a_1^+ A_3 \sigma^z(\underline{k}) + \frac{1}{N^{1/2}} \sum_{\underline{k},3} V(\underline{k}, 1, 3) A_3 a_2 \sigma^z(\underline{k}) . \tag{7.43}$$

Taking the thermal average of both sides, noting that the average of the left hand side must vanish, and decoupling the right hand side in the usual way one obtains

$$\langle a_1^+ a_2 \rangle = \frac{n_2 - n_1}{\hbar(\omega_1 - \omega_2)} V(0,1,2) \langle \sigma^z \rangle \tag{7.44}$$

Similarly one can show that

$$\langle A_1 A_2 \rangle = 2 \left[\frac{n_2 - n_1}{\hbar(\omega_1 - \omega_2)} + \frac{n_1 + n_2 + 1}{\hbar(\omega_1 + \omega_2)} \right] V(0,1,2) \langle \sigma^z \rangle \tag{7.45}$$

Below T_D the phonon modes are mixed together because of the non zero average of $\langle \sigma^z \rangle$ as shown for instance by

(7.38). This means that the equation of motion of $\ll A_1 A_2, \sigma^z \gg$ in (7.42) involves products of different phonon operators so the equations become difficult to handle. However if the mixing is small, or more precisely if $|V(0,1,2)/\hbar[\omega_1 - \omega_2]| \ll 1$ then this effect can be ignored in a first approximation and everything goes through as before. With this assumption G^{zz} becomes

$$G^{zz}(\underline{k},\omega) = \frac{4\Delta\langle\sigma^x\rangle}{4\left[(J'+V(0,0))\langle\sigma^z\rangle\right]^2 + 4\Delta\left[\Delta - \{J(\underline{k})+V(\underline{k},\omega)\}\langle\sigma^x\rangle\right] - \hbar^2\omega^2} \tag{7.46}$$

Damping can be included in a phenomenlogical way as in the derivation of (7.33).

It should be pointed out that in addition to cubic terms of the form (7.9) interactions involving three spin operators of the form

$$\frac{1}{N^{1/2}} \sum_{\underline{k},\underline{k}'} U(\underline{k},\underline{k}')\sigma^z(\underline{k})\sigma^z(\underline{k}')\sigma^z(-\underline{k}-\underline{k}') \tag{7.47}$$

can also occur. Considering (7.47) but neglecting two phonon coupling (7.09) G^{zz} can be cast in a form similar to (7.26) but with $G_o^{pp,pp}$ replaced by $G_o^{zz,zz}$ the free two spin Green function. For $T > T_D$, $G_o^{zz,zz}$ is given by a form similar to (7.24) i.e.

$$G_o^{zz,zz} = \frac{[4\Delta\langle\sigma^x\rangle]^2}{4\hbar^2\omega_E(\underline{k})\omega_E(\underline{k}')}\left\{\frac{n_{\underline{k}}+n_{\underline{k}'}+1}{\hbar(\omega+\omega_E(\underline{k})+\omega_E(\underline{k}'))} + \frac{n_{\underline{k}}+n_{\underline{k}'}+1}{\hbar(-\omega+\omega_E(\underline{k})+\omega_E(\underline{k}'))} + \frac{2.(n_{\underline{k}}+n_{\underline{k}'})}{\hbar(\omega+\omega_E(\underline{k}')-\omega_E(\underline{k}))}\right\} \tag{7.48}$$

with $\omega_E(\underline{k})$ given by (7.15) and

$$n_{\underline{k}} = \left[\exp(\hbar\omega_E(\underline{k})/k^T) - 1\right]^{-1}$$

Hence the effects of (7.47) are qualitatively the same as those of the two phonon coupling (7.9) and will be neglected from now on. Interactions between two spin operators and a phonon are also allowed but do not give rise to an anomalous low frequency behaviour in G^{zz}.

7.3 Calculation of elastic constants.

In this section the effects of non-commutivity of the displaced phonon operators γ with the spin operators will be discussed. Adding (7.09) to the model Hamiltonian (6.41) but still neglecting the four spin term we can write the resulting Hamiltonian in the molecular field approximation as

$$\begin{aligned}\mathcal{H}_{m.f.} = & \sum_1 \hbar\omega_1 [\gamma_1^+ \gamma_1 + \tfrac{1}{2}] - \Delta \sum_l \sigma^x(l) - (J(0)\langle\sigma^z\rangle + \gamma e) \sum_l \sigma^z(l) \\ & - \frac{1}{2\sqrt{N}} \sum_{2,3} V(0,2,3) \left[\langle\sigma^z\rangle A_2 A_3 + \langle A_2 A_3\rangle \langle\sigma^z\rangle \right] \\ & + \tfrac{1}{2} N J(0) \langle\sigma^z\rangle^2 + \tfrac{1}{2} V c_0 e^2 + \sum_{2,3} V(0,2,3) \langle\sigma^z\rangle \langle A_2 A_3\rangle\end{aligned} \tag{7.49}$$

It will be assumed for simplicity that the phonons which couple directly to the spins do not also couple through the two phonon term (7.9). Diagonalizing the terms

$$\sum_2 a_2^+ a_2 \hbar\omega_2 - \sum_{2,3} V(0,2,3) \langle\sigma^z\rangle A_2 A_3 \tag{7.50}$$

to obtain the new phonon frequencies ω_2' and using the result

$$\frac{1}{2N^{1/2}} \sum V(0,2,3) \langle A_2 A_3\rangle = V(0,0) \langle\sigma^z\rangle \tag{7.51}$$

obtained from (7.45) one may rewrite (7.49) as

$$\mathcal{H}_{m.f.} = -\Delta \sum_l \sigma''(l) - [\{J(0) + V(0,0)\}\langle\sigma^z\rangle + 3e] \sum_l \sigma^z(l)$$
$$+ \tfrac{1}{2} N \left(J(0)+V(0,0)\right)\langle\sigma^z\rangle^2 + \sum_i \hbar\omega_i' n_i' + \tfrac{1}{2} N V(0,0)\langle\sigma^z\rangle^2$$

(7.52)

where a thermal average n_α' of pairs of phonon operators has been taken. The corresponding free energy is

$$F = -NkT \ln\left[2\cosh\left(\frac{W}{kT}\right)\right] + \tfrac{1}{2} N [J(0)+V(0,0)]\langle\sigma^z\rangle^2$$
$$+ \tfrac{1}{2} V c_0 e^2 + \tfrac{1}{2} V(0,0)\langle\sigma^z\rangle^2 + kT \sum_i \ln\left[1 - e^{-\hbar\omega_i'/kT}\right]$$
$$+ \tfrac{1}{2} \sum_i \hbar\omega_i'$$

(7.53)

where

$$W = \left[H_e^2 + \Delta^2\right]^{1/2}$$

(7.54)

with $H_e = \left(J(0) + V(0,0)\right)\langle\sigma^z\rangle + 3e$

This expression is rather complicated because the phonon frequencies ω_1' depend on $\langle\sigma^z\rangle$. However if $V(0,1,2)$ is small compared with $\omega_1 - \omega_2$ then $(\omega_1' - \omega_1)/\omega_1 \ll 1$ so it is a good approximation to consider only terms of order $\langle\sigma^z\rangle^2$ in the expression for ω_1'. After some algebraic manipulation the last three terms in (7.53) reduce to the unperturbed phonon contribution

$$kT \sum_i \ln\left[1 - e^{-\hbar\omega_i/kT}\right]$$

in this limit. The free energy (7.53) is now identical with the free energy of $DyVO_4$, whose properties were fully investigated in Chapter 2, except that there is an extra contribution $V(0,0)$ to the spin-spin interaction $J(0)$, arising from two phonon coupling. Taking over the theory of Chapter 2, the transition temperature T_D is given by

$$\frac{\Delta}{J'+V(0,0)} = \tanh\left(\frac{\Delta}{kT_0}\right) \tag{7.55}$$

and $\langle\sigma_x\rangle$ and $\langle\sigma^z\rangle$ are calculated from (2.7) and (2.9) respectively with H_e and W given by (7.54). The elastic constants are determined by (2.16), (2.18a), (2.19a), (2.20a) and (2.22) and vanish at the transition.

Whereas the static properties of our model are identical in form with those obtained for $DyVO_4$ in Chapter 2 it will now be shown, from the dynamics, that there is a marked frequency dependence in the elastic behaviour which is in contrast to the earlier treatment of $DyVO_4$.

Assuming that phonons which couple directly to the spins do not also contribute to the two phonon term (7.9) it is straightforward to show from the equations of motion that

$$G^{zz}(\underline{k},\omega) = \frac{4\Delta\langle\sigma^x\rangle}{4\left\{\left[(J'+V(0,0))^2\langle\sigma^z\rangle^2\right] + \Delta\left[\Delta - \{J(\underline{k})+V(\underline{k},\omega)\}\langle\sigma^x\rangle\right] - \hbar^2\omega^2 - \sum_i \frac{H_i\omega^2 4\Delta\langle\sigma^x\rangle}{(\omega_i^2-\omega^2)}\right.} \tag{7.56}$$

where $H_j(\underline{k}) = 2|\xi_j(\underline{k})|^2/\hbar\omega_j(\underline{k})$

According to the dynamic theory the transition occurs when $G^{zz}(0,0)$ diverges i.e.

$$\Delta = [J'+V(0,0)]\langle\sigma^x\rangle. \tag{7.57}$$

The static theory estimates the transition temperature from the appearance of a non zero value for $\langle\sigma^z\rangle$ and is given by (7.55). These two results, (7.55) and (7.57), are consistent with each other so molecular values of $\langle\sigma^x\rangle$ and $\langle\sigma^z\rangle$, calculated from (7.54), (2.7) and (2.9), may be

inserted in expression (7.56) for G^{zz}.

Considering just one acoustic phonon branch in the last term of (7.56), then for $\omega\tau_{LL} \ll 1$ the coupled mode frequencies, determined from the poles of G_{zz} are given by the solutions of

$$\hbar^2 [\omega^2 - \omega_a^2][\omega^2 - \omega_{E'}^2] = 4\Delta \langle \sigma_x \rangle \omega^2 K_a \tag{7.58a}$$

with

$$\tfrac{1}{4}\hbar^2 \omega_{E'}^2 = [J' + V(0,0)]^2 \langle \sigma_z \rangle^2 + \Delta[\Delta - \{J' + V(0,0)\}\langle \sigma_x \rangle] \tag{7.58b}$$

On the other hand for $\omega\tau_{LL} \gg 1$ the coupled mode frequencies are given by

$$\hbar^2 [\omega^2 - \omega_a^2][\omega^2 - \bar{\omega}_E^2] = 4\Delta \langle \sigma_x \rangle \omega^2 K_a \tag{7.59a}$$

where $\bar{\omega}_E^2$ is related to $\omega_{E'}^2$ by

$$\tfrac{1}{4}\hbar^2 \bar{\omega}_E^2 = \tfrac{1}{4}\hbar^2 \omega_{E'}^2 + \Delta \langle \sigma_x \rangle L \tag{7.59b}$$

The frequency of the acoustic like branch is given for these two cases by

$$\omega_p^2(\underline{k}) = \frac{\omega_{E'}^2}{\omega_e^2}\, \omega_a^2(\underline{k}) \tag{7.60a}$$

and

$$\omega_p^2(\underline{k}) = \frac{\bar{\omega}_E^2}{\bar{\omega}_e^2}\, \omega_a^2(\underline{k}) \tag{7.60b}$$

where

$$\tfrac{1}{4}\hbar^2 \omega_{e'}^2 = \tfrac{1}{4}\hbar^2 \omega_{E'}^2 + \Delta\mu \langle \sigma_x \rangle \tag{7.61a}$$

and

$$\frac{1}{4}\hbar^2\bar{\omega}_2^2 = \frac{1}{4}\hbar^2\bar{\omega}_E^2 + \Delta\mu\langle\sigma^{xx}\rangle \tag{7.61b}$$

For $\omega\tau_{LL}\ll 1$ where ω is the acoustic phonon frequency, the gradient of the acoustic branch vanishes at the transition. However for $\omega\tau_{LL}\ll 1$ the acoustic branch no longer flattens at T_D but extrapolates to zero at a lower temperature T_0 related to T_D by (7.37) (for $\Delta\ll kT_D$). The variation of the elastic constant with temperature in these two cases, calculated from (7.60a) and (7.60b), is shown schematically in figure 14.

It is interesting to discuss this frequency dependence in terms of the different thermodynamic regimes investigated in Chapters 2 and 3. As the tunnelling mode propagates it couples to pairs of phonons through (7.9) and induces fluctuations in the phonon occupation numbers which decay in a time τ_{LL} (7.32). These fluctuations can be regarded as a mode of the system of B_2 symmetry centred at $\omega=0$ and of width $1/\tau_{LL}$. In the regime $\omega\tau_{LL}\gg 1$, where there is no response from this mode, the populations of the phonon states remain constant so this corresponds to the 'isolated' regime, $\gamma=I$, defined in Chapter 2. For $\omega\tau_{LL}\ll 1$ the populations of the phonon states change in a way to bring the phonon system to local thermal equilibrium. This is just the 'essentially isolated' regime $\gamma=S$.

The experimental measurements of c_{66} on KDP by ultrasonic [37] and Brillouin scattering [74] techniques fall to zero at $T=T_D$. This leaves two possible conclusions:

(i) The frequencies in the Brillouin scattering experiment (~10 GHz) are much smaller than $^1/\tau_{LL}$;

(ii) The measuring frequency is greater than $^1/\tau_{LL}$ but two phonon coupling is weak.

Since KDP is highly anharmonic possibility (i) cannot be ruled out. However the size of two phonon coupling can be estimated more satisfactorily from Raman scattering data, which is the subject of the next section.

7.4 Estimate of size of two phonon coupling from Raman Scattering data.

7.4(a) Calculation of Raman scattering intensity.

The intensity of scattered light in a Raman experiment is related to fluctuations in the crystal, which are in turn related to the susceptibility as will be shown below. Hence Raman scattering is a suitable technique for investigating the low frequency response of hydrogen bonded ferroelectrics.

Denoting the polarization directions of the incident and scattered beams by suffices α and β respectively, the probability of the crystal undergoing a transition from state $|i\rangle$ to state $|f\rangle$ in which the light loses energy ω is proportional to [88]

$$I(\omega) = |\langle i|\chi^{\alpha\beta}|f\rangle|^2 \tag{7.62}$$

where $\chi^{\alpha\beta}$ is the polarizibility and

$$\hbar\omega = E_f - E_i \tag{7.63}$$

To calculate the total scattering intensity one must sum (7.62) over all final states $|f\rangle$ which satisfy (7.63) and sum over all initial states $|i\rangle$ multiplied by the probability ρ_i that the state $|i\rangle$ was initially populated. Therefore $i(\omega)$ becomes

$$i(\omega) = \sum_i \rho_i \sum_f |\langle i|\chi^{\alpha\beta}|f\rangle|^2 \delta(E_f - E_i - \hbar\omega) \,. \tag{7.64}$$

By using the integral representation of the δ function

$$\delta(x) = \frac{1}{2\pi}\int_{-\infty}^{\infty} e^{ikx}\,dk \tag{7.65}$$

one can express (7.64) in the form

$$i(\omega) = \frac{1}{2\pi}\int_{-\infty}^{\infty} \langle \chi^{\alpha\beta}(t)\,\chi^{\alpha\beta}(0)\rangle e^{i\omega t}\,dt \tag{7.66}$$

where $\langle \ldots \rangle$ denotes a thermal average. Expanding $\chi^{\alpha\beta}$ as a power series in lattice displacements

$$\chi^{\alpha\beta} = \chi_0^{\alpha\beta} + \sum_j P_j Q_j + \sum_{jj'} P_{jj'} Q_j Q_{j'} + \cdots \,, \tag{7.67}$$

retaining only linear terms, using (7.5) and the fluctuation dissipation theorem (7.6) the scattering intensity is proportional to

$$i(\omega) = \frac{1}{1 - e^{-\hbar\omega/kT}}\, \mathrm{Im} \sum_{ij} P_i P_j\, G_{ij}(\omega) \tag{7.68}$$

The soft mode in hydrogen bonded ferroelectrics such as KDP transforms according to the B_2 representation of D_{2d} and is therefore observed by polarizing the incoming beam parallel to x and the scattered beam parallel to y, or viceversa [89]. Experiments [84] show that in addition to

the soft mode, which appears as a broad response centred around $\omega=0$, there is another low frequency excitation of B_2 symmetry which must be included in a full analysis of the lineshape. The acoustic branch will be neglected since it is of too low a frequency to be observed by Raman scattering techniques.

The form of G_{ij} will be investigated for two models:

(i) The anharmonic phonon model [84] where both modes of interest are described as phonons. Expressions for the Green functions are determined from the coupled mode equation

$$\begin{bmatrix} \omega_1^2 - i\omega\gamma_1 - \omega^2 & \Sigma^2 + i\omega\Gamma_{12} \\ \Sigma^2 + i\omega\Gamma_{12} & \omega_2^2 - i\omega\gamma_2 - \omega^2 \end{bmatrix} \begin{bmatrix} G_{11} & G_{12} \\ G_{21} & G_{22} \end{bmatrix} = \begin{bmatrix} 1 & 0 \\ 0 & 1 \end{bmatrix} \quad (7.69)$$

There are an infinite number of ways to diagonalize (7.69); one may always diagonalize the real part ($\Sigma=0$) or the imaginary part ($\Gamma_{12}=0$) corresponding to a different choice of coordinates Q_1 and Q_2. For $\Gamma_{12}=0$ (7.69) becomes

$$\begin{bmatrix} \omega_1^2 - i\omega\gamma_1 - \omega^2 & \Sigma^2 \\ \Sigma^2 & \omega_2^2 - i\omega\gamma_2 - \omega^2 \end{bmatrix} \begin{bmatrix} G_{11} & G_{12} \\ G_{21} & G_{22} \end{bmatrix} \quad \begin{bmatrix} 1 & 0 \\ 0 & 1 \end{bmatrix} \quad (7.70a)$$

and for $\Sigma=0$ we can write

$$\begin{bmatrix} \omega_1'^2 - i\omega\gamma_1' - \omega^2 & i\omega\Gamma_{12} \\ i\omega\Gamma_{12} & \omega_2'^2 - i\omega\gamma_2' - \omega^2 \end{bmatrix} \begin{bmatrix} G_{11}' & G_{12}' \\ G_{21}' & G_{22}' \end{bmatrix} \quad \begin{bmatrix} 1 & 0 \\ 0 & 1 \end{bmatrix} \quad (7.70b)$$

The transition occurs when G diverges i.e.

$$\omega_1^2 \omega_2^2 - \Sigma^4 = 0 \quad (7.71a)$$

or equivalently

$$\omega_1^2,\ \omega_2^2,\ = 0 \tag{7.71b}$$

(ii) The pseudospin model in which the soft mode is described by a spin coordinate but the other excitations are represented by phonons. Neglecting two phonon coupling G_{zz}, given by (7.56), is written as

$$G^{zz}(\omega) = \frac{4\Delta\langle\sigma^x\rangle}{\hbar^2[\omega_\epsilon^2-\omega^2] - 4\Delta\langle\sigma^x\rangle\omega^2\sum_j \frac{K_j}{(\omega_j^2-\omega^2)}} \tag{7.72}$$

Considering frequencies much larger than ω_a and including just the one optic B_2 mode of interest (7.72) becomes

$$G^{zz}(\omega) = \frac{4\Delta\langle\sigma^x\rangle(\omega_j^2-\omega^2)}{\hbar^2[\omega_\epsilon^2-\omega^2][\omega_j^2-\omega^2] - 4\Delta\langle\sigma^x\rangle\omega^2 K_j} \tag{7.73}$$

where ω_e is given by (3.7). The Green functions $\ll\sigma^z, \gamma^+ + \gamma\gg$ and $\ll\gamma^+ + \gamma, \gamma^+ + \gamma\gg$ can be found from the equations of motion following the derivation of (7.73). However to make a comparison with (7.70) it is more useful to work with the original phonon operators a and a^+ rather than the γ's. The corresponding Green functions can easily be calculated once the Green functions for the γ's are known. One finds

$$\begin{vmatrix} \hbar^2(\omega_s^2-\omega^2) & 4\Delta\langle\sigma^x\rangle\xi_j \\ 2\xi_j\hbar\omega_j & \hbar^2(\omega_j^2-\omega^2) \end{vmatrix} \times \begin{vmatrix} G^{zz} & G^{zp} \\ G^{pz} & G^{pp} \end{vmatrix} = \begin{vmatrix} 4\Delta\langle\sigma^x\rangle & 0 \\ 0 & 2\hbar\omega_j \end{vmatrix} \tag{7.74}$$

where

$$\tfrac{1}{4}\hbar^2\omega_j^2 = (J'\langle\sigma^z\rangle)^2 + \Delta[\Delta - (J(0)-K_j)\langle\sigma^x\rangle] \tag{7.75}$$

Damping can be added in a phenomenological way by including imaginary terms in the diagonal elements of the left hand matrix in (7.74), i.e.

$$\begin{bmatrix} \hbar^2(\omega_s^2 - i\omega\gamma_s - \omega^2), & 4\Delta\langle\sigma^x\rangle\xi_j \\ 2\xi_j\hbar\omega_j, & \hbar^2(\omega_j^2 - i\omega\gamma_j - \omega^2) \end{bmatrix} \begin{bmatrix} G^{zz} & G^{zp} \\ G^{pz} & G^{pp} \end{bmatrix} = \begin{bmatrix} 4\Delta\langle\sigma^x\rangle & 0 \\ 0 & 2\hbar\omega_j \end{bmatrix} \tag{7.76}$$

A more satisfactory method of including damping in the spin equations of motion has recently been given [64] but does not differ substantially from (7.76) in the low frequency region of interest.

* *

Notice that (7.76) and (7.70a) have precisely the same dependence upon ω and therefore give indentical results with the correct choice of parameters. However there <u>are</u> differences in the expected temperature dependence of some of the parameters. For example in the phonon model

$$\omega_1^2 \propto (T - T_0) \quad , \quad \gamma_1 \propto T \tag{7.77a}$$

whereas in the spin model

$$\omega_s^2 \propto \frac{(T - T_0)}{T} \quad , \quad \gamma_s = \text{const.} \tag{7.77b}$$

However the relaxation times τ_1 and τ_s defined by

$$\tau_1 = \gamma_1/\omega_1^2 \quad , \quad \tau_s = \gamma_s/\omega_s^2 \tag{7.78}$$

do have the same expected temperature dependence i.e.

$$\left.\begin{matrix} T\gamma_1^{-1} \\ T\gamma_s^{-1} \end{matrix}\right\} \propto T - T_0 \tag{7.79}$$

T_0 is not the transition temperature because the condition

for G to diverge is $\omega_1^2=\Sigma^4/\omega_2^2$ (or $\hbar^2\omega_s^2 = 4\Delta\langle\sigma^x\rangle K_j$) so $\omega_1\neq 0$ at T_D. This point will be important later in an analysis of the experimental results.

However if Σ is set equal to zero the matrix on the left hand side of (7.70b) is diagonal at $\omega=0$ so the modes are effectively decoupled. Hence ω_1' corresponds to one of the excitations present in the crystal and it is for this reason that the transition occurs when $\omega_1'=0$. By contrast ω_1 is not the frequency of any of the excitations in the crystal so there is no reason it should equal zero at $T=T_D$.

Defining

$$\tau_1' = \gamma_1' / \omega_1'^2 \tag{7.80}$$

then one expects

$$\tau(\tau_1')^{-1} \propto T - T_0 \tag{7.81}$$

In the spin model one also expects the width of the coupled mode to vary like (7.81) and vanish at the transition.

Equation (7.81) neglects the anomalous low frequency response due to two phonon coupling. Since Raman experiments measure at frequencies greater than τ_{LL}^{-1} the extra response at low frequency will not be detected and the width of the coupled mode, observed in the experiment, will no longer appear to vanish at T_D. Rather the temperature dependence will be like (7.79) with $T_0<T_D$. From the difference between T_0 and T_D one can determine the strength of the anomalous low frequency response using (7.37) and

(7.35).

To conclude this section we point out that in the highly overdamped situation the spin and phonon models give identical results even including the expected temperature dependences of the parameters. In this limit

$$\begin{bmatrix} G^{zz} & G^{zp} \\ G^{pz} & G^{pp} \end{bmatrix} = \frac{1}{D} \begin{bmatrix} g_0(\omega_j^2 - i\omega\gamma_j - \omega^2)\hbar_j^2 & -2\hbar\omega_j\xi_j g_0 \\ -2\hbar\omega_j\xi_j g_0 & 2\hbar\omega_j(1-i\omega\tau_s) \end{bmatrix} \tag{7.82}$$

where

$$D = (1-i\omega\tau_s)(\omega_j^2 - i\omega\gamma_j - \omega^2)\hbar^2 - g_0\hbar_j\omega_j^2\hbar^2 \tag{7.83}$$

and

$$g_0 = \frac{4\Delta\langle\sigma^x\rangle}{\hbar^2\omega_s^2} \tag{7.84}$$

which varies like $T-T_0$ for $\Delta \ll kT_D$. For the phonon model one obtains a result identical to (7.82) except that

$$g_0 = \frac{1}{\omega_a^2} \tag{7.85}$$

which also varies like $T-T_0$.

7.4(b) Comparison of theory with experiment.

A detailed series of Raman experiments on KDP, KDA, and CsDA have been performed by Ryan [85]. A typical spectrum, taken for KDP at 235°K is shown in figure 15. The soft mode appears as a large overdamped response centred at $\omega=0$ but there is a second mode at about 170 cm^{-1} which must be included in an analysis of the lineshape. In the overdamped case the width of the soft mode is given by $1/\tau_1=\omega_1^2/\gamma_1$ and any set of parameters for ω_1 and γ_1 which

leave the width unchanged fit the data almost equally well. Consequently the analysis will deal with τ_1 rather than a_1. Notice that τ_1 is expected to have the same temperature dependence in both the spin and phonon models.

The width of the soft mode in KDP is plotted in figure 16 as a function of temperature and is found to vary linearly as expected. The temperature T_0 at which the width extrapolates to zero is found to be

$$T_0 = 53 \pm 6\,^\circ K \quad \text{for } \Gamma_{12} = 0 \tag{7.86a}$$

$$T_0 = 112 \pm 5\,^\circ K \quad \text{for } \Sigma = 0 \tag{7.86b}$$

As discussed in the previous section the size of the anomalous low frequency response is determined from the difference between the transition temperature ($122^\circ K$) and T_0 evaluated with $\Sigma=0$. Part of the difference, however, is due to acoustic mode coupling the magnitude of which was found in §6.5(i) to be $4^\circ K$. Clearly then the anomalous low frequency behaviour due to two phonon coupling is a very small effect in KDP. The results of [85] for KDA are very similar to those for KDP so will not be reproduced here.

Ryan's analysis of the data for CsDA, plotted in figure 17a, shows for $\Gamma_{12}=0$, the expected linear dependence of the width against temperature with $T_0=69\pm7^\circ K$, well below the transition temperature of $143^\circ K$ also as expected. For $\Sigma=0$ the width of the soft mode (mode 1) falls as T is reduced but does not tend to zero close to T_D as expected.

However the width of mode 2 which is usually thought of as being underdamped and essentially temperature independent, does tend to zero close to T_D. This strange result is probably due to difficulties in decoupling the modes satisfactorily in CsDA.

What is important here is that the width of the low frequency peak in the Raman spectrum extrapolates to zero at a temperature just below the transition as will now be shown. For $\Sigma=0$, with both modes overdamped, the intensity is proportional to

$$\frac{1}{1-i\omega\tau} \tag{7.87}$$

at small ω, with τ given by

$$\tau = \tau_1' + \tau_2' = \frac{\gamma_1'}{\omega_1'^2} + \frac{\gamma_2'}{\omega_2'^2} \tag{7.88}$$

The variation of T/τ with temperature, determined from Ryan's data, is shown in figure 17(b). Although there is some scatter in the experimental points T/τ clearly extrapolates to zero about $15^{\circ}K$ below the transition showing that two phonon coupling is of about the same order of magnitude as in KDP, i.e. is a small effect.

In the analysis of the data for KDA and CsDA given in [70] and [84] the width was plotted as a function of temperature with $\Gamma_{12}=0$. Since this width extrapolates to zero below the transition it was concluded that there is a large anomaly at low frequencies in these materials. This is incorrect because, as pointed out earlier, the matrix

(7.70a) for G is not diagonal at $\omega=0$ when $\Gamma_{12}=0$ (but $\Sigma\neq 0$). Hence ω_1 is not the frequency of any excitation of the crystal, but is merely a parameter used to fit the data, so there is no reason why ω_1 (or $1/\tau_1$) should vanish at the transition. A correct analysis shows that the low frequency anomaly is a small effect in KDP, KDA and CsDA.

Nonetheless there is evidence from EPR [90], NQR [91] and low frequency dielectric measurements [92] of a zero frequency peak in the spectrum for $T>T_D$ in the arsenates. Experiments on mixed KDP-KDA crystals indicate that this effect is not present in the phosphates (R. Blinc, private communication). These results have been interpreted by Blinc [64] as the effects of large spontaneous fluctuations, represented in his model by a stochastic internal field acting on the pseudospins. There is no obvious explanation why the zero frequency peak should be present in the arsenates and not in the phosphates either from the stochastic approach or the two-phonon coupling mechanism.

To conclude this discussion it is pointed out that Wilson and Cummins [93] and She et al. [94] claim to be able to measure the temperature variation of ω_1 and γ_1 separately. For ω_1 they find

$$\omega_1^2 \propto (T-T_0)^{0.76} \qquad (7.89a)$$

and

$$\omega_1^2 \propto (T-T_0) \qquad (7.89b)$$

respectively. The latter result is consistent with the

anharmonic phonon model, in contrast to the earlier results of Kaminov and Damen [75] that

$$\omega_1^2 \propto \frac{T - T_0}{T} \tag{7.90}$$

which is expected on the spin model. If (7.89b) is correct the validity of the spin model must seriously be questioned. However the difference between the spectra obtained from (7.89) and (7.90) is very small and we believe this remains an open question. It would be interesting to analyse the data using the overdamped expression (7.82), which can be derived either from the spin or the phonon models. If a satisfactory fit to the measurements can be obtained this would show that Raman data above the transition is unable to distinguish the two theories. However below T_D Raman experiments on KDP show an underdamped mode, interpreted as the soft mode which hardens below the transition [64]. Similar experiments on deuterated KDP [64] are unable to detect a similar mode. This is easily understandable on the spin model since the intensity is proportional to $\Delta\langle\sigma^x\rangle$ (see 7.72)) and Δ is much smaller in the deuterated compound. There does not appear to be such a straightforward explanation in the anharmonic phonon theory.

CONCLUSIONS

For crystals which undergo a second order structural phase transition general arguments show that an elastic constant must vanish at the transition temperature T_D and that the 'soft' mode is a long wavelength acoustic phonon. We have developed a detailed theory for several such crystals and have shown that this is indeed the case. The temperature dependence of the elastic constants has been well confirmed experimentally for the Jahn-Teller coupled systems $DyVO_4$ and $TbVO_4$. A similar theory has given a good description of the data on $TmVO_4$ [95]. The difference between $DyVO_4$ on the one hand and $TbVO_4$ and $TmVO_4$ on the other lies in the fact that there is a degeneracy in the Tb^{3+} and Tm^{3+} levels. A zero frequency mode associated with this degeneracy produces a frequency dependence in the appropriate elastic constant and a satisfactory description of this frequency dependence has been obtained.

The observation that an elastic constant of $DyVO_4$ and $TmVO_4$ vanishes at T_D confirms that the transitions are of second order, or at least very close to being second order. The elastic constants which exhibit this behaviour are $\frac{1}{2}(c_{11}-c_{12})$ in $DyVO_4$ and c_{66} in $TbVO_4$ and $TmVO_4$. The reduction in symmetry is therefore caused by a $\underline{k}=0$ B_{1g} mode in $DyVO_4$ and a $\underline{k}=0$ B_{2g} mode in $TbVO_4$ and $TmVO_4$. Hence for $TbVO_4$ the space group below T_D is D_{2h}^{24} which contradicts the results of Sayetat [13] who concluded from Xray measurements on powdered $TbVO_4$ that the space

group is D_2^7 in the low temperature phase.

A theory for the first order structural phase transition in DySb has been developed. General arguments show that an elastic constant should fall near the transition but not vanish. The theory confirms this result and accounts well for the data above T_D. However below the transition the crystal is predicted to harden considerably, in contradiction to the measurements which show an almost temperature independent behaviour in this region. Magnetic interactions drive the transition, electron lattice coupling by is found too weak.

Hydrogen bonded ferroelectrics, although physically very different, can be described by a pseudospin model similar to that for Jahn-Teller coupled systems such as $DyVO_4$. However, to account for the so-called Slater conditions, four particle interactions must be included in the model. Although a satisfactory fit to the elastic constant data can be obtained without this complication it is found necessary to include it when trying to account for polarization and elastic constant data with the same set of parameters. However some discrepancies between theory and experiment still remain.

The effect of coupling between the soft mode and pairs of phonons in hydrogen bonded ferroelectrics has been discussed in terms of the pseudospin model. An anomalous low frequency dielectric response is predicted similar to earlier work on the anharmonic phonon theory [71]. A frequency dependence in the elastic constants is expected although this effect has not yet been observed. Finally, a careful analysis of the Raman scattering data shows that the anomalous low frequency behaviour is a much smaller effect in hydrogen bonded ferroelectrics than was previously claimed [70].

REFERENCES
FOR PART I

1. Landau L. and Lifshitz E.M., "Statistical Physics" (2nd ed.) London: Pergamon Press (1969).

2. Cochran W., Adv.Phys. 9, 387 (1960); "Ibid"., 10, 401 (1961).

3. Elliott R. J., Hayes W., Palmer S.B., Sandercock J.R., Smith, S.R.P. and Young A.P., J.Phys.C, 5, 3126 (1972).

4. Elliott, R. J., Smith S.R.P. and Young, A.P., J.Phys.C., 4, L317 (1971).

5. Cooks A.H., Martin D.M. and Wells M.R., Solid St.Comm., 9, 519 (1971).

6. Cooke, A.H., Swithenby, S.J. and Wells, M.R., Solid St.Comm., 10 265 (1972).

7. Gehring, K.A., Malozemoff, A.P., Stande W. and Tyte, R.N., Solid St.Comm., 9, 511 (1971).

8. Becker P.J., Leask M.J.M. and Tyte R.N., J.Phys.C., 5, 2027 (1972).

9. Ellis C.J., Gehring K.A., Leask M.J.M. and White R.L., J. de Physique, 32, C1, 1024 (1971).

10. Elliott R.J., Harley R.T., Hayes W. and Smith S.R.P., Proc.Roy.Soc. (Lond.) A 328, 217 (1972).

11. Harley R.T., Hayes W. and Smith S.R.P., J.Phys.C., 5, 1501 (1972).

12. Forsyth J.B. and Sampson C.F., Phys.Lett., 36A, 223 (1971); Will G., Gobel H., Sampson C.F. and Forsyth J.B., Phys.Lett., 38A, 207 (1972).

13. Sayetat F., Solid St.Comm., 10, 879 (1972).

14. Gehring, G.A., Malozemoff A.P., Stande W.S. and Tyte R.N., J.Phys.Chem.Solids, 33, 1487 and 1499, (1972).

15. Goredetsky G., Luthi B. and Wanklyn B.M., Solid St.Comm. 9, 2157 (1971).

16. Wyckoff R.W.G., "Crystal Structures" (2nd ed.), chap. VIII. New York: Interscience Publishers Inc. (1965).

17. Elliott R.J. and Stevens K.W.H., Proc.Roy.Soc. (Lond.), A 218, 553 (1953).

18. Griffith J.S., "The Theory of Transition Metal Ions": Cambridge Univ.Press, (1961).

19. Jahn H.A. and Teller E., Proc.Roy. Soc. (Lond.), A 161, 220 (1937).

20. Fletcher J.R. and Sheard F.W., Solid St.Comm. 9, 1403, (1971).

21. Kanamori J., J.Appl.Phys. (Suppl.) 31, 145 (1960).

22. Sears V.F., Proc.Phys.Soc., 84, 951 (1964).

23. Elliott R.J. and Parkinson J.B., Proc.Phys.Soc., 92, 1024 (1967).

24. Van Eekelen H.A.M. and Stevens K.W.H., Proc.Phys.Soc., 92, 680 (1967).

25. Sheard F.W. and Toombs G.A., J.Phys.C. 4, 313 (1971).

26. Kobayashi K., J.Phys.Soc. Japan, 24, 497 (1968).

27. Elliott R.J. "Proceedings of International Conference on Structural Phase transitions and Soft Modes", (ed. E. J. Samuelsen, E. Anderson and J. Feder) p. 235, Universitetsforlaget (1971).

28. Kittel C., "Quantum Theory of Solids" New York: Wiley (1963).

29. Elliott R.J., "Proc.Int.Conf. Light Scattering in Solids", Paris 1971 (ed. M. Balkanski) p. 354. Paris: Flammarion Press.

30. Dvorak V., Cand.J.Phys. 45, 3303 (1967).

31. Wilcox R.M., Phys.Rev. 174, 624 (1968).

32. Tolman R.C. "The Principles of Statistical Mechanics", London: O.U.P. (1938).

33. Kadanoff L.P. and Baym G., "Quantum Statistical Mechanics" New York: Benjamin (1962).

34. Cowley R.A., Rept.Prog.Phys. 31, 123 (1968).

35. Kwok P.C. and Schultz T.P., J.Phys.C., 2, 1196 (1969).

36. Benedek G.B., "Proc.Int.Conf. of light Scattering in Solids" New York, 1968, (ed. G. B. Wright) p. 637. Berlin: Springer-Verlog.

37. Garland C.W. and Novotny D.B., Phys.Rev. 177, 971 (1969).

38. Litov E and Garland C.W., Phys.Rev., B2, 4597 (1970).

39. Melcher R.L. and Scott B.A., Phys.Rev.Lett., 28, 607 (1972).

40. Kasteleijn P.W. and Van Kranendonk J., Physica, 22, 367 (1956); "Ibid", 317. Kasteleijn P.W., Physica, 22, 387 (1956).

41. d'Ambrogio F., Bruesch P. and Kalbfleisch H., "Proc.Int.Conf.Light Scattering in Solids", Paris 1971. (ed. M. Balkanski) p. 363. Paris: Flammarion Press.

42. Bucher E., Birgeneau R.J., Maita J.P., Felcher G.P. and Brun T.O., Phys.Rev.Lett., 28 746 (1972).

43. Moran T.J., Thomas R.L., Levy P.M. and Chen H.H., Phys.Rev. B7, 3238 (1973).

44. Levy P.M., J.Phys.C. (to be published).

45. Lea K.R., Leask M.J.M. and Wolf W.P., J.Phys.Chem. Solids, 23, 1381 (1962).

46. Ray D.K. and Young A.P., J.Phys.C. (to be published).

47. Frazer B.C. and Pepinsky R., Acta Crystallogr., 6, 273 (1953).

48. Bacon G.E. and Pease R.S., Proc.Roy.Soc., A 220, 397 (1953); Ibid., A230, 359 (1955).

49. Benepe J.W. and Reese W., Phys.Rev. B3, 3032 (1971).

50. Paul G.L., Cochran W., Buyers W.J.L. and Cowley R.A., Phys.Rev. B2, 4603 (1970).

51. Shur M.S., Soviet Phys.-Solid St., 8, 43 (1966); Soviet Phys.-Crystallogr., 12, 181 (1967).

52. Skalyo J. Jr., Frazer B.C. and Shirane G., Phys.Rev., B1, 278 (1970).

53. Kaminov I.P. and Damen T.C., Phys.Rev.Lett., 20, 1105 (1968).

54. Moore M.A. and Williams H.C.W.L., J.Phys.C, 5, 3168 (1972).

55. Blinc R., J.Phys.Chem.Solids, 13, 204 (1960).

56. Thomas H., "Proceedings of International Conference on Structural Phase Transitions and Soft Modes", (ed. E.J. Samuelsen, E. Anderson and J. Feder) p. 15, Universitetsforlaget (1971).

76. Kanzig W., Solid St.Phys., (ed. F. Seitz and D. Turnbull) 4, 1 (1957).

77. Hill R.M. and Ichiki S.K., Phys.Rev., 128, 1140 (1962).

78. Azoulay J., Grinberg Y., Pelah I. and Wiener E., J. Phys.Chem.Solids, 29, 843 (1968).

79. Cochran W., Adv.Phys., 18, 157 (1969).

80. Reese W. and May L.F., Phys.Rev., 162, 510 (1967).

81. Reese W., Phys.Rev., 181, 905 (1969).

82. Jona F. and Shirane G., "Ferroelectric Crystals", Frankfurt:Pergamon Press (1962).

83. Blinc R. and Svetina S., Phys.Rev., 147, 423 (1966).

84. Katiyar R.S., Ryan J.F. and Scott J.F., "Proc.Int. Conf. Light Scattering in Solids", Paris 1971 (ed. M. Balkanski) p.354, Paris: Flammarion Press.

85. Ryan J.F., Ph.D. Thesis, University of Edinburgh (1973).

86. Zubarev D.N., Sov.Phys.Uspekhi, 3, 320 (1960).

87. Kubo R., Rept.Prog.Phys., 29, 255 (1966).

88. Born M. and Huang K., "Dynamical Theory of Crystal Lattices", London:O.U.P. (1954).

89. Loudon R., Adv.Phys., 13, 423 (1964).

90. Blinc R., Schara M. and Cevc P., Phys.Rev., 159, 411 (1967).

91. Blinc R. and Bjorkstam J.L., Phys.Rev.Lett., 23, 788 (1969).

92. Adriaenssens G.J., Bjorkstam J.L. and Aikins J., J. Mag.Res., 7, 99 (1972).

93. Wilson C.M. and Cummins H.Z., "Proc.Int.Conf. Light Scattering in Solids", Paris 1971 (ed. M. Balkanski),

p. 420 , Paris: Flammarion Press.

94. She C.Y., Broberg T.W., Wall L.S. and Edwards D.F., Phys.Rev., B6, 1847 (1972).

95. Melcher R.L., Pytte E. and Scott B.A., Phys.Rev.Lett., 31, 307 (1973).

96. Feder J. and Pytte E. (preprint).

97. Landau L. and Lifshitz E.M., "Theory of Elasticity", London: Pergamon Press (1959).

98. Kittel C., "Introduction to Solid State Physics", New York: Wiley (1966).

99. Pfeuty P., Thesis, University of Paris (1970).

100. Pytte E., Phys. Rev., B3, 3503 (1971).

PART II

ELASTIC ANOMALIES IN ANISOTROPIC FERROMAGNETS

CHAPTER 8

AN ELASTIC ANOMALY IN THE FERROMAGNETIC PHASE OF DYSPROSIUM AND TERBIUM METAL

8.1 Introduction.

Rare earth metals display many interesting magnetic properties because the 4f shell of electrons is unfilled. To a first approximation the f electrons behave like those of a free ion. The ground state is given by Hund's rules and since spin orbit coupling is relatively strong only the lowest J multiplet is normally populated at room temperature.

Rare earth ions in a crystal interact with their environment through electrostatic forces which take the form of classical coulomb terms and exchange interactions. These are both smaller that the spin-orbit splitting so J remains a good quantum number. Hence the crystal field potential $V(x,y,z)$ acting on the 4f electrons can be replaced by an equivalent operator expression $\alpha_J V(J_x, J_y, J_z)$ where α_J is a constant. In the heavy rare earths, which we shall be concerned with here, the crystal field splitting is rather weaker than exchange. A thorough description of the properties of rare earth metals is given in a recent book [1].

A variety of magnetically ordered phases are observed at low temperatures in these materials [1] but ferromagnetic ordering only occurs in Tb and Dy. These two rare earth metals crystallise in the hexagonal close packed structure shown in figure 1B with a c/a ratio somewhat smaller than the perfect value of $2\sqrt{2}/\sqrt{3}=1.633$.

Dysprosium is paramagnetic down to 176°K where it forms a planar spiral phase, in which all the moments in a given plane perpendicular to the c axis lie parallel to each other in the plane but the direction of the moments varies smoothly from plane to plane. There is no net magnetic moment. On further cooling a first order transition occurs at about 90°K to a ferromagnetic phase where all the moments lie parallel to the a axis. Terbium exhibits similar behaviour but the spiral phase exists over only a small range of temperatures from 230°K to about 220°K and the spins point along the b axis in the ferromagnetic phase.

The generally accepted view is that the paramagnetic-spiral transition is driven by exchange interaction which has a maximum at a non zero wavevector $\underline{k}_o$. An instability in a spinwave of this wavevector can lead to the observed planar spiral structure although the details of the spin ordering are determined by anisotropy. According to the theory of Ruderman, Kittel, Kasuya and Yosida [2] (RKKY for short) the exchange interaction is transmitted via the conduction electrons and the instability at $\underline{k}_o$ reflects a large response of the conduction electron system at this wavevector due to the geometry of the Fermi surface [3].

If exchange favours the spiral structure one may ask why Dy and Tb become ferromagnetic at low temperatures. The answer lies in magnetostriction which is unusually large because the J values (J=6 for Tb and J=15/2 for Dy) are big so the 4f wavefunctions are very anisotropic. According to Cooper [4] the transition to the ferromagnetic

phase releases strains which reduce the combined elastic and magnetoelastic energy. The same magnetoelastic forces give rise to interesting elastic properties in the ferromagnetic phase, which is the subject of this chapter.

8.2 An elastic anomaly: qualitative discussion

From now on we shall confine our attention to the ferromagnetic phase of Dy and Tb. The moments lie parallel to the easy direction (a axis for Dy; b axis for Tb) which is determined by anisotropy forces. Suppose a magnetic field H is applied parallel to the hard direction (b axis for Dy; a axis for Tb). As H increases the moments turn and at a critical field, H_c, they will lie parallel to the hard direction. Increasing the field further leaves the direction of the spins unchanged. The variation of the angle Φ between the magnetization and the hard direction will be derived in §8.3 and is plotted in figure 19. It will be noted that the variation of Φ with H is qualitatively similar to the dependence of the order parameter with T at a second order phase transition.

One can pursue this analogy further. The appearance of a non zero expectation value for the order parameter in a second order phase change lowers the symmetry [5]. For the situation discussed here the lattice and spin system have reflection symmetry in a plane perpendicular to the hard axis for all fields greater than H_c. However for $H<H_c$ this symmetry is broken because the spins no longer lie at 90° to the reflection plane. In other words applying a

field parallel to the hard axis leads to a type of second order phase transition but with H playing the role of temperature. Just as there is a 'soft mode' in the usual type of second order phase change (see the introduction to this thesis) we expect the frequency of one of the normal modes of Dy and Tb metal to vanish at $H=H_c$. If magnetostriction is neglected the soft mode is a spin wave [4]. On the other hand if magnetoelastic effects are included it seems likely that an acoustic branch will soften since this always lies below the spin wave at low k.

To obtain this last result the interaction between lattice strains and spins must be treated correctly, a point about which a great deal of unnecessary confusion has arisen. Two different models have been proposed [4]:

(i) the 'frozen lattice' approximation, in which it is assumed the macroscopic strain cannot follow the spin precession, and

(ii) the 'free lattice' approximation which assumes the strains follow the spins exactly.

In (i) the spin wave frequency remains finite at $H=H_c$ whereas according to model (ii) it vanishes at the critical field. Neutron diffraction [6] and high frequency (100 GH_z) ferromagnetic resonance [7] support the frozen lattice model whereas low frequency (10 GH_z) ferromagnetic resonance experiments [8] show an absorption at $H=H_c$ consistent with the free lattice picture.

To see which of these approaches is correct consider an oscillator of natural frequency ω_o. It will respond fully

to an external disturbance of frequency ω if $\omega \ll \omega_o$ and will not respond at all if $\omega \gg \omega_o$. Therefore the strains set up by an acoustic phonon of wavevector $\underline{k}$ will follow the spin precession only if the spin wave frequency $\omega_s(\underline{k})$ is much less than the acoustic phonon frequency $\omega_a(\underline{k})$. As $\underline{k} \to 0$, $\omega_a(\underline{k}) \to 0$ whereas $\omega_s(\underline{k})$ tends to a finite value so this condition can never be satisfied. However actually at $\underline{k}=0$ we must apply this argument a little more carefully. The natural frequency of oscillation of macroscopic strains in an infinite crystal is zero but in a crystal of finite size the macroscopic strains can respond in a time $t \sim \ell/v$ where ℓ is a typical dimension of the crystal and v is the sound velocity. Normally $\omega_s(\underline{k}=0)t \gg 1$ so we conclude that as far as coupling to the strains is concerned the spin wave frequencies should be calculated on the frozen lattice model. These arguments only apply to bulk models of the crystal. For surface waves the criterion for free lattice behaviour is $\omega_s(\underline{k}=0)t' < 1$ where $t' \sim d/v$ and d is a measure of the thickness of the surface layer. Since $d \ll \ell$ one is much more likely to observe free lattice behaviour in a surface than in a bulk mode and it is possible that the resonant absorption measured in [8] is due to a surface wave. This point has been investigated by Liu [9] who, however, finds the absorption intensity is much smaller than that observed. Further work to clarify this point would certainly be useful.

In addition to interactions between the static $\underline{k}=0$ strain and spin waves one should also include coupling to dynamic strains set up by acoustic phonons. We shall show

in §8.4 that this leads to coupled spin-phonon modes and in general neither the free nor the frozen lattice results give the excitation energies correctly.

8.3 The model Hamiltonian

The qualitative arguments of §8.2 will now be justified for a particular model. Since first principles calculations of the interaction strengths are very difficult one adopts a phenomenological approach, taking maximum advantage of symmetry, and adjusting the parameters in the theory to obtain agreement with experiment.

The following model Hamiltonian will be adopted

$$\mathcal{H} = \mathcal{H}_{ex} + \mathcal{H}_{c.f.} + \mathcal{H}_{el} + \mathcal{H}_{m.e.} + \mathcal{H}_{s.p.} + \mathcal{H}_{\rho} + \mathcal{H}_{Z} \tag{8.1}$$

and each term will be discussed separately.

$$\mathcal{H}_{ex} = -\tfrac{1}{2} \sum_{l \neq l'} \mathcal{J}(l,l')\, \underline{I}(l) . \underline{I}(l') \tag{8.2}$$

is the exchange interaction (assumed isotropic) between moments on sites l and l'. Although the hexagonal close packed lattice has two atoms per unit cell we shall neglect this aspect of the problem and work with a simpler model which has just one atom per cell. This is equivalent to ignoring optic spin wave and phonon branches. We have verified directly that using the correct h.c.p. lattice one obtains results for the acoustic branches of interest which are identical with those to be presented here. In what follows N is the number of atoms in the crystal.

The crystal field term, written in terms of operator

equivalents, is

$$\mathcal{H}_{c.f.} = \sum_{\ell}\left[V^{o}_{2} J^{2}_{\xi}(\ell) - \tfrac{1}{2} V^{6}_{6}\left\{\left(J_{\xi}(\ell)+i J_{\eta}(\ell)\right)^{6}+\left(J_{\xi}(\ell)-i J_{\eta}(\ell)\right)^{6}\right\}\right] \tag{8.3}$$

where ξ refers to the easy direction, η is the hard direction in the basal plane and ζ is the direction of the hexagonal axis. Figure 18 indicates these directions for Tb. Coefficients V^{o}_{4} and V^{o}_{6} have been put equal to zero because they are observed experimentally to be much smaller than V^{o}_{2}[10].

For magnetization in the basal plane only the strains $e_1(=2e_{\xi\eta})$ and $e_2(=e_{\xi\xi}-e_{\eta\eta})$ are non zero so the elastic energy $\mathcal{H}_{el}$ is given by

$$\mathcal{H}_{el} = \tfrac{1}{2} V c_o (e_1^2 + e_2^2) \tag{8.4}$$

where V is the volume of the crystal and $c_o=\frac{1}{2}(c_{11}-c_{12})$ $(=c_{66})$ (see Appendix A).

$\mathcal{H}_p$ is the usual harmonic Hamiltonian for acoustic phonons

$$\mathcal{H}_p = \sum_{j\,\underline{k}} \hbar\omega_j(\underline{k})\left[a^{+}_{j}(\underline{k})a_j(\underline{k}) + \tfrac{1}{2}\right] \tag{8.5}$$

The form of the symmetry allowed magnetoelastic coupling $\mathcal{H}_{m.e.}$ has been determined by Callen and Callen [11]. Considering only the strains e_1 and e_2 and including second and fourth rank operators for the rare earth ions $\mathcal{H}_{m.e.}$ may be written as

$$\begin{aligned}\mathcal{H}_{m.e.} = &-\sqrt{\frac{V}{N}}\frac{c_o C}{J J_1}\left[e_1\sum_{\ell}\left(J^2_{\xi}(\ell)-J^2_{\eta}(\ell)\right)+e_2\sum_{\ell}\left(J_{\xi}(\ell)J_{\eta}(\ell)+J_{\eta}(\ell)J_{\xi}(\ell)\right)\right]\\ &-\sqrt{\frac{V}{N}}\frac{c_o A}{J J_3}\left[\frac{e_1}{2}\sum_{\ell}\left[\left(J^2_{\xi}(\ell)-J^2_{\eta}(\ell)\right)^2-\left(J_{\xi}(\ell)J_{\eta}(\ell)+J_{\eta}(\ell)J_{\xi}(\ell)\right)^2\right]\right.\\ &\left.-e_2\sum_{\ell}\left(J^2_{\xi}(\ell)-J^2_{\eta}(\ell)\right)\left(J_{\xi}(\ell)J_{\eta}(\ell)+J_{\eta}(\ell)J_{\xi}(\ell)\right)\right]\end{aligned} \tag{8.6}$$

where

$$J_n = (J-\tfrac{1}{2})(J-1)\cdots(J-n/2) \tag{8.7}$$

The coefficient A is necessary to obtain agreement with experiment [6].

$\mathcal{H}_{s.p.}$ is the coupling between rare earth ions and acoustic phonons which corresponds to the static strain coupling (8.6) i.e.

$$\begin{aligned}\mathcal{H}_{s.p.} = \sqrt{\frac{V}{N}} \sum_{\underline{k}j} \sum_{l} e^{i\underline{k}\cdot\underline{R}(l)} [a_j^+(\underline{k}) + a_j(-\underline{k})] \\ \times \Big\{ \frac{U_1}{J J_1} [J_x^2(l) - J_y^2(l)] + \frac{U_2}{J J_1} [J_x(l)J_y(l) + J_y(l)J_x(l)] \\ + \frac{V_1}{2J J_3} \Big[(J_x^2(l) - J_y^2(l))^2 - (J_x(l)J_y(l) + J_y(l)J_x(l))^2 \Big] \\ - \frac{V_2}{J J_3} \Big[(J_x^2(l) - J_y^2(l))(J_x(l)J_y(l) + J_y(l)J_x(l)) \Big] \Big\}\end{aligned} \tag{8.8}$$

Coupling between phonons and angular momentum operators of other symmetries are unimportant for modes propagating in the basal plane. One could also include two ion magnetoelastic interactions and anisotropic exchange, which alter the dispersion in the modes, but this has no significant effect in the small $\underline{k}$ region of interest.

$\mathcal{H}_Z$ is the Zeeman energy in the presence of a magnetic field in the basal plane at an angle δ to the magnetization.

$$\mathcal{H}_Z = -g\beta \sum_l \underline{J}(l)\cdot\underline{H} \tag{8.9}$$

It will be assumed that anisotropy and magnetoelastic interactions are sufficiently small that they can be considered as first order perturbations to the isotropic exchange Hamiltonian. This is not a very satisfactory

approximation for the rare earths and corrections involving zero point effects and elliptical spin precession have recently been investigated [12].

The equilibrium strains $\langle e_1 \rangle$ and $\langle e_2 \rangle$ are calculated at T=0 by minimising $\mathcal{H}$ with respect to e_1 and e_2 in the ground state of the exchange Hamiltonian (8.2). If the magnetization lies at an angle Φ to the hard direction then

$$\langle e_1 \rangle = \sqrt{\frac{N}{V}} \left[-C \cos 2\phi + \tfrac{1}{2} A \cos 4\phi \right]$$

$$\langle e_2 \rangle = \sqrt{\frac{N}{V}} \left[C \sin 2\phi - \tfrac{1}{2} A \sin 4\phi \right] \qquad (8.10)$$

Expectation values of the electronic operators of interest have been tabulated by Jensen [13]. The angular dependent terms in the expression for $\langle \mathcal{H} \rangle$ at T=0 are

$$\tfrac{1}{2} N c_0 A C \cos 6\phi + N J V'_6 \cos 6\phi - g\beta H N \cos \delta \qquad (8.11)$$

Of particular interest is the case when H is along the hard direction so $\delta=\Phi$. In this case the equilibrium value of Φ, obtained by minimising (8.11).is given by the solution of

$$H \sin\phi = H_c \frac{\sin 6\phi}{6} \qquad (8.12)$$

where

$$g\beta H_c = 36 (V'_6 J_5 + \tfrac{1}{2} c A C) \qquad (8.13)$$

and $$c = c_0 / J$$

For $H>H_c$, $\Phi=0$ so the applied field has swung the moments round to the hard direction. For $H<H_c$ the solution to

(8.12) is plotted in figure 19.

The spin wave theory for such a system has been discussed by several authors [4], [13], [14] and will merely be described in outline here. One first transforms to the (x,y,z) system where $\hat{x}$ is parallel to ζ and $\hat{z}$ is parallel to the magnetization (see figure 18). The new electronic operators are expanded in spin wave creation and annihilation operators, b^+ and b respectively, retaining only quadratic terms. Jensen [13] has tabulated the results for the operators of interest. Neglecting for a moment $\mathcal{H}_{e.p.}$ one finds that the Hamiltonian becomes

$$\mathcal{H} = \frac{1}{2}\sum_{\underline{k}} A(\underline{k})\left[b^+(\underline{k})b(\underline{k}) + b(\underline{k})b^+(\underline{k})\right] + \frac{1}{2}\sum_{\underline{k}} B(\underline{k})\left[b^+(\underline{k})b^+(-\underline{k}) + b(\underline{k})b(-\underline{k})\right] \tag{8.14}$$

where

$$A(\underline{k}) \quad [g(0)-g(\underline{k})]J + V_2^0 J_1 - 21 V_6^6 J_5 \cos 6\phi + g\beta H\cos\delta + c\left[3C^2 + 5A^2/2 - (13/2)AC\cos 6\phi\right] \tag{8.15a}$$

$$B(\underline{k}) = V_2^0 J_1 + 15 V_6^6 J_5 \cos 6\phi + c\left[-C^2 - 3A^2/2 + (7/2)AC\cos 6\phi\right] \tag{8.15b}$$

In deriving (8.15) it has been assumed that e_1 and e_2 are given by their equilibrium values (8.10). This assumption is justified by the following argument. Since there is no kinetic term corresponding to the strain e it follows that the equation of motion of e is

$$\frac{de}{dt} = 0 \tag{8.16}$$

Hence e= ⟨e⟩ so the frozen lattice theory is appropriate in agreement with the discussion in §6.2.

The equations of motion of $b^{+}(\underline{k})$ and $b(\underline{k})$ are

$$[\hbar\omega + A(\underline{k})]\, b^{+}(\underline{k}) + B(\underline{k})\, b(\underline{k}) = 0$$

$$-B(\underline{k})\, b(\underline{k}) + [\hbar\omega - A(\underline{k})]\, b^{+}(\underline{k}) = 0 \qquad (8.17)$$

from which it follows that the spin wave energy is given by

$$\hbar\omega_s(\underline{k}) = \{[A(\underline{k}) + B(\underline{k})][A(\underline{k}) - B(\underline{k})]\} \qquad (8.18)$$

where

$$A(\underline{k}) + B(\underline{k}) = [g(0) - g(\underline{k})]J + 2V_2^0 J_1 - 6V_6^6 J_5 \cos 6\phi + c[2C^2 + A^2 - 3AC\cos 6\phi] + g\beta H\cos\delta \qquad (8.19a)$$

$$A(\underline{k}) - B(\underline{k}) = -36 J_5 V_6^6 \cos 6\phi + g\beta H\cos\delta + [g(0) - g(\underline{k})]J + c[4C^2 + 4A^2 - 10AC\cos 6\phi] \qquad (8.19b)$$

This is just the frozen lattice result [13] as expected.

So far attention has been focused on the spin wave spectrum. In the next section coupling between the spins and acoustic phonons will be discussed fully and expressions obtained for the elastic constants.

8.4 Calculation of the elastic constants

In discussing coupled spin-phonon modes we shall only consider propagation in the basal plane. Furthermore the largest changes in elastic constants are for acoustic vibrations transversely polarized in the basal plane so coupling to other branches will be neglected.

The coupling coefficients U_1, U_2, V_1 and V_2 in (8.6) are related to A and C (defined in (8.6)) through equation

(B.12). The terms in $\mathcal{H}_{s.p.}$ which give the largest frequency shift are of the form $b^{\dagger}a$ etc. Hence expressing the electronic operators in (8.8) in terms of spin wave operators up to first order [13] $\mathcal{H}_{s.p.}$ becomes

$$\mathcal{H}_{s.p.} = \sum_{\underline{k}} \sqrt{c\hbar\omega_a(\underline{k})}\,\left[b^{+}(\underline{k}) - b(-\underline{k})\right]\left[a^{+}(\underline{k}) + a(-\underline{k})\right] \times \left[C\cos 2(\phi-\alpha) + A\cos(4\phi+2\alpha)\right] \tag{8.20}$$

where α is the angle between $\underline{k}$ and the hard axis. The full Hamiltonian (8.5)+(8.14)+(8.20) consists entirely of quadratic terms so can be diagonalised exactly. From the equations of motion of the spin wave and phonon operators one readily obtains the following expression for the coupled mode frequencies

$$\hbar^2[\omega^2 - \omega_s^2(\underline{k})][\omega^2 - \omega_a^2(\underline{k})] - 4\hbar^2\omega_a^2(\underline{k})c\left[A(\underline{k}) + B(\underline{k})\right] \times \left[C\cos 2(\phi-\alpha) + A\cos(4\phi+2\alpha)\right]^2 \tag{8.21}$$

Figure 20 shows schematically the form of the dispersion curves. As $k \to 0$ the two solutions of (8.21) are a spin like mode with frequency

$$\omega = \omega_s(\underline{k}) \tag{8.22a}$$

and an acoustic phonon like mode with frequency

$$\omega = \omega_p(\underline{k}) \tag{8.22b}$$

where

$$\frac{\omega_p^2(\underline{k})}{\omega_a^2(\underline{k})} = 1 - \frac{4c\left[C\cos 2(\phi-\alpha) + A\cos(4\phi+2\alpha)\right]^2}{A(\underline{k}) - B(\underline{k})} \tag{8.23}$$

The largest change in the phonon frequency occurs for modes propagating parllel to the easy or the hard directions ($\alpha=\Pi/2$ or 0 respectively) with H along the hard axis ($\delta=\frac{\pi}{2}$). The effective elastic constant c_I for these modes is given by

$$\frac{c_I}{c_0} = \frac{\omega_\rho^2(\underline{k})}{\omega_a^2(\underline{k})} = 1 - \frac{4c\left[C\cos 2\phi + A\cos 4\phi\right]^2}{4c\left[C^2+A^2\right] + g\beta H\cos\phi - (g\beta H_c - 8cAc)\cos 6\phi} \tag{8.24}$$

Above the critical H_c (8.24) simplifies to

$$\frac{c_I}{c_0} = \frac{g\beta(H-H_c)}{4c(C+A)^2 + g\beta(H-H_c)} \tag{8.25}$$

showing that the elastic constant vanishes at $H=H_c$ in agreement with the general arguments of §8.2. As pointed out in §8.2 this problem can be considered as a second order phase transition with H playing the role of temperature. Indeed (8.25) can be cast in a form similar to (8.16) i.e.

$$\frac{c_I}{c_0} = \frac{1 - J' g_I}{1 - (J'-\mu) g_I} \tag{8.26}$$

where

$$\mu = 4c(C+A)^2 \qquad J' = g\beta H_c \tag{8.27a}$$

and

$$g_I = \frac{1}{g\beta H} \tag{8.27b}$$

Notice that (8.27b) is similar to the corresponding result (2.18a) for $DyVO_4$ and $TbVO_4$ in the limit $\Delta \to 0$ i.e.

$$g_I = \frac{1}{kT} \tag{8.28}$$

which confirms the analogy mentioned earlier. Figure 21 shows the variation of elastic constant with H calculated from (8.24) using the parameters $36V^6_6J_5 \sim 0$, $H_c = 31$kG and $4c(C^2+A^2) = 0.36$meV/ion obtained for Tb at 4.2°K by neutron diffraction [15]. Ultrasonic measurements to test the validity of this theory are now in progress and preliminary results seem encouraging (S.B. Palmer, private communication).

In the region of the dispersion courves (figure 20) where $\omega_a(\underline{k}) \ll \omega_s(\underline{k})$ the frequency of the spin like mode is just $\omega_s(\underline{k})$ the frozen lattice result. On the other hand if $\omega_a(\underline{k}) \gg \omega_s(\underline{k})$ the two solutions of (8.21) become (for a=0, $H>H_c$) (see figure 20)

$$\omega = \omega_a(\underline{k}) \qquad (8.29a)$$

and $\omega = \omega_1(\underline{k})$

where $\omega_1 = \{[A(\underline{k}) + B(\underline{k})][gB(H-H_d)]\}$ (8.29b)

which is just the free lattice result [13] as expected from the discussion in §8.2. For $H<H_c$ the situation is a little more complicated because different magnetoelastic terms have different angular dependences. At general wavevector the excitations are coupled magnon phonon modes and the frequencies are not given by either the free or frozen lattice results, except in the limits mentioned above.

The theory so far is valid only at T=0°K. At finite temperatures the theory goes through essentially as before except for a scaling of the parameters. Cooper [4] has shown using the theory of Callen and Callen [16] that

parameters in (8.21) and (8.19) which arise from an ℓth rank electronic operator vary with the reduced magnetization σ like $\sigma^{\frac{1}{2}\ell(\ell+1)-1]}$ at low temperatures. Hence

$$J_1 V_2^0 \rightarrow J_1 V_2^0 \sigma^2 \quad \text{and} \quad J_5 V_6^6 \rightarrow J_5 V_6^6 \sigma^{24} \tag{8.30}$$

for example. This result has been modified by Brooks [17] by treating anisotropy in zeroth order rather than as a first order perturbation. At low temperatures the main contribution to σ comes from axial anisotropy rather than exchange and Brooks finds

$$J_1 V_2^0 \rightarrow J_1 V_2^0 \sigma^1 \quad \text{and} \quad J_5 V_6^6 \rightarrow J_5 V_6^6 \sigma^{35} \tag{8.31}$$

After the theoretical work described in this chapter had been performed preprints were received from Chow and Keffer [18] and Southern and Goodings [19] who derived an expression for the coupled mode frequences consistent with (8.21). Chow and Keffer also stressed that in general the excitations are coupled magnon-phonon modes whose frequencies are given neither by the free nor the frozen lattice result. Jensen [13] does not give an expression for the coupled mode frequencies but mentions as an additional note that the elastic constant should vanish at $H=H_c$. A similar treatment of magnetoelastic effects and coupled magnon-phonon modes in spiral magnetic arrangements has recently been given [20].

8.5 Conclusions

General arguments show that an elastic constant vanishes when a magnetic field $H=H_c$ is applied which turns the moments of a ferromagnet

from the easy to the hard direction. This has been verified for a particular model of the ferromagnetic phase of Dy and Tb. As k→0 the frequency of the spin wave branch is given by the frozen lattice result and if there is a region where $\omega_a(\underline{k}) \gg \omega_s(\underline{k})$ the spin wave frequency is given essentially by the free lattice formula. However in general the excitations are coupled spin-phonon modes whose frequencies are given neither by the free nor the frozen lattice theory. The cause of the microwave absorption observed at low frequencies [8] is still not completely clear but is possibly due to a surface mode.

REFERENCES

FOR PART II

1. "Magnetic Properties of Rare Earth Metals", ed. R.J. Elliott, London: Plenum Press (1972).
2. Ruderman M.A. and Kittel C., Phys.Rev. 96, 99 (1954); Kasuya T., Progr.Theoret.Phys. (Japan), 16, 45 (1956); Yosida K.,Phys.Rev.,106, 893 (1957).
3. Freeman A.J.; Chapter VI of ref.1.
4. Cooper B.R., Solid St.Phys. (ed. F. Seitz and D. Turnbull), 21, 393 (1968).
5. Landau L. and Lifshitz E.M., "Statistical Physics" (2nd edition) London: Pergamon Press (1969).
6. Nielson M., Bjerrum Møller H., Lingard P.A. and Mackintosh A.R., Phys.Rev.Lett., 25, 1451 (1970).
7. Wagner T.K. and Stanford J.L., Phys.Rev., 184, 505 (1969).
8. Bagguley D.M.S. and Liesegang J., Proc.Roy.Soc., A 300, 497 (1967).
9. Liu S.H. (preprint).
10. Rhyne J.J. and Clark A.E., J.Appl.Phys., 38, 1379 (1967).
11. Callen E. and Callen H.B., Phys.Rev., 139, A455 (1965).
12. Brooks M.S.S. and Egami T., J.Phys.C, 6, 513 (1973).
13. Jensen J., Riso Report No. 252 (o971).
14. Mackintosh A.R. and Bjerrum Møller H; Chapter V of ref. 1.
15. Bjerrum Møller H., Houmann J.C.G., Jensen J., Lindgard P.A. and Nielsen M., Riso Report No. 256 (1972).
16. Callen H.B. and Callen E., J.Phys.Chem.Solids, 27, 1271 (1966).

17. Brooks M.S.S., Phys.Rev., B1, 2257 (1970).

18. Chow H. and Keffer F., Phys.Rev., B7, 2028 (1973).

19. Southern B.W. and Goodings D.A., Phys.Rev.,B7, 534 (1973).

20. A.H. Nayyar and D. Sherrington, J.Phys.F, 5, 993 (1973).

APPENDIX A

ELASTICITY THEORY

Elasticity theory is the study of the mechanics of solid bodies regarded as a continuous medium. It describes satisfactorily the properties of acoustic vibrations, such as those generated in the ultrasonic and Brillouin scattering experiments, discussed in this thesis, whose wavelength is much greater than the interatomic spacing. The treatment below is based on that given in [97].

A.1 Definitions of the stress, strain and elastic constant tensors

Consider a particular point in the body specified by the vector R, with components x_α. (x_α = x, y or z). Under the action of applied forces the body deforms so that the point which was initially at $\underline{R}$ is, after the deformation, specified by a different vector $\underline{R}'$, with components x_α'. The displacement $\underline{R}' - \underline{R}$ is denoted by $\underline{u}$, i.e.

$$u_\alpha = x'_\alpha - x_\alpha$$

If the radiusvector between two points before the deformation is dx_α and the distance between them $d\ell$ then after the deformation the distance becomes $d\ell'$ where

$$(d\ell')^2 = (d\ell)^2 + 2\frac{\partial u_\alpha}{\partial x_\beta} dx_\alpha dx_\beta$$

Here, and in what follows, we assume that $\underline{u}$ is infinitesimally small. Because the summation in the second term on the right is taken over both α and β we can put

$$(d\ell')^2 = (d\ell)^2 + 2 e_{\alpha\beta} dx_\alpha dx_\beta \qquad (A.1)$$

where

$$e_{\alpha\beta} = \frac{1}{2}\left(\frac{\partial u_\alpha}{\partial x_\beta} + \frac{\partial u_\beta}{\partial x_\alpha}\right) \tag{A.2}$$

is called the strain tensor. This definition differs from that given, for instance, by [98] where the strain components do not form a 2nd rank tensor. Note that for a non-uniform strain $e_{\alpha\beta}$ is a function of $\underline{R}$. From its definition we see that $e_{\alpha\beta}$ is symmetrical, i.e.

$$e_{\alpha\beta} = e_{\beta\alpha} \tag{A.3}$$

The component $\sigma_{\alpha\beta}$ of the stress tensor is defined to be the α component of the force per unit area perpendicular to the x_β axis. We are not concerned with the effects of angular acceleration on the elastic properties of the body so we consider the static situation and require that the total torque vanishes. This is equivalent to making the stress tensor symmetric, i.e.

$$\sigma_{\alpha\beta} = \sigma_{\beta\alpha} \tag{A.4}$$

In what follows it will be assumed that the deformation is reversible. With this assumption the work done by the internal stresses is [97]

$$-\int \sigma_{\alpha\beta}\, \delta e_{\alpha\beta}\, dV$$

If the strain is uniform, the charge in the free energy, F = E - TS, is then given by

$$dF = -S\,dT + V\sigma_{\alpha\beta}\, de_{\alpha\beta} \tag{A.5}$$

so the components of the stress tensor can be obtained by differentiating the free energy with respect to the components of the strain tensor at constant T, i.e.

$$\sigma_{\alpha\beta} = \left(\frac{\partial F}{\partial e_{\alpha\beta}}\right)_T \qquad (A.6)$$

If the deformation is small the free energy can be expressed as a power series in the $e_{\alpha\beta}$. The coefficient of the linear term is just the stress for zero strain, which vanishes. Including terms up to second order we have

$$F = F_o + \frac{1}{2} c_{\alpha\beta\gamma\delta} e_{\alpha\beta} e_{\gamma\delta} \qquad (A.7)$$

where $c_{\alpha\beta\gamma\delta}$ is a component of the elastic constant tensor. It follows from (A.6) and (A.7) that the stress tensor is related to the strain tensor by

$$\sigma_{\alpha\beta} = c_{\alpha\beta\gamma\delta} e_{\gamma\delta} \qquad (A.8)$$

A.2 Symmetries of the elastic constant tensor

The elastic constant tensor $c_{\alpha\beta\gamma\delta}$ defined by (A.7) is symmetric under interchange of suffix α with β and suffix γ with δ because the strain tensor is symmetric. It is also symmetric under interchange of the pair of sufficies α,β with the pair γ,δ because this leaves the product $e_{\alpha\beta}\ e_{\gamma\delta}$ unchanged. Hence

$$c_{\alpha\beta\gamma\delta} = c_{\beta\alpha\gamma\delta} = c_{\gamma\delta\alpha\beta} \qquad (A.9)$$

The number of different components of a fourth rank

tensor with these properties is 21 but this may be reduced further by the crystal symmetry. Since the elastic constant is a property of the crystal it must be invariant under those operations which leave the crystal unchanged.

All the crystals discussed in this thesis have reflection symmetry in planes perpendicular to the x and y axes. This leads to the transformations

$$x \to x \quad , \quad y \to -y \, , \quad z \to z$$

and

$$x \to -x \, , \quad y \to y \quad , \quad z \to z$$

so all components of $c_{\alpha\beta\gamma\delta}$ with an odd number of like suffices vanish. Hence the free energy is given by

$$\begin{aligned} F = {} & \tfrac{1}{2} c_{xxxx} e_{xx}^2 + \tfrac{1}{2} c_{yyyy} e_{yy}^2 + \tfrac{1}{2} c_{zzzz} e_{zz}^2 \\ & + c_{xxyy} e_{xx} e_{yy} + c_{yyzz} e_{yy} e_{zz} + c_{zzxx} e_{zz} e_{xx} \\ & + \tfrac{1}{2} c_{xyxy} (e_{xy}^2 + e_{yx}^2) + \tfrac{1}{2} c_{yzyz} (e_{yz}^2 + e_{zy}^2) + \tfrac{1}{2} c_{zxzx} (e_{zx}^2 + e_{xz}^2) \end{aligned} \qquad (A.10)$$

This result could also have been obtained by group theoretical arguments.

The elastic constants $c_{\alpha\beta\gamma\delta}$ are often wirtten in the matrix notation c_{ij}, even though c is really a fourth rank tensor, by making the substitutions:

i=1	for $\alpha\beta$ = xx
i=2	for $\alpha\beta$ = yy
i=3	for $\alpha\beta$ = zz
i=4	for $\alpha\beta$ = xz
i=5	for $\alpha\beta$ = yz
i=6	for αb = xy.

In this notation the free energy (A.10) can be written as

$$F = \tfrac{1}{2} \sum_{ij} c_{ij} e_i e_j \qquad (A.11)$$

where the c_{ij} are given by the elements of the following symmetric matrix:

$$c = \begin{bmatrix} c_{11} & c_{12} & c_{13} & 0 & 0 & 0 \\ c_{12} & c_{22} & c_{23} & 0 & 0 & 0 \\ c_{13} & c_{23} & c_{33} & 0 & 0 & 0 \\ 0 & 0 & 0 & c_{44} & 0 & 0 \\ 0 & 0 & 0 & 0 & c_{55} & 0 \\ 0 & 0 & 0 & 0 & 0 & c_{66} \end{bmatrix} \qquad (A.12)$$

Hence for orthorhombic crystals where there are no further simplifications the elastic constant tensor has nine independent components.

For tetragonal crystals, such as $DyVO_4$, $TbVO_4$, $TmVO_4$ and KDP above T_D, the x and y axes are equivalent so

$$c_{11} = c_{22} \;,\; c_{13} = c_{23} \;,\; c_{44} = c_{55} \qquad (A.13)$$

and the number of elastic constants is reduced to six.

In crystals with cubic symmetry, such as DySb above the transition, the x, y and z directions are all equivalent so in addition to (A.13) one finds

$$c_{22} = c_{33} \;,\; c_{13} = c_{12} \;,\; c_{66} = c_{44} \qquad (A.14)$$

and there are just three independent elastic constants.

Hexagonal crystals, such as the rare earth metals Dy and Tb, are invariant under a rotation of 60° about the z axis. For (A.11) to satisfy this condition it follows that

$$c_{66} = \tfrac{1}{2}(c_{11} - c_{12}) \qquad (A.15a)$$

and

$$c_{11} = c_{22}, \quad c_{13} = c_{23}, \quad c_{44} = c_{55} \tag{A.15b}$$

so there are five independent elastic constants.

For $DyVO_4$ the strain which develops below T_D is of B_{1g} symmetry (i.e. transforms like x'y'). Therefore

$$e_{B_{1g}} = e_{x'y'} + e_{y'x'} = e_{xx} - e_{yy} \tag{A.16}$$

Rearranging (A.11) one finds that $e_{B_{1g}}$ occurs as a term $\frac{1}{2}c_o e_{B_{2g}}^2$ where

$$c_o = \tfrac{1}{2}(c_{11} - c_{12}) \tag{A.17}$$

For $TbVO_4$ and $TmVO_4$ the strain is of B_{2g} symmetry (i.e. transforms like xy). Therefore

$$e_{B_{2g}} = e_{xy} + e_{yx} = 2e_{xy}$$

which occurs in (A.11) as a term $\frac{1}{2}c_o e_{B_{2g}}^2$ where

$$c_o = c_{66} \tag{A.18}$$

For KDP, $e_{B_2} = 2e_{xy}$ and the corresponding elastic constant is c_{66}.

In DySb, which has cubic symmetry, e_1 transforms like $3z^2-r^2$ and e_2 like x^2-y^2 (see (5.10)). From (A.11) one finds that these strains occur in the form $\frac{1}{2}c_o(e_1^2+e_2^2)$ where

$$e_1 = \frac{1}{\sqrt{3}}(e_{zz} - e_{xx} - e_{yy})$$

$$e_2 = e_{xx} - e_{yy} \tag{A.19}$$

and $$c_o = \tfrac{1}{2}(c_{11} - c_{12})$$

For Dy and Tb metals, which have hexagonal symmetry, e_1 transforms like xy and e_2 like x^2-y^2 in this notation (see (8.6)). From (A.11) one finds

$$e_1 = e_{xy} + e_{yx} = 2e_{xy}$$
$$e_2 = e_{xx} - e_{yy} \qquad (A.20)$$

and $$c_0 = \tfrac{1}{2}(c_{11} - c_{12})$$

A.3 Elastic waves.

The equations of motion for elastic waves in an anisotropic medium are obtained from Newton's Second Law by equating the internal force due to the stress $\partial \beta_{\alpha\beta}/\partial x_\beta$, to the product of the acceleration $\ddot{u}_\alpha$ and the density ρ, i.e.

$$\rho \ddot{u}_\alpha = \frac{\partial \beta_{\alpha\beta}}{\partial x_\beta} = c_{\alpha\beta\gamma\delta}\frac{\partial e_{\gamma\delta}}{\partial x_\beta}$$
$$= c_{\alpha\beta\gamma\delta}\frac{\partial^2 u_\delta}{\partial x_\beta \partial x_\gamma} \qquad (A.21)$$

(A.21) is just the wave equation which has solutions

$$u_\alpha = u^\circ_\alpha \exp[i(\underline{k}.\underline{r} - \omega t)]$$

where

$$\rho\omega^2 u^\circ_\alpha = c_{\alpha\beta\gamma\delta} k_\beta k_\gamma u^\circ_\delta \qquad (A.22)$$

which has non zero solutions for the u°_α when

$$|c_{\alpha\beta\gamma\delta} k_\beta k_\gamma - \rho\omega^2 \delta_{\alpha\delta}| = 0 \qquad (A.23)$$

For tetragonal crystals it follows from (A.13) and (A.23) that c_{66} is determined from the frequency of the elastic wave propagating parallel to the x or y axes trans-

versely polarized in the xy plane. On the other hand $\frac{1}{2}(c_{11}-c_{12})$ is the elastic constant appropriate to the wave propagating at 45^{o} to the x or y axes, also transversely polarized in the xy plane.

Similarly for cubic crystals the elastic constant $\frac{1}{2}(c_{11}-c_{12})$ is measured by propagating a transverse wave along one of the symmetry directions x,y or z.

In hexagonal crystals one can determine $\frac{1}{2}(c_{11}-c_{12})$ from the frequency of a wave transversely polarized in the basal plane propagating in any direction in the plane. However for the ferromagnetic phase of Dy and Tb the hexagonal symmetry is broken by the magnetization and the elastic constant does depend upon the propagation direction as discussed in Chapter 8.

APPENDIX B

LATTICE VIBRATIONS

In this section we study, in the harmonic approximation the vibrations of crystals viewed as a regular array of atoms.

Let the suffix α denote one of the n atoms in the unit cell and one of the three cartesian directions i.e. α taken 3n values. Then $u_\alpha(\ell)$ is the displacement of one of the atoms in the cell centred at $\underline{R}(\ell)$, parallel to a particular cartesian axis.

The harmonic Hamiltonian is

$$\mathcal{H} = \sum_{\alpha,\ell} \frac{p_\alpha^2(\ell)}{2m_\alpha} + \sum_{\substack{\alpha\ell \\ \alpha'\ell'}} V^{\alpha\alpha'}(\ell,\ell') u_\alpha(\ell) u_{\alpha'}(\ell') \qquad (B.1)$$

where $p_\alpha(\ell)$ is the momentum conjugate to $u_\alpha(\ell)$. Because $V^{\alpha\alpha'}(\ell,\ell')$ is only a function of $\underline{R}(\ell) - \underline{R}(\ell')$ it is well known that (B.1) can be diagonalised by a transformation of the form

$$u_\alpha(\ell) = N^{-1/2} \sum_{j\underline{k}} e^{-i\underline{k}\cdot\underline{R}(\ell)} \epsilon_{\alpha j}(\underline{k}) Q_j(\underline{k}) \qquad (B.2)$$

where the $\epsilon_{\alpha j}(\underline{k})$ are chosen to diagonalise the potential energy term.

Because $u_\alpha(\ell)$ is real

$$\epsilon^*_{\alpha j}(\underline{k}) = \epsilon_{\alpha j}(-\underline{k}) \quad , \quad Q^*_j(\underline{k}) = Q_j(-\underline{k})$$

We adopt the following orthonormality and completeness relations for the ϵ's.

$$\left.\begin{aligned} \sum_\alpha m_\alpha \epsilon_{\alpha j}(\underline{k}) \epsilon^*_{\alpha j'}(\underline{k}') &= M^c \delta_{jj'} \delta_{\underline{k}\underline{k}'} \\ m_\alpha \sum_j \epsilon_{\alpha j}(\underline{k}) \epsilon^*_{\alpha' j}(\underline{k}') &= M^c \delta_{\alpha\alpha'} \delta_{\underline{k}\underline{k}'} \end{aligned}\right\} \qquad (B.3)$$

where M^c is the mass of a unit cell.

The inverse transformation to (B.2) is therefore

$$M^c Q_j(\underline{k}) = \sum_{\alpha \ell} e^{i\underline{k}\cdot\underline{R}(\ell)} \epsilon^*_{\alpha j}(\underline{k})\, m_\alpha\, u_\alpha(\ell)\, .N^{-1/2} \qquad (B.4)$$

Defining

$$P_j(\underline{k}) = \sum_{\alpha \ell} e^{-i\underline{k}\cdot\underline{R}(\ell)} \epsilon_{\alpha j}(\underline{k})\, p_\alpha(\ell)\, N^{-1/2}$$

it follows from (B.3) and (B.4) that

$$[P_j(\underline{k}), Q_{j'}(\underline{k}')] = -i\hbar\, \delta_{jj'}\, \delta_{\underline{k}\underline{k}'} \qquad (B.5)$$

so that $P_j(\underline{k})$ is canonically conjugate to $Q_j(\underline{k})$. The Hamiltonian (B.1) can be written in terms of the new variables $Q_j(\underline{k})$ and $P'_j(\underline{k})$ as

$$\mathcal{H} = \sum_{j\underline{k}} \left[\frac{P_j(\underline{k}) P_j(-\underline{k})}{2M^c} + \frac{1}{2} M^c \omega_j^2(\underline{k}) Q_j(\underline{k}) Q_j(-\underline{k}) \right] \qquad (B.6)$$

where the frequency $\omega_j(\underline{k})$ involves the V's and the masses m_α. The phonon creation and annihilation operators $a_j^+(\underline{k})$ and $a_j(\underline{k})$ respectively are defined in the usual way in terms of the $Q_j(\underline{k})$ and $P_j(\underline{k})$,

$$\left.\begin{aligned} Q_j(\underline{k}) &= \sqrt{\frac{\hbar}{2M^c\omega_j(\underline{k})}}\, [a_j^+(\underline{k}) + a_j(-\underline{k})] \\ P_j(\underline{k}) &= i\sqrt{\frac{\hbar M^c \omega_j(\underline{k})}{2}} [a_j^+(\underline{k}) - a_j(-\underline{k})] \end{aligned}\right\} \qquad (B.7)$$

Using (B.5) it is easily shown that the a's satisfy the following commutation relations

$$\left.\begin{aligned} [a_j(\underline{k}), a_{j'}^+(\underline{k}')] = \delta_{jj'}\delta_{\underline{k}\underline{k}'} \;;\; [a_j(\underline{k}), a_{j'}(\underline{k}')] = 0 \\ [a_j^+(\underline{k}), a_{j'}^+(\underline{k}')] = 0 \end{aligned}\right\} \qquad (B.8)$$

so that $\mathcal{H}$ may be written as

$$\mathcal{H} = \sum_{j\underline{k}} \hbar\omega_j(\underline{k})\left[a_j^{\dagger}(\underline{k})a_j(\underline{k}) + \tfrac{1}{2}\right] \tag{B.9}$$

From (B.7) the relationship between $\zeta_j(\underline{k})$ and $\xi_j(\underline{k})$ (see § 1.3) is

$$\xi_j(\underline{k}) = \sqrt{\frac{\hbar}{2Mc\,\omega_j(\underline{k})}}\;\zeta_j(\underline{k}) \tag{B.10}$$

Confining our attention to acoustic modes of long wavelength we will now relate the phonon operators $a_j^{\dagger}(\underline{k})$ and $Q_j(\underline{k})$ to the strains discussed in appendix A.

For the long wavelength modes all the atoms in the unit cell move approximately in phase and we can express the displacement $\underline{u}$ as a function of the continuous variable R. Hence (B.2) becomes

$$\underline{u}(\underline{R}) = N^{-1/2}\sum_{j=\alpha,\underline{k}} e^{-i\underline{k}\cdot\underline{R}}\epsilon_j(\underline{k})\,Q_j(\underline{k}) \tag{B.11}$$

where $\epsilon_j(\underline{k})$ is a unit vector parallel to the direction of polarization. The strain $e_{\alpha\beta}(\underline{R})$, defined by (A.2) is therefore given by

$$e_{\alpha\beta}(\underline{R}) = -\frac{i}{2}\sum_{j=\alpha,\underline{k}}\left[\epsilon_j^{\alpha}(\underline{k})k^{\beta} + \epsilon_j^{\beta}(\underline{k})k^{\alpha}\right]Q_j(\underline{k})\,e^{i\underline{k}\cdot\underline{R}}$$

It follows that the expression for the strain set up by a particular mode at $\underline{R} = 0$ is given in terms of the creation and annihilation operators for that mode by

$$e_{\alpha\beta} = -\frac{i}{2}\left[\hat{k}^{\alpha}\epsilon^{\beta} + \hat{k}^{\beta}\epsilon^{\alpha}\right]\sqrt{\frac{\hbar\omega_a}{2Vc_o}}\;\left[a^{\dagger} + a\right] \tag{B.12}$$

(for clarity we have omitted some indices) where $c_o = \rho\omega^2 a$ is the elastic constant appropriate to the mode and $\hat{k}_a = k_a/k$.

The coupling of the 'spins' to long wavelength acoustic phonons is proportional to the strain so $\xi_a(\underline{k}) \sim k^{\frac{1}{2}}$ (see §1.4). If the coupling is to a strain $e = e_{xy} + e_{yx} = 2e_{xy}$ (as in $TbVO_4$, $TmVO_4$ and KDP) it follows from (B.12) that the maximum coupling is for modes transversly polarized in the basal plane, propogating parallel to the x or y axes (see §3.1). For $e = e_{xx} - e_{yy}$ (as in $DyVO_4$) the corresponding modes are also transversly polarized in the basal plane, but propogate at 45° to the x or y axes (see §3.1a). In either case the strain coupling η is related to $\xi_a(\underline{k})$ by

$$N^{-1/2} |\xi_a(\underline{k})| = \sqrt{\frac{\hbar \omega_a(\underline{k})}{2Vc_o}}\ \eta \qquad (B.13)$$

for modes with the maximum coupling. This can be expressed as

$$\mu = \frac{\eta^2}{c_o}\left(\frac{N}{V}\right) = K_a(\underline{k}) \qquad (B.14)$$

(see §2.1).

APPENDIX C

CLUSTER THEORY

To improve on the results of molecular field theory the free energy and hence the elastic constants of $DyVO_4$ have been calculated using a cluster theory based upon the constant coupling approximation [40].

The general thermodynamic relationships (2.21) and (2.24) show that $c_S = c_{S'} = c_T$ for $T \geq T_D$ so the elastic constant is unaffected by exchange of energy between the spin system and the phonons. For this reason only the spin and strain terms in the Hamiltonian (1.34) are considered, i.e.

$$\mathcal{H} = -\Delta \sum_{\ell} \sigma^x(\ell) - \tfrac{1}{2} \sum_{\ell\ell'} J(\ell,\ell') \sigma^z(\ell)\sigma^z(\ell') - \eta e \sum_{\ell} \sigma^z(\ell) + \tfrac{1}{2} V c_0 e^2 \qquad (C.1)$$

As discussed in §4.1 we approximate the interaction $J(\ell,\ell')$ by splitting it into short and long range components. The short range part is assumed to equal to j for z nearest neighbours and zero otherwise while the long range part is $J_\infty = \mu - \nu$ (4.2). μ corresponds to the strain interaction, which is considered as a separate term in (C.1), while the term in ν is treated by molecular field theory. The resulting form for $\mathcal{H}$ is

$$\mathcal{H} = -\Delta \sum_{\ell} \sigma^x(\ell) - (\eta e - \nu \langle \sigma^z \rangle) \sum_{\ell} \sigma^z(\ell) - \tfrac{1}{2} j \sum_{\ell,\ell'} \sigma^z(\ell)\sigma^z(\ell') + \tfrac{1}{2} V c_0 e^2 - \tfrac{1}{2} N \nu \langle \sigma^z \rangle^2 \qquad (C.2)$$

The term $-\frac{1}{2}N\nu \langle\sigma^z\rangle^2$ at each of the N unit cells. Defining the total interaction to be J' we require that

$$J' = \mu - \nu + zj .$$

In molecular field theory the ground state is fully aligned so J' can be calculated from the zero temperature splitting of the electronic levels but it is not obvious that this is satisfactory when large deviations from molecular field theory occur. However for zero crystal field ($\Delta = 0$) the spin system is essentially that of an Ising model for which general arguements, not depending upon molecular field theory, show that the ground state is fully ordered. The crystal field splitting, which acts like a transverse field [99], causes fluctuations in the moments even at T = 0 (i.e. zero point motion) which are large if Δ is large and the interactions are of short range. For $DyVO_4$ $\Delta \ll k T_D$ so at T = 0 the fluctuations will be small and the moments almost fully aligned even when there are strong short range interactions which cause deviations from molecular field theory. It is therefore a good approximation to determine J' from the molecular field expression for the splitting of the electronic levels in the region $T \ll T_D$. From Raman scattering data [10] it is found that $J' = 13.75\ cm^{-1}$.

We now return to the calculation of the free energy for Hamiltonian (C.2). The last two terms of (C.2) can be added separately to the final expression for the free energy because they do not contribute to the entropy, and the remaining terms can be written as a sum of pair Hamiltonians, i.e.

$$\mathcal{H} + \tfrac{1}{2}N\nu\langle\sigma^z\rangle^2 - \tfrac{1}{2}VC_0e^2 = \tfrac{1}{2}\sum_{ll'}\mathcal{H}^{(2)}(l,l') \qquad (C.3)$$

where

$$\mathcal{H}^{(2)}(l,l') = -\frac{\Delta}{z}\left[\sigma^x(l)+\sigma^x(l')\right] - j\sigma^z(l)\sigma^z(l') - \frac{1}{z}\left(\gamma e - \nu\langle\sigma^z\rangle\right)\left[\sigma^z(l)+\sigma^z(l')\right] \qquad (C.4)$$

The thermal average of a quantity $A(l,l')$ involving pairs of spins can therefore be expressed in terms of an effective density matrix for a pair $\rho^{(2)}(l,l')$, defined by

$$\langle A\rangle = \tfrac{1}{2}Nz\,\mathrm{Tr}\,\rho^{(2)}(l,l')A(l,l')$$

One can write $\rho^{(2)}$ in terms of an effective Hamiltonian $\mathcal{H}^{(e)}$ by

$$\rho^{(2)} = \exp\left[-\mathcal{H}^{(e)}/kT\right] \Big/ \mathrm{Tr}.\exp\left[-\mathcal{H}^{(e)}/kT\right]$$

So far the formalism has been exact and the approximations consist of taking a simple form for $\mathcal{H}^{(e)}$. In the constant coupling approximation, the Ising interaction between the pair is considered explicitly while the effect of the other spins is represented by an average field i.e.

$$\mathcal{H}^{(e)}(l,l') = -j\sigma^z(l)\sigma^z(l') - A\left[\sigma^z(l)+\sigma^z(l')\right] - B\left[\sigma^x(l)+\sigma^x(l')\right] \qquad (C.5)$$

where A and B are parameters to be determined. One recovers the results of molecular field theory by neglecting the interaction between the pair.

As $N \to \infty$, we assume that all the contribution to the partition function Z comes from states with the equilibrium values of $\langle\sigma^x\rangle$ and $\langle\sigma^z\rangle$. The energy, for a particular

temperature T, $\langle\sigma^x\rangle$ and $\langle\sigma^z\rangle$ is determined from the partition function by.

$$E(\beta, \langle\sigma^x\rangle, \langle\sigma^z\rangle) = -\frac{\partial}{\partial\beta}\left[\ln Z(\langle\sigma^x\rangle, \langle\sigma^z\rangle)\right]$$

where $\beta = 1/kT$. We write this in abbreviated notation as

$$E_\sigma(\beta) = -\frac{\partial}{\partial\beta}\left[\ln Z_\sigma\right]$$

where the suffix 'σ' refers to both $\langle\sigma^x\rangle$ and $\langle\sigma^z\rangle$. Integrating at constant $\langle\sigma^x\rangle$, $\langle\sigma^z\rangle$ and e one obtains

$$\ln Z_\sigma(\beta) = -\int_0^\beta E_\sigma(\beta')\,d\beta' + C$$

For $\beta \to 0$, $T \to \infty$ and the partition function is just equal to the number, $g(\langle\sigma\rangle)$, of states belonging to a given value of $\langle\sigma^x\rangle$, $\langle\sigma^z\rangle$ i.e.

$$g(\langle\sigma\rangle) = \frac{N!}{\left[\frac{1}{2}N(1+\langle\sigma\rangle)\right]!\left[\frac{1}{2}N(1-\langle\sigma\rangle)\right]!}$$

so

$$C = \ln g(\langle\sigma\rangle) = -N\left\{\frac{1+\langle\sigma\rangle}{2}\ln\left[\frac{1+\langle\sigma\rangle}{2}\right] + \frac{1-\langle\sigma\rangle}{2}\ln\left[\frac{1-\langle\sigma\rangle}{2}\right]\right\}$$

where $\langle\sigma\rangle = [\langle\sigma^x\rangle^2 + \langle\sigma^z\rangle^2]^{\frac{1}{2}}$.

Hence the partition function may be written as

$$\ln Z_\sigma(\beta) = -\int_0^\beta E_\sigma(\beta')\,d\beta' + \ln g(\langle\sigma\rangle) \qquad (C.6)$$

It is shown in [40] that for the form of $\mathcal{H}^{(e)}$ taken in the constant coupling approximation

$$\frac{\partial}{\partial\beta}\left[\beta E_\sigma(\beta) + \tfrac{1}{2}Nz\,\mathrm{Tr}\,\rho^{(2)}\ln\rho^{(2)}\right] = E_\sigma(\beta) \qquad (C.7)$$

From (C.6) and (C.7) it follows that

$$\ln Z_\sigma = -\beta E_\sigma(\beta) - \tfrac{1}{2}Nz\,\mathrm{Tr}\,\rho^{(2)}\ln\rho^{(2)} + \ln g(\langle\sigma\rangle) + C' \qquad (C.8)$$

C' is given by the value of $-\frac{1}{2}Nz\ \mathrm{Tr}\ \rho^{(2)}\ \ln\ \rho^{(2)}$

evaluated at infinitely high temperature but with the given values of $\langle\sigma^x\rangle$ and $\langle\sigma^z\rangle$. This is just the molecular result, i.e.

$$C' = -Nz \ln g(\langle\sigma\rangle) \tag{C.9}$$

From (C.6), (C.7) and (C.9) it follows that the free energy F is given by

$$F = N(zB-\Delta)\langle\sigma^x\rangle + N(zA-\eta e + \nu\langle\sigma^z\rangle/2)\langle\sigma^z\rangle - \tfrac{1}{2}NzkT \ln T_r \exp[-\alpha^{(e)}/kT] + N(z-1)kT \ln g(\langle\sigma\rangle) + \tfrac{1}{2}VC_0e^2. \tag{C.10}$$

Minimising F with respect to $\langle\sigma^x\rangle$ and $\langle\sigma^z\rangle$ we find

$$\tfrac{1}{2}kT(z-1)\frac{\langle\sigma^x\rangle}{\langle\sigma\rangle}\ln\left[\frac{1+\langle\sigma\rangle}{1-\langle\sigma\rangle}\right] + \Delta - zB = 0 \tag{C.11}$$

and

$$\tfrac{1}{2}kT(z-1)\frac{\langle\sigma^z\rangle}{\langle\sigma\rangle}\ln\left[\frac{1+\langle\sigma\rangle}{1-\langle\sigma\rangle}\right] + \eta e - \nu\langle\sigma^z\rangle - zA = 0 \tag{C.12}$$

There are four unknown quantities, A, B, $\langle\sigma^x\rangle$ and $\langle\sigma^z\rangle$ so, in addition to (C.11) and (C.12) we need two more equations to determine them. These come from the condition that $\langle\sigma^x\rangle$ and $\langle\sigma^z\rangle$ are equal to the thermal averages of σ^x and σ^z respectively for each spin of the pair. For $T \geq T_D$, both e and A are zero when there is no applied stress so the elastic constants can be determined by considering only terms up to first order in A. For $T \geq T_D$ the thermal averages. $\langle\sigma^x\rangle$, and $\langle\sigma^z\rangle$ are, in this approximation, given by

$$\langle\sigma^x\rangle = \frac{2B}{W}\frac{\sinh(W/kT)}{\cosh(j/kT)+\cosh(W/kT)} \tag{C.13}$$

$$\frac{\langle\sigma^z\rangle}{A} = \frac{-jB^{-2}e^{j/kT} + W^{-1}(W+j)(W-j)^{-1}e^{W/kT} - W^{-1}(W-j)(W+j)^{-1}e^{-W/kT}}{\cosh(j/kT)+(\cosh(W/kT)} \tag{C.14}$$

where

$$W = [j^2 + 4B^2]^{1/2}$$

The stress in the B_{1g} acoustic mode is still given by (2.10) and the elastic constant by (2.15). For $T > T_D$, $c_T = c_S = c_I$ where

$$\frac{c_T}{c_0} = 1 - \mu\left\{\nu + \frac{zA}{\langle\sigma^z\rangle} - \frac{1}{2}(z-1)\frac{kT}{\langle\sigma^x\rangle}\ln\left[\frac{1+\langle\sigma^x\rangle}{1-\langle\sigma^x\rangle}\right]\right\}^{-1} \qquad (C.15)$$

The transition occurs when (C.12) is satisfied with $\langle\sigma^z\rangle \neq 0$ in zero stress i.e.

$$\frac{1}{2}kT_0\,\frac{z-1}{\langle\sigma^x\rangle}\ln\left[\frac{1+\langle\sigma^x\rangle}{1-\langle\sigma^x\rangle}\right] + (\mu-\nu) - \frac{zA}{\langle\sigma^z\rangle} = 0 \qquad (C.16)$$

which is just the condition that c_T, given by (C.15) vanishes.

(C.15) is the desired expression for the elastic constant, with $A/\langle\sigma^z\rangle$ given by (C.14) and $\langle\sigma^x\rangle$ determined self consistently from (C.11) and (C.13). In comparing this expression with the experimental measurements in §4.1 we have taken z = 4, assuming that number of interacting neighbours is equal to the actual number of nearest rare earth neighbours.

The constant coupling approximation does not give completely satisfactory results below the transition temperature when applied to the Heisenberg ferromagnet and antiferromagnet [40]. In the present case we do not expect the theory to work well at low temperatures either especially for large Δ. In particular it is unsatisfactory when Δ is sufficiently large that it destroys the ordering in σ^z even at T = 0. From (C.11) and (C.13) it follows that $\langle\sigma^x\rangle = \Delta/W$ in this limit, independent of z, whereas we expect that for $z \to \infty$ the molecular field

result $\langle\sigma^x\rangle = 1$ should be recovered. We do not therefore attempt to apply the theory $T < T_D$. For $T > T_D$, we expect the constant coupling approximation to be significantly better than the molecular field theory when Δ is small and there is a large short range interaction, such as in $DyVO_4$.

APPENDIX D

CALCULATION OF THE ELASTIC CONSTANTS OF DySb BELOW THE TRANSITION

The equilibrium balue of $\langle q_2 \rangle$ is zero even in the ordered phase, but if an external stress $\mathcal{S}_2$ is applied then $\langle q_2 \rangle \neq 0$ and is given by (5.25) i.e.

$$\langle q_2 \rangle = \sum_{i=1}^{6} a_i P_i H_2 \tag{D.1}$$

with H_2 defined in (5.18b). From (5.21), (5.22) and (D.1) it follws immediately that

$$g_x^{(2)} = g_T^{(2)} = \sum_{i=1}^{6} a_i P_i \tag{D.2}$$

which together with (5.31) yields $c^{(2)}$.

The calculation of $c^{(1)}$ is more involved since we must take account of the fact that $\langle m_z \rangle$ as well as $\langle q_1 \rangle$ alters when a stress is applied. We begin by rewriting (5.25) as

$$\langle q_1 \rangle = Q(H_1, H_2, T) = \frac{1}{4}\left[P_1(1+3F_1)+P_2(1-3F_1)+P_3(1+3F_2)+P_4(1-3F_2) - 2P_5 - 2P_6\right]$$

$$\langle m_z \rangle = M(H_1, H_2, T) = \frac{1}{2}\left[-P_1(1+F_1)+P_2(-1+F_1)+P_3(1+F_2)+P_4(1-F_2)\right] \tag{D.3}$$

Since $Q = -(\partial g/\partial H_1)$ and $M = -(\partial g/\partial H_z)$ we can readily obtain the following useful results

$$\left(\frac{\partial Q}{\partial H_2}\right) = \left(\frac{\partial M}{\partial H_1}\right) \tag{D.4}$$

and

$$\left(\frac{\partial Q}{\partial T}\right) = \left(\frac{\partial S}{\partial H_1}\right), \quad \left(\frac{\partial M}{\partial T}\right) = \left(\frac{\partial S}{\partial H_2}\right)$$

which are simply the Maxwell equations for this problem. S is defined to be the entropy per electronic site, i.e. $S = -(\partial g/\partial T)$.

If the populations of the electronic levels are kept constant (this constraint is denoted by the suffix 'I') then

$$d\langle q_1\rangle = \left(\frac{\partial Q}{\partial H_1}\right)_I dH_1 + \left(\frac{\partial Q}{\partial H_z}\right)_I dH_z \qquad (D.5)$$

$$d\langle m_z\rangle = \left(\frac{\partial M}{\partial H_1}\right)_I dH_1 + \left(\frac{\partial M}{\partial H_z}\right)_I dH_z \qquad (D.6a)$$

Since $\langle m_z\rangle = H_z/I$ we can express (D.6a) as

$$0 = \left(\frac{\partial M}{\partial H_1}\right)_I dH_1 + \left[\left(\frac{\partial M}{\partial H_z}\right)_I - \frac{1}{I}\right] dH_z \qquad (D.6b)$$

From (D.5) and (D.6b) it follows that

$$g_I^{(1)} = \left(\frac{\partial\langle q_1\rangle}{\partial H_1}\right)_I = \left(\frac{\partial Q}{\partial H_1}\right)_I - \frac{\left(\frac{\partial Q}{\partial H_z}\right)_I\left(\frac{\partial M}{\partial H_1}\right)_I}{\left[\left(\frac{\partial M}{\partial H_z}\right)_I - \frac{1}{I}\right]}$$

which can be rewritten, using (D.4) as

$$g_I^{(1)} = \left(\frac{\partial Q}{\partial H_1}\right)_I - \left(\frac{\partial Q}{\partial H_z}\right)_I^2 \Big/ \left[\left(\frac{\partial M}{\partial H_z}\right)_I - \frac{1}{I}\right] \qquad (D.7)$$

The same arguments show that for the isothermal regime

$$g_T^{(1)} = \left(\frac{\partial Q}{\partial H_1}\right)_T - \left(\frac{\partial Q}{\partial H_z}\right)_T^2 \Big/ \left[\left(\frac{\partial M}{\partial H_z}\right)_T - \frac{1}{I}\right] \qquad (D.8)$$

To calculate $g_S^{(1)}$ we write

$$d\langle q_1\rangle = \left(\frac{\partial Q}{\partial H_1}\right)_T dH_1 + \left(\frac{\partial Q}{\partial H_z}\right)_T dH_z + \left(\frac{\partial Q}{\partial T}\right) dT \qquad (D.9a)$$

$$0 = \left(\frac{\partial M}{\partial H_1}\right) dH_1 + \left[\left(\frac{\partial M}{\partial H_2}\right) - \frac{1}{I}\right] dH_2 + \left(\frac{\partial M}{\partial T}\right) dT \tag{D.9b}$$

and at constant entropy

$$dS = 0 = \left(\frac{\partial S}{\partial H_1}\right) dH_1 + \left(\frac{\partial S}{\partial H_2}\right) dH_2 + \left(\frac{\partial S}{\partial T}\right) dT \tag{D.9c}$$

Hence

$$g_S^{(1)} = \left(\frac{\partial \langle q,7\rangle}{\partial H_1}\right)_S = \begin{vmatrix} \left(\frac{\partial Q}{\partial H_1}\right)_T & \left(\frac{\partial Q}{\partial H_2}\right)_T & \left(\frac{\partial Q}{\partial T}\right) \\ \left(\frac{\partial M}{\partial H_1}\right)_T & \left(\frac{\partial M}{\partial H_2}\right)_T - \frac{1}{I} & \left(\frac{\partial M}{\partial T}\right) \\ \left(\frac{\partial S}{\partial H_1}\right)_T & \left(\frac{\partial S}{\partial H_2}\right)_T & \left(\frac{\partial S}{\partial T}\right) \end{vmatrix} \Bigg/ \begin{vmatrix} 1 & \left(\frac{\partial Q}{\partial H_2}\right)_T & \left(\frac{\partial Q}{\partial T}\right) \\ 0 & \left(\frac{\partial M}{\partial H_2}\right)_T - \frac{1}{I} & \left(\frac{\partial M}{\partial T}\right) \\ 0 & \left(\frac{\partial S}{\partial H_2}\right)_T & \left(\frac{\partial S}{\partial T}\right) \end{vmatrix} \tag{D.10}$$

$$= \left(\frac{\partial \langle q,7\rangle}{\partial H_1}\right)_T - \frac{\left(\frac{\partial Q}{\partial T}\right)^2 + \frac{I\,(\partial Q/\partial H_2)_T}{1 - I\,(\partial M/\partial H_2)_T}\left[2\left(\frac{\partial Q}{\partial T}\right)\left(\frac{\partial M}{\partial T}\right) - \frac{C_H}{T}\left(\frac{\partial Q}{\partial H_2}\right)_T\right]}{\frac{C_H}{T} + \frac{I}{1 - I\,(\partial M/\partial H_2)}\left(\frac{\partial M}{\partial T}\right)^2} \tag{D.11}$$

where we have used (D.4). C_H is the specific heat per electronic site evaluated at constant H_1 and H_2.

The elastic constants $c_\gamma^{(1)}$ for γ=I, S or T are given by (5.31) with g_I, g_S and g_T given by (D.7), (D.11), and (D.8) respectively. It only remains, therefore, to give the explicit forms of the derivatives appearing in these expressions. We find

$$\left(\frac{\partial Q}{\partial H_1}\right)_I = \frac{3}{4}\left[-P_1 x_1 + P_2 x_1 - P_3 x_2 + P_4 x_2\right]$$

where

$$x_1 = \frac{3}{2}\frac{1}{\left[\left(\Delta + H_2 - \frac{3}{2}H_1\right)^2 + 8\Delta^2\right]^{1/2}}\left[1 - \frac{\left(\Delta + H_2 - \frac{3}{2}H_1\right)^2}{\left[\left(\Delta + H_2 - \frac{3}{2}H_1\right)^2 + 8\Delta^2\right]}\right]$$

$$x_2 = \frac{3}{2}\frac{1}{\left[\left(\Delta - H_2 - \frac{3}{2}H_1\right)^2 + 8\Delta^2\right]^{1/2}}\left[1 - \frac{\left(\Delta - H_2 - \frac{3}{2}H_1\right)^2}{\left[\left(\Delta - H_2 - \frac{3}{2}H_1\right)^2 + 8\Delta^2\right]}\right]$$

$$\left(\frac{\partial Q}{\partial H_1}\right)_T = \left(\frac{\partial Q}{\partial H_1}\right)_I + \frac{1}{kT}\left\{\frac{P_1}{16}(1+3F_1)^2 + \frac{P_2}{16}(1-3F_1)^2 + \frac{P_3}{16}(1+3F_2)^2 + \frac{P_4}{16}(1-3F_2)^2 + \frac{P_5}{4} + \frac{P_6}{4} - \langle q_1\rangle^2\right\}$$

$$\left(\frac{\partial Q}{\partial H_2}\right)_I = \frac{1}{2}\left[P_1 x_1 - P_2 x_1 - P_3 x_2 + P_4 x_2\right]$$

$$\left(\frac{\partial Q}{\partial H_2}\right)_T = \left(\frac{\partial Q}{\partial H_2}\right)_I + \frac{1}{kT}\left\{-\frac{P_1}{8}(1+F_1)(1+3F_1) - \frac{P_2}{8}(1-F_1)(1-3F_1) + \frac{P_3}{8}(1+F_2)(1+3F_2) + \frac{P_4}{8}(1-F_2)(1-3F_2) - \langle q_1\rangle\langle m_2\rangle\right\}$$

$$\left(\frac{\partial M}{\partial H_2}\right)_I = \frac{1}{3}\left[-P_1 x_1 + P_2 x_1 - P_3 x_2 + P_4 x_2\right]$$

$$\left(\frac{\partial M}{\partial H_2}\right)_T = \left(\frac{\partial M}{\partial H_2}\right)_I + \frac{1}{kT}\left[\frac{P_1}{4}(1+F_1)^2 + \frac{P_2}{4}(1-F_1)^2 + \frac{P_3}{4}(1+F_2)^2 + \frac{P_4}{4}(1-F_2)^2 - \langle m_2\rangle^2\right]$$

$$\left(\frac{\partial Q}{\partial T}\right) = \frac{1}{kT^2}\left[\frac{P_1}{4}\lambda_1(1+3F_1) + \frac{P_2\lambda_2}{4}(1-3F_1) + \frac{P_3\lambda_3}{4}(1+3F_2) + \frac{P_4\lambda_4}{4}(1-3F_2) - \frac{P_5\lambda_5}{2} - \frac{P_6\lambda_6}{2}\right]$$

$$-\frac{1}{kT^2}\langle q_1\rangle\left[P_1\lambda_1 + P_2\lambda_2 + P_3\lambda_3 + P_4\lambda_4 + P_5\lambda_5 + P_6\lambda_6\right]$$

$$\left(\frac{\partial M}{\partial T}\right) = \frac{1}{kT^2}\left[-\frac{P_1}{2}\lambda_1(1+F_1) - \frac{P_2}{2}\lambda_2(1-F_1) + \frac{P_3}{2}(1+F_2) + \frac{P_4}{2}(1-F_2)\right] - \frac{1}{kT^2}\left[P_1\lambda_1 + P_2\lambda_2 + P_3\lambda_3 + P_4\lambda_4 + P_5\lambda_5 + P_6\lambda_6\right]\langle m_2\rangle$$

$$C_H = \left[\sum_{i=1}^{6} P_i\lambda_i^2 - \left(\sum_{i=1}^{6} P_i\lambda_i\right)^2\right]\frac{1}{kT^2}$$

FIGURE CAPTIONS

Fig. 1. Schematic representation of the tetragonal zircon structure (D_{4h}^{19}) for RVO_4 (R = rare earth). Two molecules in a unit cell are indicated. Note the coordinate axes (see §1.1).

Fig. 2. The energy of the lowest electronic levels of (a) $DyVO_4$, (b) $TbVO_4$ and (c) $TmVO_4$ both above and below the transition temperature T_D.

Fig. 3. Schematic diagram of the coupled electronic and acoustic phonon modes of $DyVO_4$. For a discussion see §3.1.

Fig. 4. Brillouin scattering measurements of $\frac{1}{2}(c_{11}-c_{12})$ for $DyVO_4$. The solid curve (see §4.1a) shows the value of c_I obtained from the cluster theory above T_D; below T_D, the dashed curve is drawn through the experimental points.

Fig. 5. Brillouin scattering (open circles) and ultrasonic (filled circles) measurements of c_{66} for $TbVO_4$. As discussed in §4.2, the solid curves show the values of c_I, c_S and c_T (for $T \geq T_D$, $c_S = c_T$). The dashed curve shows the value of $c(\omega)$ as given by (3.25) with τ_{SS} given by (3.28) with $\alpha/2\Pi = 27.5$ GHz. The scale on the right shows the actual measured Brillouin frequency.

Fig. 6. Variation of c_{66} with frequency at $T=T_D$ as measured by Brillouin scattering. The solid curve is obtained from (4.4).

Fig. 7. A comparison between the theory (full lines) for $c_S^{(1)}$, $c_T^{(1)}$ and $c_S^{(2)}$ $(=c_T^{(2)})$ and ultrasonic measurements (circles). The dashed line indicates schematically the theoretical results for $c_{S'}^{(1)}$.

Note the enlarged scale below T_D.

Fig.8(a) A (001) projection of the strucuture of KH_2PO_4. The heights of the PO_4 tetrahedra are shown.

Fig.8(b) A diagram of the primitive unit cell of KH_2PO_4 indicating schematically the positions of the PO_4 tetrahedra (the filled circles and the open circles corresponding to the two sublattices A and B respectively) and the hydrogen bonds.

Fig. 9. A sketch of the proton displacements in a single cell of KDP which transform according to representations of the crystal point group D_{2d}.

Fig.10(a) A schematic representation of the potential for the soft mode in an order disorder transition (i) $T>T_D$, (ii) $T<T_D$.

Fig.10(b) A schematic representation of the potential for the soft mode in a displacive transition (i) $T>T_D$, (ii) $T=T_D$, (iii) $T<T_D$.

Fig.11, A comparison between the theory for c_I (full curve)

and the Brillouin scattering (circles) and ultrasonic (triangles) measurements of KDP. The dashed curve shows the value of c_T below T_D obtained from the theory.

Fig. 12. Spontaneous polarization measurements of KDP taken by Benepe and Reese (circles) and Von Arx and Bantle (crosses). The solid curve is calculated from Benepe and Reese's phenomenological theory and the dashed curve is the best fit from the pseudospin model.

Fig. 13. A comparison between the Brillouin scattering measurements (dots) on KDP below the transition and the theory for c_S, $c_{S'}$, and c_T (lines).

Fig. 14. A schematic representation of the variation of the elastic constant in KDP with temperature for $\omega\tau_{LL} \gg 1$ and $\omega\tau_{LL} \ll 1$ according to the theory.

Fig. 15. Low frequency Raman spectrum of KDP at 235°K (from [85]).

Fig. 16. Variation of T/τ for KDP (where τ is the relaxation time) obtained by Ryan from Raman scattering measurements. Filled circles are for $\Gamma_{12}=0$ and open circles for $\Sigma=0$.

Fig. 17(a) Variation of T/τ for CsDA obtained by Ryan from Raman scattering measurements. Filled circles: $\Gamma_{12}=0$; open circles: ferroelectric mode with $\Sigma=0$; triangles: 'underdamped' mode with $\Sigma=0$.

Fig. 17(b) Variation of width of low frequency peak in Raman spectrum (multiplied by T) for CsDA.

Fig. 18. The hexagonal close packed structure and the definition of the coordinate system (ξ, η, ζ).

Fig. 19. Variation of $\emptyset$, the angle between the magnetization and the hard axis, as a function of H applied along the hard direction.

Fig. 20. A schematic drawing of the coupled magnon-phonon dispersion curves in Dy and Tb metal.

Fig. 21. Variation of the elastic constant with magnetic field applied in the hard direction for modes propagating along the easy direction in the basal plane and transversely polarized also in the basal plane. The parameters are discussed in the text.

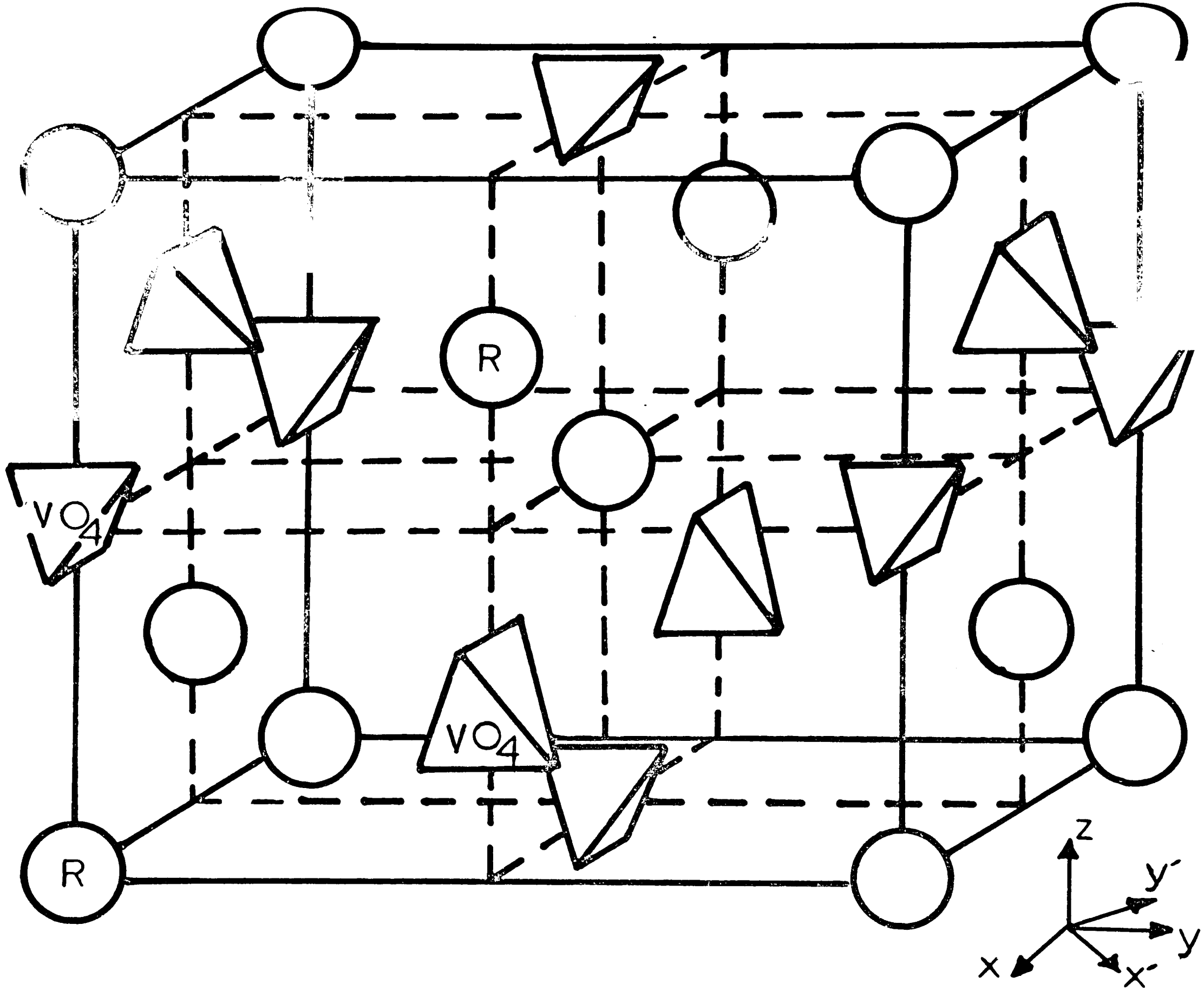

Fig.1

Fig.2

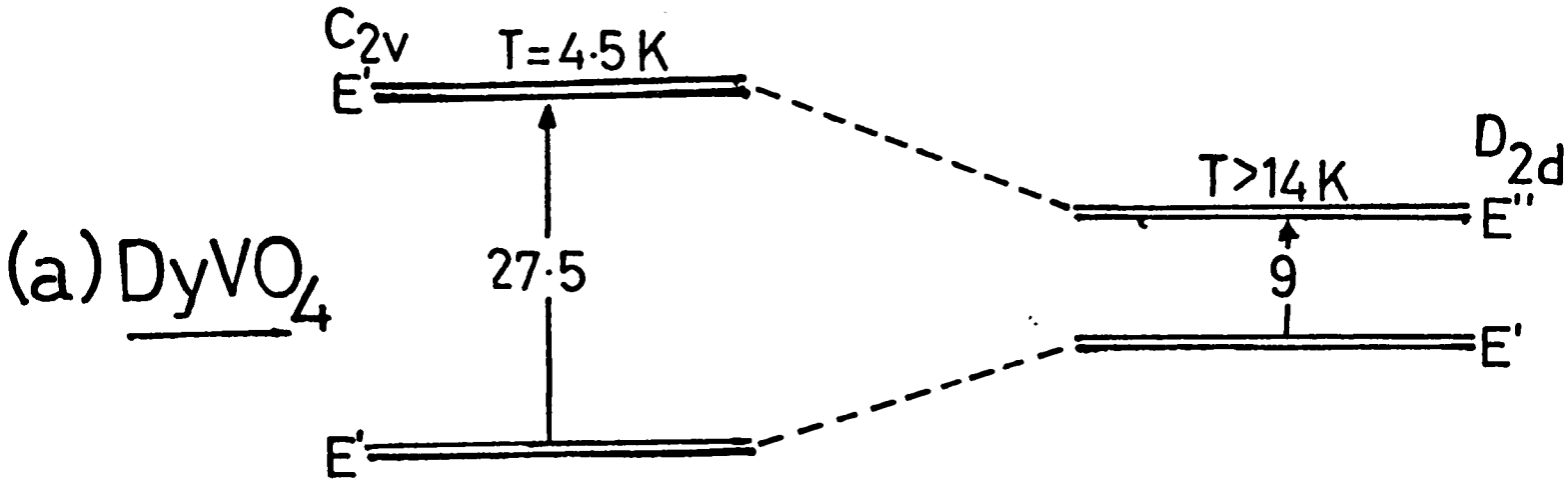
(a) DyVO4
C2v
E'
T=4·5 K
27·5
E'
D2d
T>14 K
E''
9
E'

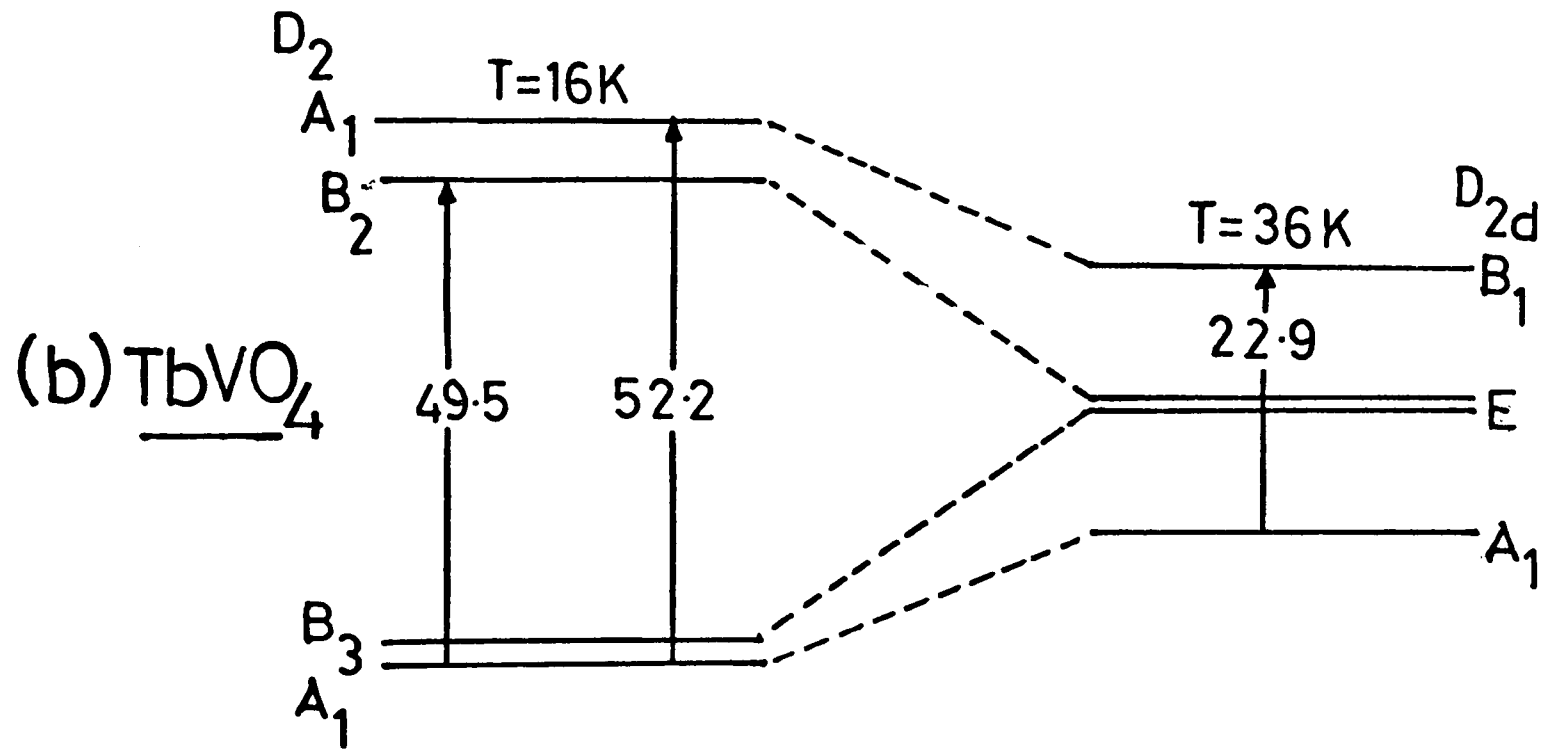
(b) TbVO4
D2
A1
B2
T=16K
49·5
52·2
B3
A1
D2d
T=36K
B1
22·9
E
A1

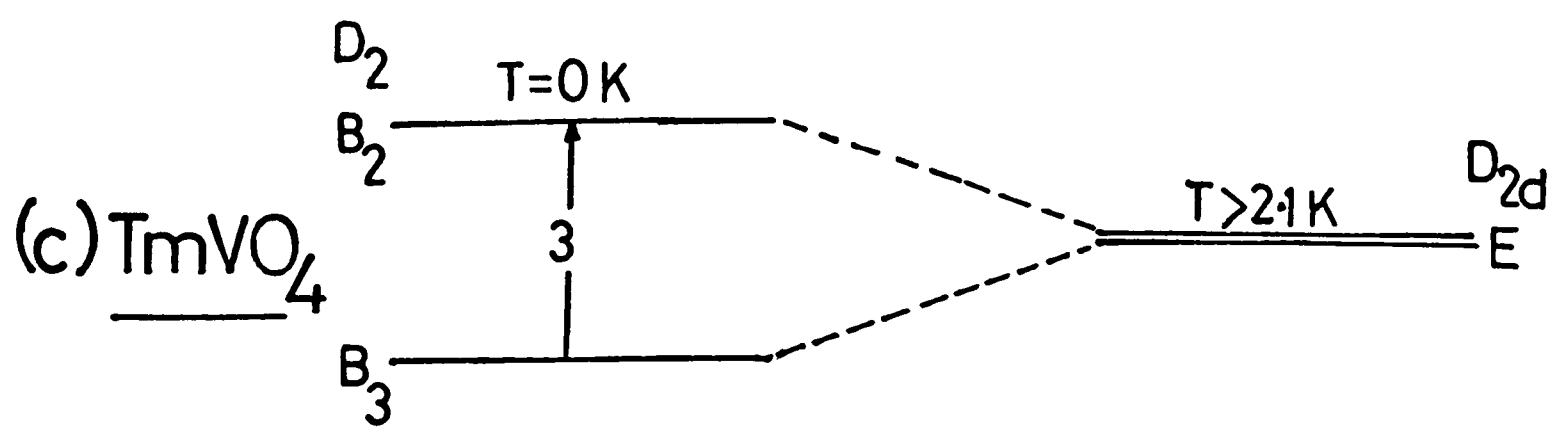
(c) TmVO4
D2
B2
T=0K
3
B3
D2d
T>2·1K
E

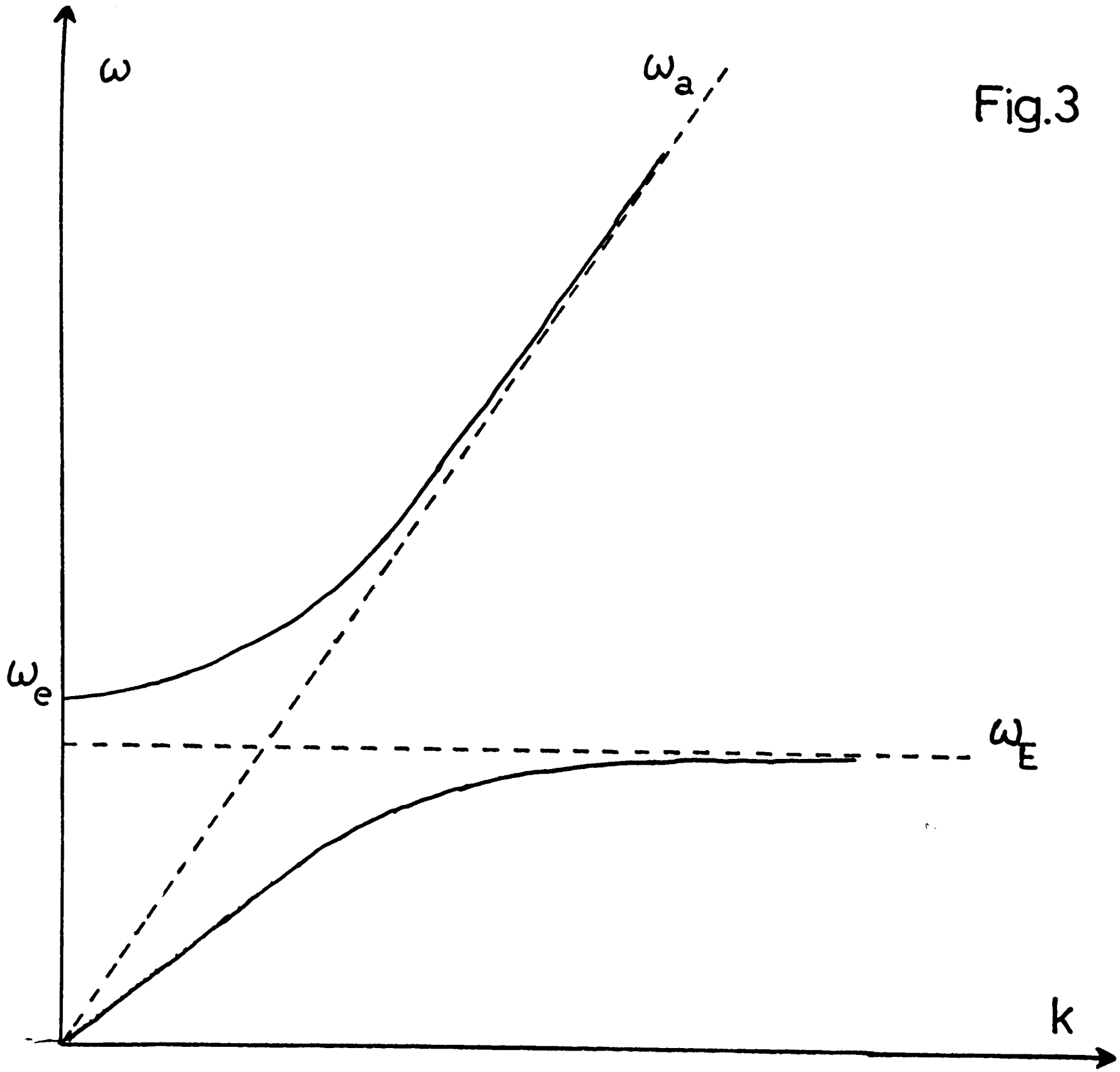

Fig.3

Fig. 4

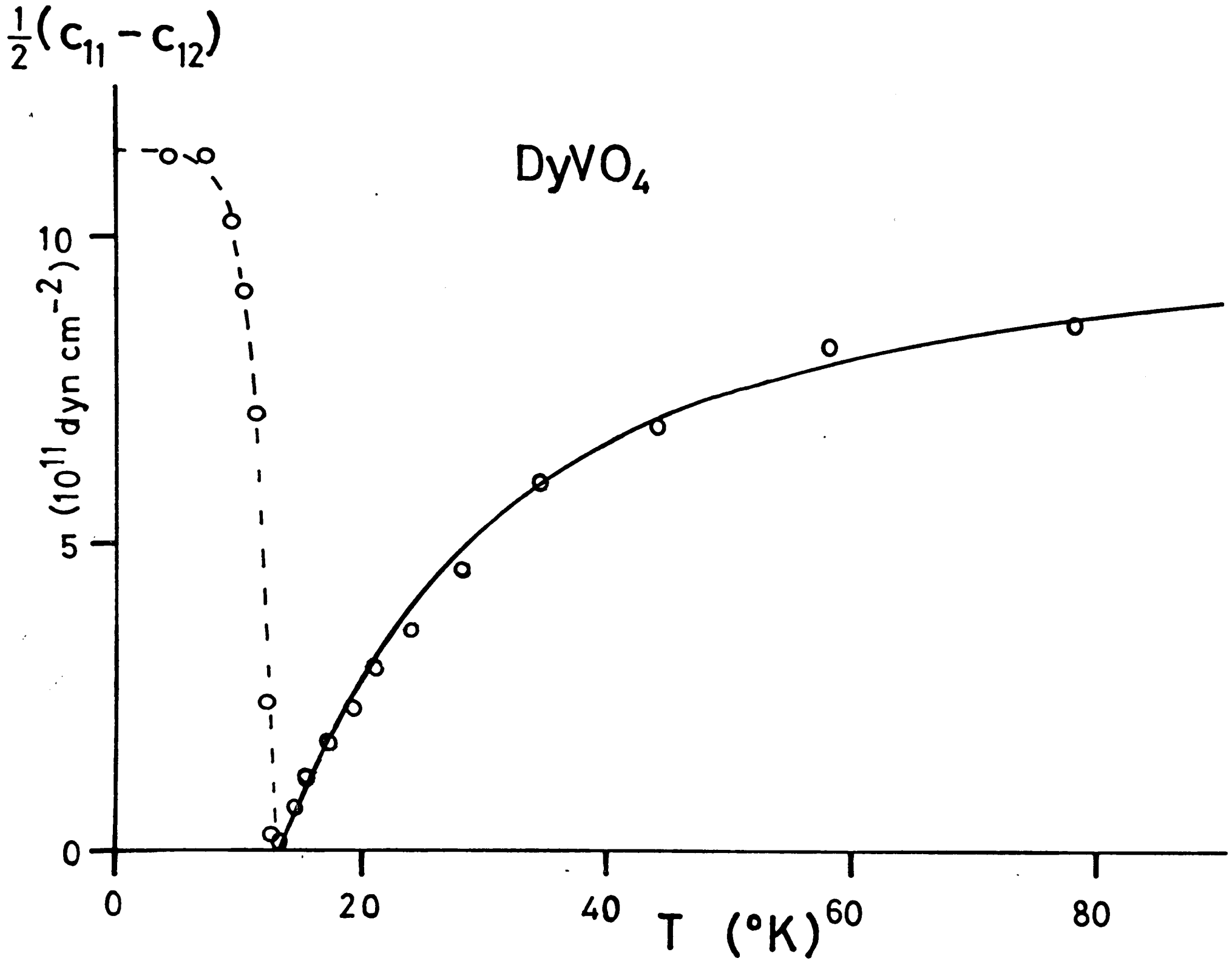

Fig. 5

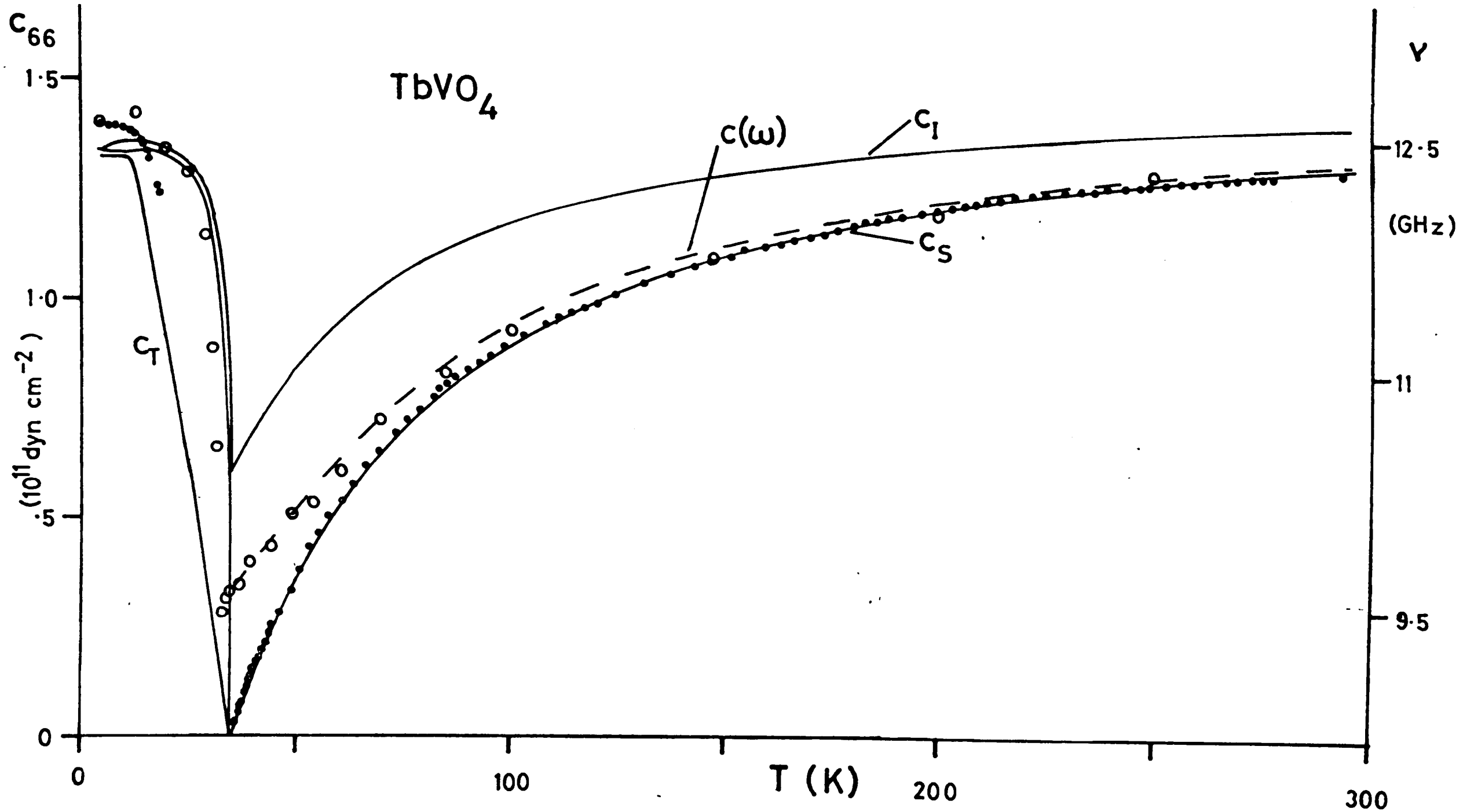
C_{66}
1·5
1·0
·5
0
$(10^{11}$ dyn cm$^{-2})$
$TbVO_4$
C_T
$C(\omega)$
C_I
C_S
ν
12·5
(GHz)
11
9·5
0
100
T (K)
200
300

Fig. 6

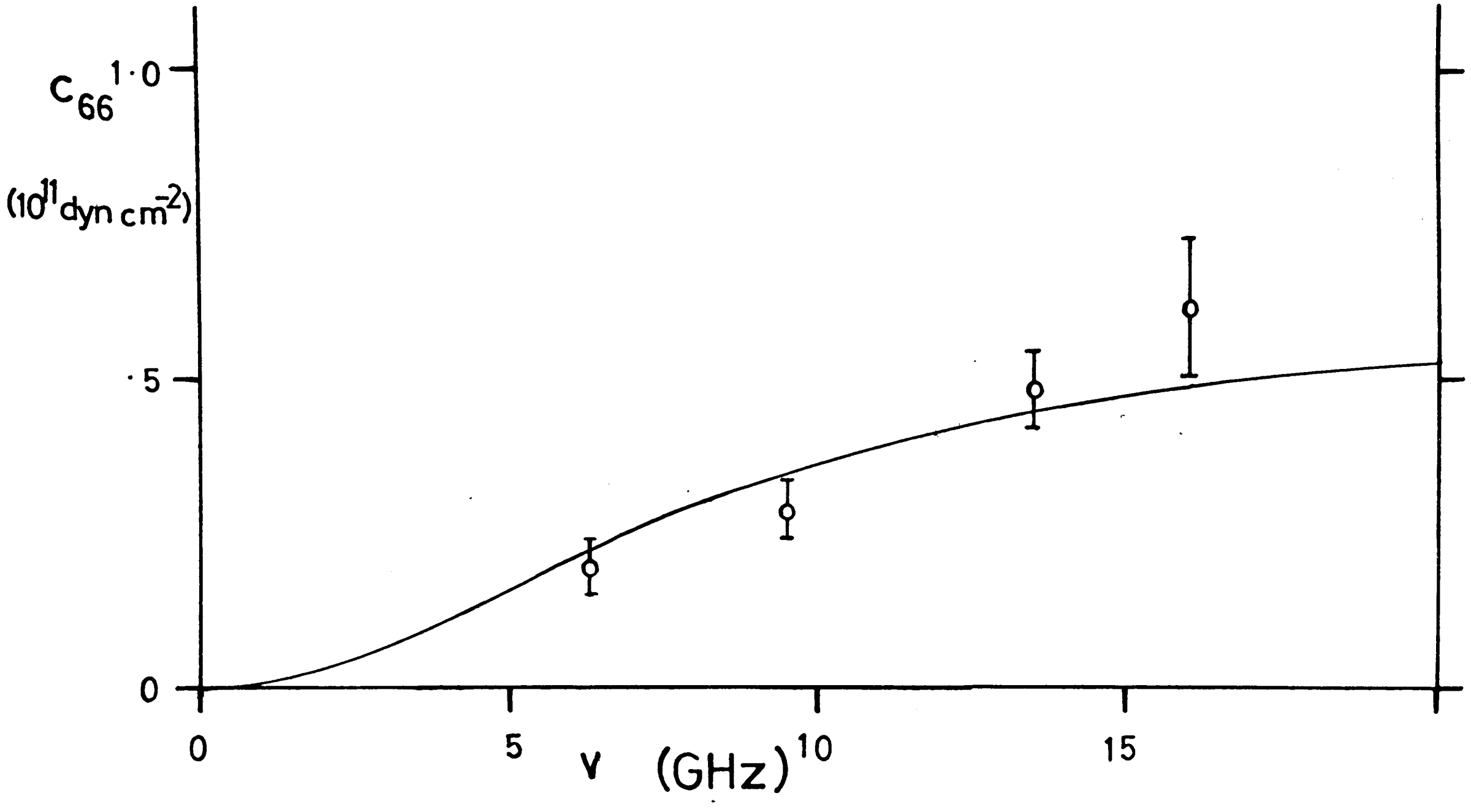

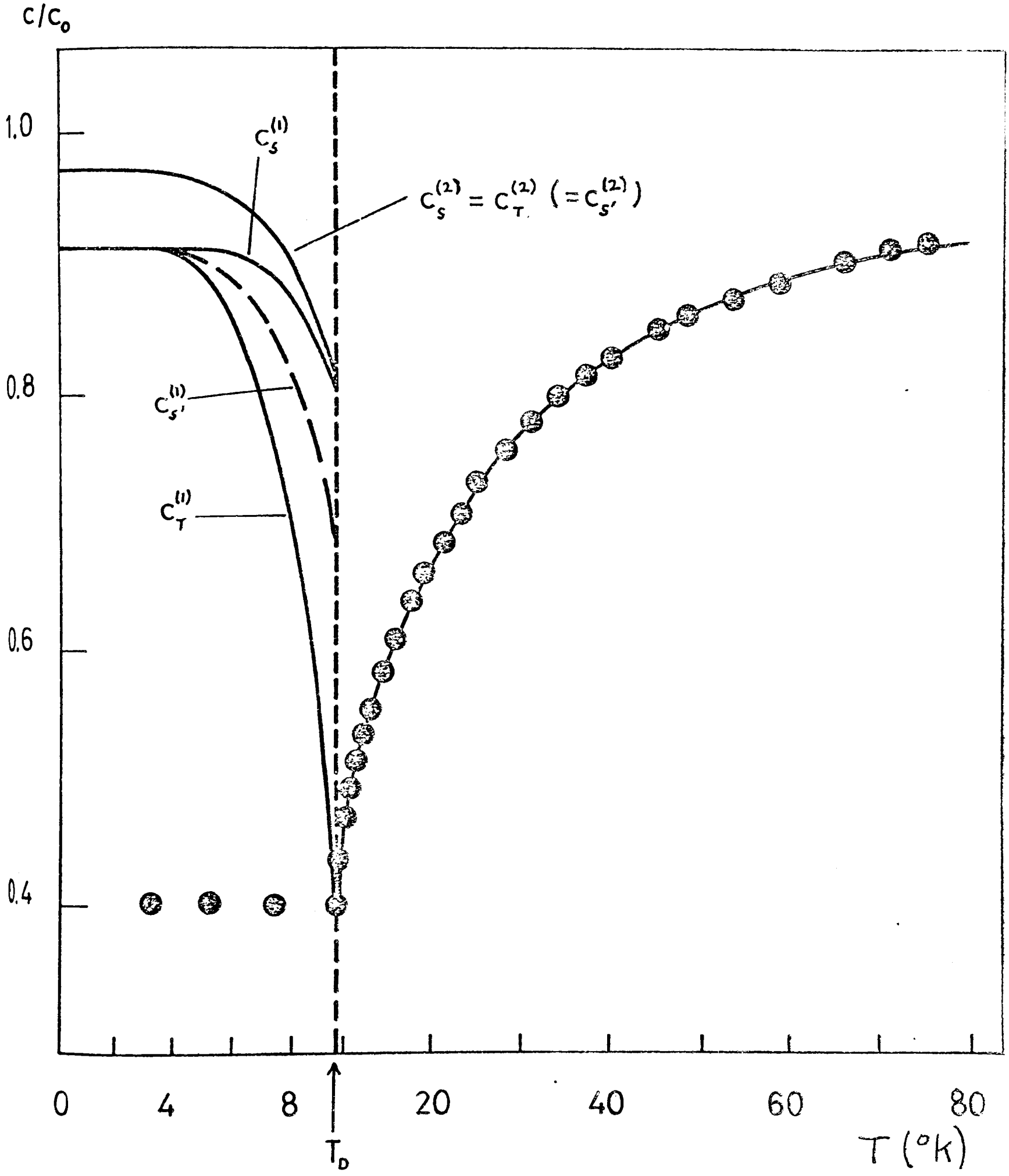

Fig. 7

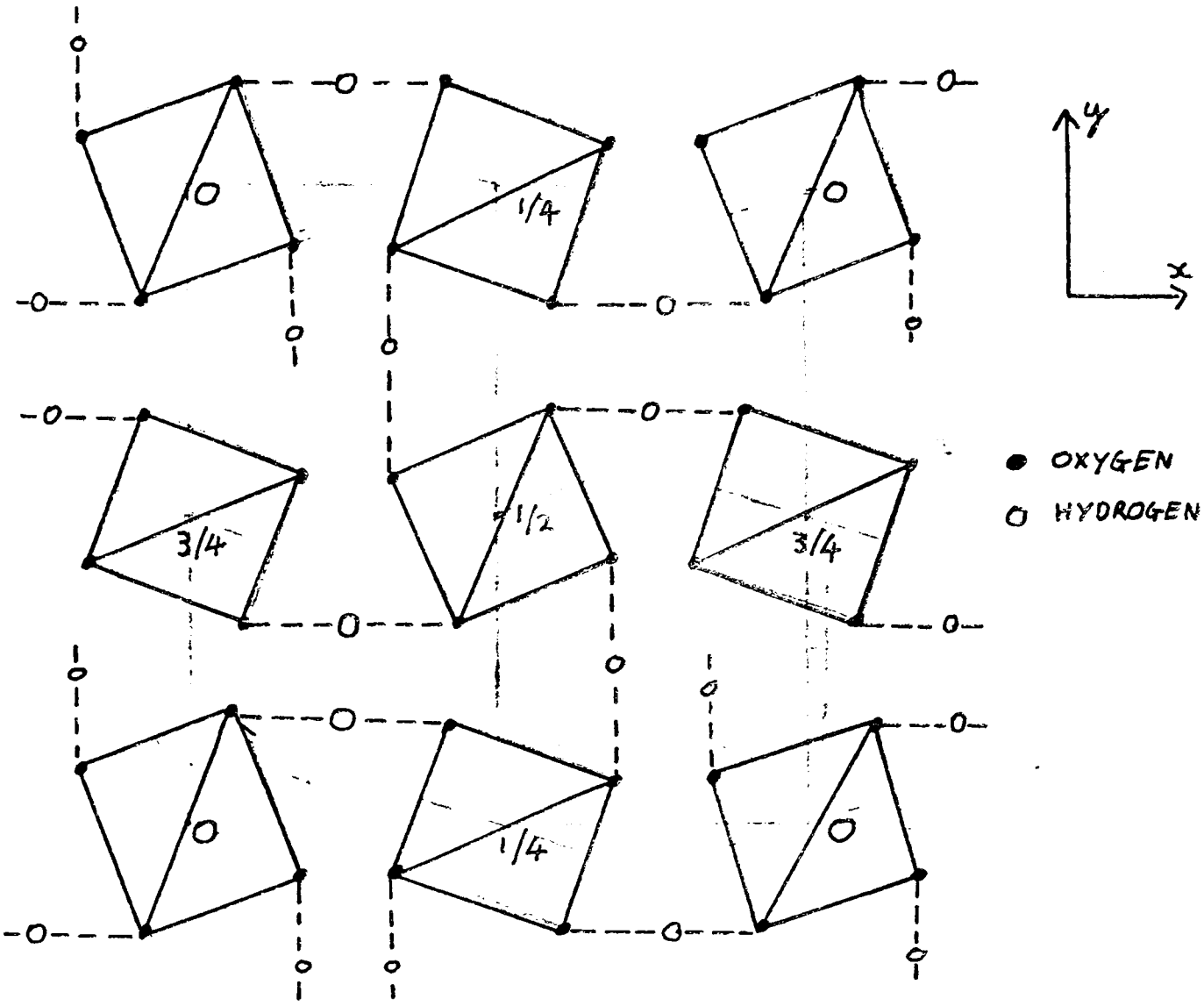
y
x
OXYGEN
HYDROGEN
1/4
3/4
1/2
3/4
1/4

(a)

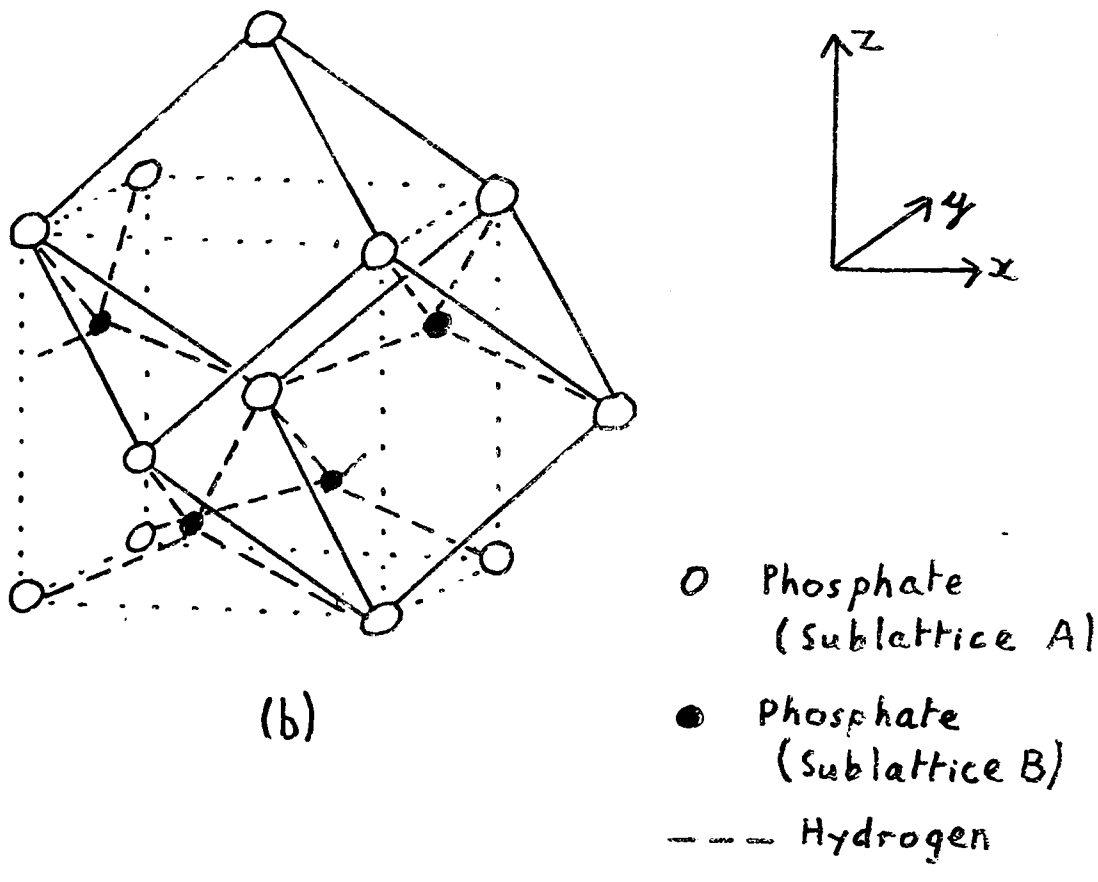
z
y
x
Phosphate (Sublattice A)
Phosphate (Sublattice B)
Hydrogen

(b)

Fig. 8

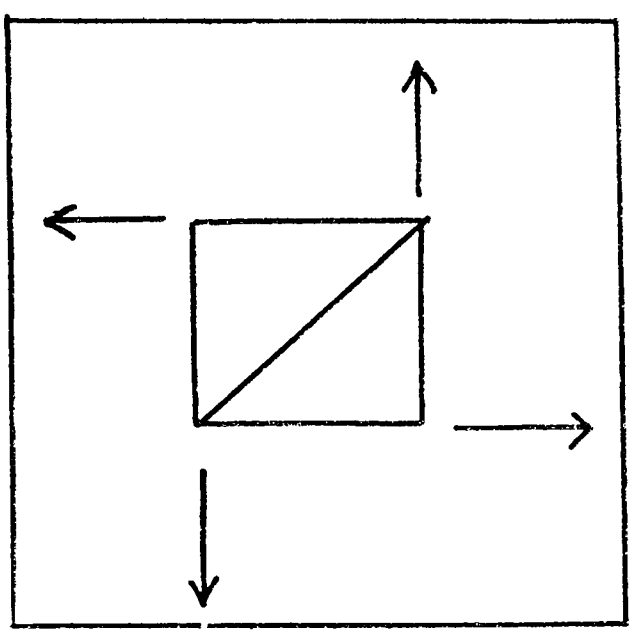

A_2

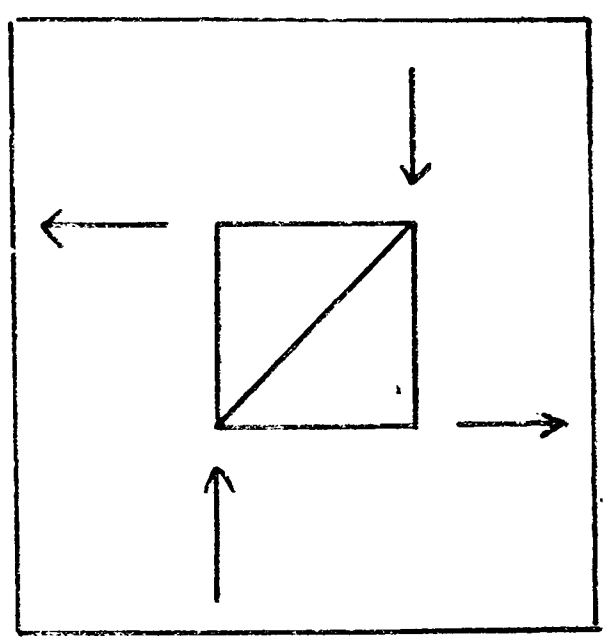

B_2

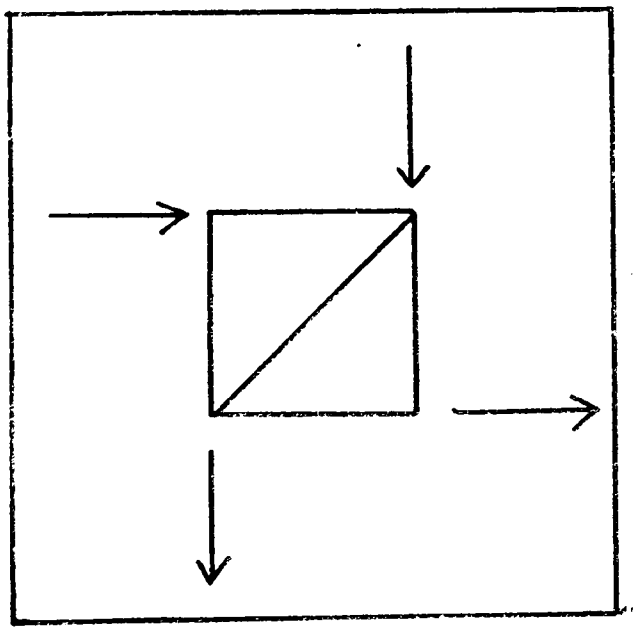

E_1

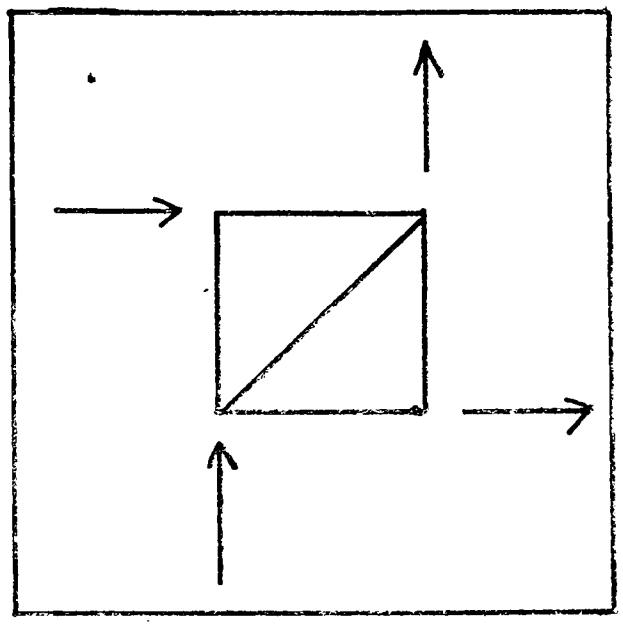

E_2

Fig. 9

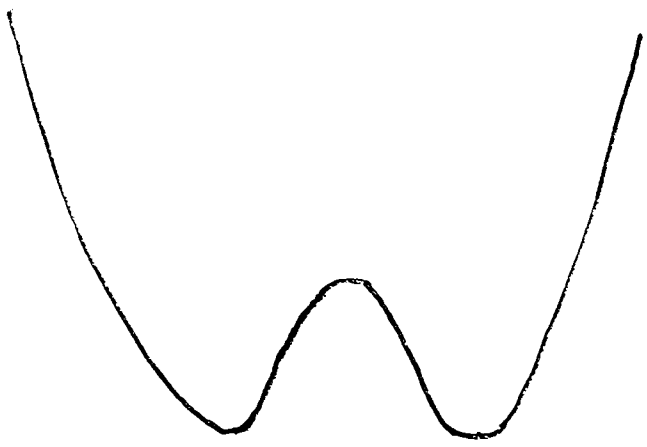

(a)(i)

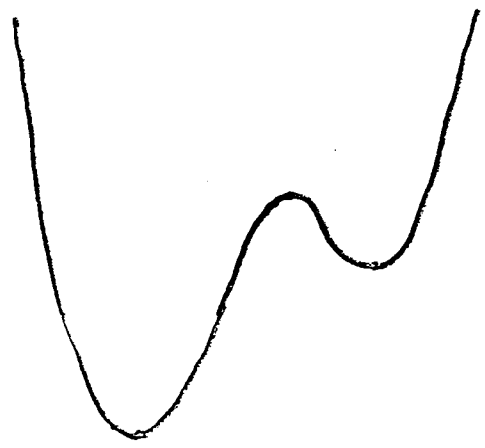

(a) (ii)

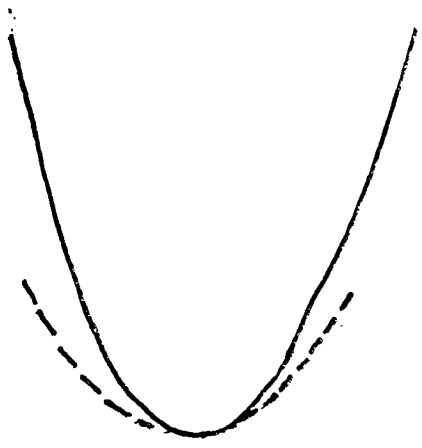

(b) (i)

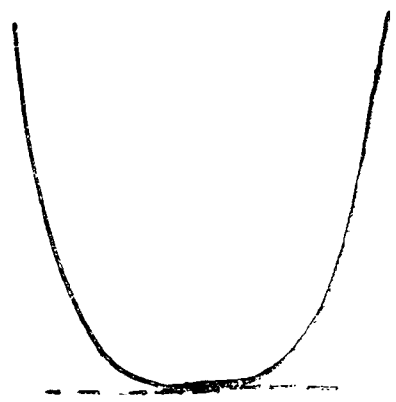

(b) (iii)

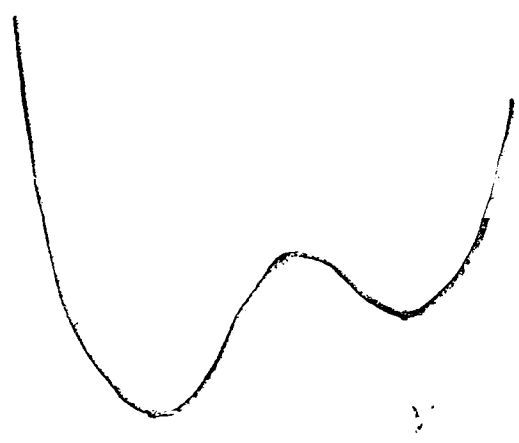

(b) (iii)

Fig. 10

Fig. 11

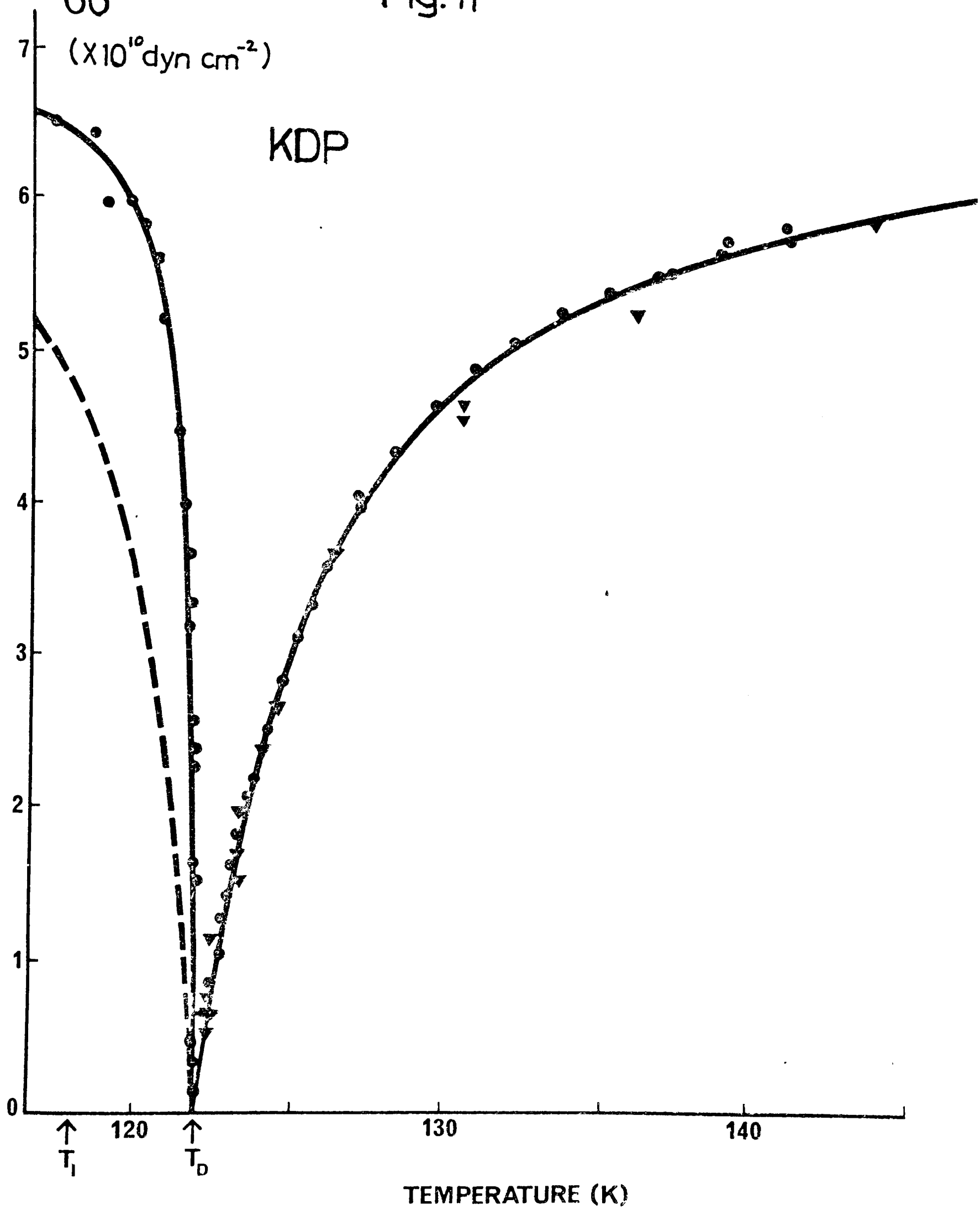
C_{66}
($\times 10^{10}$ dyn cm^{-2})
KDP
7
6
5
4
3
2
1
0
120
130
140
T_I
T_D
TEMPERATURE (K)

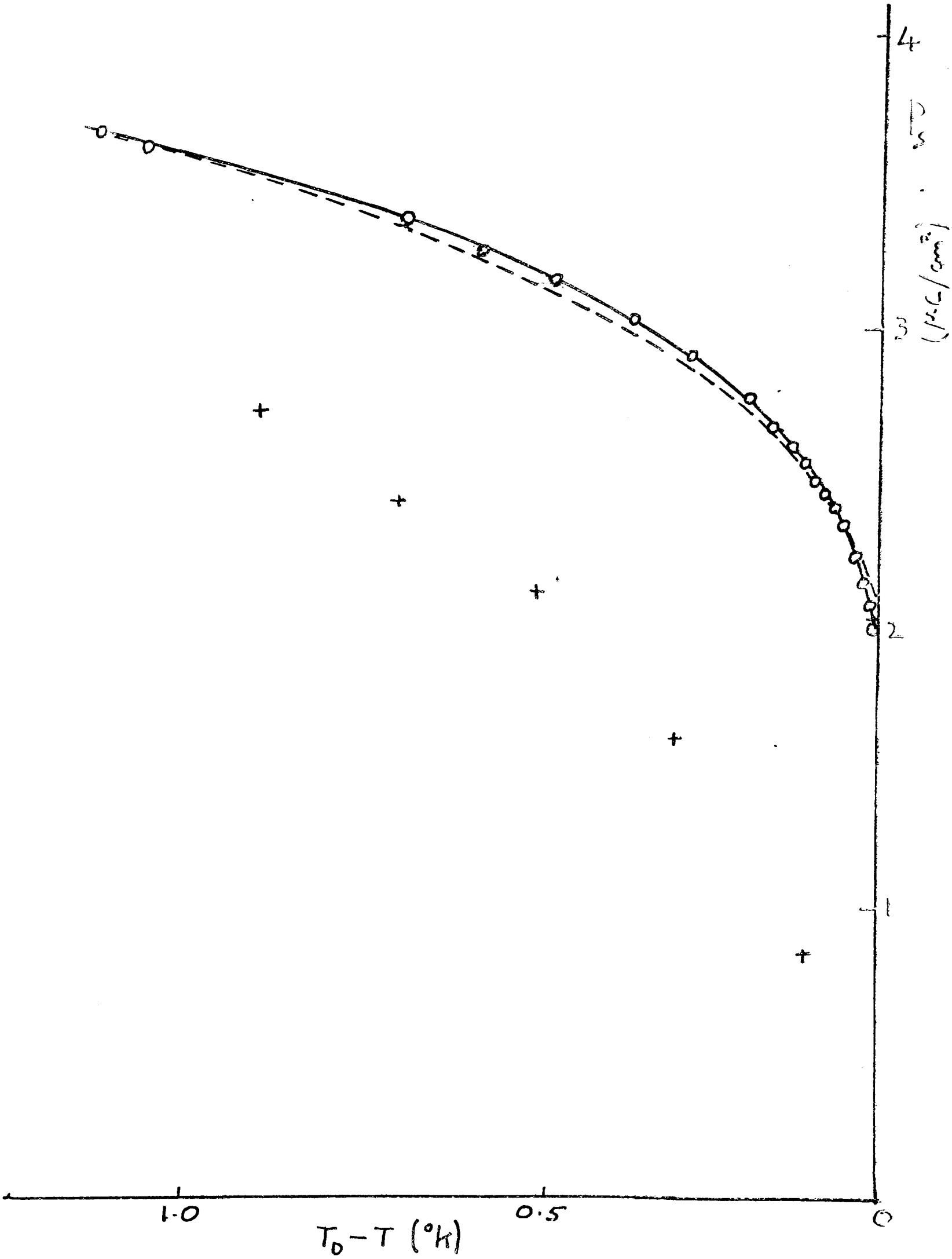

Fig. 12

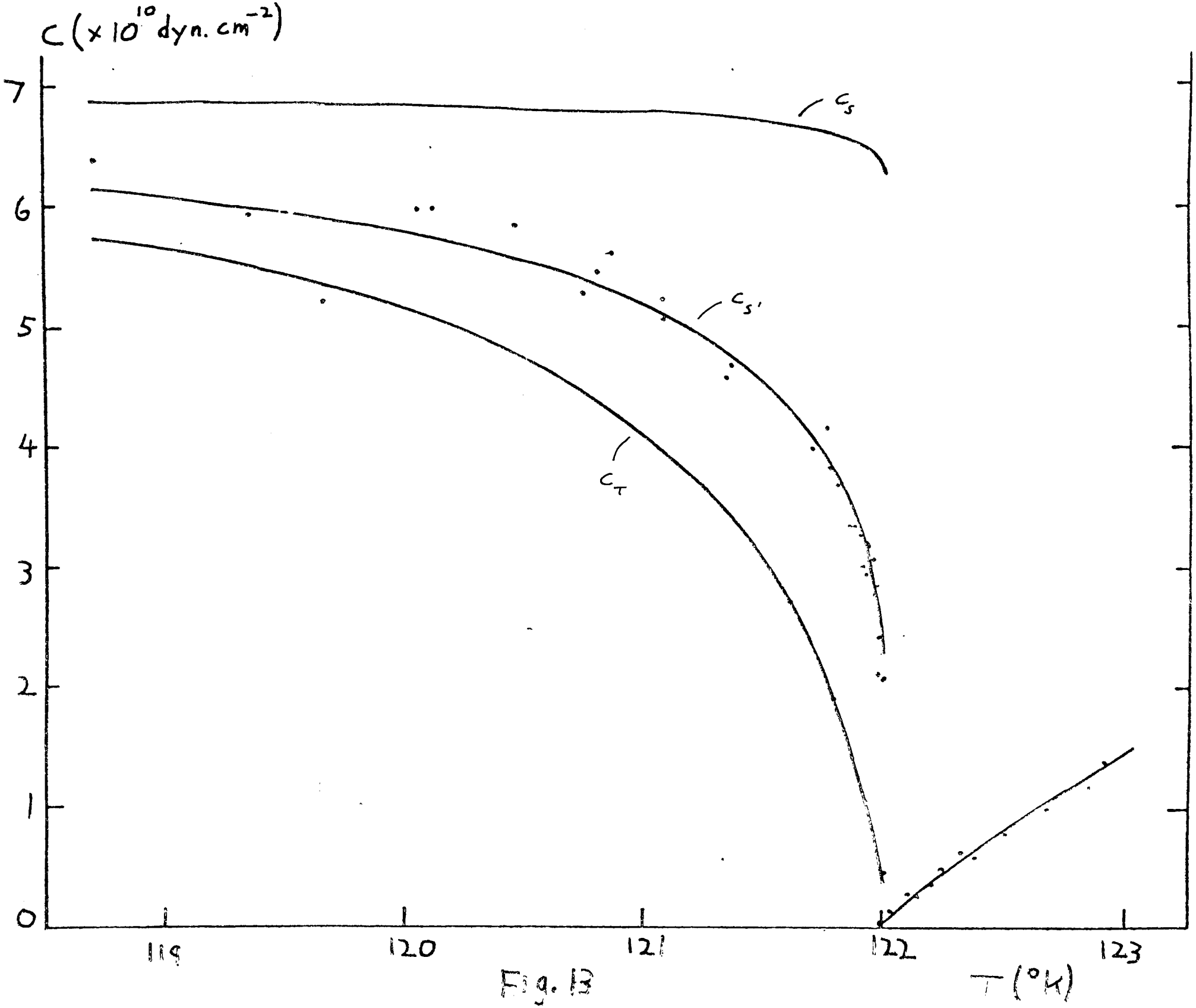

Fig. 13

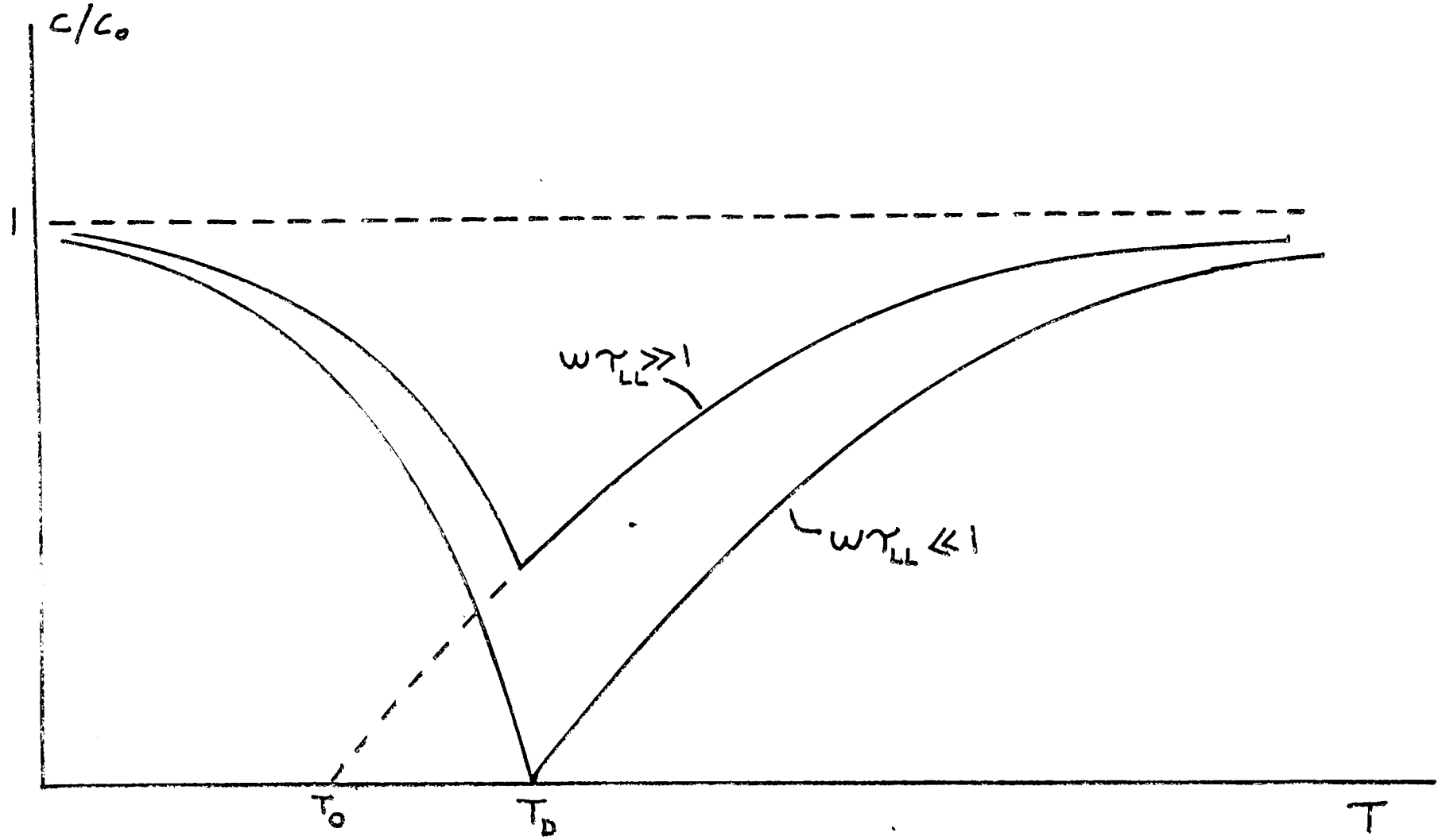

Fig. 14

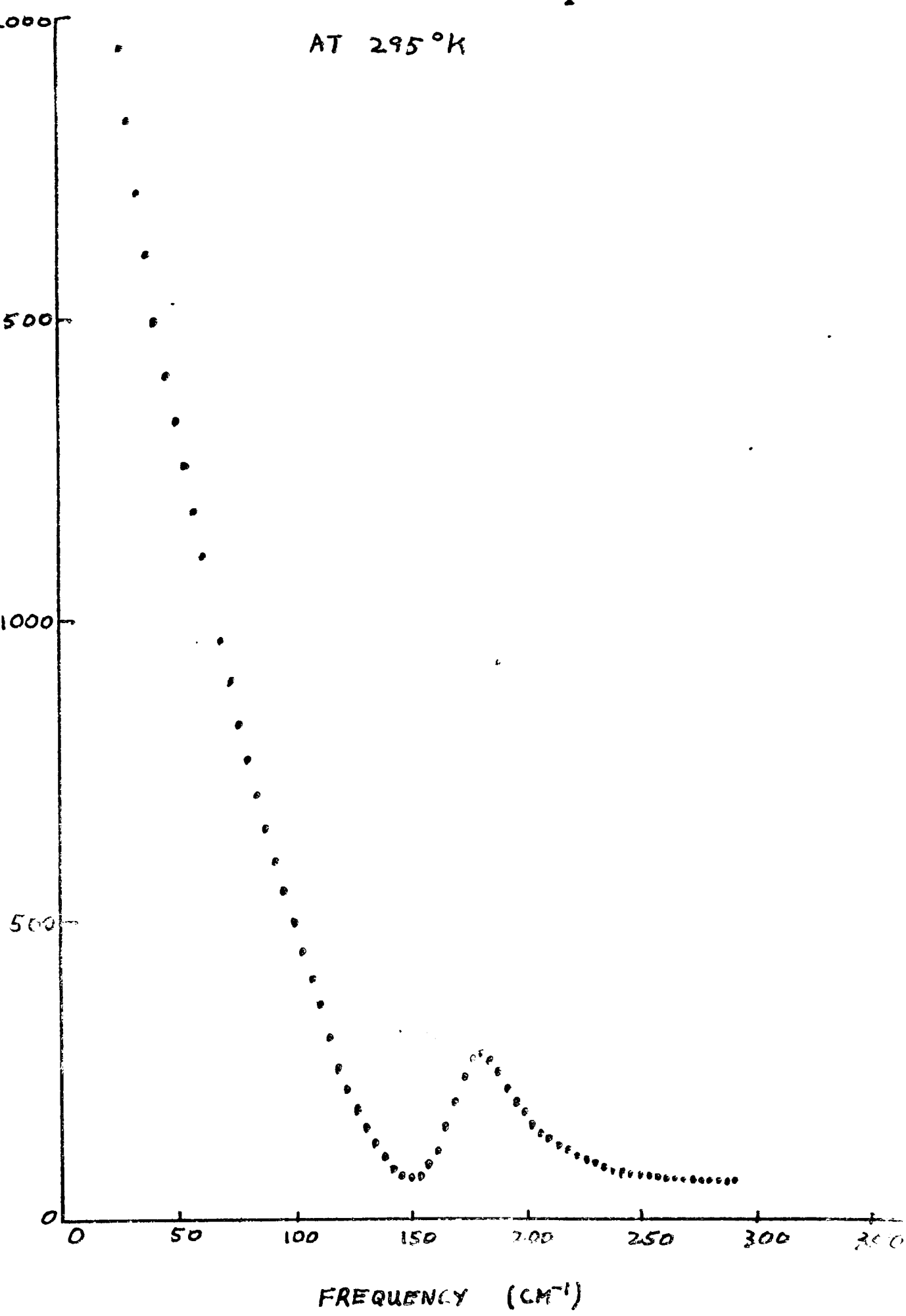
RAMAN SPECTRUM OF KDP B_2 – SYMMETRY
AT 295°K
2000
1500
1000
500
0
0
50
100
150
200
250
300
FREQUENCY (CM⁻¹)

Fig. 15

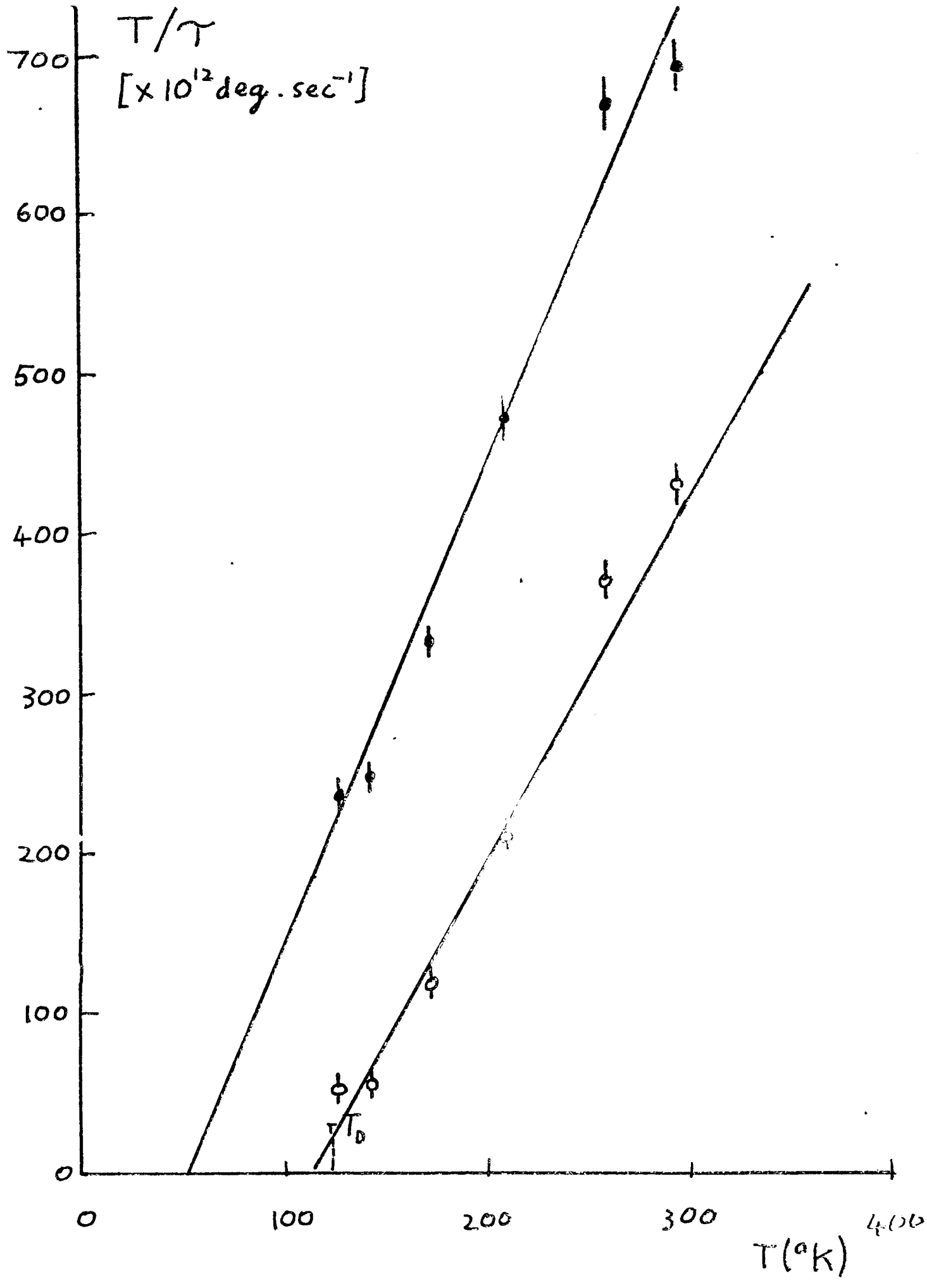
T/τ
[×10^12 deg. sec^-1]
700
600
500
400
300
200
100
0
0
100
200
300
400
T_D
T(°K)

Fig. 16

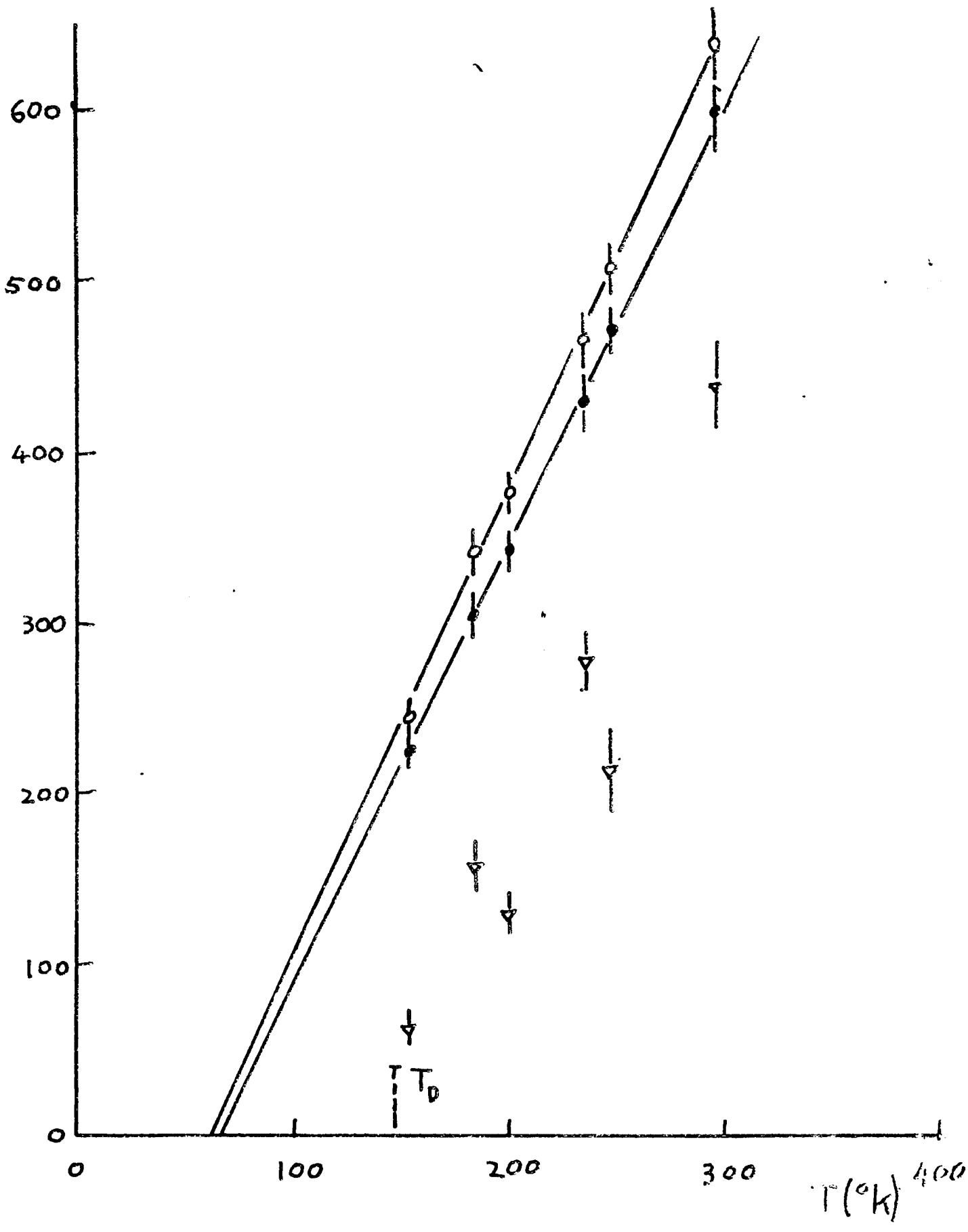

Fig. 17 (a)

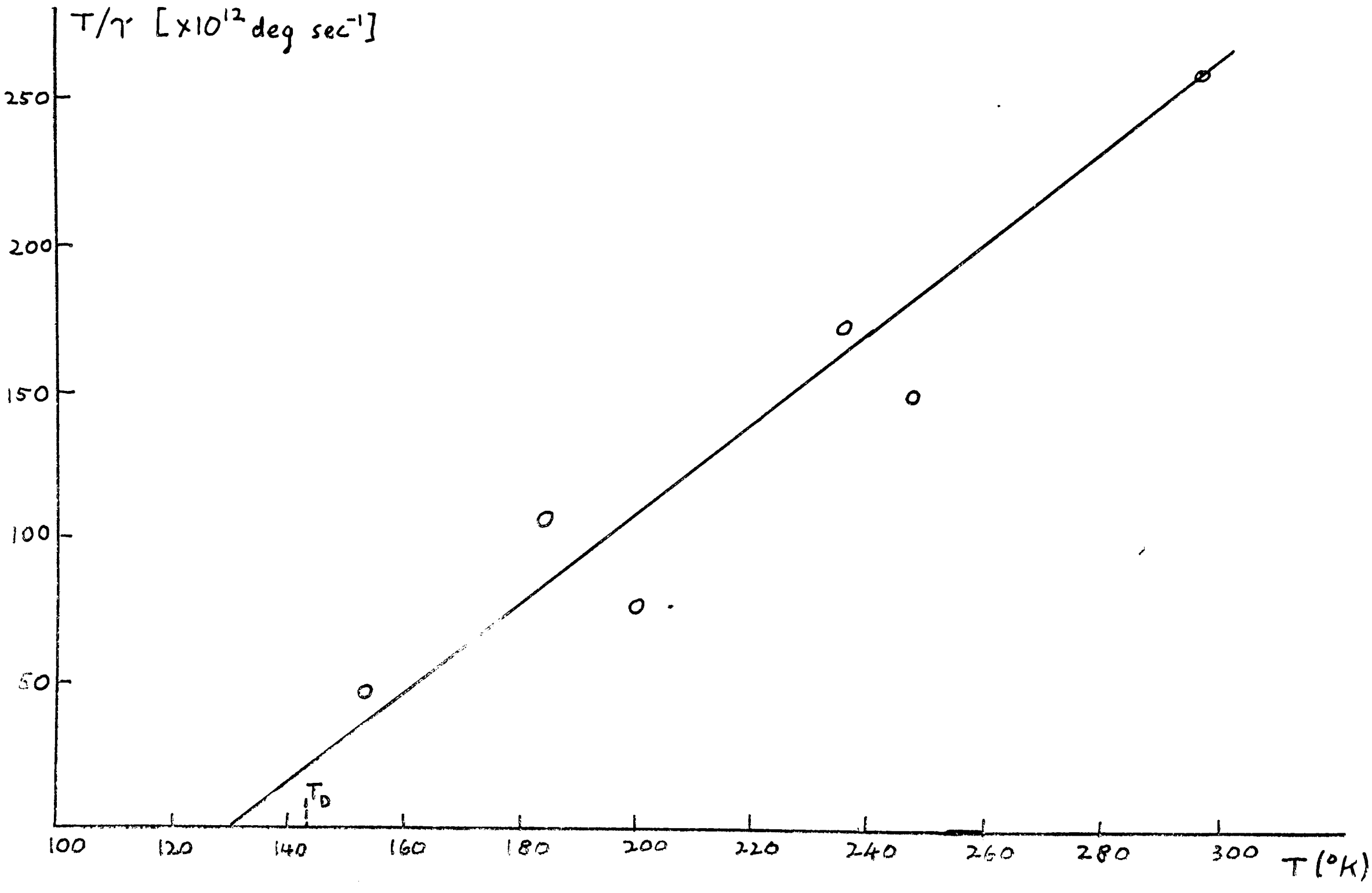
T/γ [×10^12 deg sec^-1]
250
200
150
100
50
T_D
100
120
140
160
180
200
220
240
260
280
300
T (°K)

Fig. 17 (b)

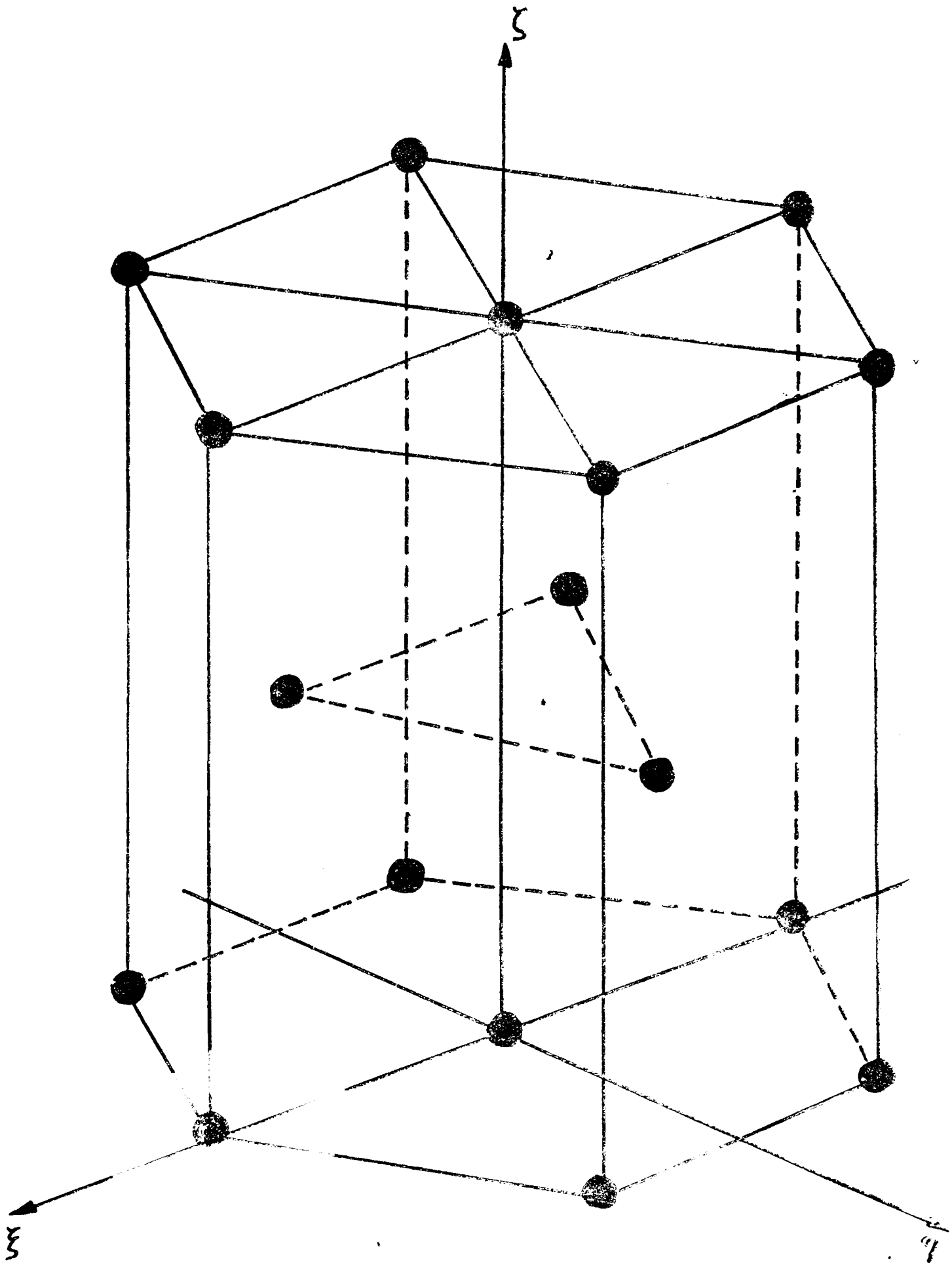

Fig. 18

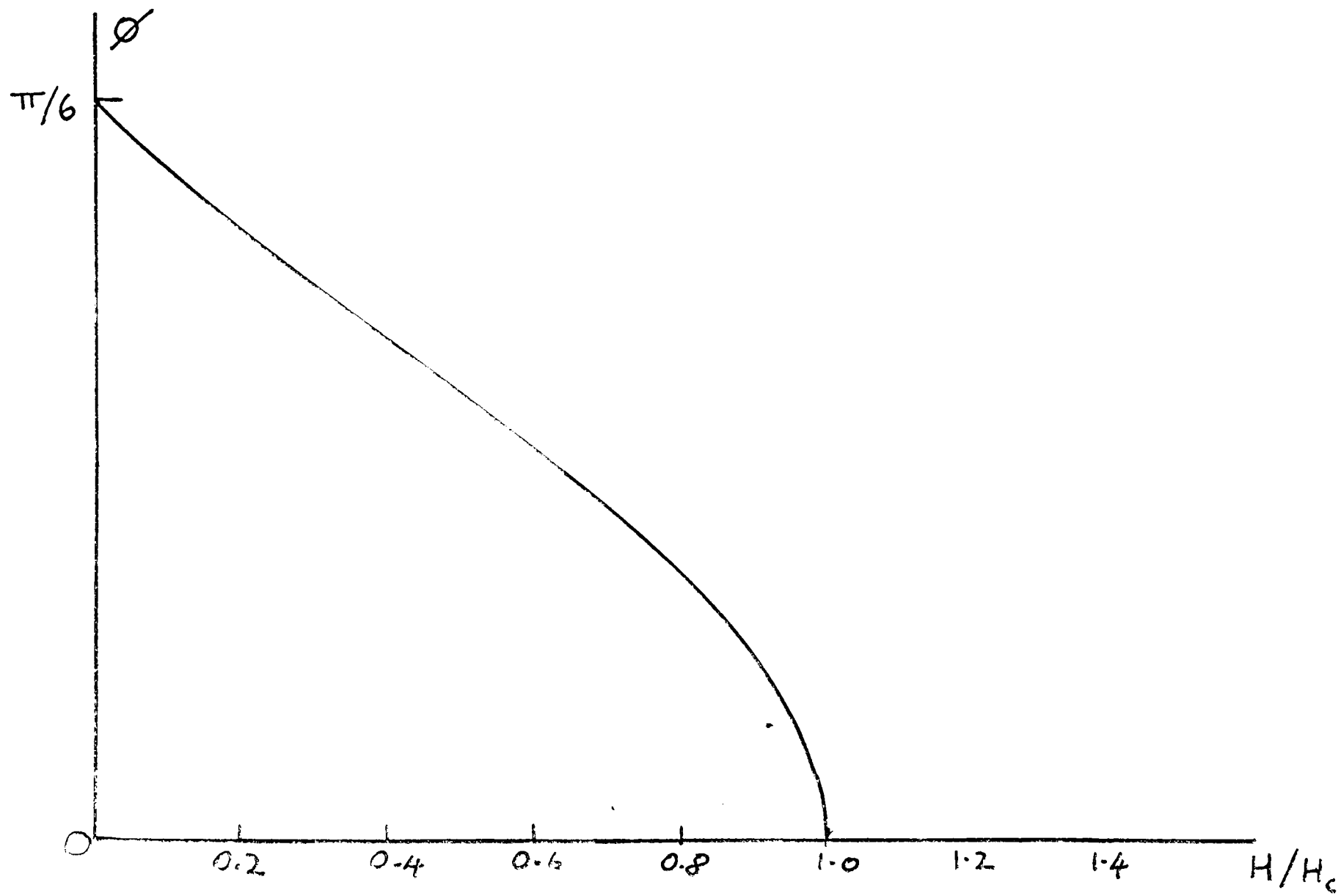

Fig. 19

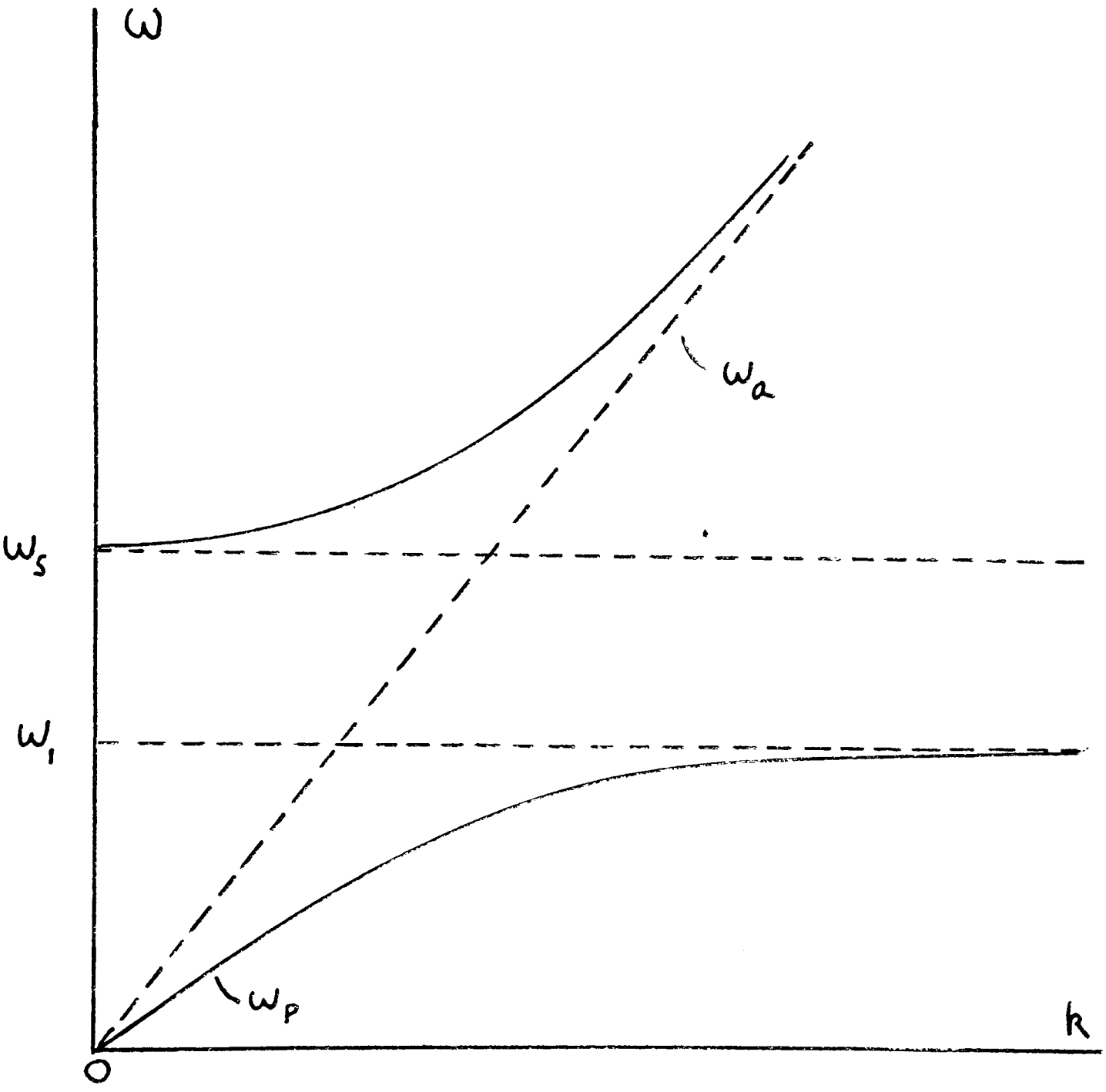

Fig. 20

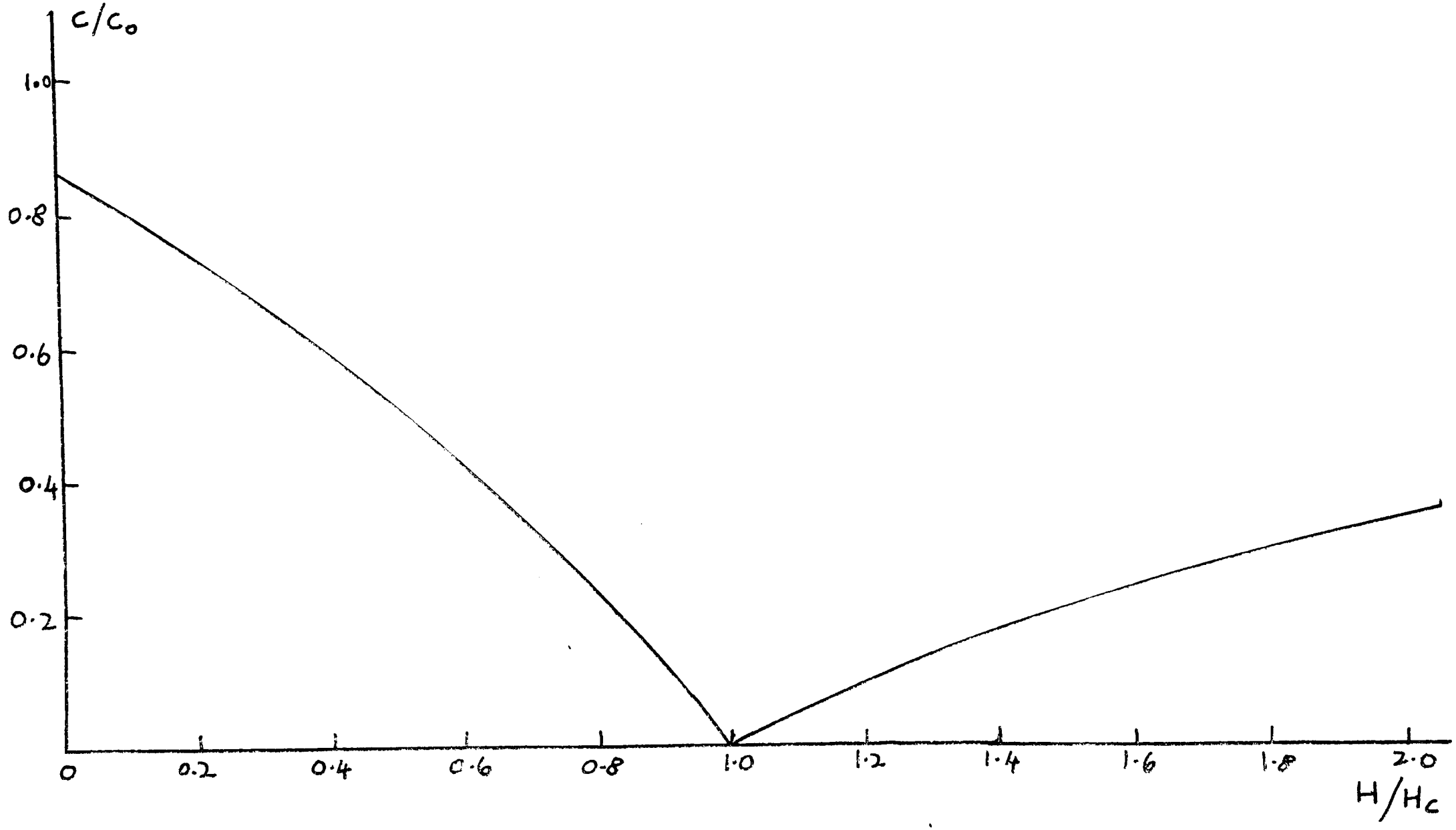

Fig. 21